

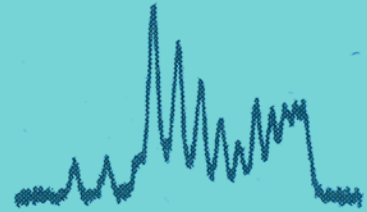


TP

europ physics
conference
abstracts



40th EGAS
GRAZ



Editor: L. Windholz

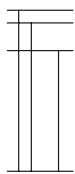
Published by: European Physical Society

Series Editor: Prof. O. Scholten, Groningen

Managing Editor: P. Helfenstein, Mulhouse

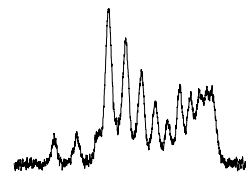
32E

ISBN 2-914771-53-3



40th G
ER
EGAS
GRAZ
S

40th EGAS Conference
Technische Universität Graz
Institut für Experimentalphysik
2 - 5 July 2008



European
Group for
Atomic
Systems

ABSTRACTS



Editor: L. Windholz

ORGANIZING COMMITTEE:

W.E. Ernst (Vice Chairman), T. Neger, G. Pottlacher, L. Windholz (Chairman)









CONTACT ADDRESS:









Institut für Experimentalphysik, Technische Universität Graz,
Petersgasse 16, A-8010 Graz
Tel. ++43 316 873 8144 (8141), Fax ++43 316 873 8655
e-mail: windholz@tugraz.at

This volume is published under the copyright of the European Physical Society (EPS). We want to inform the authors that the transfer of the copyright to EPS should not prevent an author to publish an article in a journal quoting the original first publication or to use the same abstract for another conference. This copyright is just to prevent EPS against using the same material in similar publications.

The EGAS logo shows the hyperfine pattern of a Pr I line in which the intensities of the components does not follow the theoretically predicted rules.

The 40th EGAS Conference is sponsored by

	<p>Bundesministerium für Wissenschaft und Forschung http://www.bmwf.gv.at</p>
	<p>Landeshauptmann Mag. Franz Voves Landesrätin Mag. Kristina Edlinger- Ploder</p>
	<p>http://www.graz.at/EN</p>
	<p>Technische Universität Graz http://www.tugraz.at</p>
	<p>TOPTICA Photonics AG http://www.toptica.com</p>
	<p>Springer-Verlag GmbH http://www.springer.com</p>
	<p>piezosystem jena GmbH http://www.piezojena.com/</p>
	<p>Coherent (Deutschland) GmbH http://www.coherent.de/</p>

	<p>Pfeiffer Vacuum GmbH http://www.pfeiffer-vacuum.de/</p>
	<p>Kurt J. Lesker Company GmbH http://www.lesker.com/</p>
	<p>Radiant Dyes Laser & Accessories GmbH http://www.radiant-dyes.com/</p>
	<p>iseg Spezialelektronik GmbH http://www.iseg-hv.de/</p>
	<p>ILMVAC GmbH http://www.ilmvac.de/</p>
	<p>Journal of Physics B: Atomic, Molecular and Optical Physics http://www.iop.org/journals/jphysb</p>
	<p>MEWASA FLEX GmbH http://www.mewasaflex.de/</p>
	<p>Bernhard Halle Nachfl. GmbH http://www.b-halle.de/</p>

Members of the board of the EUROPEAN GROUP FOR ATOMIC SYSTEMS

Prof. Hartmut HOTOP , CHAIR

Fachbereich Physik, Universität
Kaiserslautern
Postfach 3049
D-67653 KAISERSLAUTERN, Germany
Tel.: +49-631-205-2328
Fax: +49-631-205-3906
E-mail: hotop@physik.uni-kl.de

Prof. Michael DREWSEN

Department of Physics and Astronomy
University of Aarhus
NY Munkegade, BYG.520
DK-8000 AARHUS, Denmark
Tel.: +45 8942 3752
Fax.: +45 8612 0740
E-mail : drewsen@phys.au.dk

Prof. Frédéric MERKT (SECRETARY)

Laboratorium für Physikalische Chemie
ETH Zurich, HCI Hönggerberg
CH-8093 ZURICH, Switzerland
Tel.: +41-44 632 4367
Fax.: +41-44 632 1021
E-mail : frederic.merkt@ethz.ch

Prof. Wolfgang E. ERNST

Institute of Experimental Physics
Graz University of Technology
Petersgasse 16
A-8010 GRAZ, Austria
Tel. : +43 316 873 8140
Fax : +43 316 873 8655
E-mail : wolfgang.ernst@tugraz.at

Dr. Christian BORDAS

Laboratoire de spectrométrie ionique et
moléculaire (LASIM)
université Lyon I bâtiment Kastler
43, boulevard du 11-Novembre 1918
F 69622 VILLEURBANNE, France
Tel. : +33 4 7243 1086
Fax : +33 4 7243 1507
E-mail : bordas@lasim.univ-lyon1.fr

Prof. Jürgen ESCHNER

ICFO, Institute of Quantum Optics
Jordi Girona 29, Nexus II
08034 BARCELONA, Spain
Tel: +34-933964695
Fax: +34-934137943
E-mail : Juergen.Eschner@icfo.es

Prof. Mike CHARLTON

Department of Physics
University of Wales Swansea
Singleton Park
SWANSEA SA2 8PP, United Kingdom
Tel. : +44 (0)1792 295 372
Fax : +44 (0)1792 295 324
E-mail : M.Charlton@swansea.ac.uk

Prof. Nikolay KABACHNIK

Department of physics
Moscow State University,
Leninskiz Gory, Moscow 119992,
Russia
Tel. +7 495 939 3605
Fax +7 495 939 0896
E-mail : nkabach@mail.ru

Prof. Eva LINDROTH

Atomic Physics, Fysikum
Stockholm University
AlbaNova University Centre
SE-106 91 STOCKHOLM, Sweden
Tel.: +46-8 5537 8616
Fax.: +46-8 5537 8601
E-mail : lindroth@physto.se

Prof. Krzysztof PACHUCKI

Institute of Theoretical Physics
Warsaw University
Ul. Hoza 69
PL - 00-681 WARSAW, Poland
Tel.: +48-22-5532246
Fax: +48-22-6219475
E-mail: Krzysztof.Pachucki@fuw.edu.pl

Prof. Antonio SASSO

Università di Napoli Federico II
Dipartimento di Scienze Fisiche
Complesso Universitario Monte S.
Angelo
Via Cinthia, I-801236 NAPOLI, Italia
Tel. +39 081 67 6120 / 6273
Fax +39 081 67 6346
E-mail: sasso@na.infn.it

Prof. Kenneth TAYLOR

Department of applied mathematics and
theoretical physics
Queen's University of Belfast
BELFAST BT7 1NN, Northern Ireland,
UK
Tel. : 028 9033 5049
Fax : 028 9023 9182
E-mail : k.taylor@qub.ac.uk

Prof. Nikolay V. VITANOV

Department of Physics,
Sofia university
James Bourchier 5 Blvd.
Tel. +359 2 8161 652
Fax +359 2 9625 276
E-mail: vitanov@phys.uni-sofia.bg

Prof. Marc J.J. VRAKKING

AMOLF-FOM
Institute for Atomic and molecular
Physics
Kruislaan 407
1098 SJ AMSTERDAM, The
Netherlands
Tel. ?
Fax +31 20 6684106
E-mail: vrakking@amolf.nl

Webmaster**Prof. Henri-Pierre GARNIR**

Université de Liège
IPNAS, Sart Tilman B15
B-4000 LIEGE, belgium
Tel. +32 4 366 3764
Fax +32 4 366 2884
E-mail: hpgarnir@ulg.ac.be

Contents

This book contains all abstracts arrived in Graz before June 15, 2008

A Brief History of Elemental Carbon

R.F. Curl, jr.

*University Professor Emeritus, Pitzer-Schlumberger Professor of Natural Sciences
Emeritus, Professor of Chemistry Emeritus, Department of Chemistry, Rice University,
Houston, Texas, U.S.A., rfcurl@rice.edu*

Carbon is the only element that humanity has routinely been in contact with in reasonably pure form since the origin of the species. With this much experience with it, one might think that the chemistry of pure carbon is completely understood and developed. Nothing could be further from the real situation. Although many important advances have been made recently, there is much that is not understood and probably much to be discovered about the chemistry and uses of this extremely flexible element. This talk will be a rapid survey of human experience with elemental carbon and the variety of forms it can take.

Non-demolition photon counting and field quantum state reconstruction in a cavity: a new way to look at light

Serge Haroche

ENS and Collège de France, Paris

While usual photo-detection destroys light quanta, we have developed a quantum non-demolition way to count photons trapped in a cavity without absorbing them, making it possible to measure the same field repeatedly. We use as detectors atoms prepared in Rydberg states which cross the cavity one at a time and behave as microscopic clocks whose ticking rate is affected by light. By measuring the clocks' delay, information is extracted without energy absorption and the field progressively collapses into a well-defined photon number state. Quantum jumps between decreasing photon numbers are recorded as the cavity field subsequently relaxes towards vacuum. This new way to look at light can also generate coherent superpositions of photonic states with different phases called "Schrödinger cats". By exploiting information provided by sequences of atoms crossing the cavity and interacting non-destructively with its field, we reconstruct these Schrödinger cat states which are represented in phase space by Wigner functions exhibiting striking non-classical features. We directly monitor in this way the process of decoherence in experiments opening new avenues for the exploration of the boundary between the quantum and classical worlds.

Theory and Spectroscopy of Parity Violation in Chiral Molecules

Martin Quack

*ETH Zürich, Laboratorium für Physikalische Chemie, Wolfgang-Pauli-Str. 10,
CH-8093 Zürich,
web: www.ir.ethz.ch; email: Martin@Quack.ch*

Parity violation plays a crucial role in the Standard Model of Particle Physics and according to current understanding it has crucial connections to fundamental symmetry violations in general and to such fundamental phenomena as the existence of mass of the elementary particles (see [1,2]) and references cited therein). In chemistry, one important consequence is a “parity violating energy difference” $\Delta_{PV}E$ of the ground state energies of enantiomers of chiral molecules, corresponding to a non zero enthalpy of stereomutation or enantiomerisation $\Delta_R H_0^0 = N_A \Delta_{PV}E$, which would be exactly zero if perfect inversion symmetry were true. An experiment to measure this very small energy difference in the sub-femto-eV (or atto-eV) range, typically, has been proposed some time ago [3]. Recent improved theory [4,5,6] predicts parity violating potentials to be larger by about two orders of magnitude for the prototype compound H_2O_2 and related molecules, as compared to older theories, and this large increase has been confirmed by subsequent independent theoretical results in several groups. Thus the prospects for successful experiments look brighter today than ever before [7].

In the lecture we will discuss the current status of the field and report in some detail on the various spectroscopic approaches, which can be used, as well as the current challenges of these experiments [7]. If time permits, even more fundamental symmetry violations such as CP and CPT violation will be discussed [1,8].

References

- [1] M. Quack, in “Modelling Molecular Structure and Reactivity in Biological Systems”, Proc. 7th WATOC Congress, Cape Town January 2005 (Eds.: K. J. Naidoo, J. Brady, M. J. Field, J. Gao, M. Hann), Royal Society of Chemistry, Cambridge (2006), ISBN 0-85404-668-2, pages 3 - 38
- [2] M. Quack, *Nova Acta Leopoldina* **81**, 137 (1999), (earlier version of [1], in German).
- [3] M. Quack, *Chem. Phys. Lett.* **132**, 147 (1986); M. Quack, *Angew. Chem. Int. Ed. (Engl.)* **28**, 571 (1989).
- [4] A. Bakasov, T. K. Ha, M. Quack, in “Chemical Evolution, Physics of the Origin and Evolution of Life”, Proc. of the 4th Trieste Conference (1995) (Eds.: J. Chela-Flores, F. Raulin), Kluwer Academic Publishers, Dordrecht (1996), ISBN 0-7923-4111-2, pages 287-296.
- [5] A. Bakasov, T. K. Ha, M. Quack, *J. Chem. Phys.* **109**, 7263 (1998).
- [6] R. Berger, M. Quack, *J. Chem. Phys.* **112**, 3148 (2000).
- [7] M. Quack, J. Stohner, M. Willeke, *Annu. Rev. Phys. Chem.* **59**, 741 (2008).
- [8] M. Quack, Paper at EGAS Conference 2 to 5 July (2008)

Precision Experiments with Highly Charged Ions

H.-Jürgen Kluge for the HITRAP Collaboration

GSI/Darmstadt and University of Heidelberg, Germany

Highly-charged ions (HCI) confined in Penning traps and storage rings have been applied for high-precision experiments such as mass spectrometry or x-ray, laser and radio-frequency spectroscopy. Storage and cooling of HCI in trapping devices are prerequisites for such high-accuracy experiments in which even a single stored particle can be observed. In the case of a radioactive ion, the fate of an individual ion, undergoing a nuclear decay, can be studied in detail by observing the disappearance of the signal of the mother and the appearance of that of the daughter isotope. Since the mass resolving power of mass spectrometry using Penning traps or storage rings increases with the charge state, charge breeding and the use of HCI is planned for quite a number of radioactive beam facilities. Few-electron ions are simple systems which are calculable by theory with high accuracy. In such systems, the electric field strength increases roughly with the third power of the nuclear charge and reaches values much larger than presently achievable with the most powerful short-pulse lasers. These HCI up to hydrogen-like U^{91+} are testing grounds for QED in the little explored regime of extreme electromagnetic fields.

In order to increase the accuracy further for investigating simple systems, the Highly-charged Ion TRAP (HITRAP) facility is presently being built up at GSI. Stable or radioactive HCI are produced by stripping relativistic ions in a target and injecting them into the storage ring ESR at GSI. After electron cooling and deceleration to 4 MeV per nucleon, these ions are ejected out of the storage ring, decelerated further in a linear decelerator, and injected into a Penning trap where a temperature of 4 K is reached by electron and resistive cooling. From here, the cooled HCI are transferred at low energies to experimental setups. A large number of unique experiments with very heavy ions up to hydrogen-like U^{91+} are being prepared by the international HITRAP Collaboration:

- Clean samples of stored and cooled HCI in a chosen specific charge state can be investigated by observation of x-rays from a quasi point-like source.
- If the accuracy of QED calculations is improved, the fine structure constant α can be determined with high accuracy measuring the g-factor of the bound electron.
- Mass measurements can be performed with extreme accuracy of better than 10^{-11} and with single-ion sensitivity by using stored HCI.
- A measurement and comparison of the nuclear g-factor of the bare nucleus with that of the neutral atom allows one to check calculations of the diamagnetic correction for the first time.
- The hyperfine structure of the ground state in hydrogen-like systems can be determined. Optical pumping of the M1 transition will result in electronic and nuclear polarization enabling clean nuclear-decay experiments and, in this way, sensitive tests of weak interaction.
- Recoil ion momentum spectroscopy, ion-surface interaction experiments, and hollow-atom spectroscopy can be performed in a regime of extr. low energies using HCI.

AtomChips: Integrated circuits for matter waves

Jörg Schmiedmayer

Atominstitut der Österreichischen Universitäten, TU-Wien

AtomChips [1] aim at the miniaturization and integration of quantum optics and atomic physics on to a single chip, analogous to electronic circuits. It combines the best of both worlds: The perfected manipulation techniques from atomic physics with the capability of nanofabrication. AtomChips promise to allow coherent manipulation of matter waves on the quantum level by using high spatial resolution electro magnetic potentials from structures on the atom chip or by employing adiabatic radio frequency (RF) or micro wave (MW) potentials.

The talk will give an overview of the recent advances in the concepts, fabrication and experimental realization of AtomChips by illustrating the many different tasks that can be performed using ultra cold or Bose-Einstein condensed (BECs) atoms manipulated on the chip. These range from measuring magnetic and electric fields with unprecedented sensitivity by observing the density modulations in trapped highly elongated 1d BECs [2], to fundamental studies of the universal properties in low dimensional systems like non equilibrium dynamics and coherence decay [3] or signatures of thermal and quantum noise [4] in one dimensional super fluids. The talk will give an overview of the recent advances and experiments.

This work was supported by the European Union MC network AtomChips, integrated project SCALA, the DIP the FWF and the Wittgenstein Prize.

[1] For an overview see: Microscopic atom optics: from wires to an atom chip. Folman, R., Krger, P., Schmiedmayer, J., Denschlag, J. Henkel,C., Adv. At. Mol. Opt. Phys. **48**, 263 (2002).

[2] St. Wildermuth et al. Nature **435**, 440 (2005); S. Aigner et al. Science **319**, 1226 (2008)

[3] Hofferberth et al. Nature **449**, 324 (2007)

[4] Hofferberth et al. Nature Physics (2008), DOI:10.1038/nphys941; arXiv:0710.1575

Optical Atomic Clocks at the Frontiers of Metrology

Fritz Riehle

Physikalisch-Technische Bundesanstalt, Bundesallee 100, 38 116 Braunschweig Germany

Several optical atomic clocks are now beginning to outperform the best caesium atomic clocks that represent the realization of the definition of the unit of time in the International Systems of Units (SI). Consequently, four optical frequency standards have recently been selected and recommended as secondary representations of the second by the International Committee of Weights and Measures. Among them are the $^{171}\text{Yb}^+$ frequency standard at 688 THz which is based on an electric quadrupole transition of a single, laser-cooled ion held in a rf Paul trap and the ^{87}Sr standard at 429 THz based on a cloud of neutral atoms in an optical lattice at the magic wavelength. Due to the large number of atoms that can be interrogated in parallel, neutral atom optical frequency standards and clocks allow for unprecedented high short-term stability as compared to single ion standards whereas up to now single-ion standards seem to have the best prospects for fractional uncertainties around 10^{-17} and below. In the talk the status of both standards at PTB and elsewhere will be reviewed.

Apart from possible future realizations of the second those optical clocks are used to give upper limits for a possible drift of fundamental constants that is asked for by a certain class of theories that aim to combine quantum theory and General Relativity.

The unprecedented high accuracies and stabilities of optical clocks require novel solutions for meaningful comparisons of remote optical clocks. A particular interesting, novel and challenging approach is to phase-coherently shift the frequency of a particular optical atomic clock to the 1.54 μm band by means of a femtosecond comb, to transfer this frequency over an existing commercial telecommunication network and to employ a second frequency comb at the user end for comparison or calibration of the optical frequency standard at this place. First experimental results and planned realizations will be reported.

The remote comparison of optical clocks with fractional uncertainties around 10^{-18} is extremely challenging. A frequency shift of this magnitude results e.g. from the Doppler effect already by a relative motion of a few micrometers per day or by the gravitational red shift due to a vertical height difference of 1 cm in the gravitational potential near the surface of the Earth. It can be expected that frequency stabilized lasers of such high accuracy apart from their use as precise clocks might be used as sensitive probes for their relativistic environment and for other novel applications.

Alkali Atoms, Dimers, Exciplexes and Clusters in ^4He Crystals

A. Weis, P. Moroshkin, V. Lebedev, and A. Hofer

Physics Department, University of Fribourg, Chemin du Musée 3, CH-1700 Fribourg

A closed-shell He atom and a single-electron alkali atom strongly repel each other because of the Pauli principle. As a consequence, an alkali atom immersed into condensed (superfluid or solid) ^4He forms a spherical bubble state, in which the alkali repels the He quantum fluid/solid by imposing its own symmetry on the local He environment. For 15 years we have investigated such atomic bubbles in solid ^4He using optical and magnetic resonance spectroscopy.

In this talk I will first review our high resolution magnetic resonance studies performed on solid He matrix-isolated alkali atoms in the radio-frequency and microwave domains with special emphasis on their sensitive dependence on the crystalline structure (body-centered cubic, bcc, versus hexagonally close-packed, hcp) of the helium matrix.

In recent years we have extended the purely atomic studies to larger bound complexes, such as exciplexes, dimers and clusters. I will present some of our intriguing recent results:

- In their respective ground states, alkali and He atoms are the worst enemies in the periodic table and strongly repel each other. Excited alkali atoms, however, attract He atoms and form bound states (so-called exciplexes), in which up to 7 He atoms can be attached to one alkali atom.
- Cs_2 and Rb_2 dimers in solid He can be excited via a large variety of absorption bands, and the deexcitation proceeds either by photodissociation or by emission of radiation. We made the strange observation that, irrespective of the excitation band, dimer fluorescence is only emitted on the $(1)^3\Pi_u \rightarrow X^1\Sigma_g$ triplet-singlet transition which is forbidden in the free dimer.
- When the first excited $P_{1/2}$ state of an alkali atom is populated by direct atomic excitation, it fluoresces at 879 nm (1.7% blueshifted from the free atomic transition at 894 nm), a quantitatively well explained fact. However, when the same state is populated by photodissociation of the dimer, the emission wavelength is 885 nm. We attribute this effect to the formation of an entangled diatomic bubble state.
- The doped region of the He crystal has a bluish color that originates from Mie scattering by alkali clusters, the size distribution of which can be inferred from the extinction spectrum.
- When the doped He crystal is molten by lowering the He pressure, the doped (column-shaped) region remains solid at pressures, where pure He is superfluid. We present experimental support for our hypothesis that this new form of solid He is an amorphous or crystalline ionic structure formed by snowballs (nanoscopic solid He structures formed around positive ions) and electron bubbles.

Generation of Short Wavelength Radiation via Coherent Hyper Raman Superradiance

Marlan O. Scully

Texas AM University and Princeton University

We find that intense short pulses of XUV radiation can be produced by cooperative spontaneous emission from visible or IR laser pulses driving atoms or ions. The process depends on the generation and utilization of atomic coherence as is the case in lasing without inversion. However, the radiation process is not stimulated emission, but is rather cooperative spontaneous emission in the sense of Dicke. More precisely, the many atom mathematics of the problem is the same as that of coherent anti-Stokes Raman scattering.

Cold Atom Interferometry for Gravitational Experiments

G. M. Tino

*Dipartimento di Fisica and LENS Laboratory - Università di Firenze
Istituto Nazionale di Fisica Nucleare, Sezione di Firenze
via Sansone 1, Polo Scientifico, I-50019 Sesto Fiorentino (Firenze), Italy
E-mail: guglielmo.tino@fi.infn.it*

Experiments we are performing using atom interferometry to determine the gravitational constant G [1] and test the Newtonian gravitational law at micrometric distances [2] will be presented. Other experiments in progress, planned or being considered using atom interferometers in ground laboratories [3] and in space [4] will be also discussed.

References

1. G. Lamporesi, A. Bertoldi, L. Cacciapuoti, M. Prevedelli, and G. M. Tino, *Phys. Rev. Lett.* **100**, 050801, (2008).
2. G. Ferrari, N. Poli, F. Sorrentino, and G. M. Tino, *Phys. Rev. Lett.* **97**, 060402, (2006).
3. M. de Angelis, A. Bertoldi, L. Cacciapuoti, A. Giorgini, G. Lamporesi, M. Prevedelli, G. Saccorotti, F. Sorrentino, G.M. Tino, *to be published*.
4. G. M. Tino, L. Cacciapuoti, K. Bongs, Ch. J. Bordé, P. Bouyer, H. Dittus, W. Ertmer, A. Görlitz, M. Inguscio, A. Landragin, P. Lemonde, C. Lammerzahl, A. Peters, E. Rasel, J. Reichel, C. Salomon, S. Schiller, W. Schleich, K. Sengstock, U. Sterr, M. Wilkens, *Nuclear Physics B (PS)* **166**, 159, (2007).

Photodetachment microscopy in a magnetic field

C. Blondel, W. Chaibi, C. Delsart and C. Drag

*Laboratoire Aimé-Cotton, Centre national de la recherche scientifique,
Univ. Paris-sud 11, bâtiment 505, F-91405 Orsay, France*

Among some remarkable properties of charged-particle interferometry, one has known for sixty years of the case where a perturbation can induce a shift of interference fringes even though no physical field acts on the classical particle trajectories [1,2]. In such an extreme case, of course, all trajectories remain unperturbed, and the fringes shift with respect to a motionless envelope.

Less attention was paid to the other extreme situation, where a uniform, e.g. magnetic field acts on all possible trajectories of the interferometer volume. In this case, the Lorentz force is expected to bend all trajectories, while the added magnetic flux is expected to change the interferometer phase. No doubt that, on a microscopic scale, the latter (phase shift) is the quantum-mechanical explanation of the former (trajectory shift). Interferometers, however, provide a situation where the added magnetic flux is no longer between infinitesimally close trajectories, but between pairs of trajectories with a macroscopic separation. In the ordinary photodetachment microscopy situation [3], a μT is enough to produce a 100 radian phase shift between trajectories of the most sensitive pairs, which is definitely beyond the perturbative regime.

A review of past interference experiments shows that the identity of fringe and trajectory shifts was actually seldom addressed. The well-known sensitivity of interferometers to external perturbations can even be misinterpreted as an argument for a greater shift of the interference fringes. On the other hand, analogy of the magnetic field action to the effect of rotation of the whole apparatus can serve as an argument for the identity of fringe and trajectory displacements. Rotation vs. magnetic field analogy is however only a first-order approximation.

Photodetachment microscopy provides us with a remarkable situation where the electron interference pattern has a clear-cut envelope. Experiments done with and without a magnetic field show a pattern shifted with no internal change, which demonstrates that all trajectories and fringes undergo the same macroscopic displacement together [4]. This has important consequences for the reliability of electron affinity measurements performed by photodetachment microscopy. The property can actually be demonstrated by vector analysis. A non-zero second-order effect is expected however, which produces but a negligible phase-shift in the present experimental situations.

References

- [1] W. Ehrenberg and R.E. Siday, Proc. Phys. Soc. B **62**, 8 (1949)
- [2] Y. Aharonov and D. Bohm, Phys. Rev. **115**, 485 (1959)
- [3] C. Blondel, C. Delsart and F. Dulieu Phys. Rev. Lett. **77**, 3755 (1996)
- [4] W. Chaibi, C. Blondel, C. Delsart and C. Drag, Europhys. Lett. **82**, 20005 (2008)

Laser Induced – Tunneling, Electron Diffraction and Molecular Orbital Imaging

Paul Corkum

*University of Ottawa
National Research Council of Canada
Ottawa, Ontario, Canada*

Multiphoton ionization in the tunneling limit is similar to tunneling in a scanning tunneling microscope. In both cases an electron wave packet tunnels from a bound (or valence) state to the continuum. I will show that multiphoton ionization provides a route to extend tunneling spectroscopy to the interior of transparent solids. Rotating the laser polarization is the analogue of scanning the STM tip - a means of measuring the crystal symmetry of a solid [1].

In gas phase molecules the momentum spectrum of individual electrons can be measured. I will show that, as we rotate the molecule with respect to the laser polarization, the photoelectron spectrum samples a filter projection of the momentum wave function (the molecular analogue to the band structure) of the ionizing orbital [2].

Some electrons created during multiphoton ionization re-collide with their parent ion. I will show that they diffract, revealing the scattering potential of the ion - the molecular structure [3]. The electron can also interfere with the initial orbital from which it separated, creating attosecond XUV pulses or pulse trains. The amplitude and phase of the radiation contains all information needed to re-construct the image of the orbital [4] (just as a sheared optical interferometer can fully characterize an optical pulse).

Strong field methods provide an extensive range of new tools to apply to atomic, molecular and solid-state problems.

[1] M. Gertsvolf, D. Grojo, D. Rayner and P. B. Corkum, unpublished results.

[2] A. Staudte, D. M. Villeneuve, M. Yu Ivanov and P. B. Corkum, unpublished results.

[3] M. Meckel, D. Comtois, D. Zeidler, D. M. Villeneuve, R. Dörner and P. B. Corkum, unpublished results.

[4] J. Itatani et al, Nature **432**, 867 (2004).

Few-electron dynamics in the interaction with strong fields

Armin Scrinzi

Vienna U. of Technology, Photonics Institute

Simple single active electron models have been highly successful in describing the interaction of strong laser fields with atoms and have inspired a large number of experiments. Still, the validity and predictive power of these models for few-electron atoms and in particular for molecules remains to be investigated. There are only few (semi-)analytical models that include electron correlation. Alternatively, the numerical integration of the time-dependent Schrödinger equation (TDSE) is a challenging task because of the exponential growth of the problem size with the particle number, which has largely limited computations to $n = 2$ active electrons.

In recent years, we have developed the MCTDHF (Multi-Configuration Time-Dependent Hartree-Fock) method for the solution of the TDSE for atoms and molecules in IR laser fields. The method scales like $\sim n^4$ with the number of active electrons, as opposed to the exponential scaling encountered in direct discretizations of the TDSE. Different from time-dependent density-functional theory, which has an even more favorable n^2 -scaling, MCTDHF allows for the straight forward computation of two-electron observables and for systematic convergence studies.

As examples, we show calculations of the strong field ionization of linear molecules with up to 6 active electrons, electron-assisted laser ionization of an atom, high harmonic generation on a diatomic 4-electron molecule, and the XUV-IR pump-probe ionization of Helium. While for our parameters, the effects of electron correlation on ionization are rather straight forward and can be incorporated into simple models, we find dramatic qualitative modifications of the high harmonic spectrum by multi-electron effects. For the pump-probe scenario, we find significant crosstalk between the XUV pump and the IR probe pulses.

Molecular reaction dynamics at low energies

Roland Wester

Department of Physics, University of Freiburg, Hermann-Herder-Str. 3, 79104 Freiburg, Germany

Low-energy collisions of small molecules represent model systems for complex quantum reaction dynamics. The dynamics of negative ion reactions are particularly interesting, being characterized by a corrugated potential energy landscape that originates in the competition of long-range attractive and short-range repulsive forces. Scattering on such multi-dimensional potentials only leads to reaction products if the different molecular degrees of freedom are sufficiently coupled. This leads to unexpected dynamical features in the scattering cross sections.

To study ion-molecule reaction dynamics, we have developed two complementary experimental approaches. Using velocity map imaging in combination with crossed beams at low energy, the differential scattering cross section of negative ion reactions is measured at a controlled relative energy [1]. This setup has allowed us to image the nucleophilic substitution reaction, a prototypical reaction in organic synthesis, and we have observed several distinct reaction mechanisms as a function of collision energy [2]. Currently we are preparing experiments to investigate the stereodynamics of reactions that take place in a strong laser field.

Using a 22-pole ion trap, which allows for efficient buffer gas cooling of all degrees of freedom of trapped molecular ions, we study reaction rates of negative ions at cryogenic temperatures down to 8 Kelvin [3,4]. Due to the recent detection of negative ions in interstellar molecular clouds, these measurements have become important for understanding the interstellar abundance of anions. Absolute cross sections for anion photodetachment, a significant destruction mechanism in photon dominated regions, are measured in our 22-pole trap with high systematic accuracy [5]. In addition, we have observed unexpected temperature-dependences for a proton transfer reaction as well as for a ternary cluster stabilization reaction at low temperatures [6,7]. In the future this work will be extended to ultracold ion-atom interactions.

[1] J. Mikosch, U. Fröhling, S. Trippel, D. Schwalm, M. Weidemüller, R. Wester, *Phys. Chem. Chem. Phys.* 8, 2990 (2006)

[2] J. Mikosch S. Trippel, C. Eichhorn, R. Otto, U. Lourderaj, J. X. Zhang, W. L. Hase, M. Weidemüller, R. Wester, *Science* 319, 183 (2008)

[3] J. Mikosch, U. Fröhling, S. Trippel, D. Schwalm, M. Weidemüller, R. Wester, *Phys. Rev. Lett.* 98, 223001 (2007)

[4] J. Mikosch *et al.*, submitted

[5] S. Trippel, J. Mikosch, R. Berhane, R. Otto, M. Weidemüller, R. Wester, *Phys. Rev. Lett.* 97, 193003 (2006)

[6] R. Otto *et al.*, submitted

[7] J. Mikosch *et al.*, submitted

1, 2, 3 Photons for Trapped Ion Spectroscopy

C. Champenois, G. Hagel, M. Houssin, C. Zumsteg, F. Vedel, and M. Knoop

*CNRS/Université de Provence, Centre de St.Jérôme, Case C21,
13397 Marseille Cedex 20, France*

Rf trapped ions are versatile candidates for a large panel of applications ranging from quantum information to the creation of cold molecules. Sample size can range from a single to 10^6 ions, and the internal and external energy states of the atoms can be controlled with high precision. In our experiment, we focus on different protocols in frequency metrology using rf trapped Ca^+ ions.

A single Ca^+ ion, cooled in a miniature radiofrequency trap and confined in the Lamb-Dicke regime, is an almost perfectly isolated atomic system suited for long interrogation times. The electric quadrupole transition between the ground $4S_{1/2}$ and the upper metastable $3D_{5/2}$ state is a first choice for a frequency standard in the optical domain, its natural linewidth below 200 mHz results in a quality factor $\nu/\Delta\nu$ higher than 2×10^{15} [1]. Probing of the clock transition of a single ion is carried out using quantum jump statistics which requires interrogation times of several seconds to avoid power broadening. Care must be taken to eliminate residual effects which may perturb the **one-photon** interrogation. The line width of the probe laser (local oscillator) should reach the hertz level for a duration at least as long as the interrogation time to take full advantage of the quality factor of the clock transition.

Clock performances are limited by the signal to noise ratio which can be obtained on a single ion. We propose a novel interrogation protocol allowing to separate the **two-photon** two-color cooling laser and the fluorescence detection in two distinct wavelength domains, which allows detection without background and thus high cycle times. An additional advantage is the tuning of the limit temperature only by the variation of laser detuning and power [2]. This protocol implying cooling on a dipole forbidden transition has been demonstrated experimentally [3].

The interrogation of an ion cloud by a **three-photon** protocol can be made in a Doppler-free configuration of the laser beams [4]. A coherent superposition of the two metastable states is obtained by a coherent population trapping protocol, providing a high-resolution dark line in the THz domain. The referenced 1.8 THz signal can be propagated over long distances, as the useful information is carried by three optical photons.

[1] C. Champenois et al., Phys. Lett. A **331/5**, 298-311 (2004)

[2] C. Champenois et al., Phys. Rev. A **77**, 033411 (2008)

[3] R. Hendricks et al., Phys. Rev. A **77**, 021401(R) (2008)

[4] C. Champenois et al., Phys. Rev. Lett. **99**, 013001 (2007)

Non-linear Photoionization in the Soft X-ray Regime

Mathias Richter and Andrei A. Sorokin

Physikalisch-Technische Bundesanstalt, Berlin, Germany

The investigation of non-linear effects on photon-matter interaction like multi-photon ionization was restricted, for many years, to optical wavelengths. This has changed with the development of X-ray lasers like the Free-Electron LASer in Hamburg FLASH [1]. First gas-phase studies performed at FLASH demonstrate that non-linear photoionization in the spectral range of the classical photoelectric effect, i.e. at photon energies above atomic ionization thresholds, differs in some respect from the behaviour in the optical regime [2-4]. Here, we present results of ion Time-Of-Flight (TOF) spectroscopy on rare gases at peak irradiance levels above 10^{13} W cm $^{-2}$ up to 10^{16} W cm $^{-2}$ and photon energies around 40 eV and 90 eV. Non-linearities due to space-charge effects, target depletion, and sequential and direct multi-photon ionization were observed. Our result of 21-fold ionization of xenon seems to be even beyond a perturbative description [4]. The work is related to the development of photon diagnostic tools that are based on gas-phase photoionization but might be of significance for any experiment at current and future X-ray laser facilities.

References

- [1] W. Ackermann *et al.*, Nat. Photonics **1**, 336 (2007)
- [2] A.A. Sorokin, S.V. Bobashev, K. Tiedtke, M. Richter, J. Phys. B **39**, L299 (2006)
- [3] A.A. Sorokin, S.V. Bobashev, K. Tiedtke, M. Wellhöfer, M. Richter, Phys. Rev. A **75**, 051402(R) (2007)
- [4] A.A. Sorokin, S.V. Bobashev, T. Feigl, K. Tiedtke, H. Wabnitz, M. Richter, Phys. Rev. Lett. **99**, 213002 (2007)

Multi-photon ionization and excitation of the rare gases by Free Electron Laser radiation

Uwe Becker

Fritz-Haber-Institut der Max-Planck-Gesellschaft, Berlin, Germany

Multi-photon processes in the vacuum ultraviolet and soft X-ray regions became experimentally accessible only very recently when the Free Electron Laser FLASH at DESY in Hamburg was put into operation. The high brilliance of its light pulses makes it possible to study non-linear processes in the photoionization of atoms, molecules and clusters. First priority in the study of these processes has the spectroscopy of atoms, in particular rare gas atoms. The study of non-linear processes in these atoms was due to their high ionization thresholds with normal laser radiation not feasible; only the SASE-FEL with its ultra-bright VUV radiation made this now possible.

Studying the intensity dependence proved the well-known relationship between the number of involved photons and the exponential behavior of photon intensity versus ionization probability. More interesting was the relationship between simultaneous and sequential double photo-ionization. Our preliminary data analysis points to a predominance of the latter by two photons, if the necessary threshold energy for this process is exceeded. The last in a way most interesting aspect in this regard is the angular distribution of the corresponding photoelectrons.

Multi-photon processes are characterized by photoelectron angular distributions, which reflect the number of photons involved in the ionization process. This general rule is clearly exhibited in our angular distribution results. However, the different photolines show very distinct differences in this respect, which needs further theoretical explanation.

Ultracold deeply-bound Rb₂ molecules

F. Lang¹, K. Winkler¹, C. Strauss¹, R. Grimm^{1,2} & J. Hecker Denschlag¹

¹ *Institut für Experimentalphysik und Quantenzentrum, Universität Innsbruck, A-6020 Innsbruck, Austria*

² *Institut für Quantenoptik and Quantuminformation der sterreichischen Akademie der Wissenschaften, A-6020 Innsbruck, Austria*

The tremendous success of the field of ultracold atomic gases has triggered the quest for ultracold molecular gases. The production of such molecular gases was hindered by the absence of standard laser cooling techniques for molecules because of their richer internal structure. Other pathways to cold and dense samples of molecules such as sympathetic cooling or association of ultracold atoms are required. Association via Feshbach resonances has already led to quantum degenerate or nearly quantum degenerate ultracold molecular gases, but only in very weakly bound states with high vibrational quantum numbers. Such molecules are in general unstable under collisions with each other.

We overcome this limitation by optically transferring weakly bound Rb₂ Feshbach molecules to the intrinsically more stable ro-vibrational ground state of the triplet potential. The transfer is carried out in a single step using stimulated Raman adiabatic passage (STIRAP) with an efficiency of about 60%, which is only technically limited. Because we begin with a nearly quantum degenerate gas of Feshbach molecules, we thus enter for the first time the regime of an ultracold and dense ensemble of tightly bound molecules. The molecules which are held in a 3D optically lattice exhibit a lifetime longer than 100 ms.

These results open the door for a new generation of experiments with tightly bound ultracold molecules allowing for investigations of ultracold collisions and chemistry, production of a molecular BEC, as well as molecular quantum optics.

Manipulating cold molecular gases with intense optical fields

P. F. Barker

Department of Physics and Astronomy, University College London

Over last few years we have been exploring the application of intense, far off-resonant, optical fields for manipulating the centre-of-mass motion of molecular gases using large optical potentials in the 100 K range. This unique means of control, which can be applied to essentially any gas, has been used to decelerate molecular beams from supersonic speeds to rest to creating cold stationary molecular ensembles. Using these tailored light fields we have also focused molecular beams to micron dimensions and have even briefly trapped room temperature gases. In this update I will review these experiments and describe more recent work, which is studying the role of laser-induced molecular alignment on the manipulation of molecules, and also the trapping and sympathetic cooling of molecules with ultracold atoms.

Resonant laser spectroscopy in the soft X-ray region

José R. Crespo López-Urrutia, S. W. Epp, and J. Ullrich

*Max Planck Institute for Nuclear Physics,
Saupfercheckweg 1, 69117 Heidelberg, Germany*

In vast regions of the universe highly charged ions (HCI) are the predominant form of visible matter. They also appear in nuclear fusion devices as well as in high-temperature laser produced plasmas. Yet, their electronic structure still remains a challenge for both theory and experiment. As a result of the limitations of traditional spectroscopic methods in the soft and hard x-ray regions, accuracy currently constrains our knowledge of quantum electrodynamics (QED) in strong fields. The application of laser spectroscopy to such studies, which in the visible and ultraviolet range has already led to the most comprehensive verification of a physical theory, QED, in weak fields, being even capable of testing the time drift of fundamental constants, was until now not possible due to the lack of appropriate light sources. Extending such precision tests to strong fields beyond perturbation theory has general implications for the formalism of other quantum field theories, nuclear physics and parity-non-conservation studies. In our experiment [1], HCIs stored in an electron beam ion trap (EBIT) were excited by tunable ultra-intense soft x-rays generated at the Free electron LASer in Hamburg (FLASH), the first free electron laser in the world operating in that spectral range. With this setup, resonant laser excitation of bound-bound electronic transitions, namely the $1s^2 2s^2 S_{1/2}$ to $1s^2 2p^2 P_{1/2,3/2}$ lines of the Li-like Fe^{23+} ion at 48.6 and 65.5 eV and of the isoelectronic Cu^{26+} , became possible in an energy range hitherto unattainable with powerful lasers. This and more recent experiments, yielding a relative statistical error of only 2 ppm corresponding to 0.1% of the QED contributions, demonstrate immediate potential to push the current limits of precision by up to three orders of magnitude. They allow for tests of the QED theory in a regime in which standard perturbation methods fail, in the environment of the highest stationary electromagnetic fields found in nature, in the vicinity of the nucleus. Future experiments at upcoming x-ray free electron lasers (X-FEL) like the Stanford Linear Coherent Light Source (LCLS) or the European X-FEL will pave the way into the hard x-ray region, at energies appropriate for even deeper probing of strong field QED effects. Investigations of the photoionization of HCI and precision determinations of the lifetimes of excited states are possible with this EBIT method. It will also allow establishing atomic frequency standards at these high photon energies by coupling laser emission by e.g. high-harmonic generation directly to bound-bound transitions of – ideally – hydrogen-like ions, overcoming the present uncertainties found in x-ray standards derived from solid-state samples.

- [1] S.W. Epp, J. R. Crespo López-Urrutia, G. Brenner, V. Mäckel, P. H. Mokler, R. Treusch, M. Kuhlmann, M. V. Yurkov, J. Feldhaus, J. R. Schneider, M. Wellhöfer, M. Martins, W. Wurth, and J. Ullrich, *Phys. Rev. Lett* **98**, 183001 (2007)

Resonances in Rare Gas Atoms: Many-Electron Theory and Experiment

V. L. Sukhorukov

*Rostov State University of Transport Communications,
344038 Rostov-on-Don, Russia
E-mail: vls@rgups.ru*

Excitation processes in the rare gas atoms Ne, Ar, Kr and Xe with energies between the two lowest ionization thresholds $mp_{3/2}^5$ and $mp_{1/2}^5$ ($m = 2-5$) are dominated by resonances stemming from $mp_{1/2}^5 n\ell'[K]_J$ autoionizing Rydberg states (ARS). These states provide very suitable objects for the investigation of many-electron effects, both outside the atomic core, where the $n\ell'$ -electron is localized, and inside the core, which is responsible for the lifetime of the ARS. Starting with the pioneering work of Beutler [1] these resonances have been intensively studied experimentally (see, e.g. [2-5]). The two main properties of the resonances which are derived from experimental spectra are the quantum defect μ_ℓ , which determines the resonance energy, and the autoionization width Γ_n , i.e. the resonance lifetime $\tau_n = \hbar/\Gamma_n$.

In this talk we focus on the influence of many-electron effects on the processes responsible for the excitation and decay of the ARS. The lineshapes used for the evaluation of μ_ℓ and Γ_n are strongly dependent on the level from which the ARS are excited. In order to gain detailed insight into the dynamics for excitation and decay of the ARS, we applied the configuration interaction Pauli-Fock approach including the effects of core polarization (CIPFCP) [6,7]. Using the CIPFCP method, we calculated resonance parameters (μ_ℓ , Γ_n) [4,8,9] and the absolute photoionization cross sections (including the lineshapes) [5,9-11] for a broad range ($\ell' = 0 - 5$) of the autoionizing resonances in the rare gas atoms Ne-Xe. By comparing measured ARS lineshapes with the computed profiles and adopting step-by-step inclusion of many electron effects in the calculations, the important types of electron correlations are identified.

Support of this work by the Deutsche Forschungsgemeinschaft is gratefully acknowledged.

References

- [1] H. Beutler, *Z. Phys.* **93**, 177 (1935).
- [2] J. Berkowitz, *Adv. Chem. Phys.* **72**, 1 (1988).
- [3] H. Hotop, D. Klar, and S. Schohl, *Proc. 6th Int. Symp. on Resonance Ionization Spectroscopy (RIS-92)* volume **128** of *Inst. Phys. Conf.*, 45 (1992).
- [4] I. D. Petrov, V. L. Sukhorukov, and H. Hotop, *J. Phys. B* **35**, 323 (2002).
- [5] I. D. Petrov *et al* *J. Phys. B* **39**, 3159 (2006).
- [6] I. D. Petrov, V. L. Sukhorukov, and H. Hotop, *J. Phys. B* **32**, 973 (1999).
- [7] I. D. Petrov *et al* *Eur. Phys. J. D* **10**, 53 (2000).
- [8] I. D. Petrov, V. L. Sukhorukov, and H. Hotop, *J. Phys. B* **36**, 119 (2003).
- [9] T. Peters *et al* *J. Phys. B* **38**, S51 (2005).
- [10] I. D. Petrov *et al* *Eur. Phys. J. D* **40**, 181 (2006).
- [11] I. D. Petrov, V. L. Sukhorukov, and H. Hotop, *J. Phys. B* **41**, 065205 (11pp) (2008).

Attosecond spectroscopy in atoms and solids

Reinhard Kienberger

Max-Planck-Institut für Quantenoptik, Hans-Kopfermann-Straße 1, D-85748 Garching

The generation of ever shorter pulses is a key to exploring the dynamic behavior of matter on ever shorter time scales. Over the past decade novel ultrafast optical technologies have pushed the duration of laser pulses close to its natural limit, to the wave cycle, which lasts somewhat longer than one femtosecond ($1 \text{ fs} = 10^{-15} \text{ s}$) in the visible spectral range. Time-resolved measurements with these pulses are able to trace atomic motion in molecules and related chemical processes. However, electronic dynamics inside atoms often evolve on an attosecond ($1 \text{ as} = 10^{-18} \text{ s}$) timescale and require sub-femtosecond pulses for capturing them. Atoms exposed to a few oscillation cycles of intense visible or near-infrared light are able to emit a single electron and XUV photon wavepacket of sub-femtosecond duration [1, 2]. Precise control of these sub-femtosecond wavepackets have been achieved by full control of the electromagnetic field in few-cycle light pulses [3]. These XUV pulses together with the few-cycle (few-femtosecond) laser pulses used for their generation have opened the way to the development of a technique for attosecond sampling of electrons ejected from atoms or molecules [4]. This is accomplished by probing electron emission with the oscillating electric field of the few-cycle laser pulse following excitation of the atom by the synchronized sub-femtosecond XUV pulse. Sampling the emission of photo electrons in this manner allows time-resolved measurement of the XUV pulse duration as well as of the laser field oscillations [5]. After the full characterization of these tools, first experiments have been carried out to measure sub-femtosecond behavior of matter. Recently, the dynamics of the photoionization process on solids has been studied [6]. Not only that attosecond metrology now enables clocking on surface dynamics, but also the individual behaviour of electrons of different type (core electrons vs. conduction band electrons) can be resolved. Here, we measured a time delay of about 100 as on the emission of the aforementioned two types of electrons. The information gained in these experiments may have influence on the development of many modern technologies including semiconductor and molecular electronics, optoelectronics, information processing, photovoltaics, electronically stimulated chemistry on surfaces and interfaces, optical nano-structuring, and interference effects in spectroscopy.

References

- [1] M. Hentschel et al., Nature 501 (2001).
- [2] R. Kienberger et al. Science 297, 1144 (2002).
- [3] A. Baltuska et al., Nature 421, 611 (2003).
- [4] R. Kienberger et al., Nature 427, 817 (2004).
- [5] E. Goulielmakis et al. Science 305, 1267 (2004).
- [6] A. Cavalieri et al., Nature 449, 1029 (2007).

Above, Around, and Below Threshold Ionization using Attosecond Pulses

Johan Mauritsson*

Department of Physics, Lund University, P.O. Box 118, SE-221 00 Lund, Sweden

Attosecond pulses offer a new route to produce temporally localized electron wave packets that can easily be tailored by altering the properties of the attosecond pulses. In this talk we will present three different experiments where attosecond pulses are used to inject electron wave packets into a continuum which is dressed by an infrared laser field. By tuning the central frequency of the attosecond pulses and/or changing the target gas, the initial energy of the wave packets is set to be either above, around, or below the ionization potential.

To capture the motion of electron wave packets created above or around the ionization potential we have developed a quantum stroboscope to record the electron momentum distribution from a single ionization event. The quantum stroboscope is based on a sequence of identical attosecond pulses that are used to release electrons into a strong laser field exactly once per laser cycle. With this periodicity, the pulses create identical electron wave packets that add up coherently, with the result that the properties of an individual wave packet can be studied stroboscopically. We use this technique to study the coherent electron scattering of electrons that are driven back to the ion by the laser field [1].

For electron wave packets created below the ionization potential we find that the ionization is greatly enhanced by the presence of the infrared laser field and that this enhancement strongly depends on the timing between the attosecond pulses and the laser field. We show that this effect can be attributed to interference between consecutive wave packets, which indicates that the wave packets stay in the vicinity of the ion over an extended time period [2].

Using instead isolated attosecond pulses generated from an ultrashort, carrier-envelope-phase stabilized infrared laser with a time-dependent polarization [3] we show that it is possible to also probe ultrafast bound electron dynamics. These attosecond pulses are broad enough to excite coherently all the p -states in Helium and a fraction of the continuum. The wave packets created in Helium, partly trapped in the atomic potential, are probed by a 7 fs 750 nm infrared laser field, with an intensity of 3×10^{12} W/cm². Using this method we can extract the amplitudes and the phase evolutions of the bound, excited states.

* *Part of the work was done in collaboration with LSU, AMOLF, MPQ and CUSBO.*

References

- [1] J. Mauritsson et al., Phys. Rev. Lett. 100, 073003 (2008).
- [2] P. Johnsson et al., Phys. Rev. Lett. 99, 233011 (2007).
- [3] G. Sansone et al., Science 314, 443 (2006).

Few-body physics with ultracold Cs atoms and molecules

F. Ferlaino, S. Knoop, M. Mark, M. Berninger, H. Schöbel, H. C. Nägerl, and R. Grimm

*Institut für Experimentalphysik, Innsbruck, Austria Institut für Quantenoptik und
Quanteninformation, Innsbruck, Austria*

Ultracold gases are versatile systems to study few-body physics because of full control over the external and internal degrees of freedom. Scattering properties can be controlled because of the magnetic tunability of the two-body scattering length in the proximity of a Feshbach resonance and weakly bound dimers can be produced. Here we experimentally study three- and four-body physics by investigating ultracold (30-250 nK) atom-dimer and dimer-dimer collisions with Cs Feshbach molecules in various molecular states and Cs atoms in different hyperfine states. Resonant enhancement of the atom-dimer relaxation rate is observed in a system of three identical bosons and interpreted as being induced by a trimer state, possibly an Efimov state. A strong magnetic field dependence of the relaxation rate is also observed in a atom-dimer mixture made of non-identical bosons. Dimer-dimer inelastic collisions have been studied in a pure, trapped sample of Feshbach dimers in the quantum halo regime. We identify a pronounced loss minimum with varying scattering length along with a further suppression of loss with decreasing temperature. This observations provide insight into the physics of a few-body quantum system that consists of four identical bosons at large values of the two-body scattering length.

Weakly bound molecules : Analysis by the Lu-Fano method coupled to the LeRoy-Bernstein model.

Haikel Jelassi, Bruno Viaris de Lesegno, Laurence Pruvost

Laboratoire Aimé Cotton, CNRS II, bat 505, campus d'Orsay

91405 Orsay, France

E-mail: laurence.pruvost@lac.u-psud.fr

We have performed experiments on photo-association spectroscopy of cold ^{87}Rb atoms, below the $(5s_{1/2}+5p_{1/2})$ dissociation limit. By applying the trap loss spectroscopy method [1] we have measured the binding energies of the weakly bound molecules, associated to the 0_g^- , 0_u^+ and 1_g symmetries.

Such weakly bound molecules are described by the dipole-dipole atom interaction which varies, according to the molecular symmetry, either as $1/R^3$ or as $1/R^6$, where R is the inter-nuclear distance. The eigen energies of the weakly bound molecules are then very close to those obtained by the well-known Le Roy-Bernstein (LRB) model [2]. The discrepancies to the LRB law are due to the short distance behavior of the molecular potentials or to couplings between molecular potentials resulting from interactions, for example spin-orbit or spin-spin interactions.

To analyze the data, we have adapted the Lu-Fano (LF) method - well-known for Rydberg atoms - to the weakly bound molecules. Using the LRB law, a molecular quantum defect is defined and deduced from the data. The LF graph - quantum defect versus the binding energy - allows us to characterize the molecular potential and the couplings.

For the 0_g^- molecular levels, we observe a linear LF graph, which is the signature of the short range behavior of the molecular potential. A model for the barrier allows us to connect the slope to the barrier location [3]. The method has also been applied to ^{85}Rb and ^{133}Cs [4].

For 0_u^+ molecular levels, the LF graph exhibits sharp variations which indicate a coupling with a neighboring molecular series. The coupling is due to the spin-orbit interaction in the molecule. A two series model allows us to evaluate the coupling, to identify two perturbing levels of the $(5s_{1/2}+5p_{3/2})$ 0_u^+ series and to predict the energy position and the width of its first pre-dissociated level. An experimental signal agrees with the prediction [4]. The method has also been successfully applied to ^{133}Cs .

References

- [1] P. D. Lett et al., Phys. Rev. Lett. **71**, 2200 (1993)
- [2] R. J. Le Roy, R. B. Bernstein, J. Chem. Phys. **52**, 3869 (1970)
- [3] H. Jelassi, B. Viaris De Lesegno, L. Pruvost, Phys. Rev. A. **73**, 32501 (2006)
- [4] H. Jelassi, B. Viaris De Lesegno, and L. Pruvost, AIP Conference Proceedings, ISC 2007, **935**, 203, (2007)
- [5] H. Jelassi, B. Viaris De Lesegno, L. Pruvost, Phys. Rev. A. **74**, 12510 (2006)

Calculations of static polarizabilities of alkali dimers and alkali hydrides. Prospects for alignment of ultracold molecules.

Mireille Aymar,⁺ Johannes Deiglmayr^{*}, and Olivier Dulieu ⁺

⁺*Laboratoire Aimé Cotton, CNRS and Univ Paris Sud, Bât. 505, 91405 Orsay Cedex, France*

^{*}*Physikalisches Institut, Universität Freiburg, Hermann-Herder-Strasse 3, 79104 Freiburg, Germany.*

The rapid development of experimental techniques to produce ultracold alkali molecules opens the ways to manipulate them and to control their dynamics using external electric fields. A prerequisite quantity for such studies is the knowledge of their static dipole polarizabilities.

We computed the variations with internuclear distance and with vibrational index of the static dipole polarizability components of all homonuclear alkali dimers including Fr₂, and of all heteronuclear alkali dimers involving Li to Cs, in their electronic ground state and in their lowest triplet state and of alkali hydrides LiH to CsH in their ground state. We use the same quantum chemistry approach than in our work on dipole moments [1] based on pseudopotentials for atomic core representation, Gaussian basis sets, and effective potentials for core polarization. Polarizabilities are extracted from electronic energies using the finite-field method [2].

For the heaviest species Rb₂, Cs₂ and Fr₂ and for all heteronuclear alkali dimers and for CsH, such results are presented for the first time. The accuracy of our results on atomic and molecular static dipole polarizabilities is discussed by comparing our values with the few available experimental data and elaborate calculations. We found that for all alkali pairs, the parallel and perpendicular components of the ground state polarizabilities at the equilibrium distance R_e scale as $(R_e)^3$. Prospects for possible alignment and orientation effects with these molecules in forthcoming experiments are discussed.

[1] M. Aymar and O. Dulieu, *J. Chem. Phys.* **122**, 204302(2005).

[2] J. Deiglmayr, M. Aymar, M. Weidemüller, R. Wester, and O. Dulieu, submitted to *J. Chem. Phys.*

Electrostatically extracted cold molecules from a cryogenic buffer gas

Laurens D. van Buuren, Christian Sommer, Michael Motsch, Markus Schenk,
Pepijn W.H. Pinkse, and Gerhard Rempe

*Max-Planck-Institut für Quantenoptik,
Hans-Kopfermann-Str. 1, 85748 Garching, Germany*

Dense samples of cold polar molecules offer new perspectives in physics [1]. Studies of cold collisions and chemical reactions as well as high precision measurements will benefit from these samples. For this kind of studies there is still need for new sources which deliver a high density and a high flux of cold molecules.

We present a source which delivers a continuous, high-density beam of slow and internally cold polar molecules. In the source, warm molecules are injected into a cryogenic cell, in which their external and internal degrees of freedom are cooled by collisions with a helium buffer gas [2]. Cold molecules are extracted out of the cryogenic environment by means of an electric quadrupole guide. Information on the state purity of the extracted beam is obtained by laser depletion of H_2CO within the guide [3]. In future, the beam can be loaded into a large volume electrostatic trap (as previously shown [4]) to perform for example collision experiments.

References

- [1] J. Doyle, B. Friedrich, R. V. Krems and F. Masnou-Seeuws, Eur. Phys. J. D **31**, 149 (2004).
- [2] J. Weinstein, R. DeCarvalho, T. Guillet, B. Friedrich and J. Doyle, Nature (London) **395**, 148 (1998).
- [3] M. Motsch, M. Schenk, L.D. van Buuren, M. Zeppenfeld, P.W.H. Pinkse, and G. Rempe, Phys. Rev. A **76**, 061402R (2007).
- [4] T. Rieger, T. Junglen, S.A. Rangwala, P.W.H. Pinkse, and G. Rempe, Phys. Rev. Lett. **95**, 173002 (2005).

***In-situ* non-invasive quality control of packaged meat using a micro-system external cavity diode laser at 671 nm for Raman spectroscopy**

Heinz-Detlef Kronfeldt¹, Heinar Schmidt¹, Bernd Sumpff², Martin Maiwald²,
Götz Erbert², Günther Tränkle²

¹*Technische Universität Berlin, Institut für Optik und Atomare Physik
Sekt. EW 0-1, Hardenbergstr. 36, 10623 Berlin, Germany*

²*Ferdinand-Braun-Institut für Höchstfrequenztechnik, Gustav-Kirchhoff-Straße 4,
12489 Berlin, Germany*

Diode lasers are highly attractive for spectroscopic field applications where small sizes and low power consumption are prerequisites. They are available as light sources from the blue up to the mid infrared spectral range and are commonly used in sensor systems. However, in the ultraviolet and visible spectral ranges, which are of special interest to fluorescence and Raman spectroscopy, compact diode laser based devices with narrow spectral width are not commercially available.

In this presentation, we will show how micro-system technology can overcome these problems with a small size high power external cavity diode laser (ECDL) emitting at 671 nm with a small emission width suitable for Raman spectroscopy. All elements used in these devices are mounted on micro optical benches with a dimension of only (13 x 4 x 1) mm³. For our experiments the subassemblies were mounted on conduction cooled packages (CCP) with footprints of only (25 x 25) mm².

The ECDL system includes a broad area device as gain material, micro-optics for beam shaping and a reflecting Bragg grating for wavelength stabilization. We present results for devices with an output power of 200 mW and a stable emission at 671 nm. The spectral width of $\Delta\lambda = 80$ pm ($\Delta\tilde{\nu} \approx 2$ cm⁻¹), which includes 95% of intensity fits within the required spectral width of $\Delta\lambda = 450$ pm ($\Delta\tilde{\nu} \approx 10$ cm⁻¹) for Raman bands of most liquid and solid samples.

This micro-system laser device is implemented into a specifically designed Raman sensor for *in-situ* measurements of meat. Raman spectroscopy offers the advantages to measure non invasive and through the packaging. The sensor exploits the fingerprinting characteristics of Raman spectra for substance identification and to follow the physicochemical and biochemical changes upon aging of meat products.

The Raman probe is characterized and first results of time-dependent Raman measurements of *porcine musculus longissimus dorsi* aged for up to 4 weeks at 5 °C will be presented. The usefulness of Raman spectroscopy will be discussed with a view of integrating the sensor in a handheld laser scanner for food control.

This work was supported by the BMBF funded project „FreshScan“ 16SV2332.

$^3\text{H}/^3\text{He}$ mass ratio experiment MPIK/UW-PTMS in the context of ν -mass measurements

David Pinegar¹, Christoph Diehl¹, Robert Van Dyck, Jr.², and Klaus Blaum¹

¹*Max-Planck-Institut für Kernphysik, Saupfercheckweg 1, D-69117 Heidelberg, Germany*

²*Department of Physics, University of Washington, Seattle, WA 98195-1560, USA*

e-mail: pinegar@mpi-hd.mpg.de

Beta-spectrometer experiments to constrain neutrino masses (such as KATRIN [1] and the completed Mainz experiment [2]) have a long history, as do independent helium–3 and tritium mass difference measurements like the most precise result from SMILETRAP [3]. The main goal of MPIK/UW-PTMS, the Max-Planck-Institute for Nuclear Physics / University of Washington Penning Trap Mass Spectrometer collaboration, is to use simultaneous axial-frequency-lock in two externally-loaded hyperbolic Penning traps to perform single-ion cyclotron frequency measurements for a determination of the ^3H to ^3He mass ratio with 10^{-11} uncertainty. Ideally their mass difference (which is easily calculated from the mass ratio) will be found with an uncertainty much smaller than the tritium β -spectrum endpoint can be determined by the KATRIN experiment. For KATRIN, the uncertainty on the endpoint depends on absolute calibration of the spectrometer retarding potential as well as several other factors. Because mechanisms causing systematic uncertainty in beta-spectrometers generally effect both the fitted endpoint E_0 and the fitted electron neutrino mass m_ν , agreement between the spectrum endpoint and independent mass difference measurements should reinforce confidence in the understanding of KATRIN systematic uncertainties. Hopefully, in the future agreement at the ~ 50 meV level will be found, just as good agreement was found at the ~ 2 eV level between earlier ^3H to ^3He mass difference measurements and beta-spectrometers of lower resolution than KATRIN.

References

- [1] J. Angrik, et al., FZKA Scientific Report 7090, MS-KP-0501, (2004).
- [2] Ch. Kraus, et al., Eur. Phys. J. C, **40**, 447–468, (2005).
- [3] Sz. Nagy, et al., Europhys. Lett., **74**, 404–410, (2006).

Optical microtraps for cold atoms based on near-field diffraction

S. Nic Chormaic^{1,2}, T. N. Bandi^{2,3} and V. Minogin^{2,3,4}

¹*Physics Department, University College Cork, Cork, Ireland*

²*Photonics Centre, Tyndall National Institute, Prospect Row, Cork, Ireland*

³*Dept. of Applied Physics and Instrumentation, Cork Institute of Technology, Bishopstown, Cork, Ireland*

⁴*Institute of Spectroscopy, Russ. Ac. of Sciences, 142190 Troitsk, Moscow Region, Russia*

E-mail: S.NicChormaic@ucc.ie

In recent years there has been significant interest in studies on the development of neutral atom traps and the applications thereof [1-4]. One novel approach to the development of miniature atom traps involves the optical near-fields formed by laser diffraction on an array of circular apertures in a thin screen [5]. This approach can be adapted in order to fabricate an array of atom microtraps and, accordingly, produce a large number of trapped atomic microensembles from a single initial atomic cloud or beam.

In this paper, we propose and analyze such near-field Fresnel-type atom microtraps with a characteristic aperture size approximately equal to the optical wavelength incident on the thin screen. Our analysis of the atom microtraps shows that, for a moderate laser intensity of about 10 W/cm^2 , the traps can store atoms with a kinetic energy equivalent to $\sim 100\mu\text{K}$, and with estimated lifetimes of ~ 1 second.

Our analysis for ^{85}Rb and ^{133}Cs atoms shows that the potential well depth of the microtraps is mainly determined by the intensity of the incident laser field and the detuning. By varying these two parameters one can achieve robust control over the trap parameters. The incident laser intensity of 10 W/cm^2 corresponds to about $0.5 \mu\text{W}$ of laser power incident on each individual aperture. With such trap parameters one can perform atom optics experiments by blending microfabrication technology with cold atoms for site selective addressing of microtraps.

References

- [1] V. I. Balykin, V. G. Minogin, and V. S. Letokhov, Rep. Prog. Phys. **63**, 1429 (2000)
- [2] W. Hänsel, P. Hommelhoff, T. W. Hänsch, and J. Reichel, Nature **413**, 498 (2001)
- [3] S. K. Sekatskii, B. Riedo, and G. Dietler, Opt. Comm. **195**, 197 (2001)
- [4] K. D. Nelson, X. Li, and D. S. Weiss, Nat. Phys. **3**, 556 (2007)
- [5] V. I. Balykin and V. G. Minogin, Phys. Rev. A **77**, 013601 (2008).

Optical Spectroscopy of Rubidium Rydberg Atoms with a 297nm Frequency Doubled Dye Laser

Th. Becker, Th. Germann, P. Thoumany, G. Stania, L. Urbonas and T. Hänsch

*Max Planck Institute for Quantum Optics
Hans Kopfermann Str. 1
85748 Garching, Germany*

Rydberg atoms have played an important role in atomic physics and optical spectroscopy since many years. Due to their long lifetime and the big dipole matrix element between neighbouring Rydberg levels they are an essential tool in microwave cavity-qed experiments. Ultracold Rydberg gases are a promising candidate for realizing controlled quantum gates in atomic ensembles. In most experiments Rydberg atoms are detected destructively, where the optically excited atoms are first ionized followed by an electronic detection of the ionization products. A Doppler-free purely optical detection was reported in [1] in a room temperature cell and in [2] in an atomic beam apparatus using the technique of electromagnetically induced transparency. In all these experiments the Rydberg atoms are excited with two lasers in a two-step ladder configuration.

Here we show that Doppler-free purely optical spectroscopy is also possible with a one step excitation scheme involving a UV laser at 297 nm. We excite the ^{85}Rb isotope from the $5S_{1/2}$ ground state to the $63P_{3/2}$ state with a frequency doubled dye laser in a room temperature gas cell without buffer gas. Rydberg transitions are detected by monitoring the absorption of 780 nm laser light which is superimposed on the UV light and resonant with one hyperfine component of the Rubidium D2 line. With these two lasers we realize a V-scheme and utilize the quantum amplification effect due to the different natural lifetimes of the upper levels of the two transitions: an excitation into the 63P level hinders many absorption-emission cycles of the D2 transition and leads to a reduced absorption on that line. We discuss the shape of the observed spectra in the context of electron shelving and EIT experiments.

By applying a frequency modulation to the UV laser, we can obtain dispersive signals which can be used to stabilize the laser to a specific Rydberg transition. By shifting the frequency of the 780 nm laser to crossover resonances in the saturated absorption spectrum of the D2 line, the stabilization point of the UV laser can be detuned from the resonance by discrete values. Using this idea, we demonstrate the stability of the frequency locking scheme with an atomic beam apparatus: if the detuned laser hits the atomic beam under a small angle, only atoms of a certain velocity class will be transferred to their upper level. We excite the atoms with pulses of 5 μsec duration and measure their arrival times 10 cm behind the excitation region with field selective ionization. By analyzing the time of flight spreading we can show that the long-term linewidth of the laser is below 2 MHz in the UV, which corresponds to the specified short time stability of the dye laser and the long term frequency drift can be effectively compensated.

references:

- [1] A. K. Mohapatra, T. R. Jackson, C. S. Adams, Phys. Rev. Lett. **98**, 113003 (2007).
- [2] S. Mauger, J. Millen and M. P. A. Jones, J. Phys. B: At. Mol. Opt. Phys. **40**, F319 (2007).

Helium $n^{1,3}\text{S}$ excited states obtained with an angular correlated configuration interaction method

K. V. Rodriguez^{1,4}, V. Y. Gonzalez^{1,4}, L. U. Ancarani², D. M. Mitnik^{3,4}
and G. Gasaneo^{1,4}

¹*Departamento de Física - Universidad Nacional del Sur, 8000 Bahía Blanca, Argentina*

²*Laboratoire de Physique Moléculaire et des Collisions,
Université Paul Verlaine - Metz, France*

³*Instituto de Astronomía y Física del Espacio, y Departamento de Física, Facultad de
Ciencias Exactas y Naturales, Universidad de Buenos Aires. C.C. 67, Suc. 28,
(C1428EGA) Buenos Aires, Argentina*

⁴*Consejo Nacional de Investigaciones Científicas y Técnicas, Argentina*

We construct approximate helium wavefunctions for ground and excited $n^{1,3}\text{S}$ states through the angular correlated configuration interaction (ACCI) method proposed in [1]. The trial wavefunctions are given by

$$\Psi_{C3-N} = \sum_{n_1, n_2, n_3} \varphi_{n_1}(r_1) \varphi_{n_2}(r_2) \chi_{C3}(n_{12}, r_{12}) \sum_{ijk \neq 1} c_{ijk}^{n_1 n_2 n_{12}} r_1^i r_2^j r_{12}^k$$

where r_1, r_2, r_{12} are the interparticle coordinates. The products $\varphi_{n_1}(r_1) \varphi_{n_2}(r_2) \chi_{C3}(n_{12}, r_{12})$ (with (n_1, n_2, n_{12}) integers) were proposed by Gasaneo and Ancarani in [2] as parameter-free basis functions: φ_{n_i} are $l = 0$ hydrogenic functions, and $\chi_{C3} = {}_1F_1(-n_{12}, 2, -r_{12}/n_{12})$ is the angular correlation factor [2,3] which results from the analytic continuation of the widely used double continuum three-body Coulomb (C3) wave function [4]. Each of these product satisfies exactly all two-body Kato cusp conditions. Following the methodology proposed in [1], we multiply each of them by a series which does not affect this property. The trial wavefunction involves then N linear variational parameters $c_{ijk}^{n_1 n_2 n_{12}}$ which are obtained by solving a generalized eigenvalue problem. The $n^{1,3}\text{S}$ states obtained in this way form an orthogonal set of wavefunctions.

Quite accurate energies values for both the ground and excited states can be obtained with only a relatively low number of terms, as illustrated by the following table (the construction includes the $1s1s, 1s2s$ and $1s3s$ multiple configurations and n_{12} up to 2).

N	n_1	n_2	n_{12}	$-E1^1\text{S}$	$-E2^3\text{S}$	$-E2^1\text{S}$	$-E3^3\text{S}$
24	1,2	1,2	1,2	2.90329	2.1752	2.14587	2.05589
38	1,2,3	1,2,3	1,2	2.90335	2.17521	2.14594	2.06866
52	1,2,3,4	1,2,3,4	1,2	2.90339	2.17522	2.14594	2.06869
Exact ^[5]				2.90372	2.17523	2.14597	2.06869

References

- [1] K.V. Rodriguez, G. Gasaneo and D.M. Mitnik, J. Phys. B 40 (19), 3923 (2207).
- [2] G. Gasaneo and L.U. Ancarani, Phys. Rev. A **77**, 012705 (2008)
- [3] L.U. Ancarani and G. Gasaneo, Phys. Rev. A **75**, 032706 (2007)
- [4] C.R. Garibotti and J.E. Miraglia, Phys. Rev. A **21**, 572 (1980)
- [5] G.W.F. Drake (ed) 2005 Springer Handbook of Atomic, Molecular, and Optical Physics

Atomic structure calculations of Cm^{+4} and Am^{+3} ions

G. Gaigalas^{1,2}, E. Gaidamauskas¹ and Z. Rudzikas¹

¹*Vilnius University Research Institute of Theoretical Physics and Astronomy,
A. Goštauto 12, LT-01108 Vilnius, Lithuania*

²*Vilnius Pedagogical University, Studentų 39, LT-08106, Vilnius, Lithuania
E:mail:gaigalas@itpa.lt*

Modern technologies require knowledge of atomic structure of the most complex chemical elements, actinides included. The accuracy of the results obtained depends on the degree of accounting for correlation and relativistic effects. Many phenomena or properties, e.g. effective magnetic moments of the Cm^{+4} ions measured in several compounds [1], still remain unexplained. In this report we present *ab initio* calculations of the lowest energy terms and levels of Cm^{+4} and Am^{+3} ions in nonrelativistic approach.

For the calculation of energy spectra of Cm^{+4} and Am^{+3} ions we used multiconfigurational Hartree-Fock and configuration interaction methods accounting for relativistic effects in Breit-Pauli approach. Configuration state functions of the multiconfiguration expansion additionally include single and double substitutions from the valence shell (VV correlations). All calculations were performed with the *MCHF atomic-structure package* [2]. The dependence of fine structure of the lowest term 7F of Cm^{+4} in Breit-Pauli approach on correlation effects taken into consideration is presented in Table. The results obtained demonstrate that core-valence and core-core correlations are essential for the Cm^{+4} and Am^{+3} term energy, whereas their role in the case of fine structure is much less compared to that of valence-valence correlations. Therefore the latter must be accounted for while studying the fine structure of the ions. The calculated energy levels of the Cm^{+4} are in a good agreement with experimentally obtained values [3].

Table I. The lowest 7 energy levels of Cm^{+4} in MCHF+BREIT (CI) approach with different degree of accounting for correlation effects.

States	Energy Level (cm ⁻¹)						
	AS_6	AS_7	AS_8	AS_9	AS_{10}	AS_{11}	AS_{12}
$5f^6 {}^7F_0$	0.0	0.0	0.0	0.0	0.0	0.0	0.0
7F_1	1788.0	2019.5	2105.6	2196.5	2225.6	2265.4	2292.6
7F_2	4838.0	5464.5	5691.9	5935.8	6012.4	6118.0	6182.9
7F_3	8188.9	9221.8	9566.6	9960.9	10079.6	10248.2	10340.5
7F_4	11107.3	12422.6	12797.1	13284.9	13422.3	13628.0	13728.3
7F_5	13656.3	15143.0	15492.3	16029.8	16171.7	16396.2	16494.6
7F_6	16117.2	17681.3	17974.2	18527.4	18664.4	18894.1	18983.6

References

- [1] S.E. Nave, R. G. Haire, P.G. Huray, Phys. Rev. **B. 28**, 2317 (1983)
- [2] C. Froese Fischer, G. Tachiev, G. Gaigalas, M.R. Godefroid, Comput. Phys. Comm. **176**, 559 (2007)
- [3] G.K. Liu, J.V. Beitz, Phys. Rev. **B. 41**, 6201 (1990)

MCDHF calculations of the electric dipole moment of radium induced by the nuclear Schiff moment

E. Gaidamauskas¹, G. Gaigalas¹, J. Bieron², S. Fritzsche³ and P. Jönsson⁴

¹*Vilnius University Research Institute of Theoretical Physics and Astronomy,
A. Goštauto 12, LT-01108 Vilnius, Lithuania,*

²*Instytut Fizyki imienia Mariana Smoluchowskiego, Uniwersytet Jagielloński
Reymonta 4, 30-059 Kraków, Poland*

³*Gesellschaft für Schwerionenforschung Darmstadt, Planckstr.1, D-64291 Darmstadt,
Germany*

⁴*Nature, Environment, Society Malmö University, S-205 06 Malmö, Sweden
E-mail:gaigalas@itpa.lt*

A non-zero permanent electric dipole moment (EDM) of atom, molecules or other composite or elementary particle is one of possible manifestations of parity (P) and time reversal (T) symmetry violations. During the last decade, several atoms were considered as candidates for such experiments, and currently radium appears to be the most promising one. Experiments with radium are underway in Argonne National Laboratory and in Kernfysisch Versneller Instituut. The multiconfiguration Dirac-Hartree-Fock theory has been employed to calculate the electric dipole moment of the metastable $7s6d\ ^3D_2$ state of radium. One of the most important parity and time reversal symmetry violating interaction in atoms is due to a possible Schiff moment between the electrons and the nucleus:

$$\hat{H}_{SM} = 4\pi \sum_{j=1}^N (\mathbf{S} \cdot \nabla_j) \rho(r_j). \quad (1)$$

This interaction mixes parity of atomic states and also induces a static electric dipole moment of the atom. For the calculations of the Schiff moment interaction and electric dipole moment operators matrix elements we extended the GRASP2K relativistic atomic structure package [1]. In the calculations valence and core-valence electron correlation effects have been included in a converged series of multiconfiguration expansions. In this contribution, we investigate the mixing of two atomic levels of opposite parity, $7s7p\ ^3P_1$ and $7s6d\ ^3D_2$, which are separated by a very small energy interval 5cm^{-1} . The calculated values of EDM are presented in the Table. Obtained results are in a good agreement with other theories [2].

Table 1: EDM for different isotopes of Ra in the 3D_2 state induced by the Schiff moment.

$^{223}_{88}\text{Ra} \quad I = \frac{3}{2} \quad F = \frac{3}{2}$		$^{225}_{88}\text{Ra} \quad I = \frac{1}{2} \quad F = \frac{3}{2}$	
MCDHF	RHF+CI [2]	MCDHF	RHF+CI [2]
$0.43 \times 10^9 \text{ IS}$	$0.30 \times 10^9 \text{ IS}$	$1.40 \times 10^8 \text{ IS}$	$0.94 \times 10^8 \text{ IS}$

References

- [1] P. Jönsson, X. He, C. Froese Fischer, I.P. Grant, Comput. Phys. Comm. **177**, 597 (2007)
 [2] V.A. Dzuba, V.V. Flambaum, J.S. Ginges, Phys. Rev. A **61**, 062509 (2000)

On the solution of the time dependent Dirac equation for hydrogen-like systems

S. Selstø, J. Bengtsson, E. Lindroth

*Atomic Physics, Fysikum, Stockholm University, AlbaNova University Center,
SE-106 91 Stockholm, Sweden*

The time dependent Dirac equation for a hydrogen-like system exposed to a short, intense electromagnetic pulse is solved numerically by expanding the wave function in eigenstates of the unperturbed Hamiltonian. These eigenstates are obtained by diagonalizing the Dirac Hamiltonian on an exponential grid. As the field parameters (field strength and frequency) increases, both magnetic and relativistic effects become important. Furthermore, for higher nuclear charges, relativistic effects are important even for relatively weak fields. The need for a non-dipole and relativistic treatments is investigated by direct comparison with the corresponding predictions of the Schrödinger equation in the dipole approximation.

Although the fields considered are far below the threshold for pair-creation, negative energy states may still play a role during the interaction. The possible influence of such states is considered by propagating the wave function in field dressed states, which are obtained by diagonalizing the full Hamiltonian. After each diagonalization the negative energy states are removed from the basis.

In order to minimize the number of basis states needed, complex scaling has been applied.

Calculation of parity-nonconserving amplitude in Ra^+

Rupsi Pal¹, Dansha Jiang¹, Marianna Safronova¹, and Ulyana Safronova²

¹*University of Delaware, Newark, Delaware, 19716 USA*

²*University of Nevada, Reno, Nevada, 89523, USA*

E-mail: msafrono@udel.edu

Experimental measurements of the spin-dependent contribution to the PNC $6s \rightarrow 7s$ transition in ^{133}Cs led to a value of the cesium anapole moment that is accurate to about 14% [1]. The analysis of this experiment, which required a calculation of the nuclear spin-dependent PNC amplitude, led to constraints on weak nucleon-nucleon coupling constants that are inconsistent with constraints from deep inelastic scattering and other nuclear experiments. New experiments (and associated theoretical analyses) are needed to resolve the issue.

Comparing experimental weak charges of atoms Q_W , which depend on input from atomic theory, with predictions from the standard model provide important constraints on possible extensions of the standard model. Indeed, a recent analysis [2] of parity-violating electron-nucleus scattering measurements combined with atomic PNC measurements placed tight constraints on the weak neutral-current lepton-quark interactions at low energy, improving the lower bound on the scale of relevant new physics to ~ 1 TeV.

We have calculated parity-nonconserving $7s - 6d$ amplitude $E1_{PNC}$ in Ra^+ , using relativistic high-precision all-order method where all single and double excitations of the Dirac-Hartree-Fock wave function are included to all orders of perturbation theory. Detailed study of the uncertainty of the PNC amplitude is carried out; additional calculations are performed to evaluate the effect of the triple excitations and to estimate some of the missing correlation corrections. A systematic study of the parity-conserving atomic properties, including the calculation of the transition matrix elements, lifetimes, hyperfine constants, as well as dipole and quadrupole ground state polarizabilities, is carried out. The comparisons are made between the size of the correlation corrections in Ba^+ and Ra^+ . The results are compared with other theoretical calculations and available experimental values.

References

- [1] C. S. Wood, S. C. Bennett, D. Cho, B. P. Masterson, J. L. Roberts, C. E. Tanner, and C. E. Wieman, *Science* **275**, 1759 (1997).
- [2] R. D. Young, R. D. Carlini, A. W. Thomas, and J. Roche, *Phys. Rev. Lett.* **99**, 122003 (2007).

Development of the CI + all-order method for atomic calculations

Marianna Safronova¹, M. G. Kozlov², and W. R. Johnson³

¹*University of Delaware, Newark, Delaware, 19716 USA*

²*Petersburg Nuclear Physics Institute, Gatchina, 188300, Russia*

³*University of Notre Dame, Notre Dame, Indiana, 46556, USA*

E-mail: msafro@udel.edu

The development of the relativistic all-order method where all single and double excitations of the Dirac-Hartree-Fock wave function are included to all orders of perturbation theory led to accurate predictions for energies, transition amplitudes, hyperfine constants, and other properties of monovalent atoms as well as the calculation of parity-violating amplitudes in Cs and Fr [1]. The all-order method is designed to treat core-core and core-valence correlations with high accuracy. Precision calculations for atoms with several valence electrons require an accurate treatment of the very strong valence-valence correlation; a perturbative approach leads to significant difficulties. In this work, we develop a novel method for precision calculation of properties of atomic systems with more than one valence electron. This method combines the all-order approach currently used in precision calculations of properties of monovalent atoms with the configuration interaction (CI) approach.

The precision of the CI method is generally drastically limited for large systems by the number of the configurations that can be included. As a result, core excitations are neglected or only a small number of them are included, leading to a significant loss of accuracy for heavy atoms. In the CI + all-order approach, core excitations are incorporated in the CI method by constructing an effective Hamiltonian using fully converged all-order excitations coefficients. Therefore, the core-core and core-valence sectors of the correlation corrections for systems with few valence electrons will be treated with the same accuracy as in the all-order approach for the monovalent system. The CI method will then be used to treat valence-valence correlations. This method is expected to yield accurate wave functions for subsequent calculations of various atomic properties (such as lifetimes, polarizabilities, hyperfine constants, parity-violating amplitudes, etc).

The preliminary results for Mg, Al, Sr, and Ba are presented.

References

[1] M.S. Safronova and W.R. Johnson, *Advances in Atomic, Molecular, and Optical Physics* **55**, 191 (2008).

Ground state wavefunctions for two-electron systems with finite nuclear mass

K. V. Rodriguez^{1,4}, V. Y. Gonzalez^{1,4}, L. U. Ancarani², D. M. Mitnik^{3,4}
and G. Gasaneo^{1,4}

¹*Departamento de Física - Universidad Nacional del Sur, 8000 Bahía Blanca, Argentina*

²*Laboratoire de Physique Moléculaire et des Collisions,
Université Paul Verlaine - Metz, France*

³*Instituto de Astronomía y Física del Espacio, y Departamento de Física, Facultad de
Ciencias Exactas y Naturales, Universidad de Buenos Aires. C.C. 67, Suc. 28,
(C1428EGA) Buenos Aires, Argentina*

⁴*Consejo Nacional de Investigaciones Científicas y Técnicas, Argentina*

The basis functions proposed by Gasaneo and Ancarani in [1] are used to construct trial wavefunctions for several two-electron systems. The focus here is on the study of the following negatively charged hydrogenlike ions : $^1\text{H}^-$, $^\infty\text{H}^-$; D^- , T^- and Mu^- , the negative positronium ion Ps^- , and some exotic systems $e^-e^-(nm_e)^+$ in which one of the particles is heavier than the other two. All these systems are similar to each other in the main property of their spectra, i.e. they have only one bound (ground), singlet state with angular momentum $L = 0$. The basis functions satisfy exactly all the two-body Kato cusp conditions. Following the methodology proposed in [2], each term of the basis is multiplied by a series which does not affect this property. In terms of the interparticle coordinates r_{ij} ($i \neq j$), the trial wave functions, with N the number of (linear) variational parameters, are constructed as

$$\Psi_{C3-N} = \sum_{n_1, n_2, n_3} \varphi_{n_1}(\mu_{13}, r_1) \varphi_{n_2}(\mu_{23}, r_2) \chi_{C3}(n_3, \mu_{12}, r_{12}) \sum_{ijk \neq 1} c_{ijk}^{n_1 n_2 n_3} r_1^i r_2^j r_{12}^k$$

where μ_{ij} are the reduced masses, φ_{n_i} are $l = 0$ hydrogenic functions of principal quantum numbers n_i , and $\chi_{C3} = {}_1F_1(-n_3, 2, -2\mu_{12}r_{12}/n_3)$ with n_3 a positive integer is the angular correlation factor [1,3] which results from the analytic continuation of the widely used double continuum three-body Coulomb (C3) wave function [4].

We also investigate systems of the form $e^-e^-(nm_e)^+$ where $(nm_e)^+$ refers to exotic particles with masses m_3 equal n times the mass of the positron but with the charge of the positron (+). Taking n from 1 to ∞ we have obtained approximate analytical expressions for the energies and some mean radial quantities, as functions of the mass of the heaviest particle m_3 .

Results of the mean energy and other radial quantities will be shown at the conference for the ions $^1\text{H}^-$, $^\infty\text{H}^-$; D^- , T^- , Mu^- and the exotic systems $e^-e^-(nm_e)^+$.

References

- [1] G. Gasaneo and L.U. Ancarani, Phys. Rev. A **77**, 012705 (2008)
- [2] K.V. Rodriguez, G. Gasaneo and D.M. Mitnik, J. Phys. B **40** (19), 3923 (2007)
- [3] L.U. Ancarani and G. Gasaneo, Phys. Rev. A **75**, 032706 (2007)
- [4] C.R. Garibotti and J.E. Miraglia, Phys. Rev. A **21**, 572 (1980)

Laser separation and detecting the isotopes and nuclear reaction products and relativistic calculating the hyperfine structure parameters in the heavy-elements

O.Yu. Khetselius

Odessa University, P.O.Box 24a, Odessa-9, 65009, Ukraine

Relativistic calculation of the spectra hyperfine structure parameters for heavy elements is carried out. Calculation scheme is based on gauge-invariant QED perturbation theory with using the optimized one-quasiparticle representation at first in the theory of the hyperfine structure for relativistic atomic systems [1,2]. Within the new method it is carried out calculating the energies and constants of the hyperfine structure for valent states of cesium ^{133}Cs , Cs-like ion Ba, isotopes of ^{201}Hg , ^{223}Ra , ^{252}Cf are defined. The contribution due to inter electron correlations to the hyperfine structure constants is about 120-1200 MHz for different states, contribution due to the finite size of a nucleus and radiative contribution is till 2 dozens MHz. Obtained data for hyperfine structure parameters are used in further in laser photoionization detecting the isotopes in a beam and the buffer gas for systematic studying the short-lived isotopes and nuclear isomers. We propose a new approach to construction of the optimal schemes of the laser photoionization method for further applying to problem of the nuclear reactions products detecting. It's studied the reaction of spontaneous ^{252}Cf isotope fission on non-symmetric fragments, one of that is the cesium nucleus. The corresponding experiment on detecting the reactions products is as follows. The heavy fragment of the Cf nucleus fission created in the ionized track 106 electrons which are collected on the collector during 2 mks. The collector is charged negatively 40mks later after nuclear decay and 10mks before the laser pulse action. The photo electrons, arised due to the selective two-stepped photoionization are drafted into the proportional counter for their detecting. Usually a resonant excitation of Cs is realized by the dye laser pulse, the spectrum of which includes the wavelengths of two transitions $6S_{1/2}-7P_{3/2}$ (4555Å) and $6S_{1/2}-7P_{1/2}$ (4593Å). This pulse also realizes non-resonant photoionization of the Cs excited atoms. The disadvantages of the standard scheme are connected with non-optimality of laser photoionization one, effects of impact lines broadening due to the using the buffer gas, the isotopic shift and hyperfine structure masking etc. We proposed new laser photoionization scheme, which is based on a selective resonance excitation of the Cs atoms by laser radiation into states near ionization boundary and further autoionization decay of excited states under action of external electric field [2]. The corresponding optimal parameters of laser and electric fields, atomic transitions, states, decay parameters etc are presented.

References

- [1] A. Glushkov, O. Khetselius et al, Nucl. Phys. A. **734**, e21 (2004)
- [2] A. Glushkov, O. Khetselius et al, Recent Adv. in Theory of Phys. and Chem. Syst. (Springer). **15**, 285 (2006)

QED approach to the photon-plasmon transitions and diagnostics of the space plasma turbulence

A.V. Glushkov^{1,2}, O.Yu. Khetselius², A.A. Svinarenko²

¹*Institute for Spectroscopy of Russian Academy of Sciences, Troitsk, 142090, Russia*

²*Odessa University, P.O.Box 24a, Odessa-9, 65009*

Energy approach in QED theory [1-4] is developed and applied to modelling photon-plasmon transitions with emission of photon and Langmuir quanta in space and astrophysical plasma. It is well known that the positronium Ps is an exotic hydrogen isotope with ground state binding energy of $E = 6.8$ eV. The hyperfine structure states of Ps differ in spin S , life time t and mode of annihilation. The ortho- Ps atom has a metastable state $2s1$ and probability of two-photon radiation transition from this state into $1s1$ state $0.0018s^{-1}$. In the space plasma there is the competition process of destruction of the metastable level - the photon-plasmon transition $2s - 1s$ with emission of photon and Langmuir quanta. We carried out calculation of the probability of the photon-plasmon transition in the Ps . The approach represents the decay probability as an imaginary part of energy shift dE , which is defined by S -scattering matrix. Standard S -matrix calculation with using an expression for tensor of dielectric permeability of the isotropic plasma and dispersion relationships for transverse and Langmuir waves allows getting the corresponding probability $P(ph - pl)$. Numerical value of $P(ph - pl)$ is $5.2 \cdot 10^6 U(1/s)$, where U is density of the Langmuir waves energy. Our value is correlated with others: $P(ph - pl) = 6 \cdot 10^6 U(1/s)$. Comparison of obtained probability with lifetime t (3γ) allows getting the condition of predominance of photon-plasmon transition over three-photon annihilation. The considered transition may control the population of $2s$ level and search of the long-lived Ps state can be used for diagnostics of the plasma turbulence.

References

- [1] A. Glushkov, L.N. Ivanov, Phys. Lett.A. **170**, 33 (1992); Preprint ISAN N AS-4, Moscow-Troitsk (1994)
- [2] A. Glushkov, et al, J. Phys. CS. **11**, 188 (2004)
- [3] A. Glushkov, et al, Int. Journ. Quant. Chem. **99**, 936 (2004)
- [4] A. Glushkov, Low Energy Antiproton Phys. **796**, 206 (2006)

QED theory of laser-atom and laser-nucleus interaction

A.V. Glushkov¹²

¹*Institute for Spectroscopy of Russian Academy of Sciences, Troitsk, 142090, Russia*

²*Odessa University, P.O.Box 24a, Odessa-9, 65009*

QED theory is developed for studying interaction of atoms and nuclei with an intense and superintense laser field. Method bases on a description of system in the field by the k- photon emission and absorption lines. The lines are described by their QED moments of different orders, which are calculated within Gell-Mann Low adiabatic formalism [1-4]. The analogous S-matrix approach is developed for consistent description of the laser-nucleus interaction. We have studied the cases of single-, multi-mode, coherent, stochastic laser pulse shape. An account for stochastic fluctuations in a field effect is of a great importance. Results of the calculation for the multi-photon resonance and ionization profile in Na,Cs, Yb, Gd atoms are presented. It is also studied the phenomenon of the above threshold ionization. Efficiency of method is demonstrated by QED perturbation theory calculations for the two-photon ionization cross-sections for extended photon energy range (including above-threshold ionization) in Mg. Comparison with the R-matrix calculation of Luc-Koenig et al [3] is given. There is considered a phenomenon of the Rydberg stabilization of the H atom in a strong laser field and estimated the rate of transition between the stabilized Rydberg state ($n=40, m=2$; $E \approx 10(8)V/cm$) and ground state, when it's possible the radiation of photons with very high energy (short-wave laser amplification). DC strong field Stark effect for atoms, including atoms in plasma, Rydberg atoms and confined systems is studied within new quantum approach, based on the operator PT [1]. The zeroth order Hamiltonian, possessing only stationary states, is determined only by its spectrum without specifying its explicit form. We present here the calculation results of the Stark resonances energies and widths for a number of atoms (H, Li, Tm, U etc.) and for a whole number of low-lying and also Rydberg states. We discovered and analyzed the weak field effect of drastic broadening of widths of the Letokhov-Ivanov re-orientation decay autoionization resonances in Tm etc. Developed approach can be naturally applied to studying the Stark effect in confined systems, including quantum wells, quantum dots etc, where especially interesting effects may occur.

References

- [1] A. Glushkov, L.N. Ivanov, Phys. Lett.A. **170**, 33 (1992); Preprint ISAN N AS-2, Moscow-Troitsk (1992)
- [2] A. Glushkov, et al, J. Phys. CS. **11**, 188 (2004)
- [3] A. Glushkov, et al, Int. Journ. Quant. Chem. **99**, 936 (2004); **99**, 889 (2004); **104**, 512 (2005); **99**, 562 (2005);
- [4] A. Glushkov, Low Energy Antiproton Phys. **796**, 206 (2006)

Quantum dynamics of planar hydrogen atom in a billiard with moving boundaries

Kh.Yu. Rakhimov

*Heat Physics Department of the Uzbek Academy of Sciences,
28 Katartal St., Tashkent 100135, Uzbekistan
kh_rakhimov@yahoo.com*

Particle motion in confined geometries is an important problem providing to explore many features of classical nonlinear dynamics and quantum dynamics of classically non-integrable systems. Due to recent progress in the physics of mesoscopic systems and nanophysics this problem has become attractive from the practical viewpoint, too. Such systems as quantum dots, trapped atoms, nanotubes are the realistic systems where confined electron dynamics play important role. Usually in studying these systems the boundaries of confinement are considered as strictly fixed. However, in many practically important situations the confinement boundaries are not strictly fixed and fluctuate in space, oscillate or move in one direction.

In present work we study quantum dynamics of an electron in the Coulomb field whose motion is confined by time-dependent billiard boundaries. Exploring of billiards with moving walls require solution of the two-dimensional Schrödinger equation with time-dependent boundary conditions. Here we solve the Schrödinger equation for Coulomb potential with the boundary conditions given on circle with time-dependent radius. It well known that in most of the realistic situations with atoms confined in various traps the trap boundaries are not fixed but time-dependent. Solving the problem numerically we obtain time-dependence of the electron energy and compute density of states. The results obtained show that in the case of oscillating boundaries the energy of electron grows in time. However, this growth is strongly suppressed upon reaching certain value. This value depends on the frequency and amplitude of the billiard wall oscillations.

Interchannel interaction in orientation and alignment of Kr $4p^4mp$ states in the excitation region of $3d^9np$ resonances

B.M. Lagutin¹, I. D. Petrov¹, V. L. Sukhorukov¹, A. Ehresmann², L. Werner²,
S. Klumpp², K.-H. Schartner³ and H. Schmoranzer⁴

¹*Rostov State University of Transport Communications, 344038 Rostov-on-Don, Russia,*

²*Institut für Physik, Universität Kassel, 34109 Kassel, Germany,*

³*I. Physikalisches Institut, Justus-Liebig-Universität, D-35392 Giessen, Germany,*

⁴*Fachbereich Physik, Technische Universität Kaiserslautern,*

D-67653 Kaiserslautern, Germany

E-mail: schmoran@rhrk.uni-kl.de

In combined theoretical and experimental efforts we studied the interchannel interaction influencing the population of Kr $4p^4mp$ ionic states in the excitation energy region around the $3d^9np$ resonances by photon-induced Auger decay. This resonant Auger process was shown to be treated as an interference of strong resonant and weak direct nonresonant ionization channels [1]. This interference leads to the energy dependence of the orientation, O_{10} , and the alignment, A_{20} , of the final ionic states and also of the angular distribution of outgoing electrons and fluorescence photons. The above quantities are rather sensitive to the interference mechanism, especially when studied in the wings of the resonances [2].

In the present work the theoretical treatment of the non-resonant pathway was extended with respect to the monopole shake-process considered earlier. The non-monopole processes including both intra- and intershell correlations were taken into account. The main non-monopole contributions to the direct transition amplitude stem from the $4p^5\varepsilon'\ell$ ($\ell = s, d$) and $3d^9\varepsilon'\ell$ ($\ell = p, f$) intermediate states.

Correlation effects modify the partial monopole shake-amplitudes for the outgoing waves $\varepsilon\ell$ differently and this effect changes the energy dependence of the O_{10} and A_{20} parameters. The calculated data agree closely with the measured orientation parameter for the $4p^4(^1D)5p\ ^2P_{3/2}$ final ionic state in the extended energy region between the $3d^9_{5/2}5p_{3/2}$ and $3d^9_{5/2}6p_{3/2}$ resonances. This result asks for new extended experimental data on the angular distribution parameters for other final ionic states, too.

The quality of the wavefunctions used in the calculation was checked by comparing the computed and recently measured [3] photoionization cross sections for different $4p^4(L_0S_0)mp$ satellites in the region of the $3d^9np$ resonances. Good agreement between theory and experiment was observed in all cases. The photoelectron angular distribution measured and computed in [3] for the above satellites is also compared with the present calculations.

References

- [1] Lagutin B.M. *et al.*, Phys.Rev.Lett. **90**, 073001 (2003)
- [2] Schartner K.-H. *et al.*, J.Phys.B **40**, 1443 (2007)
- [3] Sankari A. *et al.*, Phys.Rev.A **76**, 022702 (2007)

Application of new quasirelativistic approach for treatment of oxygen-like Iron and Nickel

O. Rancova, P. Bogdanovich and R. Karpušienė

Institute of Theoretical Physics and Astronomy of Vilnius University

A. Goštauto st. 12, 01108 Vilnius, Lithuania

E-mail: olga@itpa.lt

An urgent demand for high precision calculations of atomic characteristics of heavy atoms and highly charged ions with complex electron configurations encourages the development of new methods and computer codes. Possibilities of the new quasirelativistic approach designed for *ab initio* calculations of spectral characteristics of highly charged ions and heavy atoms are investigated and illustrated with an example of a study of spectral characteristics of oxygen-like ions of Iron and Nickel. Within the quasirelativistic approach the main relativistic effects are taken already into account when obtaining the radial orbitals. The main distinctions between the approach under investigation and the well-known computer code by R. D. Cowan based on the methods described in [1] are the following: the quasirelativistic equations for the radial orbitals are newly formed in a different shape [2,3], the finite size of the atomic nucleus is taken into account while solving the equations [4], the definition of the radial integrals of the energy operator is refined, the transformed radial orbitals are created for the description of virtual excitations while performing the configuration interaction.

The calculations executed within the described approach were reduplicated by the analogical calculations based on the usual non-relativistic radial orbitals. It allows one to evaluate the advantages and the new possibilities appearing while using the quasirelativistic radial orbitals against the conventional non-relativistic radial orbitals when the correlation effects are taken into account in the same way performing the configuration interaction on the basis of transformed radial orbitals.

The energy spectra, transition characteristics and lifetimes of Fe XIX and Ni XXI ions calculated by two mentioned methods are calculated. The obtained results are compared with the experimental data and with the theoretical calculations of other authors. From the comparison it is obvious that the quasirelativistic approach enables us to obtain the data of high precision and that the structure of the energy spectra calculated perfectly coincides with the experimental spectra.

Acknowledgments

This work, partially supported by the European Communities under the contract of Association between EURATOM/LEI FU06-2006-00443, was carried out within the framework of the European Fusion Development Agreement. The views and opinions expressed herein do not necessarily reflect those of the European Commission.

References

- [1] R. D. Cowan, *The theory of atomic structure and spectra*, (University of California Press, Berkeley, 1981)
- [2] P. Bogdanovich, O. Rancova, Phys. Rev. A **74**, 052501 (2006)
- [3] P. Bogdanovich, O. Rancova, Phys. Rev. A **76**, 012507 (2007)
- [4] P. Bogdanovich, O. Rancova, Lithuanian. J. Phys. **42**, 257 (2002)

Relativistic recoil and higher-order electron correlation corrections to the transition energies in Li-like ions

Y. S. Kozhedub¹, D. A. Glazov¹, I. I. Tupitsyn¹, V. M. Shabaev¹, and G. Plunien²

¹ *Department of Physics, St. Petersburg State University, Oulianovskaya 1, Petrodvorets, St. Petersburg 198504, Russia*

² *Institut für Theoretische Physik, TU Dresden, Mommsenstraße 13, D-01062 Dresden, Germany*

E-mail: kozhedub@pcqnt1.phys.spbu.ru

Traditionally, investigations of isotope shift in atomic spectra have been carried out mainly to determine the difference in the root-mean-square nuclear radii $\langle r^2 \rangle$. Recently new applications emphasized the relevance of this effect. For instance, isotope shift calculations in atoms and ions can be important for astrophysical search for possible α -variation, where the isotope shift induces valuable systematic error. Moreover, investigations of this effect could provide information about isotopic abundances in the early Universe, which is tightly linked with the general evolution of the Universe. The study of isotope shifts in highly charged ions has the potential advantage of an increased sensitivity to nuclear size and relativistic effects due to the stronger overlap of the electronic wave function with the nuclear matter and of the simpler electronic structure of few-electron ions as opposed to their neutral atomic counterparts.

Nuclear recoil effect is the most difficult part of isotope shift to evaluate. In the present paper, we perform accurate calculations of the nuclear recoil effect for ions along the lithium isoelectronic sequence. The full relativistic theory of the nuclear recoil effect can be formulated only in the framework of QED [1]. In order to evaluate the recoil effect within the lowest-order relativistic approximation one can use the relativistic recoil operator. Within this approximation the recoil correction is calculated with many-electron wave functions in order to take into account the electron-correlation effect. The one- and two-electron contributions to the recoil effect are evaluated to all orders in αZ . Comparing the isotope shifts calculated with recent experimental data indicates very good prospect for test of the relativistic theory of the recoil effect in middle- Z ions.

We present also the most accurate up-to-date theoretical values of the $2p_{1/2}$ - $2s$ and $2p_{3/2}$ - $2s$ transition energies in middle- Z Li-like ions. All presently available contributions to the transition energies are collected. Except for the one-electron two-loop corrections, all other terms up to the two-photon level are treated within the framework of bound-state QED to all orders in αZ . The interelectronic interaction beyond the two-photon level is evaluated within the Breit approximation by means of the large-scale configuration-interaction Dirac-Fock-Sturm method. We report accurate numerical values of the higher-order interelectronic-interaction correction for Li-like ions up to uranium. The results obtained for the transition energies are in good agreement with recently published experimental data. In the case of lithiumlike scandium, they were reported in Ref. [2].

References

- [1] V. M. Shabaev, Phys. Rev. A 57, 59 (1998); Phys. Rep. 356, 119 (2002).
- [2] Y. S. Kozhedub *et al.*, Phys. Rev. A 76, 012511 (2007).

Coupled tensorial forms of atomic two-particle operator

R. Jursėnas

*Institute of Theoretical Physics and Astronomy of Vilnius University, A. Goštauto 12,
LT-01108 Vilnius, Lithuania*

For many-electron atoms and ions the ability to present a two-electron operator and its matrix elements in an optimal form may be decisive for successful calculation solutions of many theoretical spectroscopy problems. Here a two-particle operator is expressed in second quantization representation (SQR). Special attention is paid to the approach when the expressions for the operator considered are given in terms of submatrix elements of the coupled two-electron wave function [1]. This gives more freedom in choosing a convenient way for the calculations of matrix elements for open-shell atoms.

In a SQR two approaches were considered to express an arbitrary two-electron operator in a coupled tensorial form for multi-shell atoms. The expressions of both topologically different approaches are applicable to the study of the operators representing atomic interactions as well as the operators describing some effective interactions appearing, for instance, in an atomic many body perturbation theory (MBPT) or a coupled cluster method.

The first approach is more suitable when one seeks effectively to calculate the matrix elements of (one) particular operator because the internal ranks of operator are involved in the calculation of many-electron angular part. The second approach is superior for the problems where several operators with different tensorial structure are considered, for example, the formation of energy matrix of atomic Hamiltonian in Breit-Pauli approximation. In this case, only the resulting ranks of operators enter in the expressions for the submatrix elements of many-electron angular part and the computer codes used for such calculations could be more efficient if they are based on the second approach.

The final result of the study is a large set of a two-particle operators acting in the space of the states of one-, two-, three- and four-shells. The expressions can be used for both nonrelativistic (LS coupling) and relativistic (jj coupling) approximations.

References

- [1]. R. Jursėnas, G. Merkelis, Lithuanian Journal of Physics, Vol.47, No.3, 255-266 (2007).

The binominal potential of electron-proton interaction alternative to the Coulomb law

V.K. Gudym¹ and E.V. Andreeva²

¹*Space National Agency of Ukraine, Kyiv, Ukraine*

²*Institute of Physics of Semiconductors of the NASU, Kyiv, Ukraine*

E-mail:vgudym@mail.ru

On the basis of only classical assumptions, we have shown earlier [1, 2, 3] that an electron and a proton interact by the binomial law

$$V = -\frac{e^2}{r} + \frac{\Gamma}{r^2} \quad (1)$$

and have determined the value of the constant Γ as 6.10276×10^{-28} *CGSE units*.

Potential (1) has been verified by us in the analysis of both the Kepler task of a hydrogen atom where the energy takes the form

$$E = \frac{m\dot{r}^2}{2} + \frac{M^2}{2mr^2} - \frac{e^2}{r} + \frac{\Gamma}{r^2} \quad (2)$$

and the Schrödinger equation

$$\Delta\Psi + \frac{2m}{\hbar^2} \left(E + \frac{e^2}{r} - \frac{\Gamma}{r^2} \right) \Psi = 0. \quad (3)$$

We have also analyzed the scattering of an electron by a proton, as a special case of the Kepler task. Below, we give the formula for the deflection angle φ_{0b} as a function of the impact parameter ρ :

$$\varphi_{0b} = \sqrt{\frac{E\rho^2}{E\rho^2 + \Gamma}} \arccos \left[\left(1 + \frac{4E(E\rho^2 + \Gamma)}{e^4} \right)^{-1/2} \right]. \quad (4)$$

The calculations have shown that the formula describing the scattering of electrons in the binomial potential well represents the process within the range of impact parameters down to $10^{-13}cm$ for the energies of an electron from several *eV* up to hundreds of *MeV*. Further, on the basis of potential (1), we have shown the basic opportunity for the solution of the classical task concerning the movement of an electron in the field of a proton for a hydrogen atom. On this way, we were succesful to clarify the nature of the Bohr postulates, the Planck constant, and some other constants which were not treated earlier within the framework of classical mechanics. For the theory of Schrödinger, we have demonstrated, with the use of potential (1), the opportunity to understand and to resolve a number of its internal contradictions. In particular, it turns out to be possible to derive, for the first time, a wave package being stable in time in the problem concerning a hydrogen atom and to explain the mechanism of birth of a quantum in the classical interpretation.

Generally, potential (1) can be considered as a link between the classical and quantum theories.

References

- [1] Gudym V.K. 2001, *Visnyk Kyiv. Univ.*, N. 3, P. 254.
- [2] Gudym V.K., Andreeva E.V. 2003, *Poverkhn.*, N. 5, P. 59-63.
- [3] Gudym V.K., Andreeva E.V. 2006, *Poverkhn.*, N. 3, P. 113-117.

The dynamics of meta-stable states described with a complex scaled Hamiltonian

J. Bengtsson, E. Lindroth, and S. Selstø

Atomic Physics, Fysikum, Stockholm University, S-106 91 Stockholm, Sweden

The laser development has given access to light pulses in the femto- and subfemtosecond regime and thereby opened the possibility to follow electron dynamics directly in the time domain. Of special interest is the dynamics of resonant states, and pioneering experimental studies were made a few years ago on the Auger decay of inner-shell vacancies [1]. One widely spread theoretical technique, that successfully describes resonant states, is that of complex scaling. With this method, the meta-stable states are obtained as unique eigenstates to the field-free complex scaled Hamiltonian. The half-width and the energy position of the meta-stable state is furthermore given directly from the imaginary and the real part of the corresponding eigenvalue respectively. Compared to many other methods, such as the stabilization method where the manifestation of a resonant state is seen as a local accumulations of pseudo-continuum states, this property is highly attractive from a numerical point of view. A second appealing property, due to complex scaling, is that the continuum is adequately represented by a very modest number of eigenstates. A similar accuracy cannot be achieved using a conventional pseudo continuum. Due to the reasons mentioned above, the method of complex scaling is also interesting for truly dynamical systems, for instance atoms exposed to short light pulses followed by the possible population of a meta-stable state. However, the complex scaled Hamiltonian is non-Hermitian and the extension to dynamical calculations is not straight forward. Here we therefore address the question of to what extent this technique might be applied to solve the time-dependent Schrodinger equation and to what extent resonant states contribute to the overall dynamical behaviour of the system. We have tested our approach against conventional methods for the case of hydrogen.

References

- [1] I. M. Drescher et al. *Nature*, 419, 807 (2002)

A simple parameter-free wavefunction for the ground state of three-body systems

L.U. Ancarani¹ and G. Gasaneo²

¹*Laboratoire de Physique Moléculaire et des Collisions,
Université Paul Verlaine - Metz, 57078 Metz, France*

²*Departamento de Física, Universidad Nacional del Sur and Consejo Nacional de Investigaciones Científicas y Técnicas, 8000 Bahía Blanca, Buenos Aires, Argentina*

The study of the structure and stability of Coulombic three-body systems $[m_1 m_2 m_3]$, with arbitrary masses m_i and charges z_i ($i = 1, 2, 3$), has been the subject of many investigations (see, e.g., the review [1]. Recently, we have proposed a pedagogical, simple and parameter-free wavefunction for the ground state of two-electron atoms [2]. The proposal was then generalized [3] to more general atomic three-body systems in which one of the particles is positively charged ($z_3 > 0$) and heavier than the other two which are negatively charged ($z_1 < 0, z_2 < 0$).

Let $\nu_{ij} = \mu_{ij} z_i z_j$ where $\mu_{ij} = \frac{m_i m_j}{m_i + m_j}$ ($i \neq j = 1, 2, 3$) are the reduced masses. In terms of the interparticle coordinates $r_1 = r_{13}, r_2 = r_{23}$ and r_{12} (particle 3 is placed at the origin of the coordinates), the proposed wavefunction reads

$$\Psi_{ARG}^{GEN} = N_{ARG}^{GEN} e^{\nu_{13} r_1 + \nu_{23} r_2} (1 + \nu_{12} r_{12}) [1 + c(r_1^2 + r_2^2)],$$

where N_{ARG}^{GEN} is the normalization constant and c is replaced by an analytical expression in terms of (m_i, z_i) in order to minimize the mean energy of the ground state.

The wavefunction Ψ_{ARG}^{GEN} : (i) has the same form for all systems; (ii) is parameter-free; (iii) is nodeless; (iv) satisfies, by construction, all two-particle cusp conditions [4]; and (v) yields reasonable ground state energies for several systems including the prediction of a bound state for H^- , D^- , T^- and Mu^- . A wavefunction with all these characteristics is presently not available in the literature. The simplicity of Ψ_{ARG}^{GEN} is such that analytical expressions for the ground state energy can be derived. Hence, we have a useful predictive and simple analytical tool (which, to our knowledge, is not available in the literature) to estimate the energy, and therefore to study the stability, of exotic Coulombic three-body systems. In addition, our proposal is simple enough, but sufficiently accurate to be used as a starting point in calculations of collision cross sections. Of course due to its simplicity, energy values cannot compete with those obtained with advanced variational wavefunctions which involve large number of basis functions. However, the latter (i) do not have a predictive character since they have to be optimized each time for a given three-body system.; (ii) in most cases, do not satisfy exactly Kato cusp conditions.

For illustration, results will be shown for the several three-body systems.

References

- [1] E. A. G. Armour, J.-M. Richard and K. Varga, Phys. Rep. **413**, 1 (2005).
- [2] L. U. Ancarani, K. V. Rodriguez and G. Gasaneo, J. Phys. B **40**, 2695 (2007).
- [3] L. U. Ancarani and G. Gasaneo, J. Phys. B **41**, in press (2008).
- [4] T. Kato, Comm. Pure Appl. Math. **10** 151 (1957).

$(e, 3e)$ and $(\gamma, 2e)$ processes on helium: interplay of initial and final states

L.U. Ancarani¹, G. Gasaneo², F.D. Colavecchia³ and C. Dal Cappello¹

¹*Laboratoire de Physique Moléculaire et des Collisions,
Université Paul Verlaine - Metz, 57078 Metz, France*

²*Departamento de Física, Universidad Nacional del Sur and CONICET,
8000 Bahía Blanca, Buenos Aires, Argentina*

³*Centro Atómico Bariloche and CONICET,
8400 S. C. de Bariloche, Río Negro, Argentina*

Information on correlations can be gained from the theoretical study of the double ionization of helium by electron impact ($(e, 3e)$ experiments) [1]. Approximate wave functions are always used in cross section calculations since no exact wave function is known for either the scattering or the bound states. The resulting $(e, 3e)$ cross sections obtained with different theoretical description of the initial and final states are not in agreement with each other. Moreover, when these are compared with absolute experimental data, a rather confusing picture emerges; this is the subject of many recent studies (as discussed and summarized in [2]). It has been mentioned throughout the literature (see, e.g., [3]) that a balanced description of the initial and final two-electron states may play a key role in reproducing experimental $(e, 3e)$ data. This issue is investigated here with a systematic study of double ionization cross sections of helium, by both electron and photon impact.

For $(e, 3e)$ processes, calculated differential cross sections can be compared with the high energy absolute experimental data [4]. The two electrons ejected in the final channel at equal energy (10 eV) are modeled here with the "pure" C3 (or BBK) wave function [5]. For the initial channel we consider different sets of double bound wave functions with only angular correlation or with both angular and radial correlation. The comparison with the measurements allows us to see which of them are balanced when describing $(e, 3e)$ processes. Moreover, the photon impact $(\gamma, 2e)$ cross sections calculated in different gauges and with the same set of initial and final channel wave functions, indicate whether the wave functions are really "balanced" or not.

Our study of the $(\gamma, 2e)$ gauge discrepancies shows that the agreement with absolute $(e, 3e)$ experimental data at 10+10 eV ejected energy obtained with simple initial states is fortuitous and can hardly be attributed to a balanced description with respect to the final state. This result is further confirmed by an investigation of the ejected energy dependence. Moreover, it seems that the approximate C3 wave function is not suitable to describe sufficiently well the double continuum of two electrons ejected at 10 eV.

References

- [1] J. Berakdar, A. Lahmam-Bennani and C. Dal Cappello Phys. Rep. **374**, 91 (2003)
- [2] L.U. Ancarani, G. Gasaneo, F.D. Colavecchia and C. Dal Cappello, submitted (2008)
- [3] J. H. Macek and S. Jones, Rad. Phys. and Chem. **75**, 2206 (2006)
- [4] A. Lahmam-Bennani *et al.*, Phys. Rev. A **59**, 3548 (1999)
- [5] C. R. Garibotti and J. E. Miraglia, Phys. Rev. A **21**, 572 (1980); M. Brauner, J. Briggs and H. Klar, J. Phys. B **22**, 2265 (1989)

A three body approach to calculate the differential cross sections for the excitation of H and He atoms by proton impact

R. Fathi², E. Ghanbari-Adivi³, F. Shojaei Baghini¹, and M.A. Bolorizadeh¹

¹*Physics Department, Shahid Bahonar University of Kerman, Kerman, Iran*

²*Physics Department, Islamic Azad University, Kerman Branch, Kerman, Iran*

³*Physics Department, Isfahan University, Isfahan, Iran.*

mabolori@mail.uk.ac.ir

A method based on the three-body formalism incorporated into the Born series have been developed to calculate the excitation of hydrogen and helium atom by proton impact at medium and high energies. The Faddeev type approaches to the scattering of charged particles are a rearrangement of Born series. However, the on shell transition matrix is not well defined by any method based on the Lippmann-Schwinger integral equation. We have developed a method incorporating the FWL formalism in conjunction with Born approximation to calculate the differential cross section for the excitation of hydrogen and helium atom by protons of energy 50 keV to 500 keV. In the case of hydrogen atom, excitation to the final states 2s, 2p and 3s were included while for the case of atomic helium the calculations were performed for the final states 2¹S and 2³S.

The excitation of atomic hydrogen is a three body process. However, the excitation of helium is simplified by an active model where the second electron is assumed frozen. The wave function for the final state of helium is chosen from literature[1]. We have also deduced a simple method using a Slater type wave function as:

$$\psi(r) = 0.854(1 - 1.15r/2) \exp(-1.15r) + 0.488 \exp(-1.6875r). \quad (1)$$

The differential cross sections for the excitation of helium and hydrogen atoms are plotted in figures 1(a) and 1(b), respectively. In the case of helium atom, the calculations were performed using two different wave functions for the final state of the helium atom, 2¹S. One was the CHF wave functions [1] and the other one was the wave function of equation 1. Figure 1(b) shows the calculations for the final state 2s and 2p of hydrogen. The results are compared with the experimental work of Park and his co-workers [2,3].

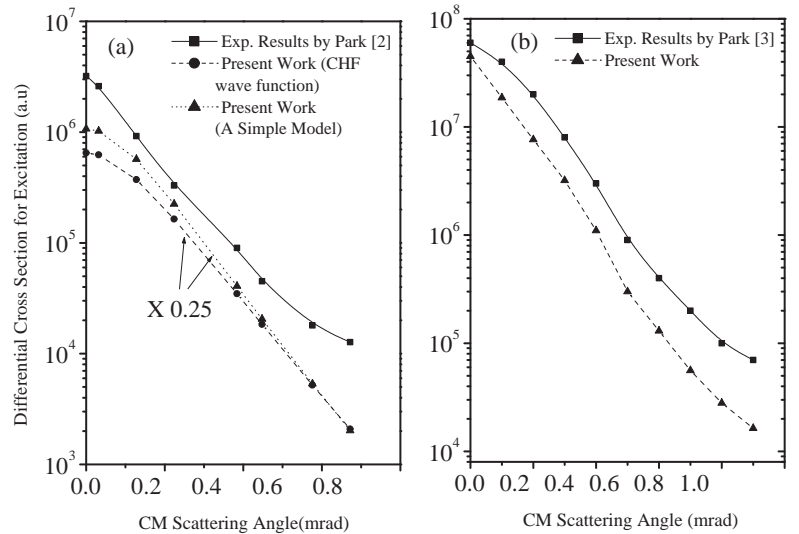


Figure 1. The excitation cross section for (a) helium and (b) hydrogen atom by proton impact at 50keV. The experimental results are from Park and co-workers.

Acknowledgement:

The authors would like to thank Dr. M. Shojaei for his help in the preparation of the manuscript.

References

- [1] G. N. Bhattacharya and G. S. Kastha, J. Phys. B: At. Mol. Phys. 14, (1981), 3007
- [2] T.J. Kvale, et al, Phys. Rev. A 32 (1985) 1369
- [3] J.T. Park, et al, Phys. Rev. A 21 (1980) 751

The peculiarities of elastic and inelastic energy losses at low-energy ion-surface interactions

Farid F. Umarov¹, Abdiravuf A. Dzhurakhalov²

¹*Kazakh-British Technical University Tole bi str., 59, Almaty, Kazakhstan*

²*Universite Libre de Bruxelles, Bd du Triomphe, B-1050, Brussels, Belgium*

An analysis of low-energy ion interaction with crystals should include both elastic and inelastic energy loss mechanisms. The problem of inelastic energy losses is highly intriguing at low-energy ion-surface interactions. Although in the low-energy range (a few keV) they make up only the small fractions (5-10%) of the total losses, they play an essential role in the ionization and electron emission processes, accompanying ion scattering, channeling and sputtering and determine to a considerable extent the charge distribution. Under the specific conditions of grazing ion scattering and channeling at the single crystal surface and subsurface layers an inelastic mechanism will predominate [1, 2]. Inelastic processes of ion-surface interactions exhibit the so-called trajectory effects [3]. In the present work the peculiarities of trajectories and elastic and inelastic energy losses at low-energy small angle correlated ion scattering and ion channeling processes have been investigated by computer simulation. The trajectories of Ne^+ , Ar^+ and Kr^+ ions with initial energy $E_0 = 1,0 - 15,0$ keV, suffering grazing scattering at the atomic chains, semichannels and channels on the Cu (100) and Ni (100) single crystals surfaces were traced in the uppermost 10 atomic layers at grazing angles interval $\psi = 3 - 15^\circ$. The trajectories have been simulated in the binary collision approximation using the universal Biersack-Ziegler-Littmark interaction potential and with regard to the time integral. The inelastic energy losses have been considered as local and calculated by modified Firsov model with their including into the scattering kinematics. Elastic and inelastic energy losses have been summed along trajectories of scattered ions. The calculations have been performed for target points, covering uniformly all surface of target area, where the full number of filling ions is equal to 5×10^4 . It is shown that the average inelastic energy losses corresponding to surface hyper-channeling (SHC) trajectories exceed those for scattering from an atomic chain by about a factor of two. The elastic energy losses for SHC in the grazing scattering region are also substantially lower than the inelastic ones. In the case of channeling of low-energy light and heavy ions it is shown that the full energy losses of paraxial part of ion beams, channeled through single crystal films increase with displacement of the aiming points from the mid-channel axis, but if in the case of light ions they were provided practically by inelastic energy losses, in case of heavy ions the main contribution to them has been made by elastic energy losses. It has been found that in case of light ions, for the paraxial part of a beam even in the low-energy region, the main contribution to energy losses is made by inelastic energy losses, whereas for heavy ions, already at $E_0 < 10$ keV, elastic energy losses exceed inelastic ones. The predominance of the inelastic energy losses should reveal itself in the efficiency of the various inelastic processes accompanying the grazing ion scattering from a single crystal surface.

[1] W. Heiland. Inelastic particle-surface collisions, in: E. Taglauer, W. Heiland (Eds), Springer, New York, 1981, p.329. [2] E.S. Mashkova, V.A. Molchanov. Medium-energy ion reflection from solids. Amsterdam: North-Holland, 1985. [3] E.S. Parilis, L.M. Kishinevsky, N.Yu.Turaev, B.E. Baklitsky, F.F. Umarov, V.Kh. Ferleger, S.L. Nizhnaya, I.S. Bitensky Atomic collisions on solid surfaces. Amsterdam: North-Holland, 1993.

Study of mechanism in alkali metal ion inert gas atom interaction

R.Lomsadze M. Gochitashvili, B.Lomsadze, N. Tsiskarishvili, D.Kuparashvili

Tbilisi State University, Department of Exact and Natural Sciences, Georgia

Absolute cross sections for inelastic processes (electron capture, ionization, stripping and excitation) have been measured for K^+ ions colliding with He atoms at laboratory energies of 0.7 - 10 keV. The experimental techniques include refined version of the potential methods, angle- and energy-dependent collection of product ions, energy-loss and optical spectroscopy. The correlation diagram of the diabatic quasimolecular terms of systems of colliding particles are used to discuss the mechanisms for inelastic processes in these collisions. It is shown that the charge exchange is caused by capture of electrons to the ground state of the atom. Corresponding quasimolecular terms are populated through Σ - Σ transitions in nonadiabatic regions. The contributions made by the various processes to the total cross sections of an electron emission in these collisions are estimated. It was found that the ionization mechanism involves the filling of quasimolecular autoionization terms, which decay in the stage in which the quasimolecule exists. The population of these terms is connected with Σ - Π and Σ - Π - Δ transitions. The stripping in K^+ - He collisions occurs by a mechanism involving transition of a diabatic term into the continuum. The increase of the excitation probability of inelastic channels at the energy loss spectrum, with increasing the angle of scattering incident ions is revealed. Anomalously small and significantly large value of the excitation cross section for the potassium atom and ion respectively, a structural peculiarity for the excitation function of resonance helium atomic line are explained.

Studies of superelastic electron scattering by the metastable thallium atoms

I.I. Shafranyosh, R.O. Fedorko, V.I. Marushka, T.A. Snegurskaya,
V.V. Perehanets, V.V. Stetsovych

Uzhgorod National University, 54 Voloshyn str., 88000 Uzhgorod, Ukraine
E-mail: shafivan@rambler.ru

Here we report on the first results of studying the superelastic electron scattering by the metastable $6s^26p\ ^2P_{3/2}$ Tl atoms in the incident electron range 0.3–3.0 eV.

The studies were carried out using the crossed electron-atomic beam technique. A five-electrode electron gun providing the low-energy electron beams (starting from 0.3 eV) with $\Delta E_{1/2} \approx 0.3$ eV (FWHM) energy resolution was used as the electron beam source. The electron energy scale was calibrated against the energy position of the resonance related to the formation of the SF_6^- negative ions, which determined the energy scale zero mark. The discharge excitation techniques was applied to produce the metastable Tl atom beam. The metastable $6s^26p\ ^2P_{3/2}$ Tl atom concentration was $4 \cdot 10^9$ cm $^{-3}$ at the divergence angle of $\sim 8.7 \cdot 10^{-2}$ rad. The scattered electron energies were analyzed using a retarding-type energy analyzer. The experimental techniques and method are described in detail in [1].

The studies performed allowed us to determine the energy dependence $\sigma^f(E)$ of the effective cross-section for superelastic electron scattering by the metastable Tl atoms and its absolute value σ^f . The experimental results are shown in figure. The absolute value of the cross section σ^f was determined at the 0.4 eV incident electron energy and reached $8 \cdot 10^{-15}$ cm 2 . The uncertainty in determining $\sigma^f(E)$ and σ^f did not exceed 8% and 60%, respectively.

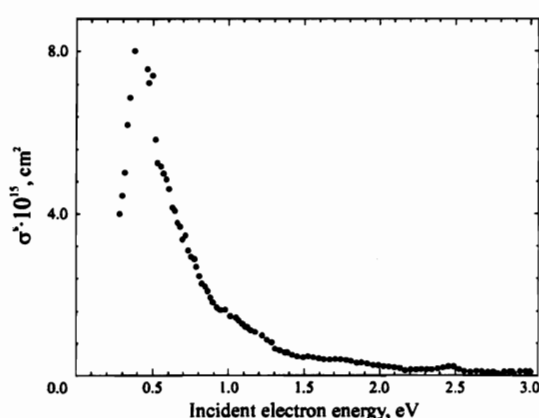


Figure. Energy dependence of the effective superelastic electron scattering by the metastable

$6s^26p\ ^2P_{3/2}$ Tl atoms

[1] V.I. Marushka, I.I. Shafranyosh. Technical Physics// 2008.– V. 53, No. 4.– P. 529–531.

The analysis of the data (see figure) has shown that the scattering cross section reveals a distinct structure in a form of narrow resonances superimposed at the 0.4 eV and 0.55 eV energies. The presence of the above structure indicates a complicated mechanism of superelastic electron scattering process, which is, possible, related to the formation and decay of the negative thallium ion.

Ionization and Dissociative Ionization of Adenine Molecules by Electron Impact near Threshold

O.B.Shpenik, A.N.Zavilopulo

Institute of Electron Physics, Ukr. Nat. Acad. Sci.

21 Universitetska str., Uzhgorod 88017, Ukraine

E-mail: an@zvl.iep.uzhgorod.ua

An increased interest to the studies of biomolecules by traditional methods of physics of electron collisions is explained by the significance of these molecules in modern life. Here we report on a study of the features of the process of ionization, including dissociative ionization, of adenine molecules under electron impact, accompanied by the formation of ionized products of reaction. The experimental setup, used for the investigation of partial cross-sections of dissociative ionization of molecules by electron impact, is described in detail in a number of our papers (See, e. g., [1]). The setup is constructed on the base of a monopole mass spectrometer with an electron ionizer and a multichannel molecule source of effusion type. The ionic products of dissociative ionization, separated by the high-frequency field of the analyser, were detected by a channeltron. The scanning of the ionizing electron energy and data acquisition were performed using a computer and a specially developed software. The duration of one measurement cycle was chosen in such a way that the number of pulses of the useful signal in the maximum of the energy dependence curve should not be less than 10^4 . In short, the measurement technique was the following. At first the adenine molecule mass spectrum was measured at the ionizing electron energy of 40 and 70 eV, then for each fragment the dissociative ionization function was measured. The mass scale was calibrated using *Ar*, *Kr* and *Xe*, and a special procedure of polynomial fitting of the threshold part of the ionization cross-section [2] was used to determine the appearance potentials of various ion fragment groups. The fragment appearance potentials were determined from the threshold dependences of the ion yield. We also studied temperature dependences of intensities of the ion fragments of the initial molecule in the temperature range 343 – 480 K. The measurement technique was reduced to the measurement of mass spectra at various temperatures at $E_{ion} = 50$ eV. From the temperature dependences, the evolution of the fragment formation could be traced and the effect of temperature on the dissociative ionization could be observed. We have measured energy dependences of the total cross-section of the adenine molecule ionization as well as the cross-sections of dissociative ionization of formation of the fragment ions. We have also determined the appearance potentials for the fragment ions with $m/e = 43, 54, 81, 108$.

This work was supported in part by the CRDF Grant $\#UKC - 2832 - UZ - 06$.

References

- [1] A.N. Zavilopulo, O.B. Shpenik, V.A. Surkov, *Anal.Chim.Acta* **573-74**, 427-431 (2006).
- [2] T. Fiegele, *at.al, J.Phys.B: Atom. Mol. Opt. Phys.* **33**, 4263-4269 (2000).

Absorption effects in intermediate-energy electron scattering by difluoroethylene

L. E. Machado*, I. Iga[†], L. M. Brescansin[§], and M.-T. Lee[†]

**Departamento de Física, UFSCar, 13565-905, São Carlos, SP, Brazil*

[†]*Departamento de Química, UFSCar, 13565-905, São Carlos, SP, Brazil*

[§]*Instituto de Física "Gleb Wataghin", UNICAMP, 13083-970, Campinas, SP, Brazil*

Although several solid-based *ab-initio* theoretical methods have been developed in the past few decades for the investigation on electron-molecule collisions, most of them can only be successfully applied in the low incident electron energy range. The extension of their application to the intermediate-energy range (roughly from the first ionization potential to around 1 keV) is not straightforward. It is known that at these energies the numerous open inelastic scattering channels are responsible for absorption effects that play important role on the collision dynamics. In the last two decades, several model absorption potentials have been proposed to include absorption effects into the scattering dynamics and so, the resolution of the scattering equations is kept in the single-channel framework.

Although these model-potential methods have shown to provide, in general, quite accurate differential (DCS), integral (ICS) and momentum-transfer (MTCS) cross sections for elastic electron-molecule collisions, most of the calculations have systematically underestimated the values of the grand-total (TCS) and total absorption (TACS) cross sections. In recent papers [1], our group has reported a modified version of the widely used Stazewska's version 3 of the quasi-free scattering model (QFSM3) absorption potential [2]. In order to obtain a better description of screening effects due to the target electronic cloud, we have proposed a multiplicative screening factor that should be applied on the original QFSM3 absorption potential. In our works [1], we have shown that such a simple modification in the absorption model potential is capable of providing significant improvement in the calculated TCS and TACS for a variety of targets for intermediate-energy electron-molecule collisions.

In the present work we apply our modified model absorption potential to study electron scattering by a strongly polar molecule, *cis*-difluoroethylene in a wide incident energy range (1-500 eV). Results of DCS, ICS, MTCS, TCS and TACS will be presented at the Conference.

References

- [1] Lee M.-T., Iga, I., Machado, L. E., Brescansin, L. M., y Castro, E. A., Sanches, I. P., and de Souza, G. L. C., J. Electron Spectrosc. Rel. Phenom. **115** 14 (2007); y Castro, E. A., de Souza, G. L. C., Iga, I., Machado, L. E., Brescansin, L. M., and Lee M.-T., J. Electron Spectrosc. Rel. Phenom. **159** 30 (2007)
- [2] Stazewska, G., Schwenke, D. W., Thirumalai, D., and Truhlar, D. G., Phys. Rev. A **28** 2740 (1983)

Charge transfer in collision of protons with water molecule and atomic helium at high energy

S. Houamer¹, Y. Popov², C. Champion³ and C. Dal Cappello³

¹*Laboratoire de Physique Quantique et Systèmes dynamiques, Département de physique, Faculté des sciences, Université Ferhat Abbas, Sétif, 19000, Algeria*

²*Nuclear Physics Institute, Moscow state University, Moscow 119899, Russia*

³*Laboratoire de Physique Moléculaire et des Collisions, Institut de Physique, 1 Boulevard Arago, 57078 Metz Cedex 3, France*

Charge transfer process in collision of protons with water molecule and helium is investigated at high energy using a first Born model in which different reaction mechanisms are considered. A sophisticated configuration interaction wave function is used to describe helium atom while the projectile is described by a plane wave.

The process is investigated for H₂O molecule in the frozen core model where the target is described by a single center wave function successfully used formerly in ionization process. The SDCS is calculated for both targets at high impact energy $E_i = 1.4 \text{ MeV}$. The TCS is then deduced by direct integration over solid angle in an energy range between 0.1 and 3 MeV. The results are finally compared with experiments in order to check the validity of the model.

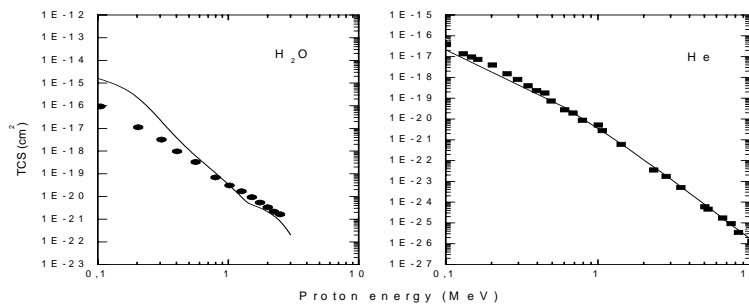


Fig. 1 Absolute TCS for electron capture in proton collision with H₂O and He. Experimental data are taken from [1] for H₂O and [2] for He.

It should be noted that for a water molecule three more integrations must be performed to average over the random orientation of the molecular target.

[1] J. H. Toburen, M. Y. Nakal and R. A. Langley, Phys. Rev. **171**, 114 (1968)

[2] I. Mancev, V. Mergel and L. Schmidt, J. Phys. B **36** 2733 (2003)

Ar($3p^5 4p$) states excitation in low-energy Ar-Ar collisions

S. Yu. Kurskov and A. S. Kashuba

*Department of Physics and Engineering, Petrozavodsk State University
Lenin 33, 185910 Petrozavodsk, Russia
E-mail: kurskov@psu.karelia.ru*

The present work is devoted to study of Ar($3p^5 4p$) states excitation in binary low-energy Ar-Ar collisions. The purpose of this work is the research of mechanisms of atomic levels excitation at collision energies that corresponds of the adiabatic approximation conditions. The results of the experimental investigation of excitation cross sections of Ar I $4p'[1/2]_1$, $4p'[3/2]_1$, $4p'[3/2]_2$ and $4p[3/2]_2$ levels in the collision energy range from threshold up to 500 eV (centre of mass system) and degree of polarization for $4s[3/2]_2^0 - 4p'[1/2]_1$ and $4s[3/2]_2^0 - 4p[3/2]_2$ transitions in this energy range are represented.

The measurements of the cross sections at interaction of an atomic beam with a gas target were carried out by optical methods on setup, controlled by computer. The measurement procedure was described in detail in the work [1].

The obtained results demonstrate that the polarization degree of emission significantly depends on collision energy – when the latter goes up, the former changes its sign. The fact that the sign of the polarization degree changes, as well as does interaction energy, proves that the mechanism of level population changes too [2]. For instance, since the angular momentum of $4p'[1/2]_1$ excitation level is equal to 1, the positive polarization degree shows that the magnetic sublevel σ_0 , that is zero momentum projection onto internuclear axis of the Ar₂ quasimolecule, is mostly populated. Negative polarization degree, in its turn, means that there is a dense population at magnetic sublevels σ_1 , corresponding to ± 1 projections. Therefore, according to the data obtained, if collision energy is higher than 400 eV, the population at the mentioned above level is determined by $\Sigma_g - \Sigma'_g$ transactions. If collision energy is equal to or lower than 300 eV, level population is guided by $\Sigma_g - \Pi_g$ transactions due to radial coupling of even terms of the Ar₂ quasimolecule. It is important to note that since output Σ_g terms of the Ar₂ quasimolecule are actually double excited terms, supposedly, the other interacting atom is excited too. This fact agrees with Wigner's law (system spin unchanged at collision) and with the research results described in works [3, 4]. The diabatic molecular orbital diagram for homonuclear system [5] and measurement results of the polarization of emission lead to the following conclusion: if collision energy is less or equal to 300 eV, the population of $4p'[1/2]_1$ level is determined by $4p\sigma - 4p\pi$ transactions due to rotational coupling at small nuclear distances. In case of higher energies, the population is governed by $5f\sigma - 5d\sigma$ transactions due to non-adiabatic radial coupling.

Reference

- [1] S.Yu. Kurskov, A.D. Khakhaev, Czech. J. Phys. **56**, B297 (2006).
- [2] K. Blum, *Density Matrix Theory and Applications* (N.Y., Plenum Press, 1981).
- [3] P.J. Martin, G. Riecke, J. Hermann et al., J. Phys. **B11**, 1991 (1978).
- [4] L. Moorman, V. van Hoegaerden, J. van Eck et al., J. Phys. **B20**, 6267 (1987).
- [5] M. Barat, W. Lichten, Phys. Rev. **A6**, 211 (1972).

Low-energy electron scattering from calcium

S. Gedeon and V. Lazur

Department of Theoretical Physics, Uzhgorod National University, 88000, Ukraine

E-mail: vfg-vik@yandex.ru

The B-spline R-matrix method (BSR) [1] is used to investigate the integrated cross sections (ICS) of elastic electron scattering from neutral calcium in the ultra-low energy range from threshold to 0.5 eV. The close-coupling expansion includes 39 bound states of neutral calcium, covering all states from the ground state to $4s8s\ ^1S$. The computational model was described in detail in [2]. Briefly, we generate an accurate target description by using multiconfiguration expansions, accounting for both valence and core-valence correlations. Very importantly, we use term-dependent valence orbitals, which are optimized individually for the various states of interest. We also account for relaxation of the core orbitals, due to the deep penetration of the 3d orbital. As a result, we have a set of normalized orthogonal one-electron orbitals for each state, but the orbitals from different sets do not form an orthonormal basis.

In this work we are compared the total and partial electron-impact cross sections from Ca in the ultra-low energy region, calculated in two different R-matrix approaches: the present BSR method and R-matrix with pseudostates method (RMPS) [4]. As seen from our calculations, basic difference between the cross sections in two R-matrix approaches comes mainly from the dominated $^2P^o$ partial wave. In the same time, partial cross sections for the $^2S^e$ and $^2D^e$ partial waves in these two methods practically coincide. In present work we also are compared the total BSR39 and RMPS cross sections with experimental data of Romaniuk et al [3]. Overall, the agreement between both R-matrix (BSR39 and RMPS) results and the experimental data [3] is satisfactory, although a few discrepancies remain. We are compared $^2S^e$, $^2P^o$ and $^2D^e$ partial eigen-phases of electron-impact scattering from Ca at low energies region between most recent calculations: BSR39 (the present calculation), RMPS [4] and method of static-exchange formalism [5]. Again, the largest discrepancy between different method was found for $^2P^o$ partial wave.

References

- [1] O. Zatsarinny, *Comput. Phys. Commun.* **174**, 273 (2006)
- [2] O. Zatsarinny et al., *Phys. Rev. A*, **74**, 052708 (2006)
- [3] N.I. Romanyuk, O.B. Shpenik, I.P. Zapesochnyi, *Pis'ma Zh. Eksp. Teor. Fiz.*, **32**, 472 (1980) [*JETP Lett.* **32**, 452 (1980)]
- [4] K. Bartschat and H.R. Sadeghpour, *J. Phys. B.* **36**, L9 (2003)
- [5] J. Yuan, Zh. Zhang, *Phys. Rev. A* **42**, 5363 (1990)

Ab initio calculation of $\text{H}+\text{He}^+$ electron transfer cross sections

J. Loreau¹, M. Desouter-Lecomte², F. Rosmej³ and N. Vaeck¹

¹*Service de Chimie Quantique, ULB, Brussels, Belgium*

²*LCP, Université de Paris XI, Orsay, France*

³*Université de Provence et CNRS, Centre St. Jérôme, PIIM, Marseille, France*

E-mail: jloreau@ulb.ac.be

Charge transfer mechanisms during collision processes between ions and neutral atoms or molecules have recently received renewed attention, due to their role in the analysis of laboratory and astrophysical plasmas.

To understand the physical processes that underlie plasma transport in magnetically confined plasmas, spectroscopic methods have turned out to be very effective. One of the most powerful of these methods is based on the space and time resolved observation of line emission from impurity ions. However, under real experimental conditions of fusion plasmas, the impurity ions interact with the plasma background H/D which leads to a change of the radial distribution of the impurity ions due to charge exchange processes [1]. As helium is of particular interest for magnetically confined fusion research (production from recombining alpha particles, ash transport), we calculate the charge exchange cross sections between He^+ and the H/D background for numerous channels at low energies (as the electron temperature of divertor plasmas is much below an atomic unit). This implies computational difficulties as a fully quantum mechanical description is needed.

We have used a quasi-molecular approach of the ion-atom collision based on the use of conventional quantum-chemistry *ab initio* methods to obtain the potential energy surfaces as well as the radial and rotational coupling matrix elements of the quasi-molecule HeH^+ . The main problem encountered in this part of our work is the large number of excited molecular states that need to be taken into account, necessitating the introduction of a new basis of molecular orbitals.

A wave packet method is used to treat the curve-crossing dynamics resulting from the failure of the Born-Oppenheimer approximation. A Gaussian wave packet is prepared in the entrance channel and propagated on the coupled effective channels. The collision matrix elements are computed from an analysis of the flux in the asymptotic region by using properties of absorbing potentials, giving access to the charge exchange cross-sections [2]. We study different propagation methods, the influence of the rotational couplings on the cross section as well as the problem of the origin-dependence of the radial and rotational couplings.

References

- [1] F. B. Rosmej, E. Stamm and V. S. Lisitsa. *Europhys. Lett.*, 73, 342 (2006).
- [2] E. Baloïtcha, M. Desouter-Lecomte, M.-C. Bacchus-Montabonel and N. Vaeck. *J. Chem. Phys.* 114, 8741 (2001).

TDCS for inner-shell (e, 2e) processes on alkali and alkali earth atoms Na, K, Be, Mg and Ca.

G. Purohit¹, U Hitawala² and K K Sud^{1,2}

¹*Department of Basic Sciences, Sir Padampat Singhania University
Bhatewar, Udaipur-313601, India*

²*Department of Physics, College of Science Campus,
M.L.S. University, Udaipur-313002, India*

The study of electron impact ionization of atoms and molecules has been of interest, since the early days of atomic and molecular physics, since the kinematics of this process are easily controlled, and the electrons or ions resulting from the reaction can be observed with relative ease. Since the first coincident measurement of (e, 2e) process on atoms by Erhardt et al[1] and Amaldi et al[2] extensive theoretical and experimental investigations have been done to measure the TDCS. A number of different theories have been developed, ranging from first-order Born calculations (and variations therein) which are successful at high incident energies and asymmetric geometries [3] to second and higher order Born calculations, which are successful at higher energies in more complex scattering geometries [4]. Variants on these models include distorted wave Born approximations (DWBAs) that have achieved success down to intermediate energies [58]. Recently U Hitawala et al [9] have calculated the (e, 2e) triple differential cross section for alkali atoms Na and K and alkali earth atoms Mg and Ca. We present in this communication the results of our calculation of triple differential cross section (TDCS) for inner-shell (e, 2e) processes on alkali Na and K and alkali earth Be, Mg and Ca atoms. We discuss the effects of incident electron energy, distortion, nuclear charge, polarization, post collisional interaction etc. for the alkali and alkali earth targets investigated by us.

References

- [1] Ehrhardt H., Schulz M., Tekaath T. and Willmann K., Phys. Rev. Lett. **22**, 89 (1969)
- [2] Amaldi U., Egidi A., Marconnero R., and Pizzella G., Rev.Sci.Instrum. **40**, 1001 (1969).
- [3] Duguet A, Cherid M, Lahmam-Bennani A, Franz A and Klar H 1987 J.Phys.B: At. Mol. Phys. **20** 6145.
- [4] Byron F.W. and Joachain C.J. 1989 Phys. Rep. **179** 211.
- [5] Zhang X, Whelan C.T. and Walters H.R.J. 1990 J.Phys. B:At. Mol.Opt.Phys. **23** L509.
- [6] Rioual S., Pochat A., Gelebart F., Allan R.J., Whelan C.T. and Walters H.R.J., 1995. J.Phys.B:At.Mol.Opt.Phys. **28** 5317
- [7] Rosel T, Roder J, Frost L., Jung K, Ehrhardt H., Jones S. and Madison D.H. 1992 Phys.Rev. **A46** 2539
- [8] Reid R.H.G., Bartchat K. and Raekar A 1998 J. Phys. B: At. Mol.Opt.Phys. **31** 563.
- [9] Hitawala U, Purohit G and Sud K K, J. Phys. B: At. Mol. Opt. Phys. (**In Press**), 2008

The relativistic J-matrix method in scattering of electrons from model potentials and small atoms

P. Syty

*Department of Theoretical Physics And Quantum Informatics
Gdańsk University of Technology
Narutowicza 11/12, 80-952 Gdańsk, Poland
e-mail: sylvas@mif.pg.gda.pl*

The J-matrix method is an algebraic method in quantum scattering theory. It is based on the fact that the radial kinetic energy operator is tridiagonal in some suitable bases. Non-relativistic version of the method was introduced in 1974 by Heller and Yamani [1] and developed by Yamani and Fishman a year after [2]. Relativistic version was introduced in 1998 by P. Horodecki [3].

The main advantage of the method is that it allows to calculate phase shifts for many projectile energies with relatively small computational time. Also, the non-relativistic limit in relativistic calculations is properly achieved. This fact was expected, since the basis sets used in relativistic calculations satisfied the so called kinetic balance condition.

Some preliminary applications of relativistic J-matrix method to scattering have been performed for some square-type potentials [4], using the newly developed Fortran 95 code JMATRIX [5]. These tests proved that the method correctly describes the scattering process.

Since these times, the JMATRIX code has been greatly extended and thoroughly tested. In the present work we applied the code (in both non-relativistic and relativistic versions) to calculate some scattering properties of electrons scattered from more complex potentials, i.e. truncated Coulomb, Yukawa and Lenard-Jones potentials and more. In its primary version, the JMATRIX program allowed for applying scattering potentials in analytical forms only. Now the code has been extended, so it allows for applying scattering potential given in any numerical form, i.e. taken from the GRASP92 code [6].

In conclusion, we present the calculated scattering phase shifts and cross sections for many energies of the incident electrons, in cases of the analytical potentials mentioned previously, as well as the numerical potentials of some small atoms. Also, we illustrate the convergence process and describe some limitations of the method.

References

- [1] E. Heller, H. Yamani, Phys. Rev. A **9**, 1201 (1974)
- [2] H. Yamani, L. Fishman, J. Math. Phys. **16**, 410 (1975)
- [3] P. Horodecki, Phys. Rev. A **62**, 052716 (2000)
- [4] P. Syty, TASK Quarterly **3 No. 3**, 269 (1999)
- [5] P. Syty, <http://aqualung.mif.pg.gda.pl/jmatrix/>
- [6] F.A. Parpia, C. Froese Fischer, I.P. Grant, Comput. Phys. Commun. **94**, 249 (1996)

Multichannel atomic scattering and confinement-induced resonances in waveguides

V.S. Melezhik^{1,*}, S. Saeidian², P. Schmelcher^{2,3}

¹*Bogoliubov Laboratory of Theoretical Physics, Joint Institute for Nuclear Research, Dubna, Russia*

²*Physikalisches Institut, Universität Heidelberg, Philosophenweg 12, 69120 Heidelberg, Germany*

³*Theoretische Chemie, Institut für Physikalische Chemie, Universität Heidelberg, INF 229, 69120 Heidelberg, Germany*

**E-mail: melezhik@theor.jinr.ru*

Pair atomic collisions in restricted geometry principally differ from the conventional two-body free-space scattering. The restricted geometry leads to quantization of the atomic motion in the direction of confinement. Another nontrivial effect for two distinguishable quantum particles in a transverse harmonic trap is the confinement induced nonseparability of the center-of-mass (CM) and the relative motions. These effects can have experimental *mesoscopic* developments for ultracold atoms in optical traps and atomic chips. However, only simple analytical estimates were performed for the special case when identical atoms occupy lowest quantum states of a confining trap. In this zero-energy limit the total atom-atom reflection has been predicted for the case of confinement-induced resonance (CIR)[1]. The origin of the CIR is a virtual transition from the ground transverse state of the confining potential to the closed excited state during the collision[2].

We have investigated what happens if the energy range of colliding atoms encompasses several quantum states of the confining potential[3]. The developed method permits to analyze the transverse excitations/deexcitations and optimal conditions for avoiding decoherence-inducing mechanisms at atomic collisions in waveguides. Special attention was paid to the analysis of the CIRs for nonzero collision energies in the multimode regimes. We have suggested a nontrivial extension of the CIRs theory developed so far only for the single-mode regime at zero-energy limit. We have also fully took into account the coupling between the CM and the relative motions in case of distinguishable atoms[4]. Specifically we explore in detail the recently discovered[5] dual CIR which is based on a destructive interference mechanism leading to complete transmission in the waveguide although the corresponding scattering in free space-exhibits strong *s* and *p* wave scattering. Possible applications include, e.g., cold and ultracold atom-atom collisions in atomic waveguides and electron-impurity scattering in quantum wires.

References

- [1] M. Olshanii, Phys. Rev. Lett. **81**, 938 (1998).
- [2] M.G. Moore, T. Begeman, and M. Olshanii, Phys. Rev. Lett. **91**, 163201 (2003).
- [3] S. Saeidian, V.S. Melezhik, and P. Schmelcher, Phys. Rev. **A 77**, 042721 (2008).
- [4] V.S. Melezhik, J.I. Kim, and P. Schmelcher, Phys. Rev. **A 76**, 053611 (2007).
- [5] J.I. Kim, V.S. Melezhik, and P. Schmelcher, Phys. Rev. Lett. **97**, 193203 (2006).

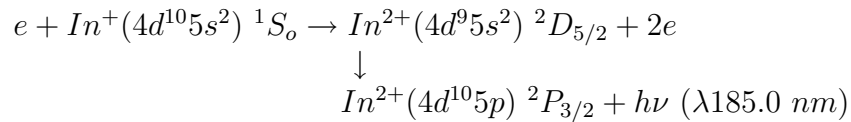
Excitation of forbidden $4d^9 5s^2 \ ^2D_{5/2} \rightarrow 4d^{10} 5s \ ^2P_{3/2}$ transition in In^{2+} ion at electron- In^+ ion collisions

E.Ovcharenko, A.Gomonai, A.Imre, Yu.Hutyach

*Institute of Electron Physics, Ukrainian National Academy of Sciences,
Universitetska 21, 88017 Uzhgorod, Ukraine, e-mail: dep@mail.uzhgorod.ua*

Here we report on the results of experimental investigation of excitation of the $4d^9 5s^2 \ ^2D_{5/2} \rightarrow 4d^{10} 5p \ ^2P_{3/2}$ transition in In^{2+} ion at electron- In^+ ion collisions, which is two-electron dipole forbidden in pure LS -coupling. The experiment was carried out by a photon VUV spectroscopy method using a crossed electron and ion beam technique. The specific features of the experimental technique for studying the processes occurring at the inelastic slow-electron collisions with indium ions are described in detail in [1].

The energy dependence of the effective excitation cross section for the In^{2+} spectral line ($\lambda 185.0 \text{ nm}$ wavelength) was studied from the excitation threshold up to 100 eV according to the following reaction scheme:



A distinct structure in the above energy dependence within the energy range from the threshold ($E_{ex} = 33.18 \text{ eV}$) of the $4d^9 5s^2 \ ^2D_{5/2}$ level up to 50 eV was observed. Since indium ion is a multielectron atomic system with pronounced correlation and relativistic effects, this leads to strong mixing of both the ionic levels and the corresponding autoionizing states (AIS).

The observed structure in the energy range from the threshold up to 40 eV may be assigned to the contribution of the highest $4d^9 5s^2 ({}^2D_{3/2}) np, mf$ AIS as well as to that of the cascade transitions from the $4d^{10} 6s-$, $4d^{10} 5d-$ and $4d^{10} 6p-$ levels, while the structure in the energy range $40 - 45 \text{ eV}$ — to those from the $4d^9 5s 5p-$ levels of In^{2+} ion [2,3] and decay of the In^+ ion autoionizing states converging to the In^{2+} states. A broad maximum above 50 eV is observed, which, we believe, reflects the mechanism of the direct d-ionization process in In^+ ion.

The result obtained, besides the fundamental significance, is of applied importance, since In^+ ion is isoelectronic to Cd atom, and the transition in In^{2+} ion at $\lambda 185.0 \text{ nm}$ is similar to the well-known $\text{Cd}^+ 4d^9 5s^2 \ ^2D_{5/2} \rightarrow 4d^{10} 5p \ ^2P_{3/2}$ laser transition at $\lambda 441.6 \text{ nm}$ in the He- Cd^+ laser. As shown in [4], this radiative transition at $\lambda 185.0 \text{ nm}$ is the best candidate for lasing in vacuum ultraviolet range.

References

- [1] A.Gomonai, E.Ovcharenko, A.Imre, Yu.Hutyach, Nucl. Instr. and Meth. in Phys. Res. B **233**, 250-254 (2005).
- [2] D.Kilbane, J-P.Mosnier, E.T.Kennedy, J.T.Costello, P. van Kampen, J. Phys. B: At. Mol. Opt. Phys. **39**, 773-782 (2006).
- [3] K.S.Bhatia, J. Phys. B: Atom. Molec. Phys. **11**, 2421-2434 (1978).
- [4] R.A.Lacy, A.C.Nilsson, R.L.Byer, J. Opt. Soc. Am. B **6**, 1209-1216 (1989).

The electron affinity of Tungsten

A. O. Lindahl¹, P. Andersson¹, C. Diehl², O. Forstner³, K. Wendt², D. J. Pegg⁴ and D. Hanstorp¹

¹*Department of physics, University of Gothenburg, SE-412 96 Gothenburg, Sweden*

²*Institut für Physik, Johannes Gutenberg-Universität, Mainz, 55099 Mainz, Germany*

³*Institut für Isotopenforschung und Kernphysik, VERA-Laboratory, University of Vienna, Kavalierstrakt A-1090 Wien*

⁴*Department of physics, University of Tennessee, Knoxville, Tennessee 37996, USA
E-mail: anton.lindahl@physics.gu.se*

An improved value of the electron affinity of Tungsten will be presented. The threshold for photodetachment of W^- forming neutral W in the ground state was investigated by measuring the total photodetachment cross section. The electron affinity was obtained from a fit of the Wigner law in the threshold region.

The experiment showed a photodetachment signal below the threshold associated with detachment from the ground state negative ions. This observation indicates the existence of a previously unobserved bound excited state in W^- .

The experiment was performed using the ion beam apparatus GUNILLA (Göteborg University Negative Ion Linear Laser Apparatus). This apparatus, which previously has been used to investigate light negative ions, has been redesigned in order to obtain a higher mass resolution and better transmission. The W^- measurement is an example of the high mass capabilities of the new apparatus. The ion optical design and performance of the apparatus will be described in some detail.

High resolution measurements of molybdenum L-shell satellites and hypersatellites excited by oxygen and neon ions

M. Czarnota¹, D. Banaś¹, M. Berset², D. Chmielewska⁴, J.-Cl. Dousse², J. Hoszowska², Y.-P. Maillard², O. Mauron², M. Pajek¹, M. Polasik³, P. A. Raboud², J. Rzakiewicz⁴, K. Słabkowska³, Z. Sujkowski⁴

¹*Institute of Physics, Jan Kochanowski University, 25-406 Kielce, Poland*

²*Department of Physics, University of Fribourg, CH-1700 Fribourg, Switzerland*

³*Faculty of Chemistry, Nicolaus Copernicus University, 87-100 Toruń, Poland*

⁴*Soltan Institute for Nuclear Studies, 05-400 Otwock-Świerk, Poland*

The observation of L-shell hypersatellites of molybdenum $L\alpha_{1,2}$ ($L_3 \rightarrow M_{4,5}$) and $L\beta_1$ ($L_2 \rightarrow M_4$) x-ray transitions excited in ion-atom collisions are reported. The high-resolution measurements of x-ray satellites and hypersatellites emitted from multiply ionized molybdenum give access to study the fine details of a structure of multi-vacancy states in mid-Z atoms. Such experiments are important for testing the atomic structure calculations, in particular, the relativistic multi-configuration Dirac-Fock (MCDF) approach, including the Breit and QED corrections. In this way the structure calculations can be tested for excited atoms having up to several vacancies in inner shells.

The high-resolution measurements of Mo $L\alpha_{1,2}$ and $L\beta_1$ x-ray satellites excited by oxygen and neon ions were performed at the Philips cyclotron in the Paul Scherrer Institute (PSI) in Villigen, Switzerland, using O^{6+} and Ne^{6+} ions with energy 278.6 MeV and 177.9 MeV respectively. The excited L-x-rays were measured with a high-resolution diffraction von Hamos spectrometer [1] having an instrumental energy resolution of 0.6 eV for studied x-rays. The absolute energy calibration of the spectrometer was about 0.3 eV [2].

In order to interpret the observed structure of $L\alpha_{1,2}$ x-ray satellites and hypersatellites and $L\beta_1$ satellites in molybdenum the relativistic MCDF calculations [3] were performed for multi-vacancy configurations ($L^{-l}M^{-m}N^{-n}$) expected to be excited in collisions with O and Ne ions. These included the x-ray diagram (L^{-1}), satellite ($L^{-1}M^{-m}N^{-n}$), hypersatellite (L^{-2}) and hypersatellite satellite ($L^{-2}M^{-m}N^{-n}$) transitions, with m and n indicating a number of vacancies in the M- and N-shell in the initial state.

To our knowledge, this is the first experimental observation of a direct ion excitation of the L-shell hypersatellites in molybdenum, which is, additionally, clearly interpreted by a complex MCDF calculations performed revealing their internal structure corresponding to the multi-vacancy ($L^{-2}N^{-n}M^{-m}$) configurations.

References

- [1] J. Hoszowska et al., Nucl. Instr. and Meth. A376, 129 (1996)
- [2] M. Czarnota et al., Nucl. Instr. and Meth. B205, 133 (2003)
- [3] M. Polasik, Phys. Rev. A52, 227 (1995)

Electron-impact scattering on boron

L. Bandurina¹, V. Gedeon²

¹*Institute of Electron Physics, Uzhgorod, 88026, Ukraine*

²*Department of Theoretical Physics, Uzhgorod National University, 88000, Ukraine*

E-mail: vfg-vik@yandex.ru

The *B*-spline *R*-matrix (BSR) method [1] is used to investigate electron-impact scattering on neutral boron over an energy range from threshold to 60 eV. A multi-configuration Hartree-Fock method with nonorthogonal orbitals is employed to generate an accurate representation of the target wavefunctions. The present close-coupling expansion includes the 8 bound states of neutral boron derived from the $1s^2 2s^2 2p$, $1s^2 2s 2p^2$, $1s^2 2s^2 3l$ ($l = 0, 1, 2$) configurations, plus twenty pseudo-states. The primary difficulties in the target structure and coupling to the target continuum for B arise from the $2s 2p^2$ configuration. The orbitals in this configuration have been corrected here through configuration interaction with the $2s 2pnl$ and $2p^2 nl$ sequences. These same pseudostate expansions also provide for coupling of $2s 2p^2$ configuration with the target continuum.

Results for angle-integrated and angle-differential cross sections and effective collision strengths are presented for important transitions from the ground state $2s^2 2p^2 P^o$ and the excited $2s^2 p^2 {}^4P$ and $2s^2 3s {}^2S$ states. Results for angle-integrated cross sections are compared with experimental data Kuchenev and Smirnov [2] and predictions from other *R*-matrix calculations Marchalant and Bartschat [3] and Ballance et al [4]. Our predictions for the angle-integrated cross sections show some discrepancies with those from previous calculations carried out with the standard *R*-matrix with pseudostates (RMPS) approach in a similar scattering model [3] and [4]. These discrepancies are mostly due to the different target descriptions, with the present one giving some better agreement with experiment [5] for energy levels. The excitation cross sections exhibit prominent resonance structures in the low-energy region. The energy positions, widths, and classifications for the detected resonances are presented.

References

- [1] O. Zatsarinny, *Comput. Phys. Commun.* **174**, 273 (2006)
- [2] A.K. Kuchenev, Yu.M. Smirnov, *Opt. spectrosc.* **51**, 116 (1981)
- [3] P.J. Marchalant and K. Bartschat, *J. Phys. B* **30**, 4373 (1997)
- [4] C.P. Ballance, D.C. Griffin, K.A. Berrington and N.R. Badnell, *J. Phys. B* **40**, 1131 (2007)
- [5] NIST Atomic Spectra Database, <http://physics.nist.gov>

Observation of He – He collisions using the anticrossing method

E. Baszanowska¹, R. Drozdowski¹, P. Kaminski¹, G. von Oppen²

¹*University of Gdansk, Institute of Experimental Physics, Wita Stwosza 57,
80-952 Gdansk, Poland*

²*Technische Universitat Berlin, Hardenbergstr. 36, D - 110623 Berlin, Germany*

Excitation of He atoms by He⁺-ion impact has been analyzed for a large range of projectile energies. Of particular interest was the intermediate energy region, where the velocity of the projectiles is comparable with the Bohr velocity of the bound electrons of the He-target atoms. It was shown [1] that it is this transition region where the excitation mechanism changes from a process, which essentially can be described within the framework of the molecular orbital model, to a process describable using the Born approximation. In this transition region, saddle dynamics [2] and electron promotion based on the atomic Paul trap mechanism [3] are suitable to describe this excitation process.

In the present investigations we analyzed the excitation of He atoms by He-atom impact in the intermediate-energy range. The post-collisional states contain components with different parity. Therefore the charge distribution of the electronic clouds of the excited atoms can be asymmetric. The charge distribution was determined by using anticrossing spectroscopy. By applying electric fields to the collision volume the singlet and triplet $1snl$ states with $l \geq 2$ can be tuned to near degeneracy. Due to the spin-orbit coupling, the Stark substates with the same rotational and reflection symmetry are strongly mixed. This mixing gives rise to the formation of anticrossings which could be detected as resonance-like variations of the intensity of the emitted spectral lines. In the experimental setup, the intensity of the selected spectral lines emitted by the collisionally excited He atoms in a direction perpendicular to the crossed beams is measured as a function of an electric field applied parallel and antiparallel to the projectile beam. Then, if the population numbers of the anticrossing singlet and triplet levels are not equal, an anticrossing intensity peak is observed. The amplitudes of these anticrossing peaks provide information about the charge distribution of the collisionally excited state. Additionally, the spectrum of the emitted light was measured for various selected values of the field strength.

The symmetric He-He collision system is composed of four equivalent electrons and two identical nuclei. In collisions, the target atom as well as the projectile atom can be excited. Singlet states are populated by direct excitation, but triplet states only by electron exchange. The evolution of the He-He system is expected to be more complex than the He⁺-He evolution, where only one electron is promoted on the two-centre potential of the He⁺ ions. But our measurements show that for intermediate-energy He-He collisions the excited He-target atoms possess electric dipole moments, that is, the charge distributions of the electronic clouds are asymmetric. Since in the He⁺-He collisions this asymmetry is mainly due to a coherent population of the $l \geq 2$ states, we conclude that the Paul-trap mechanism probably plays an important role also in these He-He collisions.

This work was supported by the BW grants of the University of Gdansk: 5200-5-0048-8 and 5200-5-0483-8
 [1] M. Busch, R. Drozdowski, Th. Ludwig and G. von Oppen, J. Phys. B **37**, 2903 (2004)
 [2] J. M. Rost, J.S. Briggs, J. Phys. B **24**, 4293 (1991).
 [3] G. von Oppen, Europhys. Lett. **27**, 279 (1994)

Spin-exchange cross sections at the interaction between ground state rubidium and metastable helium atoms

V.A.Kartoshkin, S.P.Dmitriev, and N.A.Dovator

*A.F.Ioffe Physico-Technical Institute, Russian Academy of Sciences,
Polytechnical str.26, 194021 St.-Petersburg, Russia
E-mail: victor.kart@mail.ioffe.ru.*

At the interaction between spin-polarized excited atom and ground state alkaline metal atom in gas discharge elastic and inelastic processes take place simultaneously. In such a case these two processes influence on each other giving rise to a change of the cross section's value for the elastic process. It means, that besides the chemiionization of the ground state atom at the expense of the atom's excitation energy (inelastic process), an exchange of electrons was shown to be possible without a great depolarization (s.c. spin exchange, or elastic process) [1].

Up to the present there was only one experimental work where the spin-exchange and chemiionization cross sections were measured . The experiment has been done for He* -Cs system [1] .

In order to determine interesting us cross sections we have to separate two simultaneously occurring spin-dependent processes. In the experiment on optical polarization of the helium metastable atoms these atoms may be aligned or oriented along a static magnetic field. It can be shown that the rates of the decay of the orientation $\langle S_{He} \rangle_z$ and alignment $\langle Q_{He} \rangle_{zz}$ of metastable atoms depend on chemiionization and spin-exchange processes as follows

$$1/\tau_{or} = \pi\delta f_{or} = N(1/3 C_{ci} + 1/2 C_{se}),$$

$$1/\tau_{al} = \pi\delta f_{al} = N(1/3 C_{ci} + 3/2 C_{se}),$$

here N is the alkali metal atom concentration, C_{ci} and C_{se} - are the chemiionization and spin-exchange rate constants, δf_{or} and δf_{al} are the widths of the orientation and alignment signals, $1/\tau_i$ is the rate of the decay of the metastable atom's orientation or alignment. As one can see from Eqs., the contribution to the width of the magnetic resonance line for aligned helium atoms should be different from that of oriented atoms. This difference makes it possible to determine the rate constants of the two simultaneously occurring processes. In this work the experiment on optical orientation of atoms has been done for He* -Rb system. It was established that the rate constant for spin exchange (C_{se}) in collision of metastable 2^3S_1 helium atom with a rubidium atom in $6^2S_{1/2}$ ground state equals $(1.8 \pm 0.8)10^{-9}cm^3s^{-1}$. The rate constant for chemiionization of rubidium atoms by metastable helium atoms (C_{ci}) was determined at the same time to be $(3.1 \pm 0.6)10^{-9}cm^3s^{-1}$.

References

- [1] S.P.Dmitriev, N.A.Dovator, and V.A.Kartoshkin, JETP Lett., **66**, 151-154 (1997)

Spin exchange and redistribution of the spin-polarization at the interaction between ground state alkali atoms and nitrogen atoms in gas discharge

V.A.Kartoshkin

*A.F.Ioffe Physico-Technical Institute, Russian Academy of Sciences,
Polytechnical str.26, 194021 St.-Petersburg, Russia.
E-mail: victor.kart@mail.ioffe.ru.*

In gas discharge an effective spin-exchange process is proceeding between spin-polarized ground state alkali atoms and ground state's nitrogen atoms, that demonstrates a conservation of total electron spin and, consequently, a transfer of angular momentum from an ensemble of the previously spin-polarized alkali atoms to the electronic part of the N atoms in $^4S_{3/2}$ state [1].

Consider the behavior of a quasi-molecular system consists of the nitrogen atom with electron spin angular momentum $S_A = 3/2$, and alkali atom with electron spin angular momentum $S_B = 1/2$. If the spins of the two interacting particles be S_A and S_B , there are two molecular states V_i , which correspond to different values of the total spin (S) of the quasi-molecule. In our case there are two molecular terms $V_q(S = 2)$ and $V_t(S = 1)$. Therefore the spin-exchange process can be described by two cross sections σ_1 and σ_2 corresponding to the change in the magnetic quantum numbers of the interacting particles, respectively, $3/2, 1/2 \rightleftharpoons 3/2, -1/2$; $-3/2, 1/2 \rightleftharpoons -1/2, -1/2$; $3/2, -1/2 \rightleftharpoons 1/2, 1/2$; $-1/2, -1/2 \rightleftharpoons -3/2, 1/2$ and $-1/2, -1/2 \rightleftharpoons 1/2, -1/2$; $1/2, -1/2 \rightleftharpoons -1/2, 1/2$. It can be shown that the cross sections are determined as

$$\sigma_1 = 3/4 |f_q - f_t|^2$$

and

$$\sigma_2 = 1/4 |f_q - f_t|^2,$$

where f_q and f_t are the scattering amplitudes on the quintet V_{tq} and triplet V_t terms.

At the recombination of the spin-polarized N atoms the polarization can be transmitted to the N_2 molecules. The mechanism of the N atoms recombination involves nitrogen atom recombination into the $N_2(A^5\Sigma)$ state. At the conservation of angular momentum during the interaction the transfer of angular momentum from atoms to molecules takes place being to the spin-polarization of the N_2 molecule. The redistribution of angular momentum between electron spin system and rotational system in the N_2 molecule results in rotational polarization of the molecule too.

In this work the kinetics of optical orientation and spin-exchange collisions between alkali and nitrogen atoms have been investigated and equations, describing the evolutions of the polarized moments have been received. The equations describing the redistribution of the polarization in the N_2 have been received too.

References

[1] S.P.Dmitriev, N.A.Dovator, and V.A.Kartoshkin, Optika i spektr.(in Russian) **104**, 752-755 (2008)

Large angle e-He scattering — coincidence experiment with magnetic angle changer

L. Kłosowski, M. Piwiński, D. Dziczek, K. Pleskacz and S. Chwirot

*Institute of Physics, Nicolaus Copernicus University
Grudziądzka 5/7, 87-100 Toruń, Poland
E-mail: lklos@fizyka.umk.pl*

Electron impact excitation of 2^1P_1 state of He has been the first collisional process investigated using electron–photon coincidence technique. Since then, similar studies approaching the limit of quantum mechanically complete experiments have been carried out for other collisional systems and stimulated a progress in both theoretical and experimental studies of electronic collisions. At the same time all that work has suffered from lack of experimental data on scattering parameters at large scattering angles. Such measurements could not be carried out for seemingly simple reason – finite dimensions of electron beam sources and energy analysers.

We have shown recently [1] that such measurements could be performed if trajectories of electrons were suitably modified by a so-called magnetic angle changer (MAC) [2, 3], successfully used by other groups in measurements of differential cross-sections [4].

We are presenting new experimental data for electron impact excitation of 2^1P_1 state of He atoms by 100 eV electrons. The measurements were carried out using angular correlations technique with application of MAC and yielded first experimental data on scattering parameters for large scattering angles up to 180° .

Ab initio predictions are fairly consistent for low scattering angles where they are also in good agreement with available experimental data while serious discrepancies exist at large scattering angles [5, 6], where a lack of experimental data made it difficult to improve the consistency of various theoretical models.

References

- [1] L. Kłosowski, M. Piwiński, D. Dziczek, K. Wiśniewska, S. Chwirot, *Meas. Sci. Technol.* **18**, 3801 (2007)
- [2] M. Zubek, N. Gulley, G. C. King, F. H. Read, *J. Phys. B: At. Mol. Opt. Phys.* **29**, L239 (1996)
- [3] F. Read, J. Channing, *Rev. Sci. Instrum.* **67**, 2372 (1996)
- [4] B. Mielewska, *Rad. Phys. Chem.* **76**, 418 (2007)
- [5] N. Andersen, J. W. Gallagher, I. V. Hertel, *Phys. Rep.* **165**, 1 (1988)
- [6] D. V. Fursa, I. Bray, *Phys. Rev. A*, **52**, 1279 (1995)

Diffusion coefficient and viriel coefficient of Krypton Atoms in a Argon Gas at Low and Moderate Temperature

C. Benseddik M.T. Bouazza and M. Bouledroua

¹*Physics Department and LAMA, Badji Mokhtar University, Annaba, Algeria*

²*Faculté de Médecine and LPR, Badji Mokhtar University, Annaba, Algeria*

In the present work, using the Chapman-Enskog method for dilute gases, we have calculated the diffusion coefficients of ground krypton atoms in a very weakly ionized buffer gas of argon. The calculations are carried out quantum mechanically. To do so, we have constructed the potential energy curve, relative to the $^1\Sigma^+$ molecular state, through which a Kr approaches Ar. The data points upon which the construction is made are smoothly connected to the long- and short-range forms. They are supposed to behave analytically like $1/R^n$ and $\alpha \exp(-\beta R)$, respectively. The spectroscopic data, $R_e = 7.42a_0$ and $D_e = 510.084\mu E_h$; are in accordance with what is available in literature. The isotopic effect has also been examined. The classical second virial coefficients are also calculated for several temperatures. Our computation yields a value of the Boyle temperature of about $T_B \sim 545.223K$. Generally, the results of the transport parameters with temperature show an excellent agreement with the available experimental data; the discrepancies do not exceed 5%.

A theoretical report on ultracold collisions of two monatomic cesium

M.T. Bouazza¹ and M. Bouledroua²

¹*Physics Department, Badji Mokhtar University, Annaba, Algeria*

²*Faculté de Médecine and LPR, Badji Mokhtar University, Annaba, Algeria*

In this work, we are interested in the elastic collisions of two ^{133}Cs monatoms at very low temperatures. The behavior of such cold atoms is characterized by two physical parameters: the scattering length α and the effective range r_e . The study begins by the construction of the potential-energy curves of the two possible molecular symmetries, namely, $X^1\Sigma_g^+$ and $a^1\Sigma_u^+$, through which two ground $^{133}\text{Cs}(6s)$ interact. The exchange potential of the form $AR^\alpha \exp(-\beta R)$ is also taken into account. These constructed interatomic potentials are further introduced into the radial-wave equation to determine numerically the elastic phase shifts needed in the calculations of the total and partial cross sections. The scattering length and the effective range are therefore computed by using quantum-mechanical and semiclassical approaches.

Tomography of laser cooled atoms in MOT using Rydberg state excitation

V.M.Entin*, I.I.Beterov, I.I.Ryabtsev, D.B.Tretyakov

Institute of Semiconductor Physics, Pr. Lavrentyeva 13, 630090, Novosibirsk, Russia

*E-mail: *ventin@isp.nsc.ru*

The position selective dimensional study of laser cooled atoms in magneto-optical trap (MOT) usually performed using optical detection. Nevertheless many years ago was developed more precise method of imaging of atomic beams using ionization of atoms and detection of produced electrons and ions using secondary electron multipliers[1]. This technique demonstrates possibility to detect of a few atoms that making it attractive for experiments with small density of atoms[2]. In the current paper we have performed experiment directed to observe difference in the space distribution of Rb atoms in MOT in the first excited state (5P) caused various selection (dark or bright) of the repumping transition.

In the our experiment we produced cold atomic cloud of 10^7 Rb atoms cooled using conventional MOT setup. After that atoms were optically excited to the Rydberg state using cascade transitions: $5S \rightarrow 5P \rightarrow 8S$ (decay) $\rightarrow 6P \rightarrow nS; nD$ ($n \sim 37$). First excitation pulse ($5P \rightarrow 8S$) was performed by pulsed dye laser (Rhodamine G6, 615 nm). Second, pulse of the Ti:Sa laser at 740 nm was applied to the transitions $6P \rightarrow nS; nD$. Laser beams were focused to the trap and crossed under angle near 90 degree. The Rydberg atoms were detected using selective field ionization technique. The Ti:Sa laser beam was 1D scanned across atomic cloud using deflector based on galvanometer driven lens. The optical deflection unit was controlled using computer. It allows us to make position sensitive measurement of the Rydberg state excitation rate.

Averaged data on counts of Rydberg atoms was used to determine population of the 5P state in separate parts of the atomic cloud. Experimental tomography data obtained for locking of the repumping laser to the bright or dark transition, show different 5P 1D profiles of the trap. Observed phenomena was in agreement with theoretical predictions and our previous results[3].

This technique is non-destructive method of measurement of excited state distribution in MOT. It could be used also for space selective reading (or writing) of quantum states for quantum computing experiments in optical lattices.

This work was supported by the Russian Academy of Sciences.

References

- [1] N. F. Ramsey, "Molecular Beams", Clarendon Press, Oxford, (1956).
- [2] I. I. Ryabtsev, D. B. Tretyakov, I. I. Beterov, and V. M. Entin, Phys. Rev. A, 2007, v.76, p.012722.
- [3] V. M. Entin, I. I. Ryabtsev, JETP Letters, 2004, v.80, pp.161-166.

Spatial light modulators for cold atom manipulation

Michael Mestre, Fabienne Diry, Bruno Viaris de Lesegno and Laurence Pruvost

Laboratoire Aimé Cotton, CNRS II, bat 505, campus d'Orsay

91405 Orsay, France

E-mail: laurence.pruvost@lac.u-psud.fr

Spatial Light Modulators (SLM's) are programmable optical elements that can act as dynamical phase holograms on laser beams. Thus, a laser beam can be shaped into a pattern which is the Fourier transform of the hologram. It provides a flexible method to create dipole potentials in order to manipulate small objects. In this context, our group is investigating experiments using SLM's for cold atom cloud manipulation.

First we have focused on response time and diffraction pattern quality issues. We have demonstrated a device involving a SLM and an acousto-optic modulator (AOM/SLM) with a refresh time of some micro-seconds and without bleed effect during the hologram changes [1]. This device would be well-suited for cold atom manipulation with time-dependent dipole potentials. We have also studied different algorithms to calculate holograms.

Then, we have experimented the method on cold rubidium atoms, by applying a blue detuned laser shaped into a hollow Laguerre-Gaussian beam. Such a profile is obtained by applying a helical-phase hologram to the laser beam. The cold atoms have been guided during their fall due to gravity, into the dark region of the Laguerre-Gaussian mode. Being far-detuned from resonance and dark where the atoms spend most of their time, the light field causes little scattering-induced losses and guiding is efficient. The efficiency is studied versus the detuning and the order of the Laguerre-Gaussian beam and is compared to a model for the atom capture into the two-dimensional potential.

Future applications of this technique will be presented and discussed in the context of cold atoms or Bose-Einstein condensates experiments.

References

- [1] *Fast reconfigurable and transient-less holographic beam-shaping realized by a AOM-SLM device*, M. Mestre, B. Viaris de Lesegno, R. Farcy, L. Pruvost, J. Bourderionnet, A. Delboubé, B. Loiseaux, and, D. Dolfi ; Eur. Phys. J. Appl. Phys. **40**, 269–274 (2007).

All-optical Bose-Einstein Condensation of Chromium atoms and rf spectroscopy of cold Cr_2 molecules

Q. Beaufils¹, R. Chicireanu¹, T. Zanon¹, A. Crubellier², B. Laburthe-Tolra¹, E. Maréchal¹, L. Vernac¹, J.-C. Keller¹ and O. Gorceix¹

¹*Laboratoire de Physique des Lasers, Université Paris-Nord, 99 avenue Jean-Baptiste Clément, 93430-Villetaneuse, France*

²*Laboratoire Aimé Cotton, Bat 505, Campus d'Orsay, 91405 Orsay, France
E-mail: olivier.gorceix@univ-paris13.fr*

The study of quantum gases made of chromium atoms is compelling for several reasons. Being accessible to laser manipulation, chromium has a most abundant bosonic isotope ^{52}Cr and a 9-percent abundant fermionic isotope ^{53}Cr . Most importantly, Cr atoms carry an exceptionally large magnetic moment of $6 \mu_B$. Consequently, Cr provides a valuable tool to study the physics of dipolar quantum gases as demonstrated in [1].

We present our recent achievement of a chromium Bose-Einstein Condensation (Cr-BEC) [2] using an all-optical procedure along with two innovative techniques:

- continuous accumulation of metastable ^{52}Cr atoms in a mixed optical and magnetic trap [3];
- fast and intense rf sweeps to average to zero the magnetic potential and optimize the transfer efficiency from the Cr-MOT to the optical trap [4].

We also report on the rf spectroscopy and association of weakly bound Cr_2 molecules in the decatriplet $^{13}\Sigma_g^+$ state. These latter experiments are performed in the vicinity of a d-wave Feshbach resonance at low magnetic field. Though the association rate is at present fairly low, we can study the spectroscopic properties of these cold trapped high-spin chromium molecules.

This work is supported by Conseil Régional Ile-de-France, MENESR, CNRS, ANR, EU and IFRAF.

References

- [1] T. Lahaye et al. Nature, **448**, 672 (2007)
- [2] Q. Beaufils et al., arXiv :0712.3521
- [3] R. Chicireanu et al., Eur. Phys. J. D, **45**, 189 (2007)
- [4] Q. Beaufils et al., arXiv :0711.0663

Entangled photons from excitonic decay in artificial atoms

Marek Seliger, Ulrich Hohenester, and Gernot Pfanner

Institute for Physics, Karl-Franzens-University Graz, 8010 Graz, Austria

Email: marek.seliger@uni-graz.at

We theoretically investigate the production of polarization-entangled photons through the biexciton cascade decay in a single semiconductor quantum dot. Entangled photons play a key role in quantum communication and computation schemes. Furthermore, generation of single or entangled photons on demand has widespread applications in experiments on a single photon level. Semiconductor quantum dots are very attractive for these devices due to the strong confinement of charge carriers and the resulting atomlike properties.

A biexciton decays radiatively through two intermediate exciton states. If these are degenerate, the two decay paths differ in polarization but are indistinguishable otherwise leading to polarization-entangled photons [1]. This ideal performance is usually spoiled by the electron-hole exchange interaction splitting the intermediate exciton states by a small amount and attaching a which-path information to the photon frequencies.

We discuss strategies to accomplish a high degree of entanglement, despite the exciton finestructure splitting: energetical alignment of the two exciton states [2] or post-selection of photons [3, 4]. We show how passive optical elements (spectral filtering and time shifts) at a single photon level affect the quantum information encoded in the photon wavepacket. Here the solid state environment plays a crucial role in the effective measurement of the intermediate exciton states [5]. Our results suggest that protocols for solid-state based quantum cryptography are more strict than previously thought.

References

- [1] O. Benson, et al., Phys. Rev. Lett. **84**, 2513 (2000).
- [2] R.M. Stevenson, et al., Nature (London) **439**, 179 (2006).
- [3] N. Akopian, et al., Phys. Rev. Lett. **96**, 130501 (2006).
- [4] J.E. Avron, et al., Phys. Rev. Lett. **100**, 120501 (2008).
- [5] U. Hohenester, G. Pfanner, and M. Seliger, Phys. Rev. Lett. **99**, 47402 (2007).

Optimizing number squeezing when splitting a mesoscopic condensate

J. Grond¹, U. Hohenester¹ and J. Schmiedmayer²

¹ *Institut für Physik, Karl-Franzens-Universität Graz,
Universitätsplatz 5, 8010 Graz, Austria,*

² *Atominstitut der österreichischen Universitäten, Technische Universität Wien,
Stadionallee 2, 1020 Wien, Austria
E-mail: julian.grond@uni-graz.at*

An atom interferometer can be built using Bose Einstein condensates, confined in magnetic traps, which are split by continuously transforming the trapping potential [1]. In order to minimize phase diffusion, due to the nonlinearity originating from atom-atom interactions in the condensate, number squeezing of the atoms in the wells is required. Squeezing occurs when tunneling becomes small due to the nonlinear interaction which favors a sharp number distribution in each well.

In adiabatic scenarios, squeezing is severely limited by the timescales of the tunneling dynamics, and therefore non-adiabatic strategies are favorable. In this contribution we show that optimal control theory (OCT) [2] allows to devise control strategies which significantly outperform adiabatic schemes. We first discuss number squeezing in the framework of a generic two-mode model, and give an intuitive physical explanation for the OCT control strategy. For realistic magnetic microtraps, it becomes important to include a non-adiabatic wave function evolution beyond the generic two-mode model. In this work we describe the dynamical evolution of the two orbitals occupied by the atoms within the MCTDHB equations [3], which are based on a variational principle.

Our results cover several squeezing time scales as well as different numbers of atoms in the condensate. We compare adiabatic to non-adiabatic splitting with simple control and optimal control. By using OCT, we can handle non-adiabatic wave function evolution, and obtain number squeezed states on much shorter time scales in comparison to other strategies.

- [1] T. Schumm, S. Hofferberth, L. M. Andersson, S. Wildermuth, S. Groth, I. Bar-Joseph, J. Schmiedmayer, and P. Krüger, *Nat. Phys.* 1, 57 (2005);
G.-B. Jo, Y. Shin, S. Will, T.A. Pasquini, M. Saba, W. Ketterle, D. E. Pritchard, M. Vengalattore, and M. Prentiss, *Phys. Rev. Lett* 98, 030407 (2007);
A. D. Cronin, J. Schmiedmayer and D. E. Pritchard, [quant-ph/arXiv:0712.3703](https://arxiv.org/abs/quant-ph/0712.3703) .
[2] U. Hohenester, P. K. Rekdal, A. Borz, and J. Schmiedmayer, *Phys. Rev. A* 75, 023602 (2007).
[3] O. E. Alon, A. I. Streltsov and L. S. Cederbaum, *Phys. Rev. A* 77, 033613 (2008).

Breakdown of integrability in a quasi-one-dimensional ultracold bosonic gas

I.E. Mazets^{1,2}, T. Schumm¹ and J. Schmiedmayer¹

¹*Atominstytut der Österreichischen Universitäten, TU Wien, A-1020 Vienna, Austria*

²*A.F. Ioffe Physico-Technical Institute, 194021 St. Petersburg, Russia*

We argue that virtual excitations of higher radial modes result in effective three-body collisions that violate integrability in a quasi 1 dimensional atomic Bose gas in a tightly confining waveguide and give rise to thermalization [1]. After adiabatic elimination of virtually excited radial modes, we obtain the Hamiltonian

$$\hat{H}_{3b} = -8 \log \frac{4}{3} \hbar \omega_r \alpha_s^2 \int dz \hat{\psi}^\dagger \hat{\psi}^\dagger \hat{\psi}^\dagger \hat{\psi} \hat{\psi} \hat{\psi}$$

of this effective three-body elastic process. Here ω_r is the fundamental frequency of the radial confinement, α_s is the 3D s -wave scattering length. The corresponding collision rate per atom in a non-degenerate gas is

$$\Gamma_{3b} = C_{3b} \omega_r \zeta^2, \quad \zeta = n_{1D} \alpha_s^2 \sqrt{m \omega_r / \hbar},$$

where $C_{3b} \approx 5.57$, m is the atomic mass, n_{1D} is the 1D atomic number density. We demonstrate that, for typical experimental conditions [2] ($\zeta \approx 0.007$), the three-body processes dominate over thermalization via *real* radial mode excitation in the most energetic pairwise collisions for temperatures $k_B T < 0.4 \hbar \omega_r$. We compare our theoretical findings to the experimental results [3] and stress the further inhibition of thermalization in a one dimensional gas by correlations (atomic anti-bunching due to strong repulsion).

To summarize, a radially confined atomic gas is never perfectly 1D, and radial motion can be excited, either in reality or virtually even if both its temperature and chemical potential are below $\hbar \omega_r$. Such quasi-1D systems exhibit more rich physics than predicted by the Lieb-Liniger model [4].

References

- [1] I. Mazets, T. Schumm and J. Schmiedmayer, arXiv:0802.1701 (2008)
- [2] S. Hofferberth *et al.*, Nature **449**, 324 (2007);
S. Hofferberth, *et al.*, Nature Physics (in print), arXiv: cond-mat/0710.1575.
- [3] T. Kinoshita, T. Wenger, and D.S. Weiss, Nature **440**, 900 (2006).
- [4] E.H. Lieb and W. Liniger, Phys. Rev. **130**, 1605 (1963);
E.H. Lieb, Phys. Rev. **130**, 1616 (1963).

Light-shift tomography in an optical-dipole trap

J-F. Clément, J-P. Brantut, M. Robert de St Vincent, G. Varoquaux, R.A. Nyman, A. Aspect, T. Bourdel and P. Bouyer

*Laboratoire Charles Fabry de l'Institut d'Optique, Campus Polytechnique, RD 128,
91127 Palaiseau France*

We report on light-shift tomography of a cloud of ^{87}Rb in a far-detuned optical-dipole trap. At this wavelength, the excited state of the cooling transition of ^{87}Rb is strongly red-shifted, which enables us to perform energy-resolved imaging. We take advantage of this specific feature by using it in two different situations.

(i) *Mapping of the optical potential.* Starting with a cold cloud with a smooth density profile, we switch on a trapping laser at 1565 nm, and immediately take an absorption image of the atoms in the presence of the trap. By scanning the probe laser frequency, we perform a mapping of the equal light-shift regions.

(ii) *Measurement of the atomic potential energy distribution.* By counting the total number of atoms detected at a given probe detuning, we directly measure the number of atoms having a given potential energy in the trap. We follow the evolution of this atomic distribution for a trapped cloud during the free-evaporation process, starting from a strongly out-of-equilibrium situation and relaxing towards a thermal distribution.

Using a spatially-varying light field, this technique could be used to address atoms situated in regions which size is smaller than the laser wavelength.

Matter wave interferometry with K_2 molecules

S. Liu¹, I. Sherstov², H. Knöckel¹, Chr. Lisdat², E. Tiemann¹

¹*Institut für Quantenoptik, Leibniz Universität Hannover, D-30167 Hannover, Germany*

²*Physikalisch-Technische Bundesanstalt, Bundesallee 100, D-38116 Braunschweig*

We operate a matter wave interferometer on a beam of K_2 molecules in a Ramsey-Bordé configuration [1]. The two exits of this interferometer, with molecules in either the excited state or the ground state, allow distinct detection schemes for the matter wave interference. While observation of the fluorescence of excited state molecules shows the matter wave interferences superimposed on a complicated incoherent background due to the molecular hyperfine structure, detection of ground state molecules behind the interferometer, exciting them with a fixed frequency laser, gives the interference pattern on a simple symmetric background due to a single hyperfine component. Under certain geometric conditions any of the observed matter wave interferences is composed of two distinct structures, a Ramsey-Bordé interference structure from four laser beams employed as beam splitters for the matter wave, and an additional Ramsey interference structure formed by only two laser beams acting as beam splitters.

The higher stability of the Ramsey-Bordé setup due to cancellation of phase drifts and fluctuations in corresponding laser beams promises the Ramsey-Bordé interferometer as a sensitive detector for collisions between molecules and ground state K atoms in the particle beam, when the collisions modify the phase and the damping of the interference pattern. The detection was done by deflecting atoms out of the molecular beam by a resonant laser field, thus switching the experiment between atom-molecule collisions and no collisions.

For a better understanding of the Ramsey interferences, we detected the ground state exit in two different distances near the beam splitters and further away downstream of the molecular beam. With active stabilization of the relative phases of the laser beams used as beam splitters the Ramsey interference shows a good phase stability. The better contrast of the Ramsey matter wave interferences as compared to the Ramsey-Bordé setup recommends this method as well suited for further experimental applications.

We will introduce between the beam splitters a laser field near resonant to a molecular transition from either the excited state or the ground state to another state. Such experiment allows to determine the transition matrix element of the corresponding molecular transition. By changing the collision characteristics of the K atoms by exciting them to Rydberg states, the collisions between potassium atoms and molecules will be investigated. The present status of the matter wave experiment will be presented.

References

[1] Chr. Lisdat, M. Frank, H. Knöckel, M.-L. Almazor, E. Tiemann, Eur. Phys. J. D 12, 235-240 (2000)

A magnetic lens for cold atoms tuned by a rf field

E. Maréchal, B. Laburthe-Tolra, L. Vernac, J.-C. Keller, and O. Gorceix

Laboratoire de Physique des Lasers, UMR 7538 CNRS, Université Paris Nord, 99

Avenue J.-B. Clément, 93430 Villetaneuse, France

Email : marechal@galilee.univ-paris13.fr

The combination of static inhomogeneous magnetic fields with a strong resonant rf field has been recently used in many groups to realize new trapping geometries, like double well potentials, or bubble-like traps [1, 2]. A rf field allows indeed to distort static magnetic potentials into new 'adiabatic potentials' that can be continuously tailored and tuned by changing the rf field parameters [3]. Another possibility is to use rf fields to change the properties of atom-optics elements like magnetic lenses or magnetic mirrors. Following this idea, we have experimentally investigated how the focal length of a magnetic lens can be tuned with rf.

The experiment is performed using a spin polarized cloud of cold cesium atoms. The rf dressed lens is realized with two components : a static magnetic lens, made of a simple coil, and a rf field. The inhomogeneous static field defines a surface where atoms are resonant with the rf field. As atoms cross this surface, their spin is reversed, and the effect of the lens (initially converging or diverging, depending on the initial polarization) is reversed. The magnetic lens is separated by the rf interaction surface into two parts, and become equivalent to a doublet. The position of the interaction region, and therefore the focal length of the doublet can be tuned by changing the rf frequency.

After a 72 cm free fall, atoms cross the lens center, and are focused typically 10 cm below, in a $500 \mu\text{m}$ $1/e^2$ diameter spot. We show that by changing the rf frequency between 100 MHz and 250 MHz, the 10 cm magnetic focal length can be tuned over ± 2 cm. Depending on the rf antenna position, the magnetic lens can be made more converging than without rf, and can be changed by increasing the rf frequency from a converging lens to a converging mirror. The magnetic lens, in combination with a strong rf field, is conveniently described in the dressed-atom picture. The probability that atoms follow the adiabatic rf-dressed potentials can be evaluated by a Landau-Zener model, that determines the rf power requirements to get a lens with good performances. Under our experimental conditions, 10 W of rf is necessary.

Our experimental investigation of the rf-dressed lens, supported by numerical simulations is presented in [4]. This rf-dressing procedure can be combined with the well-developed integrated atom chip technology, to add coherent control to magnetic atom chips.

We acknowledge financial support by IFRAF (MOCA project).

References

- [1] Y. Colombe, E. Knyazchyan, O. Morizot, B. Mercier, V. Lorent, H. Perrin, Europhys. Lett. **67**, 593 (2004)
- [2] I. Lesanovsky, T. Schumm, S. Hofferberth, L. M. Andersson, P. Krüger, J. Schmiedmayer, Phys. Rev. A **73**, 033619 (2006)
- [3] O. Zobay, B. M. Garraway, Phys. Rev. Lett. **86**, 1195 (2001)
- [4] E. Maréchal, B. Laburthe-Tolra, L. Vernac, J.-C. Keller, O. Gorceix, Appl. Phys. B, **91**, 233 (2008)

Stability and d -wave collapse of a dipolar Bose-Einstein condensate

T. Pfau , Th. Lahaye, J. Metz, B. Fröhlich, T. Koch, A. Griesmaier

5. Physikalisches Institut, Universität Stuttgart, Pfaffenwaldring 57, D-70550 Stuttgart, Germany
t.pfau@physik.uni-stuttgart.de

Although the phenomenon of Bose–Einstein condensation is a purely statistical effect that also appears in an ideal gas, the physics of Bose–Einstein condensates (BECs) of dilute gases is considerably enriched by the presence of interactions among the atoms. In usual experiments with BECs, the only relevant interaction is the isotropic and short-range contact interaction, which is described by a single parameter, the scattering length a . In contrast, the dipole–dipole interaction between particles possessing an electric or magnetic dipole moment is of long range character and anisotropic, which gives rise to new phenomena [1]. Most prominently, the stability of a dipolar BEC depends not only on the value of the scattering length a , but also strongly on the geometry of the external trapping potential. Here, we report on the experimental investigation of the stability of a dipolar BEC of ^{52}Cr as a function of the scattering length and the trap aspect ratio. We find good agreement with a universal stability threshold arising from a simple theoretical model. Using a pancake-shaped trap with the dipoles oriented along the short axis of the trap, we are able to tune the scattering length to zero, stabilizing a purely dipolar quantum gas [2].

We also experimentally investigate the collapse dynamics of a dipolar condensate of ^{52}Cr atoms when the s-wave scattering length characterizing the contact interaction is reduced below a critical value. A complex dynamics, involving an anisotropic, d-wave symmetric explosion of the condensate, is observed on time scales significantly shorter than the trap period. At the same time, the condensate atom number decreases abruptly during the collapse. We compare our experimental results with numerical simulations of the three-dimensional Gross-Pitaevskii equation, including the contact and dipolar interactions as well as three-body losses. The simulations indicate that the collapse is accompanied by the formation of two vortex rings with opposite circulations.

References

- [1] Th. Lahaye, T. Koch, B. Fröhlich, M. Fattori, J. Metz, A. Griesmaier, S. Giovanazzi, T. Pfau "Strong dipolar effects in a quantum ferrofluid" *Nature* **448**, 672 (2007).
- [2] T. Koch, Th. Lahaye, J. Metz, B. Fröhlich, A. Griesmaier, T. Pfau "Stabilizing a purely dipolar quantum gas against collapse", *Nature Physics* **4**, 218 (2008).

Blue cooling transitions of thulium atom

K. Chebakov, N. Kolachevsky, A. Akimov, I. Tolstikhina, P. Rodionov, S. Kanorsky, and V. Sorokin

P.N. Lebedev Physics Institute, Leninsky prosp. 53, Moscow, 119991 Russia

It has been shown recently that Yb [1] and Er [2] atoms from the lanthanides group can be efficiently laser-cooled using strong transitions near 400 nm. Degenerate Fermi gases of ytterbium have been also recently demonstrated using laser-cooling based technic [3].

Our goal was to investigate the possibility of laser cooling of Tm atom. Among other lanthanides, thulium possesses relatively simple level structure. Moreover, it has only one stable isotope ^{169}Tm with a nuclear spin of $I = 1/2$ which makes possible to use schemes for sub-Doppler cooling. Laser-cooled thulium is a favorable candidate for optical clocks applications, since the forbidden transition between the fine structure sublevels ($J_g = 5/2$) – ($J'_g = 7/2$) of the ground state $4f^{13}6s^2$ ($\lambda = 1.14$ micron) has a spectral width of approximately 1 Hz. The collisional shift of such kind of transitions in lanthanides is suppressed because of the outer closed $6s^2$ shell [4], which allows for precision spectroscopy in a dense atomic cloud.

We studied two candidates for cooling transitions from the ground state $4f^{13}6s^2$ ($J_g = 7/2$) to the states $4f^{12}(^3H_5)5d_{3/2}6s^2$ ($J_e = 9/2$) at 410.6 nm and $4f^{12}(^3F_4)5d_{5/2}6s^2$ ($J_e = 9/2$) at 420.4 nm. By means of saturation absorption spectroscopy, we measured the hyperfine structure and rates of these transitions. We evaluated the life times of appropriate excited levels as 15.9(8) ns and 48(6) ns, respectively. Decay rates from these levels to neighboring opposite-parity levels were evaluated by means of Hartree-Fock calculations [5]. The fraction of atoms which do not return to the ground state is about 10^{-5} and $5 \cdot 10^{-4}$ for the 410.6 nm and 420.4 nm transitions respectively. We conclude that the strong transition at 410.6 nm with relative slow leakage rate can be used for the efficient cooling of Tm I.

We also measured hyperfine structure of two nearby transitions from the ground state to the states $4f^{13}(^2F_{7/2})6s6p(^1P_1)$ ($J_e = 5/2$) at 409.4 nm and $4f^{12}(^3F_4)5d_{5/2}6s^2$ ($J_e = 7/2$) at 418.9 nm, which can be used for Λ -type excitation of $\lambda = 1.14 \mu\text{m}$ transition.

References

- [1] R. Maruyama et al., Phys. Rev. A **68**, 011403(R), (2003).
- [2] J.J. McClelland and J.L. Hansen, Phys. Rev. Lett. **96**, 143005 (2006).
- [3] Takeshi Fukuhara, Yosuke Takasu, Mitsutaka Kumakura, and Yoshiro Takahashi Phys. Rev. Lett. **98**, 030401 (2007).
- [4] C.I. Hancox, S.C. Doret, M.T. Hummon, L. Luo, J.M. Doyle, Nature, **431**, 281 (2004).
- [5] R.D. Cowan, The Theory of Atomic Structure and Spectra, Berkeley, CA: University of California Press, (1981).

Free-fall expansion of finite-temperature Bose-Einstein condensed gas in the non Thomas-Fermi regime

J. Szczepkowski^{1,2}, R. Abdoul^{1,5}, R. Gartman^{1,5},
W. Gawlik^{1,4}, M. Witkowski^{1,3}, J. Zachorowski^{1,4}, M. Zawada^{1,5}

¹*National Laboratory for Atomic Molecular and Optical Physics
Grudziądzka 5, 87-100 Toruń, Poland,*

²*Institute of Physics, Pomeranian University
76-200 Słupsk, Arciszewskiego 22B, Poland,*

³*Institute of Physics, University of Opole
Oleska 48, 45-052 Opole, Poland,*

⁴*Institute of Physics, Jagiellonian University
Reymonta 4, 30-057 Kraków, Poland,*

⁵*Institute of Physics, Nicolaus Copernicus University
Grudziądzka 5, 87-100 Toruń, Poland.*

E-mail: jszczepkowski@wp.pl

Since 1995 we have opportunity to experimental study degenerate and non-degenerate trapped atomic gases at ultra low temperatures. At finite temperatures the free expansion of the dilute gas leads to spatially thermal distinct and condensed phases. The thermal phase is negligible at temperatures much smaller than the critical temperature T_c , and behavior of the condensed part is mainly determined by the interplay between the trapping potential and the atomic interactions. At the temperatures close to T_c there are usually more thermal dilute gases than the condensed one. In this case also interactions between two phases, thermal and condensed, have affect on the behavior of the condensed fraction. The F. Gerbier et all[1] show influence of this interaction to evolution of free falling Bose-Einstein condensate (BEC) in the presence of the thermal fraction for the condensate with assumption the Thomas-Fermi regime in the condensate phase.

In our experiment we analyze a free expansion of ^{87}Rb BEC release from the magnetic trap[1] with presence of the thermal part dilute atomic gases using standard time-of-flight technique. As a result we note the dependence between condensed aspect-ratio (ratio of axial to radial radii) of the condensate as a function of amount of the condensate fraction in the dilute atomic gas, after 15 ms free expansion. We investigate region where the Thomas-Fermi regime is not hold in BEC. The aspect ratio dependence results from interplay between condensed and non-condensed fraction of the dilute gas and a small number of the atoms in the condensed fraction at the temperature close to T_c .

References

- [1] F. Bylicki, W. Gawlik, W. Jastrzębski, A. Noga, J. Szczepkowski, M. Witkowski, J. Zachorowski, M. Zawada, *Acta Phys. Polon. A* **113**, 691 (2008)
[2] F. Gerbier, J. H. Thywissen, S. Richard, M. Hugbart, P. Bouyer, and A. Aspect, *Phys. Rev. A* , **70**, 013607 (2004)

Resonance Interaction between Cold Rb Atoms and a Frequency Comb

E. Tereschenko^{1,2}, M. Egorov^{1,2}, A. Sokolov^{1,2}, A. Akimov^{1,2}, V. Sorokin^{1,2},
N. Kolachevsky^{1,2}

¹ *P.N. Lebedev Physics Institute, Leninsky prosp. 53, 119991 Moscow, Russia*

² *Moscow Institute of Physics and Technology, 141704 Dolgoprudny, Russia*

A long life time of atoms in a magneto-optical trap (MOT) makes it a powerful tool to study interactions with optical fields processing small cross sections (see e.g. [1]). Since the life time in MOT can reach a few seconds, even processes with characteristic rates of 1 s^{-1} can be easily analyzed if they result in losses of trapped atoms.

We have investigated the interaction of laser-cooled ^{87}Rb atoms in a MOT with a femtosecond (fs) laser radiation in the spectral region 760-820 nm. We show that in a wide range of average intensities of the fs laser field ($< 300\text{ W/cm}^2$) the dominating process is the cascade ionization. In this case the femtosecond radiation interacts with the atomic ensemble both as spectrally-narrow components (a frequency comb) and as a powerful ionizing laser field. Atoms excited by a single mode of a frequency comb from the $5P_{3/2}(F=3)$ to the $5D_{5/2}(F=2,3,4)$ hyperfine sublevels are consequently ionized by a full power of the fs laser from the $5D$ level to the continuum. By tuning the repetition rate f_{rep} of the fs laser we observe the periodic spectrum in the MOT luminescence at 780 nm (the cooling transition) reproducing the hyperfine structure of the $5D$ level (see Fig. 1a).

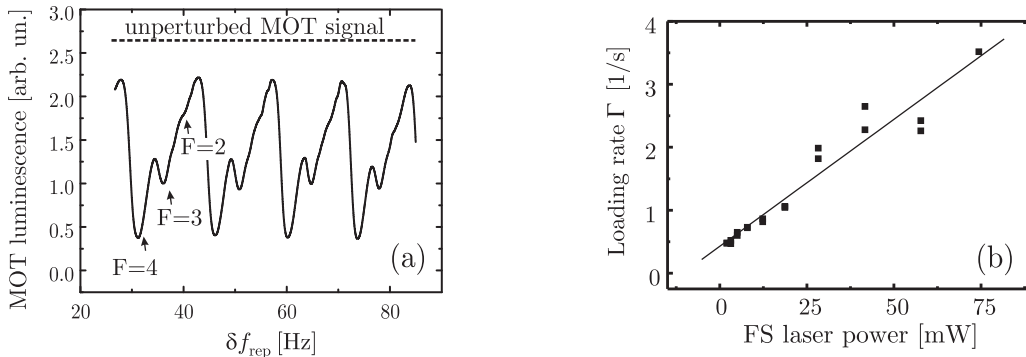


Figure 1: (a) — MOT luminescence signal *vs.* detuning of the fs laser repetition rate δf_{rep} . (b) — dependency of the MOT loading rate on the fs laser power.

We have quantitatively analyzed the ionization of the $5D_{5/2}$ level by monitoring the loading rate of the MOT at different powers of the fs laser radiation (Fig. 1b) using an auxiliary cw laser locked to the $5P_{3/2}(F=3) \rightarrow 5D_{5/2}(F=4)$ at 776 nm. A sensitive method allowing accurate determination of the $5/2$ $5D$ level population is developed [2].

[1] O. Marago, D. Ciampini, F. Fuso, E. Arimondo, C. Gabbanini, and S. T. Manson, *Phys. Rev. A* **57**, R4110 (1998).

Optical tailoring of spatial distribution of the BEC and non-degenerate cold atoms. Non-periodic optical lattice

M. Witkowski^{1,3}, R. Gartman^{1,5}, W. Gawlik^{1,4}, J. Szczepkowski^{1,2}, M. Zawada^{1,5}

¹*National Laboratory for Atomic Molecular and Optical Physics
Grudziądzka 5, 87-100 Toruń, Poland,*

²*Institute of Physics, Pomeranian University
76-200 Słupsk, Arciszewskiego 22B, Poland,*

³*Institute of Physics, University of Opole
Oleska 48, 45-052 Opole, Poland,*

⁴*Institute of Physics, Jagiellonian University
Reymonta 4, 30-057 Kraków, Poland,*

⁵*Institute of Physics, Nicolaus Copernicus University
Grudziądzka 5, 87-100 Toruń, Poland.*

E-mail: mwitkowski@uni.opole.pl

Optical lattices are the instruments of great importance in many fields of atomic physics like manipulating of neutral particles, quantum computing, etc. The common method of getting a periodic optical lattice is to use the interference of two or more laser beams which form an array of periodic light-shift potentials.

We demonstrate a new method of creating an optical lattice of either non-degenerate cold atoms or Bose-Einstein condensates. The lattice is obtained when the cloud of cold atoms is illuminated by a focused, off-resonant laser beam split into several beams by a diffraction process. The resulting lattice is non-periodic.

In our experiment we used ⁸⁷Rb atoms trapped in the magnetic trap of the Ioffe-Pritchard type. This is an anisotropic and harmonic trap characterized by frequencies: radial $\omega_r = 2\pi \cdot 137$ Hz and axial $\omega_a = 2\pi \cdot 12$ Hz [1]. The laser beam of a frequency close to the D_1 line of ⁸⁷Rb was used in the experiment.

We analyze the evolution of that kind of lattice either in a magnetic trap or during time of flight after the atoms are released from the trap. Due to interactions between atoms and near resonant light the characteristic regular structure of atoms appears. We characterize the basic properties of this structure in two cases of a nondegenerate atom cloud and a BEC. In particular, we analyze the effect of the laser frequency on the formation process of optical lattice.

Our method can be another way of studying phenomena where an optical lattice is a necessary instrument. The presented method of creating the optical lattice might be an alternative to the standard counter-propagating laser beams method.

References

[1] F. Bylicki, W. Gawlik, W. Jastrzębski, A. Noga, J. Szczepkowski, M. Witkowski, J. Zachorowski, M. Zawada, *Acta Phys. Polon. A* **113**, 691 (2008).

Laser techniques for atom-scale technologies

F. Tantussi, N. Porfido, F. Prescimone, V. Mangasuli,
M. Allegrini, E. Arimondo and F. Fuso

*CNISM and Dipartimento di Fisica Enrico Fermi, Università di Pisa
Largo Bruno Pontecorvo 3, I-56127 Pisa, Italy
e-mail: fuso@df.unipi.it*

Among the various applications envisioned for laser-cooling and manipulation of neutral atoms, those dealing with nanostructure fabrication appear particularly challenging. Atomic NanoFabrication (ANF [1]) demonstrated production of regular nanopatterns through the occurrence of dipolar forces and the consequent spatial segregation of an atom beam (optical mask). Recently, large technological interest is being attributed to develop methods for the controlled deposition of few, eventually single, atoms onto a surface. The realization of atom-scale technologies is one of the major challenges in realizing novel nanodevices from single atomic, or molecular, elements, with a potentially large impact in emerging areas such as nanophotonics, spintronics, quantum computation systems, advanced biomedical applications.

We have developed an experimental setup aimed at directly depositing few atoms onto a surface under laser-manipulation control. Core of the setup is a Cesium beam produced out of a modified magneto-optical trap (MOT) [2] which exhibits sub-thermal kinetic energy in the longitudinal direction and, after due collimation by 2D optical molasses, shows a residual divergence in the mrad range. The setup has been already employed in resist-assisted fabrication of regular arrays of nanotrenches (45 nm wide) onto Gold through interaction with a 1D optical mask [3]. We are presently exploring the regime of low flux, low temperature direct deposition [4]. Thanks to an in-situ Scanning Tunnelling Microscope (STM), sample features can be investigated at the atomic scale. A variety of substrates has been used, ranging through Graphite to organic self-assembled monolayers. Deposition of stable isolated Cesium nanostructures consisting of a few atoms has been demonstrated, with metal-like electronic features. Due to the small longitudinal velocity of the atoms, relatively long interaction times with the optical mask can be achieved, leading to the occurrence of a pure channelling regime for the guided atom trajectories. In the low surface coverage regime, the interaction produces both a spatial modulation of the deposited atom density and a peculiar nanoisland morphology, which acquires a cigar-like shape oriented in agreement with the optical mask. Results suggest however that nanostructure features are ruled by a complicated interplay between laser-manipulation and local properties of the substrate, involving a variety of surface physics effects to be still completely unravelled.

Financial support by Fondazione Cassa di Risparmio di Pisa (PR/05/137) is gratefully acknowledged.

References

- [1] For a review see, for instance, D. Meschede and H. Metcalf, *J. Phys. D* **36**, R17 (2003).
- [2] A. Camposeo, et al., *Opt. Commun.* **200**, 231 (2001).
- [3] C. O'Dwyer, et al., *Nanotechnology* **16**, 1536 (2005).
- [4] F. Tantussi, et al., *Mat. Sci. Eng. C* **27**, 1418 (2007).

Emission from Silicon/Gold nanoparticle systems

M. Bassu¹, F. Tantussi¹, L. Strambini², G. Barillaro², M. Allegrini¹, F. Fuso¹

¹ *CNISM and Dipartimento di Fisica E. Fermi, Università di Pisa, I-56127 Pisa, Italy*

² *Dipartimento di Ingegneria dell'Informazione, Università di Pisa, I-56122 Pisa, Italy*
e-mail: fuso@df.unipi.it

Investigation of systems comprising metal nanoparticles (NPs) with plasmonic features and light-emitting Silicon is stimulated by distinct motivations. First of all, integration of NPs with materials and technologies used in conventional optoelectronics represents an important step towards practical applications in the emerging areas of plasmonics and nanophotonics [1]; moreover, spectroscopy of such systems opens the way to study the interplay between distinct sub-systems with specific optical properties. When properly designed, such interplay can be used to tailor the system behavior, for instance by modifying the emission spectrum or the overall quantum efficiency.

We have analyzed photoluminescence (PL) of samples produced by a novel anodization-free electrochemical etching of Si catalyzed by Gold NPs. The process is based on the production of Au NPs through rapid thermal annealing of a thin Au film evaporated onto a Si wafer. Etching in a H₂O₂:HF (10:1) solution then leads to mesopore structures diverging from Au NPs. Microscopy of the produced samples demonstrates the achievement of a porous-Si network embedding NPs typically sized in the few tens of nanometers range. The technique, which can be considered as a variant of the HOME-HF process [2], exhibits technologically appealing features: for instance, no anodization is required, favoring integration with conventional Si technologies; by lithographical definition of the pristine Au film, porization can be easily achieved in predefined patterns, thus leading to nanostructured light-emitting samples.

Samples produced in various conditions, starting from either p- or n-doped Si, have been analyzed upon both cw and pulsed laser excitation in the violet/UV range, at room and low temperature. Results demonstrate efficient PL in the visible, peaked around 600-650 nm. Comparison with samples which underwent an Au-removal process based on chemical etching suggests that NPs play a prominent role in ruling the emission: after Au-removal the emission intensity gets remarkably smaller and is spectrally shifted. The role of NPs is well confirmed by simulations of the plasmon resonance for Au NPs in the actual conditions (size distribution and dielectric constant of the embedding medium) experienced in the samples, resulting peaked slightly above 600 nm. Analysis of the emission lifetime as a function of the temperature reveals a puzzling behavior which suggests an intriguing contribution of both radiative and non-radiative phenomena. Nanoscopic investigations have been started based on scanning near-field optical microscopy (SNOM), a technique already proven successful with similar systems [3]. Results show distinctive features for the near-field maps which describe scattering and emission, simultaneously acquired with our SNOM. Interpretation, still in progress, will shed light on the interaction between NPs and Si occurring in the near-field.

References

- [1] For a review see, for instance, S. Maier, et al., *Nature Materials* **2**, 229 (2003).
- [2] X. Li and P.W. Bohn, *Appl. Phys. Lett.* **77**, 2572 (2000).
- [3] F. Fuso, et al., *J. Appl. Phys.* **91**, 5495 (2002).

As3d core level studies of (GaMn)As annealed under As capping

I.Ulfat^{1,2}, J.Adell^{1,2}, J.Sadowski^{2,3}, L.Ilver¹ and J.Kanski¹

¹*Department of Applied Physics, Chalmers University of Technology, Goteborg, Sweden*

²*MAX-Lab, Lund University, Lund, Sweden*

³*Institute of Physics, Polish Academy of Sciences, Warszawa, Poland*

In recent years the DMS (GaMn)As has fascinated research community as a promising candidate for spintronic application. It is of exacting significance due to both its compatibility with existing III-V technology and great progress in improving its magnetic properties. Being a supersaturated solid solution of Mn in GaAs matrix, fabricated by low temperature molecular beam epitaxy (LT-MBE), the material contains a high density of various defects compensating Mn acceptors. This results in the deterioration of its magnetic properties as the ferromagnetism in (GaMn)As occurs due to an indirect exchange between magnetic moments of Mn ions mediated by free holes.

The ferromagnetic state of (GaMn)As is known to be established by post growth annealing. Until recently such annealing has been carried out in air or nitrogen. However, once the sample has been exposed to air, its surface cannot be restored. This means that (GaMn)As annealed in this way are not useful for further epitaxial overgrowth to be included in multilayer structures. In order to meet this requirement an innovative annealing procedure was devised in which the reactive medium (oxygen or nitrogen) is replaced by a surface layer of amorphous As thus removing the interstitial Mn [1].

To observe the presence of reacted surface layer containing As, As3d core level spectra taken at BL41 at Swedish National Synchrotron Radiation Facility (MAX-lab) have been analyzed. In order to identify the contribution from the reacted layer, spectra from pure GaAs and (GaMn)As subjected to post growth annealing have been investigated. Our data indicate that the interface between the out-diffusing Mn and the As capping results in a uniform epitaxial continued layer structure of MnAs. This is rather unexpected as zincblende MnAs is known to be unstable, and MBE growth of MnAs on GaAs normally results in the formation of clusters with hexagonal structure.

[1] M.Adell et al., Appl.Phys.Lett.6, 112501 (2005)

Pulsed laser Deposition Simulation for Graphite Target using Mont-Carlo Method

N. Alinejad, M. Jahangiri, F. Izadi

Physics and Nuclear Fusion Research School, Tehran, Iran

Pulsed laser deposition method for producing thin films is investigated. This deposition method include several stages such as absorption of the laser beam in the target material, evaporation of the material producing plume of atoms or molecules, strong interaction of the laser beam with the plumb to produce plasmas, and finally deposition of atoms or molecules on the substrate surface. The growth of the thin film in the initial stage is simulated using Mont Carlo method. Our simulation indicated that by decreasing the duration of the pulse together with the decrease in laser energy, the thin film growth is steady so that the uniform and homogenous layer is produced. Keywords: pulsed laser deposition, thin films, simulation, Graphite PACS No: 310.0310, 140.0140

Precision Measurement of the ${}^3\text{He}$ - ${}^3\text{H}$ mass ratio with the MPIK/UW-PTMS

Christoph Diehl¹, David Pinegar¹, Robert S. Van Dyck Jr.² and Klaus Blaum¹

¹*Max-Planck-Institut für Kernphysik, Saupfercheckweg 1, D-69117 Heidelberg, Germany*

²*Department of Physics, University of Washington, Seattle, WA 98195-1560, USA*
e-mail: christoph.diehl@mpi-hd.mpg.de

The precise determination of the ${}^3\text{He}$ - ${}^3\text{H}$ mass ratio is of utmost importance for the measurement of the electron anti-neutrino mass performed by the Karlsruhe Tritium Neutrino experiment (KATRIN) [1]. By determining this ratio to an uncertainty of 1 part in 10^{11} , systematic errors of the endpoint energy in the β -decay of ${}^3\text{H}$ to ${}^3\text{He}$ can be checked in the data analysis of KATRIN [2].

To reach this precision, a Penning Trap Mass Spectrometer (MPIK/UW-PTMS) was constructed at the University of Washington [3], which is now transferred to the Max-Planck-Institute for Nuclear Physics in Heidelberg in the new division “Stored and Cooled Ions”.

The Penning trap technique allows for the most precise mass measurements ($< 10^{-10}$ relative uncertainty for stable ions) by the determination of the eigenfrequencies of a single stored ion in a superposition of an electric and magnetic field [4].

Special design features of the MPIK/UW-PTMS are the utilization of an external ion source and the double trap configuration. The external Penning ion source efficiently ionizes the helium and tritium gas. Also, external ion creation can give superior elimination of unwanted ion species compared to the previously utilized internal field emission tips. The design as a double Penning trap allows for several monitoring capabilities (e.g. using one trap as a voltage reference), as well as for a faster measurement procedure. This should help to avoid problems due to long-term drifts in the experimental conditions.

The MPIK/UW-PTMS will be set into operation in Heidelberg by the end of 2008. We will present the design of the setup as it was constructed and tested at the University of Washington.

References

- [1] Ch. Weinheimer, Nucl. Phys. B **168**, 5 (2007)
- [2] E. W. Otten, J. Bonn, Ch. Weinheimer, Int. J. Mass Spec. **251**, 173 (2006)
- [3] D. B. Pinegar, S. L. Zafonte, R. S. Van Dyck Jr., Hyperf. Int. **174**, 47 (2007)
- [4] K. Blaum, Phys. Rep. **425**, 1 (2006)

Measured of different atomic parameters of some elements (Ca, Sn, Pb) in a plasma generated by Laser-Induced Breakdown Spectroscopy (LIBS)

A. Alonso-Medina¹, C. Colón¹ and C. Herrán-Martínez²

¹*Dpto. de Física Aplicada, EUIT Industrial, Universidad Politécnica de Madrid (UPM), Spain*

²*Dpto. de Astronomía y Astrofísica II, Facultad de Ciencias Físicas, Universidad Complutense de Madrid, Spain
aurelia.alonso@upm.es*

Data on atomic parameters, Stark widths, Transition Probabilities of spectral lines are of high interest for astrophysics and analytical techniques of stellar plasma diagnosis. The analysis of spectral lines of lead, tin and calcium allow us (with the new generation telescope such as, NASA's Next Generation Space Telescope (NGST)) to obtain information about the physical conditions of the hot stars.

The application of laser ablation for analysis of a solid sample is one of the most important applications of LIBS.

In this work stark widths and Transition Probabilities of some spectral lines of Pb I, Pb II, Pb III, Sn I, Sn II, Ca I and Ca II are measured. The obtained results are compared with available experimental and theoretical values. From the experimental point of view, Laser-Induced-Plasma (LIP) has proved to be a valuable source of spectroscopic data on neutral and ionized species, as can be seen from several recent works (see, e. g., [1-4])

The experiment system is similar to that described in the above mentioned works, a LIP was used as a spectral source. Spectra were recorded and analyzed between 1890 and 7000 Å by a time resolved optical multichannel analyzer. Experimental working conditions of stability and homogeneity of electron density and temperature in the plasma were determined by means of a study of the temporal evolution in different environmental conditions and target composition. The present measurements were carried out with different targets, Sn-Pb with 75%, 25%, 10% lead purity and Pb-Ca with a 99% lead purity, placed in several argon atmosphere and several delay times from laser light pulse. The Local Thermodynamic Equilibrium (LTE) assumption is discussed in the analysis of our experimental working conditions.

References

- [1] A. Alonso-Medina ,C. Colón and A. Zanón, MNRAS **385**, 261 (2008).
- [2] A. Alonso-Medina and C. Colón , A&A **466**, 399 (2007).
- [3] C. Colón, A. Alonso-Medina, Spectrochim. Acta B **61**, 856 (2006).
- [4] A. Alonso-Medina ,C. Colón and C. Herrán-Martínez, ApJ **595**,550 (2003).

This work has been supported by the project CCG07-UPM/ESP-1632 of the UPM. IV PRICIT of the CAM (Comunidad Autónoma de Madrid), SPAIN.

Isotope shift in the electron affinity of sulfur: observation and theory

T. Carette¹, C. Drag², C. Blondel², C. Delsart²,
C. Froese Fischer³, M. Godefroid¹ and O. Scharf¹

¹ *Service de Chimie Quantique et Photophysique, Université Libre de Bruxelles -
CP160/09, B 1050 Brussels, Belgium*

² *Laboratoire Aimé-Cotton, CNRS, Université Paris-sud, F-91405 ORSAY cedex, France*

³ *Department of Electrical Engineering and Computer Science, Box 1679B, Vanderbilt
University, Nashville TN 37235, USA*

Photodetachment microscopy [1] was performed on a beam of S⁻ generated by a hot cathode discharge in a mixture of 98% Ar and 2% CS₂, with the sulfur isotopes in natural abundances. Isotope 34 was selected by a Wien velocity filter. Laser excitation was provided by a CW ring laser operating with the Rhodamine 590 dye. The laser wavenumber was measured by an *Angström* WS-U lambdameter, with an accuracy better than 10⁻³ cm⁻¹. Subtracting the photoelectron energy found by analysing the electron interferogram from the photon energy, one can determine the electron affinity ^eA. The result for ^eA(³⁴S) is 16 752.978(10) cm⁻¹, to be compared to the previously measured ^eA(³²S)=16 752.976(4) cm⁻¹ [2]. Technical correlations between the two measurements lets the isotope shift $\Delta_{exp} = {}^eA({}^{34}S) - {}^eA({}^{32}S)$ be a little more accurate than the more imprecise electron affinity. Numerically $\Delta_{exp} = +0.002(8)$ cm⁻¹, in wich the (2 σ) error bars leave room for a normal or anomalous result.

Ab initio calculations of the isotope shift on the electron affinity from the infinite-mass systems S⁻/S were carried out, adopting the multiconfiguration Hartree-Fock (MCHF) approach using the ATSP2K package [3]. Our model includes in a systematic way valence correlation, limiting the core to the n=2 shell. The one-electron orbitals are optimized using a single- and double- multi-reference expansions. Configuration-interaction (CI) calculations including up to 6·10⁵ configuration state functions were performed in order to complete the convergence patterns of the S⁻ energy, resulting in a unextrapolated *non-relativistic* electron affinity of ^eA([∞]S) = 16 987(44)cm⁻¹. The theoretical isotope shift value $\Delta_{theor} = {}^eA({}^{34}S) - {}^eA({}^{32}S) = -0.0022(2)$ cm⁻¹ is found to be rather small but definitely negative. The analysis of the various contributions reveals a very large specific mass shift that counterbalances the normal mass shift, while the positive field shift is smaller than the total mass contribution by one order of magnitude.

[1] C. Blondel, C. Delsart, and F. Dulieu. *Phys. Rev. Lett.* **77** (1996) 3755.

[2] C. Blondel, W. Chaibi, C. Delsart, C. Drag, F. Goldfarb, and S. Kröger. *Eur. Phys. J. D* **33** (2005) 335 ; C. Blondel, W. Chaibi, C. Delsart, and C. Drag. *J. Phys. B: At. Mol. Opt. Phys.* **39** (2006) 1409;

[3] C. Froese Fischer, G. Tachiev, G. Gaigalas, and M. R. Godefroid. *Comp. Phys. Com.* **176**(2007)559

Theoretical study of attosecond chronoscopy of strong-field atomic photoionization

A.K. Kazansky^{1,2} and N.M. Kabachnik^{3,4}

¹ *Fock Institute of Physics, State University of Sankt Petersburg, Sankt Petersburg 198504, Russia*

² *Donostia International Physics Center, E-20018 San Sebastian/Donostia, Basque Country, Spain*

³ *Fakultät für Physik, Universität Bielefeld, D-33615 Bielefeld, Germany*

⁴ *Institute of Nuclear Physics, Moscow State University, Moscow 119991, Russia*

A model which describes the time evolution of strong-field photoionization of atoms is presented. Based on the numerical solution of the non-stationary Schrödinger equation, the model allows one to predict and to interpret the results of experiments on double photoionization of atoms by a combined action of a very short (attosecond) XUV pulse and a few-cycle IR pulse of a powerful laser at various delay times between the two pulses. Depending on the binding energy of the ionized electron, two types of process are considered. If the electron is tightly bound (Ne case), the XUV pulse ionizes the atom and shakes up another (outer) electron to an excited state, which is subsequently ionized by the strong IR field. For an atom with a weakly bound outer electron (Li case), the IR field ionizes the latter, while the XUV pulse, ionizing the inner shell, terminates (or suppresses) the strong field ionization. In both cases the yield of doubly ionized ions strongly depends on the delay time between the two pulses, revealing "steps", oscillations and other features which characterize the time evolution of the ionization process. The presented model describes qualitatively the results of recent experiments on Ne [1].

References

[1] M. Uiberacker et al., *Nature* **446**, 627 (2007)

Generation of ultra-short X-ray pulses in cluster system during ionization by femto-second optical pulse

A.V. Glushkov^{1,2}, O.Yu. Khetselius², A.V. Loboda²

¹*Institute for Spectroscopy of Russian Academy of Sciences, Troitsk, 142090, Russia*

²*Odessa University, P.O.Box 24a, Odessa-9, 65009*

We present the results of modelling generation of the atto-second VUV and X-ray pulses during ionization of atomic and cluster systems by femto-second optical laser pulse. The concrete data are received for the Ar cluster response, the molecular 2D H₂⁺ response for different inter nuclear distances (R=2.5, 3.5, 7.4, 16a.u.) with smoothed Coulomb potential and atomic (H) response (spectral dependence) under ionization of the system by femto-second optical pulse [1-4]. Our calculation show that the generation of the atto-second X-ray pulses in the cluster system is more effective and profitable (as minimum the 2-3 orders) than in similar molecular atomic one. The generation of the atto-second pulses in the molecular system is more profitable too (as minimum the 1-2 orders) than in similar atomic one. The last achievements in this field demonstrate a possibility of construction of the compact X-ray radiation sources.

References

- [1] A. Glushkov, L.N. Ivanov, J. Phys.B. **26**, L379 (1993)
- [2] A. Glushkov, O. Khetselius, Recent Adv. in Theory of Phys. and Chem. Syst. (Springer). **18** (2008)
- [3] A. Glushkov, et al, Int. Journ. Quant. Chem. **99**, 889 (2004)
- [4] A. Glushkov, O. Khetselius, S. Malinovskaya, Mol. Phys. **24** (2008)

Long-term stability of high-finesse Fabry-Perot resonators made from Ultra-Low-Expansion glass

J. Alnis¹, A. Matveev^{1,2}, C. Parthey¹, N. Kolachevsky^{1,2}, T.W. Hänsch^{1,3}

¹ *MPI für Quantenoptik, Hans-Kopfermann Str. 1, 85748 Garching, Germany*

² *P.N. Lebedev Physics Institute, Leninsky prosp. 53, 119991 Moscow, Russia*

³ *Ludwig-Maximilians University, Geschwister-Scholl-Platz 1, 80539 Munich, Germany*

Sub-Hz line width lasers limited by thermal noise of the high-finesse Fabry-Perot (FP) resonators used for laser stabilization are very important for optical atomic clock community. Usually thermal noise limited operation can be achieved for time scales of approximately 1 min and for longer time scales the drift starts to dominate. The most suitable material for making a stable FP cavity (spacer and mirror substrates) is Ultra Low Expansion glass (ULE). In this work we report on our observations of the long-term stability of ULE FP resonators measured against the hydrogen $1S$ - $2S$ transition and also using an optical frequency comb referenced to a hydrogen maser.

When ULE FP cavity temperature is stabilized around the zero thermal expansion point the FP resonance frequency drift is very small and it is dominated by the aging of the cavity. Our 77.5 mm long ULE FP resonator that is stabilized at the zero expansion temperature [1, 2] has a temperature sensitivity of ca 20 Hz/mK and during 2 weeks of measurements we could clearly observe a linear drift of +60(5) mHz/s (5 kHz/day) at 972 nm due to FP aging while measuring an optical beat note with a stable optical frequency comb. During two 15 h long measurement runs the deviation from a linear drift slope was within 20 Hz (using 100 s counter gate time). It was also observed that, unfortunately, the drift rate slightly changed from day to day.

Our second 972 nm ULE FP cavity (length 77.5 mm) that is stabilized 20K above the optimal zero expansion temperature is having temperature stability of 11 kHz/mK and exhibits frequency fluctuations in 20 kHz range per day that we attribute to the stability of the temperature control. When the temperature controller is activated it takes approximately 2 weeks for this ULE FP cavity resonance frequency to stabilize.

The resonance frequency of our oldest ULE FP resonator (length 15 cm) built in 2004 for dye laser stabilization at 486 nm has been tracked against the hydrogen $1S$ - $2S$ transition for 4 years now. It was observed that during the first year the drift was +80 mHz/s and at present it has decreased to +40 mHz/s at 486 nm. This can be explained by the relaxation of the cavity after mechanical machining. Positive frequency drifts indicate shrinking of the FP length.

References

- [1] J. Alnis, A. Matveev, N. Kolachevsky, Th. Udem, and T.W. Hänsch, Sub-Hz line width diode lasers by stabilization to vibrationally and thermally compensated ultra low expansion glass Fabry-Perot cavities, *Phys. Rev. A*, to appear 2008. arxiv:0801.4199.
- [2] J. Alnis, A. Matveev, N. Kolachevsky, T. Wilken, R. Holzwarth, T.W. Hänsch, Stable diode lasers for hydrogen precision spectroscopy, *Eur. Phys. J. D. Special Topics*, to appear 2008.

Application of Surface-Enhanced-Raman-Scattering (SERS) for *In-Situ* Detection of PAHs in Sea-Water

Heinar Schmidt, Heinz-Detlef Kronfeldt

*Institut für Optik und Atomare Physik, Technische Universität Berlin
Hardenbergstr. 36, 10623 Berlin, heinar@physik.tu-berlin.de*

Enforced monitoring of sea-water requires advanced instrumentation and technologies for long term and unattended observation. In particular real time and *in-situ* sensors are of interest. In this field, sensors tragetting organic pollution are scarce.

We present a sensor based on surface-enhanced Raman scattering (SERS) using disposable SERS substrates as sensing membrane which have been designed for the in-situ detection of polynuclear aromatic hydrocarbons (PAHs). Raman spectroscopy was chosen due to the fingerprinting nature of the spectra useful for the identification of organic substances and SERS was applied to achieve the sensitivity for trace detection in the environment.

The SERS sensor was developed as part of the EU-funded projects SOFIE („*Spectroscopy Using Optical Fibres in the Marine Environment*“) and MISPEC („*Multiparametric in-situ Spectroscopic Measuring Platform for Coastal Monitoring*“) where a field-operable device was constructed, characterised and field-tested in the Baltic Sea, at the Atlantic coast and in the Bosphorus. The underwater system consists (amongst other) of a robust SERS optode which is coupled to a core instrument containing a 785 nm diode laser and an axial spectrograph with TE-cooled CCD detector.

We present results of laboratory tests characterising the SERS substrates in terms of selectivity, adsorption kinetics, adsorption from mixtures of up to eight PAHs and limits of detection for selected PAHs. The influence of salinity, flow conditions and high immunity against turbidity are shown. In-situ SERS and Raman spectra from the sea trials will be presented. The potential and limitations of Raman and SERS spectroscopy will be discussed with a view to marine *in-situ* applications.

Laser Based Isotopic Separation of Atoms

Shahzada Qamar Hussain¹, M. Saleem², Dr. M. Aslam Baig

¹*Quaid-i-Azam University, Department of Physics, Islamabad*

²*COMSATS Institute of Information Technology, Department of Physics, Defence Road
Off Raiwind Road, Lahore, Pakistan*

A design and fabrication of an atomic beam system is presented. The beam source consists of a cylindrical oven made of stainless steel enclosed by a cylindrical heater for producing the vapor of the sample in the oven [1,2]. The atomic beam source is simple, versatile and can be operated at stable temperatures up to $1000K$. The atomic beam apparatus is placed inside the locally developed Time of Flight (TOF) mass spectrometer. Interaction of laser with the atomic beam in the interaction region of the TOF mass spectrometer produces ions that are resolved and detected by the TOF mass spectrometer. The observed signals from the TOF mass spectrometer are correlated with the flight times for different isotopic masses. The optimum performance of the atomic beam-TOF mass spectrometer is checked with the isotope separation of lithium and magnesium. Their relative abundance is found very close to the already cited values in the literature.

The locally designed and fabricated atomic beam-TOF mass spectrometer is therefore capable for the spectroscopic studies of the selected isotopes of elements. The apparatus can be utilized for Laser isotopic separation of light elements possessing sufficient vapor density up to $1000K$.

References:

- [1] "High temperature metal atomic beam sources", K.J. Ross and B. Sonntag, Rev. Sci. Instrum. 66(9), 4409 (1995).
- [2] "High Temperature Materials and Technology", E. Compbell and E. M. Shewood, Wiley, New York, (1967).

Atomic fluorescence coupled into a thin optical fibre

D. Gleeson^{1,2}, V. Minogin^{2,3,4} and S. Nic Chormaic^{1,2}

¹ *Physics Department, University College Cork, Cork, Ireland*

² *Photonics Centre, Tyndall National Institute, Prospect Row, Cork, Ireland*

³ *Dept. of Applied Physics and Instrumentation, Cork Institute of Technology, Bishopstown, Cork, Ireland*

⁴ *Institute of Spectroscopy, Russ. Ac. of Sciences, 142190 Troitsk, Moscow Region, Russia*

E-mail: danny.gleeson@tyndall.ie

In recent years there has been considerable interest in the problem of the interaction between optically excited atoms and dielectric nanobodies. The basic aspects of such an interaction are the modification of the spontaneous emission rate near nanobodies [1-3] and the dependence of the coupling of atomic fluorescence to the nanobody on the strength of the interaction between the atoms and the surface of the nanobody. These studies are important for developing new spectroscopic techniques to measure interactions between atoms and nanobodies as well as developing new experimental schemes to control internal and translational atomic states near optical nanobodies [4, 5].

Here, we report on the spectrum of fluorescence emitted by optically excited atoms into the fundamental guided mode of an optical nanofibre. An ensemble of two level atoms in the vicinity of a nanofibre is considered. The atoms are excited by a laser field near-resonant to the atomic dipole transition and emit fluorescent light. The frequency of the fluorescent light is chosen to be below the cut-off frequency of all guided modes bar the fundamental, and so only this mode is generated by the fluorescent light.

We find that when an atom is far from the surface of the fibre it is most effectively excited by the laser field with a frequency close to the atomic transition for the free atom. When the atom is close to the surface of the fibre, we see that it is now excited at a red-shifted frequency. This shift leads to an asymmetry of the fluorescence line, observed as the power of light coupled into the nanofibre. This selectivity can be used for measuring the strength of the interactions, including the evaluation of the van der Waals constant. It can also be used for the control of the atomic states near optical nanofibers. We evaluate the atomic fluorescence spectrum for ¹³³Cs atoms excited at the 6S-6P optical transition with wavelength 852 nm.

References

- [1] T. Sondergaard and B. Tromborg, *Phys. Rev. A* **64**, 033812 (2001)
- [2] V. V. Klimov and M. Ducloy, *Phys. Rev. A* **69**, 013812 (2004)
- [3] Fam Le Kien, S. Dutta Gupta, V. I. Balykin, and K. Hakuta, *Phys. Rev. A* **72**, 032509 (2005)
- [4] V. I. Balykin, K. Hakuta, Fam Le Kien, J. Q. Liang, and M. Morinaga, *Phys. Rev. A* **70**, 011401 (R) (2004)
- [5] K. P. Nayak, P. N. Melentiev, M. Morinaga, Fam Le Kien, V. I. Balykin, and K. Hakuta, *Opt. Express* **15**, 5431 (2007).

Nonlinear dynamics of atoms in a cavity: The role of finite temperature effects

D.U.Matrasulov¹, T.A.Ruzmetov¹, D.M.Otajanov¹, P.K.Khabibullaev¹,
A.A.Saidov¹ and F.C.Khanna²

¹*Heat Physics Department of the Uzbek Academy of Sciences,
28 Katartal Sreet, 100135 Tashkent, Uzbekistan*

²*Physics Department of the University of Alberta,
Edmonton, Alberta, T6G 2J1 Canada*

E-mail: davrano@yahoo.com

Cavity quantum electrodynamics is an area of physics studying the interaction of atoms with photons in high-finesse cavities in a wide range of the electromagnetic spectrum from microwaves to visible light. The fact that the system “atom + cavity mode” is a quantum system makes cavity quantum electrodynamics (QED) an excellent testing ground for such important issues of modern quantum physics as quantum measurement theory, entanglement, quantum computation, quantum interference and at the same time provides a unique possibility for trapping, cooling and manipulating of atoms. Practical importance of cavity QED is mainly related to potential possibility for manipulating atoms and photons in mesoscopic scales. Therefore, in recent years cavity QED has become one of the hot topics both in theoretical and experimental physics [1- 3].

Since the dynamics of a single atom trapped in a microcavity is governed by quantum electrodynamics, the cavity QED can be considered as an interdisciplinary area. Many subfield of physics, such as quantum and atomic optics, cold atom physics, physics of nanosized systems and quantum information, may use important results of the cavity QED.

Recently cavity QED is considered in the context of nonlinear dynamics [3]. Mapping quantum equations of motion onto classical ones, for the Jaynes-Cummings Hamiltonian, which includes recoil motion of the atom, Prants et. al., explored phase-space dynamics of the atom interacting with a single cavity mode by analyzing Poincare surface sections and calculating Lyapunov exponents [3].

In this work we explore finite-temperature nonlinear dynamics of an atom coupled to a single mode of the cavity field. Applying the formalism of a real-time finite-temperature field theory to the Jaynes-Cummings Hamiltonian and using the same approach as that used in we have studied classical dynamics of the “atom + cavity mode” system in the presence of coupling to a thermal bath.

Using the temperature-dependence of the equations of motion, dependence of the dynamics on heat-bath effects or finite temperature effects are considered. The results show that the dynamics is quite sensitive to the small changes of temperature. This implies that temperature of a thermal bath can be considered as an additional control parameter for the dynamics of an atom coupling to cavity modes.

References

- [1] *Cavity Quantum Electrodynamics*. Edited by P.R.Berman, (Academic, New York 1994).
- [2] Special Issue on Modern Studies of Basic Quantum Concepts. Phys. Scr., **T76** (1998).
- [3] S.V.Prants, M.Edelman, G.M.Zaslavsky, Phys. Rev. E., **66** 046222 (2002).

Storage of optical pulses in solids despite fast relaxation

G.G. Grigoryan¹, Y.T. Pashayan-Leroy², C. Leroy² and S. Guérin²

¹*Institute for Physical Research, 0203, Ashtarak-2, Armenia*

²*Institut Carnot de Bourgogne, UMR 5209 CNRS - Université de Bourgogne, BP 47870, 21078 Dijon, France*

The solid-state systems are very attractive for optical information storage due to their high density, compactness, and absence of diffusion. The main drawbacks of solid-state materials are huge inhomogeneous broadenings. In practice an efficient storage of information requires a large optical depth [1] such that even negligibly weak losses being accumulated at such long distance result in an essential loss of information. In order to reduce the inhomogeneous broadening, it was proposed in a number of works to use the so-called hole burning technique [2]. However, this technique leads to the reduction of the optical depth of the samples employed. The natural question is whether it is possible to store optical information in solids using reduced optical depths.

Analytical studies performed in the limit of short pulses showed that the length of information storage in Λ - type medium depends remarkably on the ratio between the oscillator strengths of the adjacent transitions [3]. In the present work by exploiting this property we propose a novel scheme of short length storage in media featuring fast relaxations.

We perform a complete analytical and numerical study of the full set of the density-matrix and Maxwell equations for both pulses in case of arbitrary relaxation times and arbitrary intensities of the probe and control fields in a Λ - type medium. Our detailed analysis shows that the storage of the probe field in inhomogeneously broadened media is more efficient when we use atoms of different adjacent transition strengths. In this case the control pulse should have longer duration but considerably lower intensity than the probe pulse. The possibility of the retrieval of an intense pulses stored in a medium is also discussed.

References

- [1] M. Fleischauer and M.D. Lukin, Phys. Rev. Lett. **84**, 5094 (2000); I. Novikova, A.V. Gorshkov, D.F. Phillips, A.S. Sørensen, M.D. Lukin, R.L. Walsworth, Phys. Rev. Lett. **98**, 243602 (2007).
- [2] M.S. Shahriar, P.R. Hemmer, S. Lloyd, P.S. Bhatia, A.Craig. Phys. Rev. A **66**, 032301 (2002); M. Nilsson, L. Rippe, S. Kroll, R. Klieber, D. Sutter, Phys. Rev. B **70**, 214116 (2004).
- [3] G.G. Grigoryan and Y.T. Pashayan. Phys. Rev. A **64**, 013816 (2001); G.G. Grigoryan and G.V. Nikoghosyan. Phys. Rev. A **72**, 043814 (2005).

Purcell-enhanced Rayleigh scattering into a Fabry-Perot cavity

Michael Motsch, Martin Zeppenfeld, Gerhard Rempe, and Pepijn W.H. Pinkse

Max-Planck-Institut für Quantenoptik, Hans-Kopfermann-Str. 1, 85748 Garching, Germany

In recent years a growing interest in cold molecules from fields as different as cold chemistry, precision spectroscopy and quantum information science could be observed. Velocity filtering by means of an electrostatic quadrupole guide is an efficient technique to produce slow beams of polar molecules from a thermal reservoir. For formaldehyde, ammonia, and other naturally occurring polar molecules, fluxes of the order of 10^{10} s^{-1} with velocities down to $\sim 10 \text{ m/s}$ with only a handful of occupied rotational states have been demonstrated [1,2]. However, so far no universal method was found to bridge the gap from the cold ($\sim 1 \text{ K}$) to the ultracold ($\leq 1 \text{ mK}$) regime.

Standard laser cooling schemes fail for molecules due to their complex internal level structure, and hence lack of a closed cycling transition. By replacing spontaneous emission with coherent scattering into an optical cavity, the need for a closed transition can be circumvented [3]. To avoid excitation of the molecular system, operating in the far-detuned Rayleigh scattering regime is advantageous. Since Rayleigh scattering cross sections are small compared to typical resonant cross sections and because typical densities of cold molecular samples are limited, it is unclear if enough light can be scattered into the cavity to be detected. To achieve effective cooling, the power of the coherently scattered light must be significantly higher than for detection only.

We have set up a precursor experiment using room-temperature molecules to study the feasibility of cavity-enhanced detection and cooling of thin samples of cold molecules. As a first step in this direction, we plan to experimentally demonstrate that also in the far-detuned Rayleigh scattering regime an optical cavity can enhance the scattered power. In our experiment we use a high-power single-frequency cw-laser operating at 532 nm as a transverse pump beam for Rayleigh scattering into the optical cavity. By changing the cavity finesse, the enhancement of the light scattered into the cavity mode compared to the free-space situation is shown. We study the polarization, pressure and pump power dependence of the Rayleigh scattered light into a single mode of the optical cavity and derive limits for a detectable density of cold polar molecules with the present setup.

References

- [1] T. Junglen, T. Rieger, S.A. Rangwala, P.W.H. Pinkse, and G. Rempe, *Eur. Phys. J. D* **31**, 365 (2003).
- [2] M. Motsch, M. Schenk, L.D. van Buuren, M. Zeppenfeld, P.W.H. Pinkse, and G. Rempe, *Phys. Rev. A* **76**, 061402R (2007).
- [3] P. Horak, G. Hechenblaikner, K.M. Gheri, H. Stecher, and H. Ritsch, *Phys. Rev. Lett.* **79**, 4974 (1997); D. Chan, A.T. Black, and V. Vuletić, *Phys. Rev. Lett.* **90**, 063003 (2003); P. Maunz, T. Puppe, I. Schuster, N. Syassen, P.W.H. Pinkse, and G. Rempe, *Nature* **428**, 50 (2004).

Circular and elliptical dichroism effects in two-photon disintegration of atoms and molecules

M. Ya. Agre

National University of “Kyiv-Mohyla Academy”, 04070, Kyiv, Ukraine

E-mail: magrik@ukr.net

Compact convenient for the analysis expressions for the cross sections considerably simplify studying the interaction of electromagnetic radiation with atomic systems and allow us to discover some fine effects. In present paper on the basis of the general symmetry considerations taking only into account the dipole approximation and without any other approximations used in atomic calculations we derive the compact invariant expressions for the angular distribution of photoelectrons escaping from atoms or molecules in the process of two-photon ionization and for the angular distribution of fragments forming under two-photon two-particle dissociation of molecules. The dependence on all geometric parameters – the unit vector \mathbf{p} determining the direction of photoelectron (photofragments in the case of dissociation) motion, \mathbf{k} specifying the direction of propagation for the electromagnetic radiation and the unit complex vector \mathbf{e} specifying polarization of the radiation – is completely separated in the angular distributions in the form of scalar and triple scalar products of the vectors. The information of the intrinsic structure of the atomic system is included in few constant dynamic parameters of the system that can independently be calculated using the well-known approximations.

In case of atoms and optically inactive molecules the angular distributions contain the term linear in the pseudoscalar degree of circular polarization of the electromagnetic radiation

$\xi = i\mathbf{k} \cdot (\mathbf{e} \times \mathbf{e}^*)$:

$$\xi a \operatorname{Re}[\mathbf{k} \cdot (\mathbf{p} \times \mathbf{e})(\mathbf{p} \cdot \mathbf{e}^*)], \quad (1)$$

where a is a scalar dynamic parameter of the atomic system. The term (1) leads to the interesting effect of elliptical dichroism in the angular distribution of photoelectrons (photofragments of the molecule): under elliptical polarization of the radiation, $0 < |\xi| < 1$, the density of the particle flux depends on the sign of ξ , i.e., on the clock-anticlockwise rotation of the field strength of the electromagnetic wave. However, the term (1) does not lead to the circular dichroism because it vanishes in case of circular polarization of the wave ($|\xi| = 1$). The dynamic parameter a in (1) has to change the sign under time reversion. This T-oddness can appear due to the scattering phase of the escaping particle and due to the resonance level width in case of the resonant two-photon disintegration of the atomic system.

In two-photon ionization or dissociation of optically active (chiral) molecules the angular distributions also include the additional terms linear in ξ :

$$b_1 \xi \mathbf{k} \cdot \mathbf{p} + b_2 \xi \mathbf{k} \cdot \mathbf{p} (|\mathbf{p} \cdot \mathbf{e}|^2 - \frac{1}{5}), \quad (2)$$

where b_1 and b_2 are the pseudoscalar dynamic parameters of the chiral molecule. The terms (2) do not vanish in case of circular polarization and, therefore, lead to the circular dichroism in the angular distributions.

The expressions for the angular distributions derived here could also be useful for the solution of inverse problem finding the atomic dynamic parameters from the experiment.

Thermal ionization of alkali Rydberg atoms

I. L. Glukhov and V. D. Ovsianikov

*Department of Physics, Voronezh State University, University Square 1, 394006, Russia,
Voronezh*

E-mail: GlukhovOfficial@mail.ru

The environmental blackbody radiation (BBR) is a principal factor reducing essentially lifetimes of Rydberg atoms. Of the three channels of the BBR-induced level broadening — decay to lower levels, excitation to upper levels and ionization — the latter is the most destructive one, responsible for the neutral gas breakdown and for supporting the ionized state of plasmas. Therefore, the rate of the BBR-induced ionization of atoms from Rydberg states is an important characteristic for describing both the elementary processes in excited atoms and the kinetics of non-equilibrium gases and plasmas.

We have calculated matrix elements for bound-free transitions in the dipole approximation for alkali atoms (Li, Na, K, Rb, Cs) on the basis of the Fues' model potential method [1]. The matrix elements were used for determining the rates of the BBR-induced ionization from s-, p-, d-states with the principal quantum number $n=8-45$ at different temperatures. Our results agree well with the latest available theoretical and experimental data [2,3].

We discovered that the ratio E_n/kT for the states of maximal ionization rate takes the values in the range of 0.5–1.3. Therefore, we suggest the relation of an effective principal quantum number ν , corresponding to the maximal photoionization rate, with the ambient temperature T (in Kelvin)

$$\nu = (350 \div 560) T^{-1/2}, \quad \text{where} \quad E_n = -\frac{1}{2\nu^2}.$$

We also generalize our previously reported three-term approximation [4], which was proposed for helium, to the alkali atoms. Thus, the BBR-induced ionization rate P_n in inverse seconds is

$$P_n = \frac{a_0 + a_1x + a_2x^2}{\nu^4[\exp(x) - 1]}, \quad \text{where} \quad x = \frac{1.579}{\nu^2 T} 10^5,$$

and a_i are fitted coefficients, for a given atomic series of states, smoothly dependent on temperature. This equation provides good results for states in the vicinity of the ionization rate maximum and for higher energy states. The deviation of results determined by this approximate equation from those of exact calculations for the states with principal quantum numbers up to $n = 70$ does not exceed 15%.

The temperature dependence for a -coefficients is approximated by the relation

$$a_i = \sum_{k=0}^2 b_{ik} T^{-k/2},$$

with nine coefficients b_{ik} , fixed for each series, providing rather accurate results in the ranges of $T=100-2000\text{K}$.

References

- [1] N.L. Manakov, V.D. Ovsianikov, L.P. Rapoport, Phys. Rep. **141**, 319–433 (1986)
- [2] I.I. Beterov, D.B. Tretyakov, I.I. Ryabtsev, Phys. Rev. A **75** 052720 (2007)
- [3] I.I. Beterov, I.I. Ryabtsev, D.B. Tretyakov, JETP to be published (2008)
- [4] I.L. Glukhov, V.D. Ovsianikov, Proc. of SPIE **6726**, 67261F (2007)

Hyperpolarizabilities of multiplet Rydberg states in alkali and alkaline-earth atoms

V.D. Ovsianikov ¹ and E.Yu. Ilinova ¹

¹ *Department of Physics, Voronezh State University, 394006 Voronezh, Russia*

The atomic spectra in external fields is one of the most important problems of atomic Physics and spectroscopy. Sensitive methods were developed for cooling and trapping atoms, for selective excitation to strictly indicated states, for experimental investigation of radiative properties of atoms in Rydberg states [1,2]. The spectroscopy of atoms and atomic ensembles trapped in optical lattices provides new information on the properties of quantum objects and on elementary processes of radiation-matter interaction. Precision information on the Stark effect in higher orders of perturbation theory is of a special interest in constructing optical frequency standards of a new generation, and also in processing quantum information on the basis of atomic ensembles in Rydberg states. Therefore, the development of simple methods for calculating nonlinear atomic susceptibilities, specifically those for Rydberg states, seems of primary importance.

Stark shifts of energies for Rydberg S_J, P_J, D_J ($J=L\pm S$) states of alkali ($S=1/2$) and alkaline-earth ($S=0, 1$) atoms in external electric field were determined, up to the 4-th order in the field strength. To this end, for close sublevels of multiplets, with equal values of magnetic quantum number M_J , the higher-order perturbation theory for nearly-degenerate states [3] was used. Analytical equations for energy shifts were presented in terms of irreducible (scalar and tensor) parts of polarizabilities $\alpha^{s,t}$, hyperpolarizabilities γ^{s,t,t^4} and oscillator strength sums $\beta^{s,t}$ [3]. For irreducible parts of hyperpolarizabilities and oscillator strength sums the three-term approximation in powers of the effective principal quantum number $\nu=1/\sqrt{-2E_{nl}}$ was proposed, which provides accurate estimates to these values for Rydberg states with arbitrary principal quantum number, up to $\nu = 1000$. The coefficients of the polynomials were obtained from the corresponding values, calculated for states with the radial quantum number $n_r = 25, 26, 27$.

Using the calculated data, the "critical" values of field intensities for double Stark resonance on Rydberg $36P_{3/2,1/2}, 37S_{1/2}, 37P_{3/2,1/2}$ states in Na were determined and compared with experimental and theoretical data of ref.[1]. The account of the 4-th-order terms amends the agreement with experimental data so, that the difference from the results of ref. [1] does not exceed 1-1.5 percents. Also, for Rb atom, on the basis of our data and the results previously obtained in [4], the coefficients were determined, which appear at F^4 in expansion of energy shifts in powers of field intensity. The data of calculations demonstrates significant amendments of agreement between theoretical and experimental data in comparison with that of the ref. [2].

References

- [1] I.I. Ryabtsev, D.B.Tretyakov, JETP **121** 787 (2002).
- [2] T.Haseyama, K.Kominato, M.Shibata, S.Yamada, T.Saida, T.Nakura, Y.Kishimoto, M.Tada, I.Ogawa, H.Funahashi, K.Yamamoto, S.Matsuki, Phys.Lett. A **317** 450 (2003).
- [3] I.L. Bolgova, V.D. Ovsianikov, V.G. Palchikov, A.I. Magunov, G. von Oppen, JETP **123** 1145 (2003).
- [4] A.A. Kamenski, V.D. Ovsianikov, J.Phys B:At. Mol.Opt.Phys. **39** 2247 787 (2006).

Penning ionization of cold Rb Rydberg atoms due to long-range dipole-dipole interaction

N. N. Bezuglov^{1,2}, K. Miculis¹, A. Ekers¹, J. Denskat³, C. Giese³, T. Amthor³, and M. Weidemüller³

¹ *Laser Centre, University of Latvia, LV-1002 Riga, LATVIA*

² *Faculty of Physics, St.Petersburg State University, 198904 St. Petersburg, RUSSIA*

³ *Physikalisches Institut, Universität Freiburg, D-79104 Freiburg, GERMANY*

Ionization in cold collisions of Rydberg atoms is possible via two mechanisms: associative and Penning ionization. Associative ionization is a short range process of low efficiency, because it requires close encounters enabling overlap of Rydberg atom wavefunctions (at internuclear distances $R \ll n^*$). In contrast, Penning ionization is a long-range process (at $R \gg n^*$), which is enabled by the dipole-dipole interaction (atomic units are used in this abstract)

$$V = \frac{\vec{D}_1 \vec{D}_2 - (\vec{D}_1 \vec{n})(\vec{D}_2 \vec{n})}{R^3}, \quad (1)$$

where \vec{D}_i are the dipole moments of both atoms and \vec{n} denotes the orientation of the internuclear axis.

We consider the formation of atomic ions in an Ager-type processes: one of the Rydberg atoms undergoes a dipole transition from the initial state nl to a lower state $n'l'$, while the other atom is excited from the initial state nl to the ionization continuum. Such ionization can take place if the energy released in the $nl \rightarrow n'l'$ transition is equal to (or larger than) the binding energy of electron in the nl state, which is given by the condition $n^{*'} < n^*/\sqrt{2}$ (n^* is the effective quantum number). Perturbation theory [1] allows one to express the autoionization width $\Gamma(R)$ via the photoionization cross section σ_{ph} of atom in the nl state and the reduced dipole matrix elements $|D_{nn'}|$ of the $nl \rightarrow n'l'$ transitions

$$\Gamma(R) = \frac{\tilde{\Gamma}}{R^6}; \quad \tilde{\Gamma} = \sum_{n'} \frac{c\sigma_{ph}}{\pi\omega_{nn'}} |D_{nn'}|^2 \quad (2)$$

We have evaluated the ionization rates $\tilde{\Gamma}$ using semiclassical analytical formulae for both the photoionization cross sections and the dipole matrix elements derived in [2] for alkali atoms. The resulting $\tilde{\Gamma}(n^*)$ is a function that oscillates around the power-law curve $\tilde{\Gamma} = Cn^{*16/3}$ with $C_S = 0.3$ and $C_P = 0.46$ for nS and nP states, respectively. These results should help in understanding the ionization dynamics of cold Rydberg gases [3].

Support by the EU FP6 TOK Project LAMOL, DFG, and ESF is acknowledged.

References

- [1] K. Katsuura, J.Chem.Phys., **47**, 3770 (1965).
- [2] N. N. Bezuglov, V. M. Borodin, . Opt. Spectrosc., **86**, 467 (1999).
- [3] T. Amthor, M. Reetz-Lamour, C. Giese, and M. Weidemüller, Phys. Rev. A **76**, 054702 (2007).

Ionization of alkali-metal Rydberg atoms by blackbody radiation

I.I.Beterov¹, I.I.Ryabtsev¹, D.B.Tretyakov¹, N.N.Bezuglov², A.Ekers³, and V.M.Entin^{1*}

¹*Institute of Semiconductor Physics, Pr. Lavrentyeva 13, 630090, Novosibirsk, Russia*

²*Institute of Physics, 198904, St. Petersburg, Russia*

³*Institute of Atomic Physics and Spectroscopy, LU, LV-1586 Riga, Latvia*

*E-mail: *ventin@isp.nsc.ru*

Interaction of Rydberg atoms with blackbody radiation (BBR) was studied for many years [1]. However, only few works were devoted to BBR-induced ionization of Rydberg atoms. A renewed interest to this process is related to the recently observed spontaneous formation of ultracold plasma in dense samples of cold Rydberg atoms and to the prospects of using the BBR ionization as a convenient reference signal in absolute measurements of collisional ionization rates.

In this report the results of our extended theoretical calculations of BBR-induced ionization rates of alkali-metal Rydberg atoms are presented [2,3]. Calculations have been made for nS, nP and nD states of Li, Na, K, Rb and Cs atoms, which are commonly used in a variety of experiments, at principal quantum numbers $n=8-65$ and at three ambient temperatures of 77, 300 and 600 K. A semi-classical model [4] was used to numerically calculate the bound-bound and bound-free matrix elements. A peculiarity of our calculations is that we take into account the contributions of BBR-induced redistribution of population between Rydberg states prior to photoionization and field ionization by extraction electric field pulses. The obtained results show that these phenomena affect both the magnitude of total ionization rates and shapes of their dependences on the principal quantum number n . For Li Rydberg atoms a bound-bound Cooper minimum is observed.

The theoretical ionization rates are compared with the results of our earlier measurements of BBR-induced ionization rates of Na nS and nD Rydberg states with $n=8-20$ at 300 K. A good agreement for all states except nS with $n \geq 15$ is obtained. The useful analytical formulas for quick estimates of BBR ionization rates taking into account quantum defects of Rydberg atoms are also presented. These formulas have been derived using the analytical formulas for hydrogen matrix elements obtained in [5]. The analytical estimates of BBR-induced ionization rates well agree with the results of our numerical calculations.

This work was supported by the Russian Academy of Sciences, EU FP6 TOK project LAMOL, European Social Fund, Latvian Science Council, and NATO grant EAP.RIG.981387.

References

- [1] T.F.Gallagher, "Rydberg Atoms", Cambridge University Press, Cambridge (1994).
- [2] I.I.Beterov, D.B.Tretyakov, I.I.Ryabtsev, N.N.Bezuglov, and A.Ekers, Phys. Rev. A, 2007, v.75, p.052720.
- [3] I.I.Beterov, I.I.Ryabtsev, D.B.Tretyakov, N.N.Bezuglov, and A.Ekers, JETP, 2008 (in press).
- [4] L.G.Dyachkov and P.M.Pankratov, J. Phys. B, 1994, v.27, p.461.
- [5] S.P.Goreslavsky, N.B.Delone, and V.P.Krainov, JETP, 1982, v.55, p.246.

Level-crossing transition between mixed states

B. T. Torosov and N. V. Vitanov

Department of Physics, Sofia University, James Bourchier 5 blvd, 1164 Sofia, Bulgaria

The Landau-Zener model [1] is conventionally used for estimating transition probabilities in the presence of crossing levels. Nevertheless, because of the infinite duration of the coupling in this model, the propagator involves a divergent phase. It has been shown that this phase causes undefined populations in the degenerate Landau-Zener model [2]. In this work we show that even in the original Landau-Zener model we have undefined populations when we deal with pure superposition states or with mixed states. Besides, we show that the Allen-Eberly model [3] can be used as an alternative to the Landau-Zener model to describe the dynamics of such level-crossing problems.

References

- [1] L. D. Landau, *Physik Z. Sowjetunion* **2**, 46 (1932); C. Zener, *Proc. R. Soc. Lond. Ser. A* **137**, 696 (1932).
- [2] G. S. Vasilev, S. S. Ivanov and N. V. Vitanov, *Phys. Rev. A* **75**, 013417 (2007).
- [3] L. Allen and J. H. Eberly, *Optical Resonance and Two-Level Atoms* (Dover, New York, 1987).

M1-E2 interference in the Zeeman spectra of Bi I

S. Werbowy and J. Kwela

*Institute of Experimental Physics, University of Gdansk, Wita Stwosza 57, 80-952
Gdańsk, Poland*

Precision in atomic parity nonconservation (PNC) measurements have reached the level required to provide important tests of the electroweak standard model [1]. Nevertheless, to extract the electroweak quantity of interest, the 'weak charge', from the experiment, atomic structure calculations of comparable precision are necessary. The measurement of the ratio $D = A^{E2}/(A^{E2} + A^{M1})$ of the electric-quadrupole (E2) and magnetic-dipole (M1) transition probabilities in mixed forbidden lines can provide stringent test of theoretical wave-function calculations; accurate knowledge of this quantity is essential for existing and future measurements of parity nonconserving optical rotation.

The $6s^26p^3$ ground configuration of bismuth gives rise to five levels $^4S_{3/2}$, $^2P_{3/2,1/2}$ and $^2D_{5/2,3/2}$. We report studies [2] of the interference effect in mixed-type forbidden lines: 461.5nm ($^2P_{1/2} \rightarrow ^4S_{3/2}$), 647.6nm ($^2D_{5/2} \rightarrow ^4S_{3/2}$) and 875.5nm ($^2D_{3/2} \rightarrow ^4S_{3/2}$) of Bi I. In the past, the mixed M1+E2 type lines 647.6nm and 875.5nm in bismuth were intensely exploited in PNC experiments [3, 4]. In the Zeeman effect of mixed multipole lines, the intensities of patterns are not a simple sum of two contributions for M1 and E2 radiations taken in proportion to their transition probabilities, but should be modified by an interference term. The spontaneous transition probability for a single photon emission in the presence of the magnetic field can be expressed, according to

$$a_{ab} = (1 - D)a_{ab}^{M1} + Da_{ab}^{E2} \pm 2\sqrt{D(1 - D)}a_{ab}^{M1-E2}, \quad (1)$$

where D is percentage admixture of E2 radiation, a_{ab}^{M1} and a_{ab}^{E2} are pure magnetic-dipole and electric-quadrupole components, respectively, and the cross term a_{ab}^{M1-E2} describes the interference effect. The interference effect in emission spectra causes the difference between the intensities of $\Delta M = \pm 1$ Zeeman patterns observed in longitudinal and transverse directions of observation. This phenomenon, in a series of experiments, was used for precise determination of the electric-quadrupole admixture D in forbidden lines.

A special computer program considering the M1-E2 interference was design to obtain the predicted contour of the Zeeman structure of the line. By variation of free parameters, describing the line shape and electric-quadrupole admixtures, the calculated profiles were fitted into the experimental spectra recorded by CCD detector. The E2 admixtures found are: $(7.84 \pm 0.14)\%$, $(17.5 \pm 0.4)\%$ and $(0.70 \pm 0.11)\%$ for 461.5nm, 647.6nm and 875.5nm lines, respectively. Our results were compared with recent theories and other experiments.

This work was supported by grant BW/5200-5-0482-8 and BW/5200-5-0053-8.

- [1] C. S. Wood, *at. al.*, Science **275**, 1759 (1997)
- [2] S. Werbowy and J. Kwela, Phys. Rev. A **77**, 023410 (2008)
- [3] P. E. G. Baird, *at. al.*, Phys. Rev. Lett. **39**, 798 (1977)
- [4] J. H. Hollister, *at. al.*, Phys. Rev. Lett. **46**, 643 (1981)

Numerical investigation of NeI for $2p^5 5g$ configuration and ArI for $3p^5 5g$ configuration Zeeman structure

Anisimova G.P.¹, Efremova E.A.¹, Semenov R.I.¹, Tsygankova G.A.¹

¹*St.-Petersburg State University*

Petergof, Ulianovskaja st., 1, NIIF-SPbSU, St.-Petersburg, 198504, Russia.

E-mail: efremovakat@inbox.ru

The behavior of an atom in the magnetic field can be studied numerically based on the parameters of the fine structure (the radial integrals in the energy operator matrix). A set of the fine structure parameters ensuring the correlation with experimentally observed energies [1, 2] was obtained in the previous works of the authors.

The authors provide the results of the numerical study of magnetic sublevels behavior for NeI and ArI (of specified configurations) in the magnetic fields up to 150 kOe .

Using the free momentums representation and the Clebsch-Gordan coefficients the authors succeeded to obtain the expressions for the diagonal and non-diagonal elements of the atom-field interaction matrices in $LSJM$ -representation as well as to refine the signs of the non-diagonal elements.

$$\langle \gamma \Psi_i | W | \gamma \Psi_i \rangle = \left(\frac{J(J+1) + L(L+1) - S(S+1)}{2J(J+1)} g_l + \frac{J(J+1) - L(L+1) + S(S+1)}{2J(J+1)} g_s \right) \mu_0 H M$$

$$(\Delta J = \Delta L = \Delta S = 0)$$

$$\langle \gamma \Psi_i | W | \gamma' \Psi_j \rangle = \sqrt{\frac{(J-L+S+1)(J+L-S+1)(J+L+S+2)(L+S-J)}{4(J+1)^2(2J+1)(2J+3)}} ((J+1)^2 - M^2) \times$$

$$\times (g_l - g_s) \mu_0 H$$

$$(\Delta J = \pm 1, \Delta L = \Delta S = 0, J_{min})$$

The energies of Zeeman's sublevels were calculated by means of the diagonalization of the complete energy operator matrix, which was expressed in LS -representation with additional elements accounting for the atom-field interaction. The diagonalization was carried out for all the values of the magnetic quantum number M .

The distinctive details of Zeemann's structure especially points of crossing and anticrossing areas of magnetic sublevels were obtained for $2p^5 5g$ configuration of NeI and $3p^5 5g$ configuration of ArI .

References

- [1] Chang E.S., Schoenfeed W.G., Biemont E., Quinet P., Palmeri P., Phys. Scr. **V. 49.**, 26-33 (1994)
 [2] Palmeri P., Biemont E., Phys. Scr. 1995. **V. 51.**, 76-80 (1995)

Method for quantitative study of atomic transitions in magnetic field based on vapor nanocell with $L = \lambda$

A. Papoyan¹, G. Hakhumyan^{1,2}, A. Atvars³, M. Auzinsh³ and D. Sarkisyan¹.

¹ *Institute for Physical Research, NAS of Armenia, Ashtarak-0203, Armenia*

² *Russian-Armenian State University, 123 Housep Emin str., Yerevan, 0051 Armenia*

³ *Department of Physics, University of Latvia, 19 Rainis blvd., Riga, LV-1586 Latvia*
E-mail: papoyan@ipr.sci.am

It is well known that atoms placed in an external magnetic field undergo shift of their energy levels and change in their transition probabilities. To study these changes, widely used saturation absorption technique has been used in [1]. However, the complexity of Zeeman spectra in magnetic field arises primarily from the presence of strong crossover resonances, which are also split into many components strictly limiting the range of study to $5 \div 50$ G, while the most significant changes are expected for $B \sim 1000$ G.

A method, which we call " $L = \lambda$ Zeeman technique" (λ -ZT) has been implemented for investigation of the individual transition between the Zeeman sublevels of the hf structure of alkali atoms in magnetic field $1 \div 2500$ G. The λ -ZT is based on the employment of a nanocell with the thickness of Rb vapor column equal to the wavelength of diode laser radiation resonant with D_2 line of atomic ^{85}Rb , ^{87}Rb ($\lambda = 780$ nm). At the laser intensity 1 mW/cm^2 , narrow (~ 10 MHz) resonant velocity selective optical pumping/saturation (VSOP) peaks of reduced absorption appear in the transmission spectrum localized exactly at the atomic transitions [2]. These VSOP peaks are split to separate components in magnetic field; the amplitudes (which are proportional to transition probability) and frequency positions of the components depend on B - field.

Particularly, it is revealed that in relatively weak magnetic field (~ 100 G) with σ^+ -polarized laser radiation also those atomic transitions are recorded, for which new selection rules with respect to the quantum number F take place: $^{87}\text{Rb } D_2$, $F_g=1$, $m_F=1$ $F_e=3$, $m_F=0$ transition (let call it (2)) increases with the increase of the magnetic field, and at $B \sim 200$ G becomes equal to probability of the strongest transition $F_g=1$, $m_F=+1$ $F_e=2$, $m_F=+2$ (let call it (1)) for $B = 0$. At higher magnetic field up to 2000 G probability of the atomic transition (2) is the largest, while for $B > 2000$ G again the probability of (1) is larger than that of (2). Note that implementation of λ -ZT technique is very convenient to study atomic transitions behavior also at higher magnetic field > 2000 G. Particularly, by measuring the frequency difference between transition (1) and transition (2) it is possible to measure a strongly non-homogeneous magnetic field of 150 G/mm. This is achieved by displacement of the nanocell by 10 - 20 μm in the direction of magnetic field gradient. The theoretical model very well describes the experimental results.

Also, the performed studies showed that the atomic transition $F_g=1 \rightarrow F_e=2$ of $^{87}\text{Rb } D_1$ line ($\lambda = 794$ nm) is very convenient for determination of uniform, as well as strongly non-uniform magnetic field strength in the range of $5 \div 10\,000$ G.

References

- [1] M.U. Momeen, G. Rangarajan, P.C. Deshmukh, Journ. Phys. B: At. Mol. Opt. Phys. **40**, 3163 (2007).
 [2] C. Andreeva, S. Cartaleva, L. Petrov, S.M. Saliel, D. Sarkisyan, T. Varzhapetyan, D. Bloch, M. Ducloy, Phys. Rev. A **76**, 013837 (2007).

g factor of boronlike ions

D. A. Glazov¹, A. V. Volotka², V. M. Shabaev¹, I. I. Tupitsyn¹ and G. Plunien²

¹ *Department of Physics, St. Petersburg State University, Oulianovskaya 1,
Petrodvorets, St. Petersburg 198504, Russia*

² *Institut für Theoretische Physik, TU Dresden, Mommsenstraße 13, D-01062 Dresden,
Germany*

E-mail: glazov@pcqnt1.phys.spbu.ru

High-precision measurements of the g factor of H-like carbon and oxygen, performed by the GSI - Universität Mainz collaboration, combined with the corresponding theoretical investigations, have provided a new determination of the electron mass to an accuracy that is four times better than that of the previously accepted value. An extension of the g factor experiments to higher- Z systems is anticipated in the near future at the HITRAP facility at GSI (Darmstadt). As was demonstrated in [1], investigations of a specific difference of the g factors of H- and B-like ions can provide an independent determination of the fine structure constant to an accuracy comparable to that of the recent determination by Gabrielse et al. [2].

We perform accurate calculations of the ground-state g factor of B-like ions in a wide range of nuclear charge numbers. The calculational methods were already employed in [3,4] for Li-like ions. One-loop QED corrections were evaluated in effective screening potential. To our best knowledge, this is the first correct evaluation of the QED correction to the g factor of the $2p$ state. The one-photon exchange correction was calculated in the framework of QED. The large-scale configuration-interaction Dirac-Fock-Sturm method was employed to take into account the electron-correlation effects of the order $1/Z^2$ and higher. As a result, the most accurate up-to-date values of the g factor of B-like ions are obtained.

References

- [1] V. M. Shabaev *et al.*, Phys. Rev. Lett. 96 (2006) 253002.
- [2] G. Gabrielse *et al.*, Phys. Rev. Lett. 100 (2008) 120801.
- [3] D. A. Glazov *et al.*, Phys. Rev. A 70 (2004) 062104.
- [4] D. A. Glazov *et al.*, Phys. Lett. A 357 (2006) 330.

Magnetolectric Jones spectroscopy of Li and Na atoms

V.V.Chernushkin, V.D.Ovsiannikov

*Theoretical Physics Dept, Voronezh State University, Voronezh, Russia,
E-mail: albert@phys.vsu.ru*

Magnetolectric birefringence, which was predicted by Jones¹ and first observed in liquids², may also become a useful tool for high-precision laser spectroscopy of atomic systems³.

The amplitude of the Rayleigh scattering of a monochromatic wave with the frequency $\omega = E_{nD_J} - E_{nS_{1/2}} - \varepsilon_J$ in resonance ($|\varepsilon_J| \ll \omega$) with the D-level doublet substates of the total momentum $J = 3/2, 5/2$, may be written as (taking into account only the terms with the second-order resonance singularities)

$$U = AQ \left(\frac{7}{(\varepsilon_{3/2})^2} + \frac{47}{(\varepsilon_{5/2})^2} - \frac{4}{\varepsilon_{3/2}\varepsilon_{5/2}} \right) [\varphi_0 + \varphi_1], \quad (1)$$

where the constant factor $A = F^2 F_0 B / 1500$ is proportional to the product of the square laser field F^2 , static electric field F_0 and magnetic field B . The polarization-dependent factors are

$$\varphi_0 = (\mathbf{e}_0 \cdot [\mathbf{n} \times \mathbf{e}_B]); \varphi_1 = \text{Re}\{(\mathbf{e}_0 \cdot \mathbf{e})(\mathbf{e}^* \cdot [\mathbf{n} \times \mathbf{e}_B])\},$$

where \mathbf{e}_B and \mathbf{e}_0 are unit vectors of magnetic and electric fields, \mathbf{e} and \mathbf{n} are unit polarization and wave vectors of the laser wave. The complex quantities $\varepsilon_J = \Delta_J - i\Gamma_J/2$ include both the resonance detuning Δ_J for the real part and the resonance level width Γ_J for the imaginary part. The factor Q_D is a product of the radial matrix elements for the first-order quadrupole and second-order dipole radiation transition between the ground $nS_{1/2}$ and resonance $n'D$ states (the influence of the fine structure on radial integrals is neglected):

$$Q_D = \langle nS | r^2 | n'D_{J_2} \rangle \langle n'D_{J_1} | r(g_P^\omega + g_P^0) r | nS \rangle;$$

The Jones birefringence appears, when $\mathbf{e}_0 = \mathbf{e}_B$, due to the difference between the amplitude (1) for $\mathbf{e} = \mathbf{e}^{(+)}$ and $\mathbf{e} = \mathbf{e}^{(-)}$, where $\mathbf{e}^{(\pm)} = (\mathbf{e}_0 \pm [\mathbf{n} \times \mathbf{e}_0]) / \sqrt{2}$:

$$\Delta U_D^{(J)} = U_D^{(+)} - U_D^{(-)} = 2AQ_D \left(\frac{7}{(\varepsilon_{3/2})^2} + \frac{47}{(\varepsilon_{5/2})^2} - \frac{4}{\varepsilon_{3/2}\varepsilon_{5/2}} \right).$$

Similar effects in atoms with singlet structure of levels, which correspond to $\varepsilon_{3/2} = \varepsilon_{5/2}$, were discussed in⁴.

¹R. C. Jones, J. Opt. Soc. Am. 38, 671 (1948).

²T. Roth and G. L. J. A. Rikken, Phys. Rev. Lett. 85, 4478 (2000).

³D. Budker and J. E. Stalnaker, Phys. Rev. Lett. 91, 263901 (2003).

⁴P. V. Mironova, V. V. Tchernouchkine, V. D. Ovsiannikov, J. Phys. B, **39**, 4999 (2006).

Radiative transition probabilities from D Stark states in orthohelium

A. A. Kamenski¹ and V. D. Ovsianikov¹

¹*Department of Physics, Voronezh State University, 394006, Voronezh, Russia*

The dependence of radiative line intensity on external field strength is an important characteristic of radiative properties, which gives rise to new lines in the emission and adsorption spectra and in sufficiently strong fields removes a number of lines that exist in the spectrum of a free atom. Our calculations for the pair-wise interacting sublevels were based on the integral Schrödinger equation for close levels [1]. The total momenta projection M determines a group of multiplet sublevels interacting with one another in the lowest order of external DC electric field. Even for a general case of arbitrary angular L and spin S momenta, one can find the states interacting in pairs. General analysis of different pairwise interacting substates with equal parity demonstrates common features of the field-dependent probability behaviour. In particular, we discovered the equalization of probabilities in the anticrossing field and vanishing of one of the two doublet components in a strong-field limit [1].

In this communication we present some results on the radiative transitions from triple-interacting sublevels of atoms in a DC electric field. The perturbation operator matrix takes into account the interaction of an atom with a dc field in all orders of the field amplitude. The atomic wavefunction in the field is reduced to a set of homogeneous algebraic equations for the superposition coefficients [1,2].

The simplest example of triple-interacting sublevels are D -states of orthohelium atom with $M = \pm 1$. We calculate numerically energy shift and wave function superposition coefficients for this case in the first nonvanishing order of perturbation theory. As for the pair-wise interacting levels, the sign of the tensor polarizability determines the behaviour of triplet states in the field. So the sublevels approaching each other in orthohelium atom, as field strength increases, occurs only in $3D$ -state with positive tensor part of polarizability $\alpha_{3D}^t > 0$, and does not appear for nD -states with $n \geq 4$ where $\alpha_{nD}^t < 0$ [2].

In order to reveal the impact of the anticrossing effect explicitly, we consider the field dependence of the probability of radiative transition from the triple-interacting n^3D -levels to an isolated n'^3P_J -sublevel (with $J = 1, M = 0$ or $J = 2, M = \pm 2$) or to n'^3F_3 -sublevel with $M = 0$. Such transitions give triplet structure of corresponding radiative lines. The vanishing of some fine-structure components with the growth of the field strength corresponds to our asymptotic results for orthohelium lines [1].

Such dependence is not monotonous, and we discovered zero-intensity points and intensity maximum among the fine-structure $P - D$ -lines. This effect can be useful for selective control by a dc field of the radiation processes.

References

- [1] A.A. Kamenski, and V.D. Ovsianikov, Journal of Experimental and Theoretical Physics, **100**, No 3, pp.487-504 (2005)
- [2] A. A. Kamenski and V. D. Ovsianikov, J. Phys. B: At. Mol. Opt. Phys. **39**, 2247-2265 (2006)

Light-induced quasi-static polarization in hydrogen-like atom under the action of strong electromagnetic laser field

M.V.Ryabinina, L.A.Melnikov

*Saratov State Univerisity, Physics Department
83 Astrakhanskaya, 410012, Saratov, Russia
mvr@vtt.net*

For two-level system is well known that the transitions rate parameter is Rabi-frequency. At large intensities the Rabi frequency can be comparable with an optical transition frequency ν , while laser electric field remains smaller than intra-atomic field. In this case temporal variation of probability amplitudes $a(t)$ and $b(t)$ for the levels of two-level system can occurs at frequencies comparable with $n\nu, n = 1, 2, \dots$. As a result, simple analytical solution is not possible and use of numerical methods [1] is required even for two-level system.

In present paper the transitions in hydrogen atom induced by the linearly polarized pulse with a polarization along the axis z are investigated. For hydrogen atom all matrix elements of transitions are in an analytical form as well as wave functions of discrete and continuum spectra. The dynamics of populations of $4s$ and $3p$ states and polarization of the transition $4s \leftrightarrow 3p$ are investigated theoretically and numerically at one-, two- and three-photon resonance conditions and at large detuning out of frame of perturbation theory and rotating wave approximation.

It was shown that at resonance the low frequency modulation of optical oscillations exists, producing corresponding quasi-static polarization of atoms along z -axis. The oscillations frequency becomes zero at the values of laser field amplitude corresponding to ratio of Rabi frequency to optical frequency $\wp E_0/\nu = 1.05, 2.75, 4.3, 5.8, 7.5, 9, \dots$. These low-frequency oscillations are attributed to the special displacement of quasi-energy levels. We have used the Floquet-type solution of the equations for probability amplitudes:

$$i\dot{a} = \wp_{ab}b(t)E_0(t) \cos(\nu t) \exp(i\nu t), \quad i\dot{b} = \wp_{ab}a(t)E_0(t) \cos(\nu t) \exp(-i\nu t). \quad (1)$$

$$a(t) = \exp(i\lambda t) \sum_{n=-\infty}^{\infty} a_n \exp(i\nu n t), \quad b(t) = \exp(i\lambda t) \sum_{n=-\infty}^{\infty} b_n \exp(i\nu n t).$$

$$(i\lambda + i\nu n)a_n = -i\frac{\wp_{ab}E_0(t)}{2}(b_n + b_{n-2}), \quad (i\lambda - i\nu n)b_n = -i\frac{\wp_{ab}E_0(t)}{2}(a_n + a_{n+2}). \quad (2)$$

Calculations of the values of λ gives $\lambda = \frac{1}{2}$ for mentioned values of field. In this case the quasi-levels are crossed. For two-photon transitions $\lambda = 0(n\nu)$ for $\wp E_0/\nu \approx 2.4, 4.1, 5.7, \dots$ demonstrating the same behavior of the polarization.

This effect can be used for measuring the ultra-high intensity pulse amplitudes. The influence of the transitions to continuum calculated using method of Ref.2 is discussed also.

References

- [1] Bordyug N.V. and Krainov V.P. Laser Phys. Lett. v.4, 418(2007)
- [2] Ryabinina M.V., Melnikov L.A. AIP Conference Proc. v.796, 325(2005)

Doppler-free spectroscopy of rubidium atoms placed in a magnetic field

G. Skolnik, N. Vujicic, T. Ban, S. Vdovic and G. Pichler

Institute of Physics, Bijenicka 46, Zagreb, Croatia

Saturation spectroscopy (SAS) is one type of high resolution laser spectroscopy and is widely used in alkali atomic vapour system for observing the sub-Doppler resonances [1]. In SAS technique two counter-propagating laser beams, which derive from the single laser source, simultaneously interact with zero velocity group of atoms. The pump laser beam burns a hole in the Boltzmann distribution curve of the lower level and when the probe laser beam comes across this hole, in the absorption spectrum a Lamb dip can be observed. This dip has a Doppler-free Lorentzian line shape depending on the natural, collision and the transit time broadening and on the laser linewidth.

In this work we used saturation spectroscopy and improved it with an application of a lock-in technique. This technique eliminates broad Doppler-background from the signal and enables a resolution of all hyperfine transitions. We investigated the resonance D2 line of rubidium vapour by External Cavity Diode Laser (ECDL). The observed Doppler-broadened profiles consist of four lines, two of them resulting from ^{85}Rb absorption and the other two from ^{87}Rb . In SAS technique for each absorption line three hyperfine transitions and three belonging crossovers were obtained. In addition, we performed the theoretical simulations of the measured Lorentzian profiles. In saturation spectrum of ^{87}Rb an inverse negative crossover resonance appeared as a consequence of alignment effect and its dependence on polarization of the laser beams and on the magnetic field strength was measured.

We measured line shape dependence on the magnetic field strength. Our experimental arrangement contains of two parts in order to measure magnetic field effect on rubidium vapour at one part and simultaneously compare it with the other one that has no magnetic field influence. In this way the first part serves as a reference scale for frequency valuation. An offset in the central frequency line position, increase in linewidth of each transition line and decrease in line intensity due to the enhancement of magnetic field strength were observed. Measured experimental results show good agreement with applied theoretical model.

Our experimental measurements belong to a group of nonlinear magneto-optic effects that show their significance in laser spectroscopy, where they are applied in high-precision magnetometry, weak transition researches such as magnetic dipole transition with small magnetic moment, parity violation experiments and nowadays in quantum computing processing investigations.

[1] W. Demtroeder, Laser Spectroscopy, (Springer-Verlag, Berlin, 2003)

Electric field influence on the hydrogen atom embedded in a plasma

Mariusz Pawlak and Mirosław Bylicki

*Institute of Physics, Nicolaus Copernicus University
Grudziądzka 5, PL-87-100 Toruń, Poland*

The energy levels of a hydrogen atom in a uniform strong electric field and embedded in a plasma are investigated. The plasma environment modifies the potential around the charged particle. This influence is represented by the Debye screening. Hence the Yukawa potential is used to represent the plasma-modified electron-nucleus interaction. The effect of this modification is that [1]: (i) The number of bound states of a given spherical symmetry (for a given orbital quantum number) is finite. (ii) Their energy levels are shifted up. (iii) The states whose energies are shifted just above the continuum threshold become resonances.

An external homogeneous electric field causes further changes: (iv) It breaks down the spherical symmetry. (v) It shifts the energy of some states *down* and *up* of other ones (the Stark effect). (vi) It also turns all the bound states into quasibound resonances.

We include all these effects in our complex coordinate rotation calculation within a basis set of square integrable functions. The obtained complex energies give us positions and widths of the energy levels. They migrate in the complex plane when the field strength changes. Occasionally they tend to cross. Interesting avoided crossing structures appear.

References

- [1] M. Bylicki, A. Stachów, J. Karwowski, P. K. Mukherjee, *Chem. Phys.* **331**, 346 (2007)

Dynamic and Geometric Phases in the Stark-Zeeman effect of the hyperfine structure of one-electron atoms

B. Schnizer, Th.Heubrandtner, E. Röschl, M. Musso

Institut für Theoretische Physik - Computational Physics, TU Graz, Austria
Virtual Vehicle Competence Center, Graz, Austria
Philips Research Europe - Hamburg, Germany, Sector Medical Imaging Systems
Fachbereich Materialforschung und Physik, Universität Salzburg, Austria

A theoretical investigation of the Stark-Zeeman effect of the $np\ ^2P_{3/2}$ fine structure levels of atoms with one radiant electron and a core of closed shells with nuclear spin $I = 1$ (^6Li) or $I = 3/2$ (^7Li , ^{23}Na , ^{69}Ga , ^{71}Ga) predicted crossings and anticrossings. These were confirmed in an experiment. They could be predicted in the adiabatic approximation from the structure of the energy surfaces $\mathcal{E}_n(B, E)$ in their dependence on the magnetic field B and the electric field E . Two of these surfaces meet in the crossing points. There are two types of such crossing points resulting from the quadratic dependence of the Stark effect on E . In some crossing points the energy surfaces meet in a bicone, in the other ones they have an osculating contact in the E -direction. When the electric and magnetic fields are varied such that the phase point of the atom surrounds a biconical crossing points then the wave functions of the two levels concerned change sign; on the other hand a path around a crossing point of the second type does not change the sign. We assume that the change in sign corresponds to a geometric phase of absolute value π . As a first step for the feasibility of finding this geometric phase in an experiment, the dynamic phase connected with such time-dependent field variations has been investigated. Values of all these phases will be presented.

New analytical relativistic formulae for the total photoeffect cross section for the K-shell electrons

A. Costescu¹, C. Stoica¹ S. Spanulescu²

¹*University of Bucharest*

²*Hyperion University of Bucharest*

We present a new analytical relativistic result for the total photoeffect cross section for the K-shell electrons, in the lowest order of perturbation theory. In the cases of low atomic number values, the well known Sauters formula is recovered as a rough approximation of the exact relativistic result. For high atomic numbers, due to the specific behavior at small distances from the nucleus of the ground state Dirac spinor, some subtle relativistic effects are revealed near the photoeffect threshold. Also, our formulae contain all terms contributing at high energies in the next order of the perturbation theory, obtaining in the limit of infinite photon energy the correction term due to Pratt and Gavrila. In the nonrelativistic limit, we get the right result involving all the multipoles and retardation terms without the spurious singularities presented by Fischer's formula. Numerical evaluations of these formulae give very good predictions, within 5% for photon energies up to 5 MeV, comparing with accurate relativistic calculations existing in the literature.

Using the Green function method we obtain the imaginary part of the forward elastic scattering amplitude which provides via the optical theorem the photoeffect cross section and also the pair production cross section with the electron created in the K shell.

Our formalism allows including the screening effects which may be important near the photoeffect threshold, by using an effective nuclear charge Z_{eff} depending on the photon energy ω . Taking into account the screening effects, the obtained photoeffect cross sections present an even better agreement with the experimental cross sections and other relativistic calculations in the region near the threshold.

We point out that cross section for the K -shell electrons provides, in the high energy regime, the most important contribution to the total cross section of the whole atom. Thus, our formulae are useful for an important range of the gamma spectrum, where there is a lack of accurate formulae for the photoeffect cross sections, and may present interest in various experiments where gamma interactions with intermediate and high Z targets are involved.

References

- [1] Lynn Kissel, R. H. Pratt, and S. C. Roy, Phys. Rev. A **22**, 1970 (1980);
- [2] J.H. Scofield, Lawrence Radiation Laboratory Report No. CRL 51326, Livermore, CA, 1973 (unpublished)
- [3] L. Hostler, R.H. Pratt, Phys. Rev. Lett. **10**, 469 (1963);
- [4] C.Martin, R. J. Glauber, "Relativistic Theory of Radiation Orbital Electron Capture", Phys. Rev. **109**, 1307 (1958);
- [5] J. Schwinger, J. Math. Phys, **5**, 1606 (1964);
- [6] M. Gavrila, AIP Conf. Proc. No. 94, Eugene, Oregon, 1982.

Two-photon above-threshold ionization by a VUV-light

N. L. Manakov, S. I. Marmo and S. A. Sviridov

*Department of Physics, Voronezh State University,
Voronezh, 394006, Russia
E-mail: sviridovs@yandex.ru*

Recent experiments on two-photon above-threshold ionization (2ATI) of inert gases [1,2] by a VUV radiation renewed the interest to the perturbative analysis of 2ATI (since in VUV region the perturbation theory (PT) is valid up to high light intensities). The main difficulty of such calculations is the summation over the intermediate (after absorption of the first photon) continuum states of escaping electron. In the present work, we calculate the cross sections of 2ATI for He and alkali atoms in the single-active electron approximation, using the Fues model potential (FMP) for description of an active atomic electron. The known analytical expression for the Sturmian expansion of FMP Green's function allows to present the 2ATI amplitude in terms of a single series of hypergeometric functions of two variables, F_2 (Appel functions) [3], that, however, becomes divergent for above-threshold frequencies, $\hbar\omega > |E_0|$, where E_0 is the ground state energy. For summation of this divergent series we use the Pade-approximation (ε -algorithm), similarly to that used for calculations of 2ATI for the hydrogen atom [4]. We justify the applicability of the ε -algorithm to our problem by independent calculations of the imaginary part of the 2ATI amplitude and by analytical calculations of low-frequency asymptotics in the in two-color 2ATI (by two, high-frequency and low-frequency, photons). Our numerical results are in reasonable agreement with experiments [1,2] and other theoretical results [5,6,7,8].

Supported in part by RFBR Grant 07-02-00574.

Table 1: Total cross-sections, σ (in units of 10^{-52} cm⁴s), of two-photon ionization (in linearly polarized field) of He and comparison with experiments and perturbative and non-perturbative theoretical results [5,6,7,8].

ω , eV	Exp.	[5]	[6]	[6], PT	[7]	[8]	σ_{FMP}
15.0	–	11	12	12	–	–	13
25.0	1.9 [1]	1.0	–	–	–	–	3.2
27.2	–	1.0	4.5	2.5	2.7	–	2.2
41.8	2.0 [2]	–	–	–	–	0.53	0.35
45.0	–	0.12	1.0	0.33	–	–	0.26

References

- [1] N. Miyamoto, M. Kamei, D. Yoshitomi et al., Phys. Rev. Lett. **93**, 083903 (2004).
- [2] H. Hasegawa, E.J. Takahashi, Y. Nabekawa et al., Phys. Rev. A **71**, 023407 (2005).
- [3] N.L. Manakov and V.D. Ovsiannikov, J. Phys. B **10**, 569 (1978).
- [4] S. Klarsfeld and A. Maquet, J. Phys. B **12**, L553 (1979).
- [5] L.A.A. Nikolopoulos and P. Lambropoulos, J. Phys. B **34**, 545 (2001).
- [6] J. Colgan and M.S. Pindzola, Phys. Rev. Lett. **88**, 173002 (2002).
- [7] D. Proulx and R. Shakeshaft, J. Phys. B **26**, L7 (1993).
- [8] K.L. Ishikawa, unpublished (cf. Ref. [2]).

Above-threshold polarizability of alkali-metal and noble gas atoms

N. L. Manakov, S. I. Marmo and S. A. Sviridov

*Department of Physics, Voronezh State University,
Voronezh, 394006, Russia
E-mail: sviridovs@yandex.ru*

We investigate the dynamic polarizabilities of atoms of alkali metals and inert gases in the framework of Fues model potential (FMP) method. Using FMP for the atomic valence electron provides a simple one-particle method for calculation of atomic photoprocesses [1]. The convenient Coulomb-like expressions for the optical electron's wavefunctions and Green function for FMP enables easy calculations resulting in representations of linear and nonlinear atomic susceptibilities in terms of series in hypergeometric polynomials. These series can be easily summed at below-threshold frequency values (negative energies of intermediate states) that in most cases yields the atomic susceptibilities with a reasonable degree of accuracy. However, for the above-threshold frequencies ($\hbar\omega > |E_0|$) the standard use of FMP becomes impossible since it leads to divergent series.

For the calculation of the above-threshold bound-bound transitions of optical atomic electron we develop in this work a special technique based on decomposition of FMP Green function $g_l(E; r, r')$ into double series over Sturmian functions S_{kl} [2]:

$$g_l(E; r, r') = \sum_{k, k'=0}^{\infty} g_{kk'}^l(E; \alpha) S_{kl}(2r/\alpha) S_{k'l}(2r'/\alpha). \quad (1)$$

Here $S_{kl}(x) \sim x^\lambda \exp(-x/2) L_k^{2\lambda+1}(x)$, $\lambda = \lambda(l, E)$, $g_{kk'}^l$ are expressed in terms of product of Gauss hypergeometric functions ${}_2F_1$, α is the arbitrary parameter. To choose the value of the parameter α , an algorithm is given [3] which ensures the convergence of the bound-bound matrix elements. Calculations of the above-threshold polarizabilities are performed for alkali metals and rare gases [3]. The obtained results agree well with the other author's calculations. In particular, the He polarizability in the 27...58 eV frequency range coincides (within 10% accuracy) with more rigorous many-electron calculation [4] as well as with experiment [5].

Supported in part by RFBR Grant 07-02-00574.

References

- [1] G. Simons, J. Chem. Phys. **55**, 756 (1971).
- [2] A.A. Krylovetsky, N.L. Manakov, and S.I. Marmo, Zh. Exp. Teor. Phys. **119**, 45 (2001) [Sov. Phys. JETP **92**, 37 (2001)].
- [3] N.L. Manakov, S.I. Marmo, and S.A. Sviridov, Zh. Exp. Teor. Phys. **132**, 796 (2007) [Sov. Phys. JETP **105**, 696 (2007)].
- [4] W. C. Liu, Phys. Rev. A **56**, 4938 (1997).
- [5] J. A. R. Samson, Z. X. He, and G. N. Haddad, J. Phys. B **27**, 877 (1994).

Ionization in Intense Superposed XUV + NIR Laser Fields

V. Richardson¹, J. Dardis¹, P. Hayden¹, P. Hough¹, E. T. Kennedy¹ and J. T. Costello¹,
S. Dsterer², W. Li², A. Azima², H. Redlin², J. Feldhaus², D. Cubaynes³, D. Glijer³, M.
Meyer³,

¹*School of Physical Sciences, National Centre for Plasma Science and Technology,
Dublin City University, Dublin 9, Ireland*

²*HASYLAB, DESY, Notkestr. 85, D-22607 Hamburg, Germany*

³*LIXAM/ CNRS, UMR 8624 Centre Universitaire Paris-Sud, Btiment 350, F-91405
Orsay Cedex, France*

FLASH (i.e. Free electron LASer in Hamburg) operates on the principle of Self Amplified Spontaneous Emission (SASE) and produces coherent, bright and ultrashort eXtreme-UV (XUV) pulses [1]. The current phase of the project has been in operation since mid 2005. By synchronizing FLASH with an independent optical laser, so-called 'pump-probe' experiments become possible [2,3]. These experiments are paving the way for fundamental studies of dynamical effects in inner-shell photoionisation and photodissociation, as well as molecular fragmentation [4]. Apart from pump and probe experiments, it is also possible to induce and control coherent processes in superposed intense XUV and NIR fields. One such process is photoelectron sideband generation [5]. In this class of experiment, photoelectrons are ejected by XUV radiation and simultaneously subjected to the intense field of an optical laser with which they can exchange photons. In effect, they absorb/emit photons with energy corresponding to $\hbar\omega_l$ i.e. that energy of the optical laser photons [3]. As a consequence the photoelectron spectrum is no longer comprised of a single feature corresponding to the main photoline but is straddled by additional photoelectron lines separated by $\hbar\omega_l$, these are referred to as sidebands. In our experiments at FLASH we have used the 800 nm output ($\hbar\omega_l = 1.55$ eV) from a Ti-Sapphire laser which can provide pulses of up to a 10 mJ in pulse widths from 120 fs to 4 ps.

We have studied this process at high and low optical laser intensity for a range of atoms, namely He, Ne, Kr and Xe. In extreme cases we observe a large redistribution of the ejected electrons from the main photoline to the sidebands, so much so that a pronounced suppression of the main photoelectron line (corresponding to single XUV photon absorption) occurs when the XUV and the optical pulses are perfectly superposed.

References

- [1] W. Ackermann et al, Nature Photonics 1 336 (2007)
- [2] P. Radcliffe et al, App Phys Lett, 90, 121109 (2007)
- [3] P. Radcliffe et al, Nucl. Intr. and Meth. A (2007)
- [4] J. T. Costello, J. Phys. Conf. Ser 88, (2007)
- [5] T.E. Glover et al., Phys Rev Lett. 76, 2468 (1996)

Photoionization of excited rare gas atoms $Rg(mp^5(m+1)p \ J=0 - 3)$ in the autoionization region

I. D. Petrov¹, V. L. Sukhorukov¹, and H. Hotop²

¹*Rostov State University of Transport Communications,
344038 Rostov-on-Don, Russia,*

²*Department of Physics, University of Kaiserslautern,
D-67653 Kaiserslautern, Germany
E-mail: hotop@physik.uni-kl.de*

In the present paper we study theoretically the lineshapes of the **even** autoionizing Rydberg series $mp_{1/2}^5(m+1)\ell'$ $\ell' = 0, 2, 4$, excited from the lowest-lying **odd** $mp^5(m+1)p \ J = 0 - 3$ states of Ne, Ar, Kr, and Xe atoms in the framework of the configuration interaction Pauli-Fock approach including core polarization (CIPFCP) [1–3]. In our previous work [4–6] this approximation has successfully been applied for the investigation of the odd Rydberg resonances excited from the even states in rare gas atoms.

Autoionizing $mp_{1/2}^5(m+1)\ell' [K']_J$ Rydberg states, excited from different $mp^5(m+1)p [K]_J$ levels, attain different lineshapes, as usually characterized by the profile parameter q [7]. This dependence on the initial level was first demonstrated experimentally for the Ne(ns' , $J = 1$) resonances, excited from several Ne($3p$, $J = 1, 2$) levels [8]. The comparison between the computed spectra and experimental data indicates that many-electron effects play an important role for both the resonance parameters and the lineshapes. Absolute values of the experimental cross sections, available for photoionization of the $mp^5(m+1)p \ J = 3$ levels of Ne, Ar, and Kr, are somewhat smaller than the computed values. These differences ask for new precise measurements, e.g. using cold trapped metastable $Rg(mp^5(m+1)s [3/2]_2)$ atoms, especially in view of the good agreement between the theoretical and experimental cross sections for near-threshold photoionization of the $mp^6(m+1)p$ levels in the alkali atoms Na – Cs [2,9,10].

Support of this work by the Deutsche Forschungsgemeinschaft is gratefully acknowledged.

References

- [1] I. D. Petrov, V. L. Sukhorukov, and H. Hotop *J. Phys. B* **32**, 973 (1999).
- [2] I. D. Petrov *et al* *Eur. Phys. J. D* **10**, 53 (2000).
- [3] I. D. Petrov, V. L. Sukhorukov, and H. Hotop, *J. Phys. B* **36**, 119 (2003).
- [4] T. Peters *et al* *J. Phys. B* **38**, S51 (2005).
- [5] I. D. Petrov *et al* *Eur. Phys. J. D* **40**, 181 (2006).
- [6] I. D. Petrov *et al* *J. Phys. B* **39**, 3159 (2006).
- [7] U. Fano and J. W. Cooper, *Phys. Rev.* **137**, A1364 (1965).
- [8] J. Ganz, M. Raab, H. Hotop, and J. Geiger, *Phys. Rev. Lett.* **53**, 1547 (1984).
- [9] K. Miculis and W. Meyer, *J. Phys. B* **38**, 2097 (2005)
- [10] I. D. Petrov, V. L. Sukhorukov, and H. Hotop, *J. Phys. B* **41**, 065205 (11pp) (2008).

Spin Dependent Exchange Scattering from Ferromagnetic Materials

S.Y. Yousif Al-Mulla

*University of Borås, College of Engineering, Physics and Mathematics Group, 50190
Borås, Sweden*

It is well known that the structure information through the use of Spin Polarised Low Energy Electron Diffraction (SPLEED) is highly sensitive to the interaction potential between the primary electrons and the electrons of the target, especially to the exchange interaction. Since the electrons in SPLEED penetrate the surface only a few lattice spacing, it is extremely sensitive to the spin structure of a magnetic surface. The early study of Feder [1] on Fe(110) provides a strong indication in this direction. The main objective of this work is to use the insights of our recent work [2,3] to study the spin polarisation of electron scattering from ferromagnetic materials by using the local density approximations of the exchange-correlation potential. The differential cross sections for electron scattering from atoms with net spin, namely nickel and iron, have been calculated together with studying the energy/ wave vector dependence of the exchange scattering from surfaces of nickel and iron in glasses by calculating differential cross sections and the spin asymmetry. Comparison of predictions with observed spin dependent scattering intensities in amorphous magnetic alloys will give insight into surface magnetisation in these systems.

[1] Feder R., Solid State Comm. 31, 821 (1979)

[2] S.Y. Yousif Al-Mulla, J. Phys. B: At. Mol. Opt. Phys. 37, 305 (2004)

[3] S.Y. Yousif Al-Mulla, Eur. Phys. J. D 42, 11 (2007)

Far-wing collisional broadening of the Na(3s-3p) line by helium

K. Alioua¹, M. Bouledroua¹, A. Allouche², and M. Aubert-Frécon²

¹*Laboratoire de Physique des Rayonnements, Badji Mokhtar University,
B.P. 12, Annaba 23000, Algeria*

²*LASIM, Claude Bernard University, Lyon 1, France*

In this work, we examine theoretically the absorption spectra produced by sodium atoms immersed in a bath of helium. We present our classical and quantum-mechanical calculations of the photoabsorption spectra of the Na(3s→3p) line perturbed by ground He(1s²) atoms. We particularly focus our attention on the *ab initio* computation with MOLPRO of the ground and excited potential-energy curves, through which the systems Na(3s)+Na(3s) and Na(3p)+Na(3s) interact, and of the corresponding transition dipole moments. These potentials and moments are used to analyze the absorption spectra and their possible satellite structure at various temperatures. The results are compared with previous theoretical and experimental data [1, 2].

References

- [1] C. Zhu, J.F. Babb, and A. Dalgarno, Phys. Rev. A **73**, 012506 (2006).
- [2] H.-K. Chung, M. Shurgalin, and J.F. Babb, AIP Conference Proceedings **645**, 211 (2002).

Excited and ground potassium monatoms perturbed by helium

S. Chelli and M. Bouledroua

*Laboratoire de Physique des Rayonnements, Badji Mokhtar University,
B.P. 12, Annaba 23000, Algeria*

The purpose of this work is to calculate quantum-mechanically the diffusion coefficients of atomic potassium in helium as well as the width and shift of the $K(4p \rightarrow 4s)$ resonance line perturbed by He. The diffusion coefficients of ground $K(4s)$ and excited $K(4p)$ in a helium buffer gas are analyzed and the results are compared for few temperatures with experimental and other theoretical data. Further, the pressure broadening parameters are treated by using the most recent interatomic potentials, spin-orbit effects neglected. The simplified Baranger method is particularly used to examine the linewidth and lineshift coefficients and their behavior with temperature.

Pressure broadening of calcium resonance line perturbed by helium

L. Reggami and M. Bouledroua

*Laboratoire de Physique des Rayonnements, Badji Mokhtar University,
B.P. 12, Annaba 23000, Algeria*

The aim of this work is to calculate quantum mechanically the width w and shift d of the neutral calcium lines $\text{Ca}(4s^2 \ ^1S) \longrightarrow \text{Ca}(4s4p \ ^1P)$ and $\text{Ca}(4s^2 \ ^1S) \longrightarrow \text{Ca}(4s4p \ ^3P)$ perturbed by helium He. The *ab initio* data points from Paul-Kwiek [1] are used to construct the potential-energy curves. For the ground state, $X^1\Sigma^+$, and the four excited states, $^1\Sigma^+$, $^1\Pi$, $^3\Sigma^+$, and $^3\Pi$, the potential data are smoothly connected to the appropriate long and short forms. The numerical integration of the radial wave equation provides the elastic phase shifts which allow the computation of the linewidth and lineshift parameters by adopting the pressure broadening simplified Baranger model [2]. The results show there is in general a good agreement with other experimental and theoretical data [3, 4].

References

- [1] E. Paul-Kwiek, private communication (2007).
- [2] M. Baranger, Phys. Rev. **111**, 481 (1958).
- [3] A.R. Malvern, J. Phys. B **10**, 593 (1977).
- [4] J. Röhre-Hansen and V. Helbig, J. Phys. B **25**, 71 (1992).

Broadening and intensity redistribution in the atomic hyperfine excitation spectra due to optical pumping in the weak excitation limit

E. Saks¹, I. Sydoryk¹, N. N. Bezuglov^{1,2}, I. I. Beterov³, K. Miculis¹, and A. Ekers¹

¹ *Laser Centre, University of Latvia, LV-1002 Riga, LATVIA*

² *Faculty of Physics, St. Petersburg State University, 198904 St. Petersburg, RUSSIA*

³ *Institute of Semiconductor Physics SB RAS, 630090, Novosibirsk, RUSSIA*

We analyze spectral line broadening and variations in relative intensities of hyperfine spectral components due to optical pumping at exciting laser intensities below the saturation limit. The study was motivated by the lack of availability of detailed theoretical models describing such effects in partially open level systems. In experiment, the hyperfine laser-excitation spectra of the Na(3p) state were measured in a supersonic beam as a function of laser intensity under the conditions when optical pumping time is shorter than transit time of atoms through the laser beam. The theoretical excitation spectra were calculated numerically by solving density matrix equations of motion using the split propagation technique [1, 2].

The following results will be reported: (i) it will be shown that spectral lines can be significantly broadened at laser intensities well below the saturation intensity, which is usually regarded as the threshold for onset of broadening effects; (ii) it will be shown that the presence of dark m_F sublevels can vary the effective branching coefficients of the transitions, and this variation depends on laser intensity. Changes in the effective branching coefficients lead to irregular changes of peak ratios, like minimum in the intensity dependence of the peak ratio, which deviate from those expected from the given original branching coefficients; (iii) analytical expressions will be presented, which allow the calculation of critical values for laser intensity and Rabi frequency, above which linewidths and peak ratios are notably affected by optical pumping. The critical laser intensity can be expressed via the saturation intensity I_{sat} , the branching coefficient Π of the transition, and the ratio of natural lifetime and transit time of atoms through the laser beam τ_{nat}/τ_{tr} :

$$I_{cr} = \frac{8\pi^2\hbar c}{\sqrt{\pi}3\lambda^3} \frac{1}{\tau_{tr}\Pi(1-\Pi)} = \frac{4\tau_{nat}}{\sqrt{\pi}\tau_{tr}(1-\Pi)} I_{sat}. \quad (1)$$

Importantly, the critical laser intensity depends on the branching coefficient Π and has a minimum at $\Pi = 1/2$, and it can be much smaller than the saturation intensity.

We acknowledge support by EU FP6 TOK Project LAMOL, Latvian Science Council, and European Social Fund.

References

- [1] M. D. Fiet, J. A. Fleck, and A. Steiger, *J. Comput. Phys.* **47**, 412 (1982)
- [2] I. Sydoryk, N. N. Bezuglov, I. I. Beterov, K. Miculis, E. Saks, A. Janovs, P. Spels, and A. Ekers, *Phys. Rev. A* (2008) in print

Reconsideration of spectral line profiles affected by transit time broadening

B. Mahrov¹, C. Andreeva^{1,2}, N. N. Bezuglov^{1,3}, K. Miculis¹, E. Saks¹, M. Bruvelis¹, and A. Ekers¹

¹ *Laser Centre, University of Latvia, LV-1002 Riga, LATVIA*

² *Institute of Electronics, Bulgarian Academy of Sciences, Sofia 1784, Bulgaria*

³ *Faculty of Physics, St.Petersburg State University, 198904 St. Petersburg, RUSSIA*

In the weak excitation limit in dilute gases, when saturation and collision effects are negligible, line broadening occurs due to spontaneous decay (width Γ_{sp}), Doppler effect, and, if atoms interact with tightly focused cw laser beams, also due to limited transit time τ_{tr} of atoms through the laser beam. Consider a two step excitation process, in which Doppler broadening is avoided using counterpropagating laser fields. The conventional knowledge says that the resultant lineshapes are given by the Lorentz profile [1]

$$P(\Delta) = \pi\tilde{\Gamma} / (\Delta^2 + \tilde{\Gamma}^2); \quad 2\Delta\omega = \tilde{\Gamma} = \Gamma_{sp} + 1/\tau_{tr}, \quad (1)$$

where Δ is the detuning of the laser fields off from the two-photon resonance, and $2\Delta\omega$ is the FWHM width. If an atom from a supersonic beam at a flow velocity v_f crosses a Gaussian laser beam of FWHM L , then it is reasonable to assume $\tau_{tr} = L/v_f$.

We consider excitation of the Na($5S_{1/2}$) HF sublevel $F = 2$ with lifetime $\tau_{sp} = 76ns$ by two counter-propagating laser beams, which models an effective two-level quantum system. Laser in the first step is focused to $L_1 = 30\mu m$ using a cylindrical lens and detuned by $\Delta\nu_1=100MHz$ off from resonance with the $3S_{1/2}, F'' = 1 \rightarrow 3p_{1/2}, F' = 2$ transition. The second laser is collimated to $L_2 = 1000\mu m$, while its frequency is scanned across the two-photon resonance. The detuning $\Delta\nu_1$ is sufficient to ensure that the intermediate level is virtual. Both lasers cross the atomic beam with flow velocity of $v_f = 1200m/s$ at right angles. The time dependence of their Rabi frequencies are given by $\Omega_i(t) = \Omega_0^{(i)} \exp(-2t^2/\tau_{i,tr}^2)$, which corresponds to a Gaussian laser intensity profiles $I_i(z) = I_0^{(i)} \exp(-4z^2/L_i^2)$ along the atomic beam axis z . The spatial distribution of the corresponding effective Rabi frequency is given by $\Omega_{eff}(z) = \Omega_1(z)\Omega_2(z)/\Delta\omega_1$.

We have obtained analytical solutions to this model problem which show that the lineshape of excitation of the upper state is described by the Voigt profile with FWHM which can be approximated (within the accuracy level of 10%) by the expression

$$2\Delta\omega_{res} = \sqrt{\Gamma_{sp}^2 + 19.2 \cdot \ln(2)/\tau_{tran}^2}. \quad (2)$$

Importantly, the value of the width $2\Delta\omega_{res}$ exceeds the intuitive one $2\Delta\omega$ (1) by a factor of four if the broadening occurs predominantly due to limited transit time, i.e. when $\tau_{tran} < 1/\Gamma_{sp} = \tau_{sp}$.

We acknowledge support by EU FP6 TOK Project LAMOL (Contract MTKD-CT-2004-014228), Latvian Science Council, European Social Fund.

References

[1] B.W.Shore, *The Theory of Coherent Atomic Excitation* (Wiley, New York, 1990).

Alkali doped Helium Droplets in a Magnetic Field

G. Auböck, J. Nagl, C. Callegari, W.E. Ernst

Institute of Experimental Physics, Graz University of Technology, Austria

Helium nanodroplets are produced by supersonic free jet expansion and provide a cold environment ($T \approx 0.4$ K) for dopant atoms and molecules. Helium droplets can dissipate energy very efficiently by evaporating some of their own atoms. Alkali atoms are deposited onto the droplet by passing the droplet beam through one or more heated pick-up cells containing alkali vapor. Capture of multiple atoms per droplet leads to molecular formation; alkali-metal species are unique dopants in that they remain on the droplet's surface. Most degrees of freedom of dopant atoms and molecules are immediately cooled to the droplet's internal temperature and the energy released leads to further evaporation of helium atoms. This applies in particular to the energy of formation of complexes, which may be large enough to cause them to be expelled from the droplet: due to their smaller binding energy it is the high spin alkali complexes (triplet dimers, quartet trimers) which preferentially remain on the droplet after formation.

High-spin molecules are very interesting systems, and relate to a variety of topics such as Bose-Einstein condensation, molecule formation by photoassociation or magnetic tuning, many-body forces, reactivity and magnetism of small metal clusters, the Jahn-Teller effect, electron- and nuclear-spin resonance.

Here we summarize several results of our investigations of alkali doped He droplets in a magnetic field. This series of experiments was initially started to investigate the feasibility of optical preparation and detection of spin states for further electron spin resonance experiments. For atom doped droplets (K and Rb) we found that the spin state does not thermalize with the He droplet on the time scale of our experiment (we can extract a relaxation rate $< 1000/s$). Usually alkali atoms (molecules) are evaporated from the droplet surface upon electronic excitation what can be used for the preparation of a spin polarized beam by spin selective optical depletion for K. Contrary to common wisdom, we found that nondestructive excitation is possible at the Rb D1 line, this makes optical pumping feasible.

Unlike atoms, the spin state fully thermalizes with the internal temperature of the droplet for dimers and trimers. Then the population difference of the ground state Zeeman sublevels causes the appearance of a C-type magnetic circular dichroism (MCD). In fact the amplitude of the MCD signal can be used to determine the temperature on the droplet surface which is a priori not necessarily equal to the temperature measured in the interior. For dimers, the MCD spectrum further allowed us to interpret consistently the structure of $(1)^3\Pi_g - (a)^3\Sigma_u^+$ transitions for several molecules (K_2 , Rb_2 , Cs_2 , KRb , $LiCs$, $NaCs$) as an interplay of a perturbation of the excited state electronic wave function by the droplet surface and spin orbit coupling. For trimers we investigated the LIF and MCD spectra of the $(2)^4E' - (1)^4A_2'$ transition of K_3 and Rb_3 . We interpret these spectra as $e \otimes E$ vibronic coupling plus spin-orbit coupling. This is to our knowledge the first observation of relativistic vibronic coupling in a quartet states.

Quartet alkali trimers on He nanodroplets: Laser spectroscopy and *ab initio* calculations

J. Nagl, G. Aubock, A. W. Hauser, O. Allard, C. Callegari, and W. E. Ernst

Institute of Experimental Physics Graz University of Technology Graz Austria

Helium nanodroplets ($N = 10^4$) are produced by supersonic free jet expansion and provide a cold environment ($T = 0.4$ K) for dopants; the droplets can dissipate energy very efficiently by evaporating their own atoms (binding energy per He atom: 5 cm^{-1}). Alkali atoms are deposited on the helium surface by passing the droplet beam through one or more heated pick-up cells containing alkali vapor. Capture of multiple atoms per cluster leads to molecular formation. Due to the amount of binding energy released into the cluster, in general a strongly bound low-spin molecule will be expelled from the droplet beam, while a weakly bound high-spin van der Waals molecule will not. A variety of electronic spectra of the homo- and heteronuclear trimers K_3 , Rb_3 , K_2Rb and KRb_2 in their high-spin quartet state lie in the wavelength range $10500\text{--}17500 \text{ cm}^{-1}$. We measured them and applied various schemes of beam depletion spectroscopy, such as two-laser excitation and mass-selective depletion to separate overlapping spectral features, and to assign the individual bands.

We find several regular patterns in the spectra of these trimers, which we are in the process of explaining by means of symmetry arguments and simplified models of their level structure. The experiments are supported by high-level *ab-initio* electronic structure calculations.

References

- [1] Johann Nagl, Gerald Aubock, Andreas W. Hauser, Olivier Allard, Carlo Callegari, and Wolfgang E. Ernst. *Heteronuclear and homonuclear high-spin alkali trimers on helium nanodroplets*. Phys. Rev. Lett. **100**, 063001 (2008).
- [2] Johann Nagl, Gerald Aubock, Andreas W. Hauser, Olivier Allard, Carlo Callegari, and Wolfgang E. Ernst. *High-spin alkali trimers on helium nanodroplets: Spectral separation and analysis*. J. Chem. Phys. **128**, 154320 (2008).

Group Dynamics of 2-Atom Even-Electron Molecules and Ions

R. Hefferlin

*Physics Department, Southern Adventist University
Collegedale, Tennessee 37315, United States of America
E-mail: hefferln@southern.edu*

The group $SO(3)$ is used to characterize even-electron atoms on the basis of their electron counts. The atoms are arranged in multiplets that have “chemical angular momentum” quantum numbers l and z -component m_l [1-3]. Atoms in group 2 have $(l, m_l) = (0, 0)$; atoms in groups 14, 16, and 18 have $l = 1$ and $m_l = -1, 0, +1$. Negatively-charged atoms of groups 1, 13, 15, and 17 have the same quantum numbers; unipositive ions of atoms in groups 3, 15, 17, and (from the next higher period number) 1 also have the same quantum numbers; more highly-ionized species follow the same pattern.

Odd-electron atoms may be characterized in the very same way. Neutral atoms in group 1 have $(l, m_l) = (0, 0)$; atoms in groups 13, 15, and 17 have $l = 1$ and $m_l = -1, 0, +1$. Their ions follow the same pattern. Likewise, transition-metal and rare-earth atoms are arranged in multiplets with $l = 2$ and 3. (The period numbers are not defined in the algebra and may be chosen at will.)

Atoms or ions are now defined as vectors in the space $H(1)$. The bosonic raising operator of $SO(3)$ [4,5] is used to combine two even-electron multiplets, or two odd-electron multiplets, of atoms or ions to form multiplets of even-electron vectors in the space $H(2)$ of diatomic molecules and ions. These multiplets are then combined, using an empirical function of the two period numbers, to construct the group-dynamic periodic system of the even-electron gas-phase diatomic species. Some forecasted data for spectroscopic properties of the species are presented.

References

- [1] Y.B. Rumer, A.I. Fet, *Teor. Mat. Fiz. (Russ.)* **9**, 203 (1971)
- [2] A.I. Fet, *Theor. Math. Phys.* **22**, 227 (1975)
- [3] A.O. Barut, *Group Structure of the Periodic System*, in B. Wybourne, Ed., *Structure of matter (Proceedings of the Rutherford Centenary Symposium, 1971)*: University of Canterbury Press, Canterbury, 1972, pp. 126-136.
- [4] G.V. Zhuvikin, R. Hefferlin, *The Periodic system of Diatomic Molecules: Group-Theoretical Approach*, *Vestnik Leningradskovo Universiteta*, No. 16, 1983, pp. 10-16.
- [5] G.V. Zhuvikin, R. Hefferlin, *Joint Report #1 of the Physics Departments of Southern College [SAU], Collegedale, TN, USA and St. Petersburg University, St. Petersburg, Russia, Southern Adventist University: Collegedale, Tennessee, 1994.*

Cavity-QED with ion Coulomb crystals

A. Dantan, P. Herskind, J. Marler, M. Albert, M.B. Langkilde-Lauesen, M. Drewsen

*QUANTOP, Department of Physics and Astronomy, University of Aarhus,
Ny Munkegade, bygning 1520, D8000 Aarhus, Denmark*

In addition to its fundamental interest for atom-light studies, Cavity Quantum Electrodynamics (CQED) represents an interesting avenue for engineering efficient light-matter quantum interfaces for quantum information processing. Experiments with neutral atoms have been very successful in strongly coupling single atoms to cavities of extremely small mode volume and very high finesse. However, these experiments are challenged by the difficulty in confining and storing the atoms in the cavity for a long time [1].

Ions, on the other hand, have proved to be an excellent medium for quantum information processing and benefit from very long trapping times, a good localization and are robust against decoherence. However, minimizing the mirror separation, without severely modifying the trapping potential has made it extremely difficult to reach the strong coupling regime with a single ion [2,3]. The small mode volume requirement can be relaxed for ensembles of atoms or ions due to the enhancement of the collective coupling strength of the ensemble. In addition to tight confinement and long storage times, ion Coulomb crystals also have a number of advantages over cold atomic samples. As the ions are confined in a crystal lattice, the decoherence rate due to collisions is very low and their low optical densities (10^8cm^{-3}) make optical pumping and state preparation unproblematic. Finally, the inherent lattice structure in conjunction with the standing wave field of the optical resonator opens up for new possibilities to engineer the atom-photon interaction.

We will present recent experimental results on CQED with cold ion Coulomb crystals of calcium, obtained by using a novel linear ion trap incorporating a moderately high finesse cavity ($F \sim 3200$). Even though the 3-mm diameter dielectric cavity mirrors are placed between the trap electrodes and separated by only 12 mm, it is possible to produce *in situ* ion Coulomb crystals containing more than 10^5 calcium ions of various isotopes and with lengths of up to several millimetres along the cavity axis [4]. Single to a few thousands of ions can be stored in the cavity mode volume and efficiently prepared by optical pumping in a given magnetic substate of the metastable $4d^2D_{3/2}$ level of $^{40}\text{Ca}^+$. The first results on the crystal-light coupling strength - evaluated by probing the ion-cavity system at the single photon level - and the possibilities for CQED offered by this new system will be discussed.

[1] P.R. Berman (Ed.) Cavity Quantum Electrodynamics, Academic Press inc., London (1994)

[2] M. Keller, B. Lange, K. Hayasaka, W. Lange, H. Walther, Nature **431**, 1075 (2004)

[3] A.B. Mundt, A. Kreuter, C. Russo, C. Becher, D. Leibfried, J. Eschner, F. Schmidt-Kaler, R. Blatt, Appl. Phys. B **76**, 117 (2003)

[4] P. Herskind, A. Dantan, M.B. Langkilde-Lauesen, A. Mortensen, J. L. Sørensen, M. Drewsen, quant-ph/0804.4589.

Spin flip lifetimes in superconducting atom chips

Ulrich Hohenester¹, Asier Eiguren², Stefan Scheel³, and E. A. Hinds³

¹*Institut für Physik, Karl–Franzens–Universität Graz, Austria*

²*Donostia International Physics Center (DIPC), San Sebastian, Spain*

³*Quantum Optics and Laser Science, Imperial College London, United Kingdom*

Over the last few years, enormous progress has been made in magnetic trapping of ultracold neutral atoms near microstructured solid-state surfaces, sometimes known as atom chips [1]. The atoms can be manipulated through variation of the magnetic confinement potential, either by changing currents through gate wires mounted on the chip or by modifying the strength of additional radio-frequency control fields. These external, time-dependent parameters thus provide a versatile method of atom manipulation, and make atom chips attractive for various applications, including atom interferometry, quantum gates and coherent atom transport.

The proximity of the ultracold atoms to the solid-state structure introduces additional decoherence channels, which limit the performance of the atoms. Most importantly, Johnson-Nyquist noise currents in the dielectric or metallic surface arrangements produce magnetic-field fluctuations at the positions of the atoms. Upon undergoing spin-flip transitions, the atoms become more weakly trapped or are even lost from the microtrap. This constitutes a serious limitation for atom chips. Superconductors could reduce the magnetic noise level significantly and thereby boost the spin flip lifetimes by many orders of magnitude. Indeed, superconducting atom chips have already been fabricated and tested [2, 3] with the aim of realizing controllable composite quantum systems.

In this contribution we investigate theoretically the magnetic spin-flip transitions of neutral atoms trapped near a superconducting slab [4, 5]. We find that below the superconducting transition temperature the spin-flip lifetime becomes boosted by several orders of magnitude, a remarkable finding which is attributed to: (1) the opening of the superconducting gap and the resulting inability to deposit energy into the superconductor, (2) the highly efficient screening properties of superconductors, and (3) the small active volume within which current fluctuations can contribute to field fluctuations. Our numerical results based on the Eliashberg theory show that the expected spin-flip lifetime for an atom placed one micrometer away from a 4.2 K superconducting planar niobium surface exceeds several thousand seconds. Hence, superconducting surfaces provide an extremely low-noise environment for magnetically trapped neutral atoms and thus have great potential for coherent manipulation of atoms.

References

- [1] J. Fortagh and C. Zimmermann, *Rev. Mod. Phys.* **79**, 235 (2007)
- [2] T. Nirrengarten, A. Qarry, C. Roux, A. Emmert, G. Nogues, M. Brune, J. M. Raimond, and S. Haroche, *Phys. Rev. Lett.* **97**, 200405 (2006)
- [3] C. Roux, A. Emmert, A. Lupascu, T. Nirrengarten, G. Nogues, M. Brune, J.-M. Raimond, and S. Haroche, *Euro. Phys. Lett.* **81**, 56004 (2008)
- [4] B. S. Skagerstam, U. Hohenester, A. Eiguren and P. K. Rekdal, *Phys. Rev. Lett.* **97**, 070401 (2006)
- [5] U. Hohenester, A. Eiguren, S. Scheel, and E. A. Hinds, *Phys. Rev. A* **76**, 033618 (2007)

Interaction-Free Measurement of the Degree of Polarization of an Atomic Ensemble

Alessandro Cerè,¹ Valentina Parigi,² Marta Abad,¹ Florian Wolfgramm,¹
Ana Predojevic¹ and Morgan W. Mitchell¹

¹*ICFO-Institut de Ciències Fotoniques, Mediterranean Technology Park, Castelldefels,
08860 Barcelona, Spain*

²*LENS, Via Nello Carrara 1, 50019 Sesto Fiorentino, Florence, Italy*

In the last years, several proposals for quantum information and quantum communication schemes require the use of atomic media together with single photons. Among the possible interactions, much interest has been generated by non destructive techniques, like the quantum non-demolition measurement. We present here instead a characterization of the polarization state of an atomic sample via the non-interaction of our sample with the probe, thus reducing, in principle, the damage to the sample for successful event to zero.

The term “interaction-free” applies to a measurement process where the probe carries information about a system without interacting with it, possible thanks to the quantum nature of the interference process. After the proposal of Elitzur and Vaidman [1], an experimental demonstration was provided by Kwiat et al. [2]. We have realized an interaction free measurement of the spectrum and polarization state of a hot ensemble of ⁸⁷Rb by inserting it in a polarization interferometer, where a different optical density for one of the polarization modes is revealed by detection of light at the output dark in the balanced case. The probe is a narrowband coherent light, strongly attenuated to the single photon level, with a central frequency that can be scanned by some GHz in the region of the Rb D1 line. The atoms are optically pumped by an intense beam into the $m_F=1,2$ Zeeman substates of the $F=2$ hyperfine level. Observing the output of the dark port while scanning the probe frequency, the obtained trace presents a peak in correspondence with the transitions involving the hyperfine ground level $F=2$. The profile of the trace corresponds to the profile of the transition, power broadened by the intense pumping necessary for polarization.

The demonstrated scheme suffers from limited statistical efficiency, equal to 1/4 in theory and further reduced because of experimental imperfections. It has been demonstrated that combining the interaction free measurement approach and an implementation of the quantum Zeno effect it is possible reach a theoretical efficiency close to unity [3]. Moreover, this scheme could be used to measure the degree of polarization of a sample of atoms reducing the damage compared with standard absorption techniques [4].

References

- [1] A. Elitzur and L. Vaidman, *Foundations of Physics* **23**, 987 (1993).
- [2] P. G. Kwiat *et al.*, *Phys. Rev. Lett.* **74**, 4763 (1995).
- [3] P. G. Kwiat *et al.*, *Phys. Rev. Lett.* **83**, 4725 (1999).
- [4] P. Facchi *et al.*, *Phys. Rev. A* **66**, 012110 (2002).

Entangled atom-pairs from dissociated dimers: an experimental test of Bell inequality for atoms

J. Koperski¹, M. Krośnicki², and M. Strojecki¹

¹*Smoluchowski Institute of Physics, Jagiellonian University
Reymonta 4, 30-059 Krakow, Poland*

²*Institute of Theoretical Physics and Astrophysics
University of Gdansk, Wita Stwosza 57, 80-952 Gdansk, Poland
E-mail: ufkopers@cyf-kr.edu.pl*

In 1964 Bell showed that in all local realistic theories, correlations between the outcomes of measurements in different parts of a physical system satisfy certain class of inequalities [1]. Furthermore, he found that certain predictions of quantum mechanics violate these inequalities. Starting with the first experimental tests of Bell inequalities with photons [2], violation of a Bell inequality has been observed for protons [3], K mesons [4], ions [5], neutrons [6], B mesons [7], atom-photon systems [8], and atomic ensembles [9].

Production of entangled *atom-pairs* via stimulated two-photon Raman dissociation of dimers produced in supersonic free-jet pulsed beam will be described. The process relies on the proposal of Fry et al. [10] for experimental realization of Bohm's spin-1/2 particle version of the Einstein-Podolsky-Rosen (EPR) experiment. The first stage of the experiment, designed for ¹⁹⁹Hg atoms, is underway at Texas A&M University. The real challenge is to isolate a particular rotational transition within a triplet-singlet D³1_u–X¹0_g⁺ electronic transition in ¹⁹⁹Hg₂ propagating in the beam [11], and then dissociate the excited isotopomer using a stimulated Raman process. Pairs of entangled ¹⁹⁹Hg atoms obtained in this way are going to be spin-state-selectively detected in two different atom detectors located in two parallel planes of detection.

An alternative approach is to selectively dissociate ¹¹¹Cd₂ isotopomers produced in a continuous supersonic free-jet using selected rotational transition within a singlet-singlet A¹0_u⁺–X¹0_g⁺ electronic transition in ¹¹¹Cd₂. During the conference the advantages of using the latter approach and recent developments in the endeavor of testing Bell inequality for ¹¹¹Cd atoms planned in Krakow will be reported.

This work was financed from 2007-2010 funds for science of Polish Ministry of Science and Higher Education (research project N N202 2137 33).

References

- [1] J.S. Bell, Physics (Long Island City, N.Y.) **1**, 195-200 (1964).
- [2] S.J. Freedman, J.F. Clauser, Phys. Rev. Lett. **28**, 938-941 (1972).
- [3] M. Lamehi-Rachti, W. Mittig, Phys. Rev. **D14**, 2543-2555 (1976).
- [4] A. Bramon, M. Nowakowski, Phys. Rev. Lett. **83**, 1-5 (1999).
- [5] M.A. Rowe et al., Nature (London) **409**, 791-794 (2001).
- [6] Y. Hasegawa et al., Nature (London) **425**, 45-48 (2003).
- [7] A. Go, J. Mod. Opt. **51**, 991-998 (2004).
- [8] D. L. Moehring et al., Phys. Rev. Lett. **93**, 090410 (2004).
- [9] D. N. Matsukevich et al., Phys. Rev. Lett. **96**, 030405 (2006).
- [10] E. Fry, T. Walther, S. Li, Phys. Rev. **A 52**, 4381-4395 (1995).
- [11] J. Koperski et al., Chem. Phys. (2008), in press.

Primary gas thermometry by means of near-infrared laser absorption spectroscopy and determination of the Boltzmann constant

G. Casa¹, A. Castrillo¹, G. Galzerano², R. Wehr¹, A. Merlone³, D. Di Serafino⁴, P. Laporta² and L. Gianfrani^{1,†}

¹*Dipartimento di Scienze Ambientali, Seconda Università di Napoli, Caserta, Italy*

²*Dipartimento di Fisica, Politecnico di Milano and Istituto di Fotonica e Nanotecnologie (IFN-CNR), Milano, Italy*

³*Istituto Nazionale di Ricerca Metrologica, Torino, Italy*

⁴*Dipartimento di Matematica, Seconda Università di Napoli, Caserta, Italy*

[†]*livio.gianfrani@unina2.it*

We report on a new method for primary gas thermometry, based on high-precision, intensity-stabilized laser absorption spectroscopy in the near-infrared. Initially designed and developed for the accurate determinations of absolute linestrength factors [1], the method consists in retrieving the Doppler width from the absorption line shape corresponding to a given vibration-rotation transition in a CO₂ gaseous sample at thermodynamic equilibrium. There is presently a strong interest in new primary thermometric methods, likely to be employed for direct and highly accurate determinations of the Boltzmann constant k_B , in view of a possible new definition of the unit kelvin [2].

We probed the R(12) component of the $\nu_1+2\nu_2^0+\nu_3$ combination band, using a distributed feedback diode laser, which was mounted in a mirror-extended cavity configuration. Consisting of a cylindrical cavity inside an aluminum block, with inner and external surfaces carefully polished, the absorption cell was housed inside a stainless steel vacuum chamber and its temperature was stabilized at a level of ~ 10 mK by means of an active system based on four Peltier elements and a PID controller. The gas temperature was measured by means of precision platinum resistance thermometers, carefully calibrated at the triple point of water and at the gallium melting point with an overall accuracy better than 10 mK. By doing Doppler broadening measurements as a function of the gas temperature, which was varied between 270 and 305 K, we determined the Boltzmann constant with an uncertainty of 1.6×10^{-4} , including statistical and systematic errors [3].

We also report on the status of a second-generation experiment, in which a pair of phase-locked extended-cavity diode lasers are being employed in order to improve significantly the capability of measuring laser frequency variations.

References

- [1] G. Casa, D. A. Parretta, A. Castrillo, R. Wehr, and L. Gianfrani, *J. Chem. Phys.* **127**, 084311 (2007)
- [2] B. Fellmuth et al., *Meas. Sci. Technol.* **17**, R145 (2006)
- [3] G. Casa, A. Castrillo, G. Galzerano, R. Wehr, A. Merlone, D. Di Serafino, P. Laporta and L. Gianfrani, *Phys. Rev. Letters*, in press

Towards precision spectroscopy in the XUV

Valentin Batteiger¹, Maximilian Herrmann¹, Sebastian Knünz¹, Akira Ozawa¹, Andreas Vernaleken¹, Guido Saathoff¹, Mariusz Semczuk¹, Feng Zhu², Hans Schuessler², Theodor W. Hänsch¹ and Thomas Udem¹

¹*Max-Planck-Institut für Quantenoptik, Hans-Kopfermann-Strasse 1, D-85748 Garching*

²*Department of Physics, Texas A&M University, College Station, Texas 77843, USA*

Recent developments of XUV frequency combs [1],[2] open up the possibility of high resolution spectroscopy in the XUV wavelength regime. The 1s-2s two photon transition in hydrogen-like Helium at 60 nm is a particular interesting candidate allowing a further test of bound state QED. Our proposed spectroscopy scheme is based on the detection of ionization events out of the 2s state and sympathetic cooling by co-stored Magnesium ions in a RF-trap. Experimental progress is presented, including an absolute frequency measurement on cooling transitions in Mg⁺.

References

- [1] C. Gohle et. al., Nature 436, 234 (2005)
- [2] R. J. Jones et al., PRL 94, 193201 (2005)

Probing isotope effects in chemical reactions using single ions

Peter F. Sta anum¹, Klaus Høj bjerre¹, Roland Wester² and Michael Drewsen¹

¹*Department of Physics and Astronomy, University of Aarhus, Aarhus, Denmark*

²*Physikalisches Institut, Universität Freiburg, Freiburg, Germany*

Isotope effects often play an important role for the outcome of chemical reactions. For instance the chemical composition of interstellar clouds is strongly influenced by isotope effects in certain reactions [1]. In laboratory experiments, isotope effects observed in isotopic analogs of chemical reactions can provide important information about details of the reaction dynamics.

Here we present a recent study of isotope effects, in reactions between Mg^+ in the $3p^2P_{3/2}$ excited state and molecular hydrogen at thermal energies, through *single* reaction events observed in a Paul trap [2]. From only ~ 250 reactions with HD, the branching ratio between formation of MgD^+ and MgH^+ is found to be larger than 5. From additional 65 reactions with H_2 and D_2 we find that the overall decay probability of the intermediate MgH_2^+ , MgHD^+ or MgD_2^+ complexes is the same. These results suggest that the observed isotope effect in reactions with HD arise through a dynamic mechanism in the exit channel of the reaction, which may also explain the isotope effect observed in reactions with ground state Mg^+ ions at much higher collision energies [3].

Our study shows that few *single* ion reactions can provide *quantitative* information about branching ratios and relative reaction rate coefficients in ion-neutral reactions. Hence, the method is particularly well suited for reaction studies involving rare species, e.g., rare isotopes or short-lived unstable elements, as well as for studies involving state prepared molecular ions [4], more complex molecular ions [5, 6] or of astrophysically relevant reactions [7, 8].

References

- [1] T. J. Millar, Space Science Reviews **106**, 73 (2003).
- [2] P. F. Sta anum, K. Høj bjerre, R. Wester and M. Drewsen, arXiv:0802.2797v1.
- [3] N. Dalleska, K. Crellin and P. Armentrout, J. Phys. Chem. **97**, 3123 (1993).
- [4] I. S. Vogelius, L. B. Madsen and M. Drewsen, Phys. Rev. Lett. **89**, 173003 (2002); Phys. Rev. A **70**, 053412 (2004).
- [5] A. Ostendorf *et al.*, Phys. Rev. Lett. **97**, 243005 (2006).
- [6] K. Høj bjerre *et al.*, Phys. Rev. A **77**, 030702(R) (2008).
- [7] D. Gerlich, E. Herbst and E. Roueff, Planetary and Space Science **50**, 1275 (2002).
- [8] S. Trippel *et al.* Phys. Rev. Lett. **97**, 193003 (2006).

Laser cooling of unbound atoms in nondissipative optical lattice

N. A. Matveeva¹, A. V. Taichenachev^{1,2}, A. M. Tumaikin¹ and V. I. Yudin^{1,2}.

¹ *Novosibirsk State University*

Pirogova 2, 630090 Novosibirsk, Russia

²*Institute of Laser Physics SB RAS*

Laurenteva 13/3, 630090 Novosibirsk, Russia

E-mail: matveeva1314@ngs.ru

Laser cooling of neutral atoms plays a very important role in optical metrology. In particular, the transversal cooling (collimation) of an atomic beam below μK would allow one to achieve the higher precision and stability in the modern atomic frequency standards (atomic fountains, atomic clock in condition of microgravitation). This collimation can be made by the method of sideband-resolved Raman cooling (SRLC). The experiments on SRLC of neutral cesium atoms [1] were carried out in the 2D nondissipative (far-off-resonance) optical lattice with pre-cooling in a near-resonance lattice, which complicated experimental realization. Similar experiments on the high-effective 3D - SRLC were made without pre-cooling stage [2], but the exhaustive theoretical explanation of high cooling efficiency has not been presented. Then SRLC was applied at the attempt of the improvement of the continuous atomic fountain [3]. In these experiments one used 2-D cooling scheme similar to described in [2]. However, the efficiency of cooling was poor and appreciably lower in comparison with the previous results [2]. The causes of this were not explained. Thus the necessity of more detailed investigation of cooling in nondissipative optical lattices has arisen. One of the purposes of such consideration is to find the fields of parameters where cooling mechanisms of unbound and bound atoms co-exist.

In the present work the semiclassical approach is applied for the analysis of cooling of unbound atoms with optical transitions $J \rightarrow J - 1$ in a one-dimensional nondissipative optical lattice. For slow atoms in the low-saturation limit the analytical expressions for coefficients of friction and diffusion are obtained for the simplest $1 \rightarrow 0$ transition. However, in this case it is necessary to go beyond the slow atom approximation for the full description of atomic kinetic. For this purpose the dependence of force on atom and the coefficient of diffusion on the atomic velocity are found. At the weak Raman transition the heating takes place for small velocity that corresponds to the results of the slow atom approximation. At the increasing of atomic velocity the direction of kinetic process changes and cooling occurs. In addition there are the selective velocity Raman resonances in the force, that have some specific features for $J \rightarrow J - 1$ atomic transitions. The kinetic temperature is estimated on the base of the numerical solution of Fokker-Plank equation for Wigner distribution function.

References

- [1] S. E. Hamann, D. L. Haycock, G. Klose *et al.*, Phys. Rev. Letters **80**, 4149 (1998)
- [2] A. J. Kerman, V. Vuletic, C. Chin, and S. Chu, Phys. Rev. Letters **84**, 439 (2000)
- [3] G. Di Domenico, N. Castanga, G. Miletì *et al.*, Phys. Rev. A **69**, 063403 (2004)

Investigations on the lin|| lin CPT and its application in quantum sensors

R. Lammegger¹, E. Breschi², G. Kazakov³, G. Mileti², B. Matisov³ and L. Windholz¹

¹*Institute of Experimental Physics TU-Graz, Petersgasse16, 8010 Graz*

²*Laboratoire Temps-Fréquence, University of Neuchâtel, rue A.-L.-Breguet 1, CH-2000 Neuchâtel*

³*St. Petersburg State Polytechnic University, Polytechnicheskaya 29, 195251 St. Petersburg, Russia*

Coherent Population Trapping (CPT) is a resonance phenomenon due to a quantum mechanical interference effect in an atomic system. The resonantly driven atomic level population is being trapped into a so called dark state, yielding the atomic medium transparent for the exciting electromagnetic fields.

We present experimental investigations on the behavior of CPT resonances in Rubidium (⁸⁷Rb Isotope) due to the interaction of a linear polarized bichromatic laser light (lin|| lin CPT) in presence of longitudinal magnetic fields[1]. In this configuration the coherence has a quadrupol like nature and is strongly influenced by the hyperfine structure of the excited state. The hyperfine structure of the excited states gives rise to degenerate CPT resonances. By comparing the multi-level model calculations with the experimental results we demonstrate that the quantum interference between the multi-CPT states is an essential feature in this interaction scheme.

We investigate the lin|| lin CPT signal depending on the relationship of pressure broadening and laser linewidth. Therefore CPT signals obtained by excitation with a vertical surface emitting laser system (linewidth 100MHz) and a system of phase locked lasers (linewidth 40kHz) are compared. The experimental and theoretical results allow us to quantify the contribution from different CPT-states to the total lin|| lin CPT signal. Based on our experiment, we can define the conditions in which the laser linewidth does not degrade the amplitude of the lin|| lin CPT signal and, thus the optimal performance for compact atomic clocks and magnetometers based on lin|| lin CPT.

References

[1] E. Breschi, G. Kazakov, R. Lammegger, G. Mileti, B. Matisov and L. Windholz, arXiv:0804.4627v1 [quant-ph]

Optically Driven Atomic Coherences: From the Gas Phase to the Solid State

J. Klein, F. Beil, and T. Halfmann

Institute of Applied Physics, Technische Universität Darmstadt, Germany

Coherent interactions between strong radiation and quantum systems provide well-established tools to control optical properties and processes. Among others, applications aim at efficient data storage and processing of optically stored data, e.g. as required in quantum information processing. Thus, a large number of experimental studies in quantum information science have been conducted in atomic media in the gas phase. Only few experiments on coherent, adiabatic interactions were conducted in solid state media. Appropriate solid materials for such investigations are quantum dots, color centers, or rare-earth doped solids. The latter combine the advantages of atoms in the gas phase, i.e. spectrally narrow transitions and long dephasing times, with the advantages of solids, i.e. large density and scalability. In the talk we present implementations of coherent interactions in a rare-earth doped solid, i.e. a Pr:YSO crystal [1]. In particular we report on the experimental implementation of stimulated Raman adiabatic passage (STIRAP) in Pr:YSO. Our data provide clear and striking proof for complete population inversion between hyperfine levels in the Praseodymium dopants. Time-resolved absorption measurements serve to monitor the adiabatic population dynamics during the STIRAP process. We will discuss the possibilities of STIRAP and related techniques to drive atomic coherences in the solid state environment, e.g. for applications in optical and quantum information processing.

References

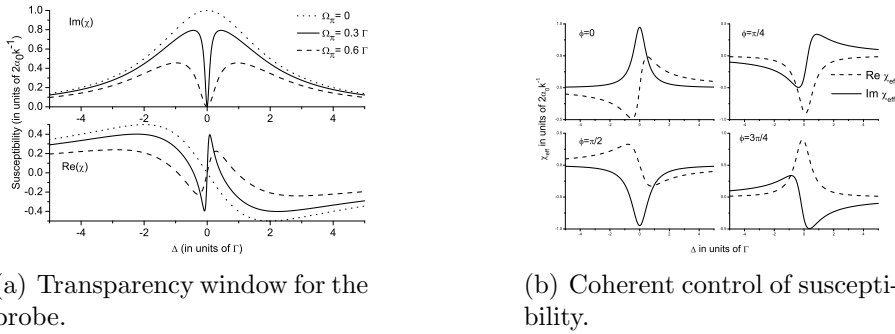
- [1] J. Klein, F. Beil, and T. Halfmann, Phys. Rev. Lett. **99**, 113003 (2007)

Slowing light and coherent control of susceptibility in a duplicated two-level system

F.A. Hashmi, M.A. Bouchene

*Laboratoire de Collision Agrégats Réactivité, C.N.R.S UMR 5589, IRSAMC
Université Paul Sabatier, 118 Route de Narbonne, 31062 TOULOUSE, FRANCE*

We present a new method of slowing light that can be realized in a double two level system by exciting it with two orthogonally polarized light pulses that propagate along different axis ¹. Spatio-temporal dephasing of the total polarization induces a grating in the ground zeeman coherence. The stronger of the two fields (the control field) is diffracted from this grating into the direction of the weak probe field compensating for the absorption of this latter field. A transparency window is thus created in the absorption spectrum of the probe leading to the slowing down of light [Fig. 1(a)]. The transparency window exhibits characteristics identical to the one obtained by EIT method. However, the important difference between our method and the traditional EIT method is that ours doesn't rely on realizing dark state in the system. This may open the possibility of slowing down light in more complex atomic media.



(a) Transparency window for the probe.

(b) Coherent control of susceptibility.

Figure 1: Real and Imaginary parts of the susceptibility. Ω_π is the strength of the control field, Δ is the detuning for the probe in (a) and detuning of both probe and control in (b)

For the case when the two fields have the same frequency and the same axis of propagation, linear susceptibility vanishes and higher order, phase dependent non-linear susceptibility becomes important, allowing coherent control of the optical response of the medium ². Coherent control of the medium gain for double two level system in the femtosecond pulse regime has already been discussed ³. Here we demonstrate that for long pulses the effective susceptibility for the probe behaves as $\chi_{lin} e^{-2i\phi}$ where χ_{lin} is linear susceptibility and ϕ is the phase difference between two fields. Depending on the relative phase between the two fields the system can be converted into an absorber or the gain medium for the probe with normal or anomalous dispersion [Fig. 1(b)]. At larger optical thickness, phase growth during propagation destroys this coherent control and effective susceptibility turns into χ_{lin}^* , turning an absorber into an amplifier without effecting the dispersion.

¹F.A. Hashmi and M.A. Bouchene, *Slowing light through Zeeman Coherence Oscillations in a duplicated two-level system*, submitted to Phys.Rev.A (2008)

²F.A. Hashmi and M.A. Bouchene, *Coherent control of the effective susceptibility through wave mixing in a duplicated two-level system (2008)*, submitted to Phys.Rev.Lett.

³J.C. Delganes and M.A. Bouchene, Phys. Rev. Lett. **98**, 053602 (2007)

Rydberg excitation of a Bose–Einstein condensate

T. Pfau , R. Heidemann, U. Raitzsch, V. Bendkowsky, B. Butscher, R. Löw

5. Physikalisches Institut, Universität Stuttgart, Pfaffenwaldring 57, D-70550 Stuttgart, Germany
t.pfau@physik.uni-stuttgart.de

Rydberg atoms provide a wide range of possibilities to tailor interactions in a quantum gas. Here we report on Rydberg excitation of Bose-Einstein condensed ^{87}Rb atoms. The Rydberg fraction was investigated for various excitation times and temperatures above and below the condensation temperature. The excitation is locally blocked by the van der Waals interaction between Rydberg atoms to a density-dependent limit. Therefore the abrupt change of the thermal atomic density distribution to the characteristic bimodal distribution upon condensation could be observed in the Rydberg fraction. The observed features are reproduced by a simulation based on local collective Rydberg excitations [1]. The excitation dynamics was investigated for a large range of densities and laser intensities and shows a full saturation and a strong suppression with respect to single atom behaviour. The observed scaling of the initial increase with density and laser intensity provides evidence for coherent collective excitation. This coherent collective behaviour, that was observed for up to several thousand atoms per blockade volume is generic for all mesoscopic systems which are able to carry only one single quantum of excitation [2]. Despite the strong interactions the evolution can still be reversed by a simple phase shift in the excitation laser field. We experimentally prove the coherence of the excitation in the strong blockade regime by applying an optical rotary echo technique to a sample of magnetically trapped ultracold atoms, analogous to a method known from nuclear magnetic resonance. We additionally measured the dephasing time due to the interaction between the Rydberg atoms. [3]

References

- [1] R. Heidemann, U. Raitzsch, V. Bendkowsky, B. Butscher, R. Löw, and T. Pfau
 "Rydberg excitation of Bose-Einstein condensates"
 Phys. Rev. Lett. **100** , 033601 (2008).
- [2] R. Heidemann, U. Raitzsch, V. Bendkowsky, B. Butscher, R. Löw, L. Santos, T. Pfau
 "Evidence for coherent collective Rydberg excitation in the strong blockade regime"
 Phys. Rev. Lett. **99**, 163601 (2007).
- [3] U. Raitzsch, V. Bendkowsky, R. Heidemann, B. Butscher, R. Löw, T. Pfau
 "An echo experiment in a strongly interacting Rydberg gas"
 Phys. Rev. Lett. **100** , 013002 (2008).

Progress towards a high-precision measurement of the g -factor of a single, isolated (anti)proton in a double Penning trap

S. Kreim¹, K. Blaum^{2,3}, H. Kracke¹, A. Mooser¹, W. Quint², C. Rodegheri¹, S. Ulmer^{2,4}, J. Walz¹

¹*Institut für Physik, Johannes Gutenberg-Universität, 55099 Mainz, Germany*

²*GSI Darmstadt, 64291 Darmstadt, Germany*

³*Max-Planck-Institut für Kernphysik, 69117 Heidelberg, Germany*

⁴*Ruprecht Karls-Universität, 69047 Heidelberg, Germany*

E-Mail: kreim@uni-mainz.de

This experiment is aimed at measuring the magnetic moment or g -factor of a single, isolated proton stored in a cylindrical Penning trap with a relative uncertainty of 10^{-9} or better, which will be the first direct measurement of the proton g -factor ever performed. Determining the g -factor of a particle results from an accurate measurement of its cyclotron and spin precession frequency. The Larmor frequency can be extracted by inducing radio-frequency transitions between the two spin states in the homogeneous magnetic field region of the first, precision Penning trap. The resulting spin state is then detected non-destructively in the magnetic bottle field of the analysis trap. There, the magnetic moment is coupled to the axial eigenmotion shifting this frequency according to the spin direction. The value of the frequency shift scales with the magnetic moment of the particle and the strength of the magnetic bottle. Thus, a novel trap design was developed which we call *hybrid Penning trap* [1] to increase the axial frequency jump to a detectable range.

To achieve a high-precision determination of the proton g -factor, long storage times are required which is realized by performing the experiment in a closed setup at 4 K yielding extremely low background pressure ($p < 10^{-16}$ mbar). This environment bears great challenges for the electronics needed to non-destructively detect the trapped proton, however, it leads to a low electronic noise. In addition, the use of superconductive resonant circuits increases the signal-to-noise ratio of the detection system by some orders of magnitude.

Since the sealed system requires an in-trap creation of protons, a newly developed cryogenic electron gun [2] will function as an electron beam ion source permitting the creation of protons inside the magnetic field and at 4 K. Commissioning experiments with electron gun and fully cabled system will be presented where the performance of the trap tower and the thermal behavior of electronic components were examined. At present, the detection circuits are implemented to yield spectra of particle clouds shortly.

Besides the proton g -factor, future experiments aim at determining the antiproton g -factor. Comparison of the two experimental values will provide a stringent test of CPT invariance on the baryonic sector. Furthermore, the hybrid trap design enables a variety of new experiments such as investigating the magnetic moments of bare light nuclei like ³He or tritium.

References

- [1] J. Verdu *et al.*, LEAP Conf. Proc., 260 (2005), J. Verdu *et al.*, submitted (2008)
- [2] F. Maurer, *et al.*, Nucl. Instr. Meth. B **54**, 234 (2005)

Helium-4 Clusters Doped with Excited Rubidium Atoms

Robert E. Zillich¹, Markku Leino², Alexandra Viel²

¹*Institute of Theoretical Physics, Johannes Kepler Universität Linz, Austria*

²*Institute of Physics of Rennes, UMR 6251 du CNRS, Université de Rennes 1, France*

We report on a quantum Monte Carlo study of helium nanodroplets doped with an electronically excited rubidium atom, Rb^* . Our work is motivated by recent experiments conducted in Graz and Freiburg.

The Rb-He_N potential energy surface (PES) is simply a sum of pair potentials if the Rb is in the electronic ground state. If Rb is in an electronically excited state (Rb^*), the PES of $\text{Rb}^*\text{-He}_N$ is based on the diatomics-in-molecules model, thus it is different from a pair potential. Moreover, the spin-orbit coupling cannot be neglected and it is responsible for different equilibrium structures when compared with potassium.

We use the diffusion Monte Carlo (DMC) method to obtain ground state energies along with different unbiased pair distribution densities. For the first excited state of Rb, the PES could accommodate a planar ring of $N = 8$ helium atoms, but the DMC simulations show that only $N = 7$ atoms fit into the ring, because of the large zero point motion of He atoms. Adding more atoms creates a very diffuse second ring.

For simulations at the temperature of large ^4He droplets of about $T = 0.3 - 0.4\text{K}$, we employ the path integral Monte Carlo (PIMC) method. If Rb is in the electronic ground state, Rb-He_N is a weakly bound complex. Increasing N to $N = 100$ it becomes a He droplet with Rb sitting in a “dimple” on the surface. For Rb in the first excited state, PIMC simulations confirm the DMC results, that a ring of up to 7 He atoms forms around the Rb atom.

In order to model the experiments where Rb is excited from the electronic ground state to the first excited state, we performed PIMC simulations where we start from equilibrium configurations of Rb-He_N and then switch to the PES of the 1st excited state. In this case, we do not find any signature of a He ring around Rb^* , but instead Rb^* is promoted to a very weakly bound, metastable state where it sits in a shallow He dimple. This result agrees with the interpretation of recent experiments [1]. We used the same modeling for the excitation from the ground state to the 2nd excited state of Rb. In this case, we found a clear signature of the formation of a Rb^*He exciplex, which is weakly bound to the cluster of $N - 1$ He atoms. We plan to investigate the dynamics upon such electronic excitations of Rb using correlated basis function theory.

References

[1] W. Ernst et al., private communication

Progress in optically-detected spin-resonance on helium droplets

M. Koch, J. Lanzersdorfer, G. Auböck, J. Nagl, C. Callegari, and W. E. Ernst

Institute of Experimental Physics, Graz University of Technology, Graz, Austria

We demonstrate the possibility of optically detecting the spin state of alkali metal atoms and molecules weakly bound on the surface of helium nanodroplets, immersed in a magnetic field. This allows us to show that the electronic spins of atoms do not relax within the timescale of the experiment ($\sim 10^{-3}$ s) and those of molecules do. With this prerequisite knowledge, we demonstrate that electron spins on a He droplet can be manipulated. We show why Rb do not desorb from the droplet upon laser excitation, and how this leads to optical pumping, which we achieve experimentally.

With the addition of a microwave field, we have just succeeded in optically detecting an electron-spin transition, on K atoms; the perturbation due to the helium results in a distinct shift of the g value, which we are in the process of accurately quantifying; the same measurements will be done on Rb, and the latest results will be presented at the meeting.

References

- [1] J. Nagl, G. Auböck, C. Callegari and W. E. Ernst, *Phys. Rev. Lett.* **98**, 075301 (2007).
- [2] G. Auböck, J. Nagl, C. Callegari and W. E. Ernst, *J. Phys. Chem. A* **111**, 7404 (2007).
- [3] G. Auböck, J. Nagl, C. Callegari and W. E. Ernst, *submitted to Phys. Rev. Lett.* (2008).

Effect of finite detection efficiency on the observation of the dipole-dipole interaction of a few Rydberg atoms

I.I.Ryabtsev, D.B.Tretyakov, I.I.Beterov, and V.M.Entin

Institute of Semiconductor Physics, Pr. Lavrentyeva 13, 630090 Novosibirsk, Russia
E-mail: ryabtsev@isp.nsc.ru

Studies of the long-range interactions in small ensembles of closely placed Rydberg atoms are important to implement quantum logic gates of a quantum computer. As such gates imply coherent interactions of two Rydberg atoms, or excitation of only one Rydberg atom at the dipole blockade, the key issue in these studies is the high detection efficiency of Rydberg atoms and the need to distinguish between the signals measured for 1, 2, 3, etc., atoms with high fidelity.

Selective Field Ionization (SFI) technique [1] is most appropriate to detect single Rydberg atoms. However, microchannel plate detectors commonly used in experiments do not provide the single-atom resolution. Therefore, in our work we focused on detecting Rydberg atoms with a channeltron. In our experiments we have found that the histograms of its output pulses have prominent maxima corresponding to 1-5 detected atoms. Combined with the post-selection technique, this provides a tool to investigate the signals measured in experiments on long-range interactions of definite small numbers of Rydberg atoms.

We have developed a simple theoretical model [2] describing multiatom signals that we measure in the experiments on Stark-tuned resonant dipole-dipole interactions [1] of a few Rydberg atoms in an atomic beam and frozen Rydberg gas. We have shown that finite efficiency of the SFI detector leads to the mixing up of the spectra of resonant collisions registered for various numbers of Rydberg atoms. The formulas are presented, which help to estimate an appropriate mean Rydberg atom number for a given detection efficiency. The dependences of the measured signals on the number of atoms, excitation volume, energy and interaction time were investigated. We have also found that a measurement of the relationship of the amplitudes of resonances observed in the one- and two-atom signals provides a straightforward determination of the absolute detection efficiency and mean Rydberg atom number excited per laser pulse. This method is advantageous as it is independent of the specific experimental conditions.

Finally, we have performed the testing experiments on resonant dipole-dipole interactions $\text{Na}(37\text{S})+\text{Na}(37\text{S})\rightarrow\text{Na}(36\text{P})+\text{Na}(37\text{P})$ in a small excitation volume of a sodium atomic beam [2] and $\text{Rb}(nP)+\text{Rb}(nP)\rightarrow\text{Rb}(n\text{S})+\text{Rb}((n+1)\text{S})$ in a rubidium magneto-optical trap. The resonances obtained for 1 to 5 of detected Rydberg atoms have been analyzed and compared with the theory. The peculiarities of the obtained results will be discussed in this report.

This work was supported by the Russian Academy of Sciences.

References

- [1] T.F.Gallagher, "Rydberg Atoms", Cambridge University Press, Cambridge (1994).
- [2] I.I.Ryabtsev, D.B.Tretyakov, I.I.Beterov, and V.M.Entin, Phys. Rev. A, 2007, v.76, p.012722.

Energy approach to discharge of metastable nuclei during negative muon capture

A.V. Glushkov^{1,2}, O.Yu. Khetselius², S.V. Malinovskaya², Yu.V. Dubrovskaya²

¹*Institute for Spectroscopy of Russian Academy of Sciences, Troitsk, 142090, Russia*

²*Odessa University, P.O.Box 24a, Odessa-9, 65009*

A negative muon captured by a metastable nucleus may accelerate the discharge of the latter by many orders of magnitude [1]. For a certain relation between the energy range of the nuclear and muonic levels the discharge may be followed by the ejection of a muon, which may then participate in the discharge of the other nuclei. We developed new, QED energy approach (EA) to calculating characteristics for the discharge of a nucleus with emission of quantum and further muon conversion, which initiates this discharge. Traditional process of the muon capture are in details studied earlier and here is not considered. The intensities of satellites (decay probability) are linked with imaginary part of the "nucleolus core+ proton +muon" system. Three channels should be taken into account: 1). radiative purely nuclear 2j-poled transition (probability P1; this value can be calculated on the basis of known traditional formula); 2). Non-radiative decay, when a proton transits into the ground state and a muon leaves the nuclei with energy $E = E(p - N1J1) - E(i)$, where $E(p - N1J1)$ is an energy of nuclear transition, $E(i)$ is an energy of bond for muon in the 1s state (P2); 3). A transition of proton into the ground state with excitation of muon and emission of the quantum with energy $E(p - N1J1) - E(nl)$ (P3). Under condition $E(p-N1J1) \geq E(i)$ a probability definition reduces to QED calculation of probability of the autoionization decay of the two-particle system. Numerical calculation is carried out for the Sc nucleus. The probabilities of the meso atom decay for different transitions: $P2(p1/2-p3/2) = 3.93 \cdot 10^{15}$, $P2(p1/2-f7/2) = 3.15 \cdot 10^{12}$, $P2(p3/2-f7/2) = 8.83 \cdot 10^{14}$. For above indicated transitions the nucleus must transit the momentum no less than 2,4 and 2 according to the momentum and parity rules. If a meso-atom is in the initial state p1/2, than the cascade discharge occur with ejection of muon on the first stage and the quantum emission on the second stage. To consider a case when the second channel is closed and the third one is opened, suppose: $E(p1/2) - E(p3/2) = 0.92$ MeV. Energy of nuclear transition is not sufficient to transit the muon into the continuum state and it may excite into the 2p state. In this case there is the proton transition p1/2-p3/2 with virtual excitation of muon into states of series nd and quantum emission with energy $EE = Ep(p1/2) + E(1s) - Ep(p3/2) - E(2p)$. The dipole transition 2p-1s occurs with probability: $P3 = 1.9 \cdot 10^{13} s^{-1}$ that is more than probabilities of the p1/2-p3/2 and p1/2-f7/2 transitions without radiation.

References

- [1] V.I.Gol'dansky, V.S.Letokhov, JETP. **67**, 513 (1974); L.N.Ivanov, V.S.Letokhov, JETP. **70**, 19 (1976); A. Glushkov, L.N. Ivanov, Phys. Lett.A. **170**, 33 (1992)
- [2] A. Glushkov et al, Recent Adv. In Theory of Phys. and Chem Systems (Springer). **15**, 301 (2006).
- [3] A.V.Glushkov, S.V.Malinovskaya, In: New projects and New lines of research in Nuclear Phys., eds.Fazio G.,Hanappe F., World Sci.,Singapore, 242 (2003); Nucl. Phys. A. **734**, 21 (2004)

Resonance phenomena in heavy ions collisions and structurization of positron spectrum

A.V. Glushkov¹²

¹*Institute for Spectroscopy of Russian Academy of Sciences, Troitsk, 142090, Russia*
²*Odessa University, P.O.Box 24a, Odessa-9, 65009*

A great interest to this topic has been, in particular, stimulated by inaugurating the heavy-ion synchrotron storage cooler ring combination SIS/ESR at GSI [1]. The known discovery of existence of a narrow and unexpected e⁺ line in the positron spectra obtained from heavy ions collisions near the Coulomb barrier. Here a consistent unified QED approach is developed and applied for studying the low-energy heavy ions collision, including the electron- positron pair production (EPPP) process too. To calculate the heavy ions (atoms, nuclei) (EPPP) cross-section we use modified versions of the relativistic energy approach, based on the S-matrix Gell-Mann and Low formalism and QED operator perturbation theory [2]. The nuclear subsystem and electron subsystem has been considered as two parts of the complicated system, interacting with each other through the model potential. The nuclear system dynamics has been treated within the Dirac equation with effective potential. All the spontaneous decay or the new particle (particles) production processes are excluded in the 0th order. Resonance phenomena in the nuclear system lead to the structurization of the positron spectrum produced. Analysis of data for cross-section at different collision energies (non-resonant energies, resonant ones, corresponding to energies of s-resonances of compound U-Cf, U-U, U+Ta system) is presented. The special features are found in the differential cross-section for the nuclear subsystem collision energies, for example, for U-U susyem as follows: (a) E1 = 162.0 keV (3rd s-resonance), (b) E1 = 247.6 keV (the 4th s-resonance), (c) E1=352,2 keV (5th upper s-resonance).

References

- [1] J.Reinhardt, U. Muller, W.Greiner, Z. Phys.A. **303**, 173 (1981); V.Zagrebaev, W.Greiner, J. Phys. G. **34**, 1 (2007); V.Zagrebaev, V.Samarin, W.Greiner, Phys.Rev.C. **75**,035809 (2007); A.Glushkov, JETP Lett. **55**, 95 (1992); Low Energy Antiproton Phys., AIP Serie. **796**, 206 (2005); A.Glushkov, L.Ivanov, Phys.Lett.A. **170**, 33 (1992); L.Ivanov, A.Glushkov etal, Preprint Inst.for Spectroscopy RAS, AS-5, Moscow (1991); L.Ivanov, T.Zueva, Phys.Scr. **43**, 374(1991).
- [2] A. Glushkov, et al, J. Phys. CS. **11**, 188 (2004); **11**, 199 (2004); **35**, 420 (2005); Int.J.Quant.Chem. **104**, 512 (2005); **104**, 562 (2005).

Dynamics of the resonant levels for atomic and nuclear ensembles in a laser pulse: optical bi-stability effect and nuclear quantum optics

O.Yu. Khetselius

Odessa University, P.O.Box 24a, Odessa-9, 65009, Ukraine

Present paper has for an object (i) to carry out numerical quantum computation of a temporal dynamics of populations differences at the resonant levels of atoms in a large-density medium in a non-rectangular form laser pulse and (ii) to determine possibilities that features of the effect of internal optical bi-stability at the adiabatically slow modification of effective field intensity appear in the sought dynamics. It is known that the dipole-dipole interaction of atoms in dense resonant mediums causes the internal optical bi-stability at the adiabatically slow modification of radiation intensity. The experimental discovery of bistable co-operative luminescence in some matters, in crystal of $Cs_3Y_2Br_9Yb_3+$ particularly, showed that an ensemble of resonant atoms with high density can manifest the effect of optical bi-stability in the field of strong laser emission. The Z-shaped effect is actually caused by the first-type phase transfer. On basis of the modified Bloch equations, we simulate numerically a temporal dynamics of populations differences at the resonant levels of atoms in the field of pulse with the non-rectangular ch form. Furthermore, we compare our outcomes with the similar results, where there are considered the interaction between the ensemble of high-density atoms and the rectangularly- and sinusoidally-shaped pulses. The modified Bloch equations describe the interaction of resonance radiation with the ensemble of two-layer atoms taking into account the dipole-dipole interaction of atoms [1]. A fundamental aspect lies in the advanced possibility that features of the effect of internal optical bi-stability at the adiabatically slow modification of effective field intensity for pulse of ch form, in contrast to the pulses of rectangular form, appear in the temporal dynamics of populations' differences at the resonant levels of atoms. Modelling nuclear ensembles in a super strong laser field provides opening the field of nuclear quantum optics [2,3].

References

- [1] A. Glushkov, O. Khetselius et al, J. Phys.CS. **35**, 420 (2006)
- [2] A. Glushkov, O. Khetselius, Recent Adv. in Theory of Phys. and Chem. Syst. (Springer). **18** (2008)
- [3] A. Glushkov, O. Khetselius, S. Malinovskaya, Europ. Phys. Journ. **32** (2008)

Spectroscopy of the hadronic atoms and superheavy ions: Spectra, energy shifts and widths, hyperfine structure

A.V. Glushkov^{1,2}, O.Yu. Khetselius², E.P. Gurnitskaya², Yu.V. Dubrovskaya²,
D.E.Sukharev²

¹*Institute for Spectroscopy of Russian Academy of Sciences, Troitsk, 142090, Russia*
²*Odessa University, P.O.Box 24a, Odessa-9, 65009*

Paper is devoted to calculation of the spectra, radiative corrections, hyperfine structure parameters for exotic hadronic atoms and heavy ions with account of the definite nucleus structure modelling. One of the main purposes is establishment a quantitative link between quality of the nucleus structure modelling and accuracy of calculating energy and spectral properties of systems. We apply our numerical code [1,2] to calculating spectra of the hadronic (pion, kaon, hyperon) atoms. A new, highly exact, ab initio approach [2] to relativistic calculation of the spectra for superheavy ions with an account of relativistic, correlation, nuclear, radiative effects on the basis of gauge-invariant QED perturbation theory is used. Zeroth approximation is generated by the effective ab initio model functional, constructed on the basis of the comprehensive gauge invariance procedure [2]). The wave functions zeroth basis is found from the Klein-Gordon (pion atom) or Dirac (kaon, hyperon) equation. The potential includes the core ab initio potential, the electric and polarization potentials of a nucleus (the Fermi model, the gaussian form of charge distribution in the nucleus and the uniformly charged sphere are considered). For low orbits there are important effects due to the strong hadron-nuclear interaction (pion atom). The energy shift is connected with length of the hadron-nuclear scattering (scattering amplitude under zeroth energy). For superheavy ions the correlation corrections of high orders are accounted within the Green functions method. The magnetic inter-electron interaction is accounted in the lowest order, the Lamb shift polarization part- in the Uhling-Serber approximation, self-energy part - within the Green functions method. We carried out calculations :1).energy levels, hfs parameters for superheavy H and Li-like ions for different models of charge distribution in a nucleus and super heavy atom Z=114; 3). Shifts and widths of transitions (2p-1s,3d-2p, 4f-3d) in some pionic and kaonic atoms (18O, 24Mg etc.) and also K-4He [3].

References

- [1] A. Glushkov, L.N. Ivanov, Phys. Lett.A. **170**, 33 (1992)
- [2] A. Glushkov, et al, J. Phys. CS. **11**, 188 (2004); **11**, 199 (2004); **35**, 420 (2005); Int.J.Quant.Chem. **104**, 512 (2005); **104**, 562 (2005).
- [3] A. Glushkov, O. Khetselius, S. Malinovskaya, Mol. Phys. **24** (2008); A. Glushkov, O. Khetselius, Recent Adv. in Theory of Phys. and Chem. Syst. (Springer). **18** (2008); EUrop. Phys. Journ. (2008).

Ar I transition probabilities and excitation cross sections involving the 4s metastable levels and the 4/5p configurations

K. Katsonis¹, Ch. Berenguer¹, R. Srivastava², L. Sharma², R.E.H. Clark³, M. Cornille⁴
A.D. Stauffer⁵

¹*GAPHYOR, Lab. de Physique des Gaz et des Plasmas, UMR 8578, Univ. Paris-sud
91405 Orsay, FRANCE*

²*Dept. of Physics, Indian Institute of Technology, Roorkee 247667 INDIA*

³*Nuclear Data Section, IAEA, Vienna, AUSTRIA*

⁴*LUTH, Observatoire de Paris, CNRS, Univ. Paris Diderot, 5 Place Jules Janssen,
92190 Meudon, FRANCE*

⁵*Dept. of Physics and Astronomy, York University, Toronto, ON, M3J1P3 CANADA
E-mail: konstantinos.katsonis@u-psud.fr, GAPHYOR.lpgp@u-psud.fr*

Evaluation of transition probability $A_{i,j}$ and electron collision excitation $\sigma_{j,i}$ are required for the development of satisfactory Collisional - Radiative (C-R) models for use with optical diagnostics and in the modeling of low temperature plasmas. The present evaluation was made with diagnostics of Ar fed plasma thrusters in mind. Part of this work is also related to emission spectroscopy diagnostics of the WEGA Stellarator and to a coordinated research project of the IAEA in support of controlled fusion applications.

For $A_{i,j}$ evaluations within the Ar I 4s - 4/5p multiplets, we have compared theoretical results coming from: (a) CbA, a Coulomb Approximation code [1], (b) the code contained within the SUPERSTRUCTURE package [2] and (c) the Los Alamos National Laboratory (LANL) atomic physics codes available through the Internet [3]. These data are compared with the evaluated sets available at NIST [4].

Recent theoretical work on Ar I 4s - 4/5p electron impact excitation cross sections has been carried out using R-matrix calculations [5] and relativistic quantum calculations [6,7]. These cross sections have been compared to DW calculations results obtained with the LANL codes [3], CTMC evaluations and empirical formulas. Experimental data [8] have also been used when available. Compilation of the evaluated data is given in a recent report [9].

References

- [1] D.R. Bates, A. Damgaard, *Phil. Trans. Roy. Soc. (London)* **A242** 101 (1949).
- [2] W. Eissner, M. Jones, H. Nussbaumer, *Compt. Phys. Commun.* **8** 270 (1974).
- [3] <http://aphysics2.lanl.gov/tempweb/>
- [4] http://physics.nist.gov/cgi-bin/AtData/main_asd
- [5] K. Bartschat, V. Zeman, *Phys. Rev. A* **59** R2252 (1999).
- [6] R. Srivastava, A.D. Stauffer, L. Sharma, *Phys. Rev. A* **74** 012715 (2006).
- [7] L. Sharma, R. Srivastava, A.D. Stauffer, *Phys. Rev. A* **76** 024701 (2007) and references therein.
- [8] J.B. Boffard, A.G. Piech, M.F. Gehrke, M.E. Lagus, L.W. Etersson, C.C. Lin, *Phys. Rev. A* **59** 2749 (1999).
- [9] K. Katsonis, Ch. Berenguer, M. Cornille, "Ar I Transition Probabilities and Excitation Cross Sections Involving the 4s Metastable Levels and the 4/5p Configurations", Report LPGP-GA-22 (2008).

Radiative data in the Zr I spectrum

G. Malcheva¹, K. Blagoev¹, R. Mayo², M. Ortiz², J. Ruiz², L. Engström³, H. Lundberg³,
S. Svanberg³, H. Nilsson⁴, P. Quinet^{5,6} and É. Biémont^{5,6}

¹*Institute of Solid State Physics, 72 Tzarigradsko Chaussee, BG - 1784 Sofia, Bulgaria*

²*Department of Atomic, Molecular and Nuclear Physics, Univ. Complutense de Madrid,
E-28040 Madrid, Spain*

³*Department of Physics, Lund Institute of Technology, P.O. Box 118, S-221 00 Lund,
Sweden*

⁴*Lund Observatory P.O. Box 43, S-221 00 Lund, Sweden*

⁵*IPNAS (Bt. B15), University of Lige, Sart Tilman, B-4000 Lige, Belgium*

⁶*Astrophysics and Spectroscopy, University of Mons-Hainaut, B-7000 Mons, Belgium
E-mail: bobcheva@issp.bas.bg*

Radiative data in the Zr I spectrum, in particular radiative lifetimes of excited states and transition probabilities of electric dipole (E1) transitions, are of interest for the determination of the Zr abundance in stars, including the Sun. These data are also important for the investigation of plasmas, particularly the plasmas near the walls in high-temperature devices.

In the present work radiative lifetimes for 17 levels belonging to the odd $4d^25s5p$ configuration are reported. They were measured using a time-resolved laser-induced fluorescence (TRLIF) technique [1]. The levels investigated are: y^3S_1 ; $u^3P_{0,1,2}$; $v^3P_{1,2}$; t^3P_1 ; $t^3D_{1,2,3}$; $u^3F_{2,3,4}$; x^3G_5 and $w^3G_{3,4,5}$. A single-step laser-excitation process, either from the ground state or from appropriate metastable states, was used.

Free zirconium atoms were generated by laser ablation in a vacuum chamber with 10^{-6} - 10^{-5} mbar background pressure. For the ablation, an Nd:YAG laser with 10 ns pulse duration was used. The laser system for the excitation of the Zr I levels consisted of a dye laser which had a pulse duration of about 1-2 ns.

For 14 of the investigated states, radiative lifetimes were obtained for the first time. The error bars are in the interval 4-10%. Measurements of branching fractions are also in progress by means of the Laser Induced Breakdown Spectroscopy (LIBS) technique.

The relativistic Hartree-Fock (HFR) method, as described by Cowan [2], has been used to compute radiative lifetimes and transition probabilities and the results are compared with the experimental data. In the calculations, core-polarization effects and extensive configuration interaction effects have been taken into account.

This work was financially supported by the Swedish Research Council; by the EU-TMR access to Large-Scale Facility Programme (contract RII3-CT-2003-506350) and by the National Science Foundation of Bulgaria (grant 1516/05).

References

- [1] Z. G. Zhang, S. Svanberg, P. Quinet, P. Palmeri and É. Biémont, *Phys. Rev. Lett.* **87**, 273001 (2001)
- [2] R. D. Cowan, "The Theory of atomic Structure and Spectra" (University of California Press, Berkley, California, USA, 1981)

Energy levels, oscillator strengths and lifetimes in Cl IV

G. P. Gupta

*Department of Physics, S. D. (Postgraduate) College, Muzaffarnagar 251 001,
(Affiliated to Chowdhary Charan Singh University, Meerut - 250 004), INDIA
E-mail: g-p-gupta1@yahoo.co.in*

Emission lines due to allowed and intercombination transitions in multiply charged Si-like ions are observed in solar corona and laser produced plasma. The lines arising from intercombination transitions have been shown to be very useful, for instance, in understanding density fluctuations and elementary processes which occur in both interstellar and laboratory plasma and the determination of transition energies, oscillator strengths and transition probabilities of these lines as needed for a qualitative analysis of the spectra are not well known. This is mainly because these weak lines are usually sensitive to the theoretical modeling and have been a challenge for the atomic structure theory.

We have calculated the excitation energies, oscillator strengths and transition probabilities for electric-dipole-allowed and intercombination transitions among the fine-structure levels of the terms belonging to the configurations $(1s^2 2s^2 2p^6) 3s^2 3p^2$, $3s 3p^3$, $3s^2 3p 3d$, $3p^4$, $3s^2 3p 4s$, $3s^2 3p 4p$, $3s 3p^2(^2S) 4s$, $3s 3p^2(^2P) 4s$, $3s 3p^2(^4P) 4s$, $3s 3p^2(^2D) 4s$, $3s^2 3p 4d$ and $3s^2 3p 4f$ of Si-like Chlorine, using extensive configuration-interaction (CI) wavefunctions [1]. The relativistic effects in intermediate coupling are incorporated by means of the Breit-Pauli Hamiltonian [2]. Small adjustments to the diagonal elements of the Hamiltonian matrices have been made so that the energy splittings are as close as possible to the experiment. From our radiative rates, we have also calculated the radiative lifetimes of the levels. In this calculation we have investigated the effects of electron correlations on our calculated data, particularly on the intercombination transitions, by including orbitals with up to $n=5$ quantum number. We considered up to two electron excitations from the valence electrons of the basic configurations and included large number of configurations. These configurations represent all major internal, semi-internal and all-external electron correlation effects [3].

The mixing among several fine-structure levels is found to be very strong. These levels are identified by their eigen-vector composition [4]. The energy splitting of 85 fine-structure levels, oscillator strengths, transition probabilities for electric-dipole-allowed and intercombination transitions and the lifetimes of several fine-structure levels are presented and compared with available experimental levels and the other theoretical results. Significant differences between our calculated and the other sophisticated theoretical lifetimes for several fine-structure levels are discussed.

References

- [1] A. Hibbert, *Comput. Phys. Commun.* **9**, 141 (1975)
- [2] R. Glass, A. Hibbert, *Comput. Phys. Commun.* **16**, 19 (1978)
- [3] I. Oksuz, O. Sinanoglu, *Phys. Rev.* **181**, 42 (1969)
- [4] G. P. Gupta, K. M. Aggarwal, A. Z. Msezane, *Phys. Rev.* **A70**, 036501 (2004)

Large scale CIV3 calculations of fine-structure energy levels and lifetimes in Al-like copper

G. P. Gupta¹ and A. Z. Msezane²

¹*Department of Physics, S. D. (Postgraduate) College, Muzaffarnagar 251 001, (Affiliated to Chowdhary Charan Singh University, Meerut - 250 004), INDIA*

²*Department of Physics and Center for Theoretical Studies of Physical Systems, Clark Atlanta University, Atlanta, Georgia 30314, USA*

E-mail: g-p-gupta1@yahoo.co.in

We have performed large scale CIV3 calculations of excitation energies from ground states for fine-structure levels as well as of oscillator strengths and radiative decay rates for all electric-dipole-allowed and intercombination transitions among the fine-structure levels of the terms belonging to the configurations $(1s^2 2s^2 2p^6) 3s^2 3p$, $3s 3p^2$, $3s^2 3d$, $3p^3$, $3s 3p 3d$, $3p^2 3d$, $3s 3d^2$, $3p 3d^2$, $3s^2 4s$, $3s^2 4p$, $3s^2 4d$, $3s^2 4f$, and $3s 3p 4s$ of Cu XVII, using very extensive configuration-interaction (CI) wave functions [1]. The important relativistic effects in intermediate coupling are incorporated by means of the Breit-Pauli Hamiltonian which consists of the non-relativistic term plus the one-body mass correction, Darwin term, and spin-orbit, spin-other-orbit, and spin-spin operators [2]. The errors, which often occur with sophisticated *ab initio* atomic structure calculations, are reduced to a manageable magnitude by adjusting the diagonal elements of the Hamiltonian matrices. In this calculation we have investigated the effects of electron correlations on our calculated data, particularly on the intercombination transitions, by including orbitals with up to $n=5$ quantum number. We considered up to three electron excitations from the valence electrons of the basic configurations and included large number of configurations (1164) to ensure convergence.

Our adjusted excitation energies, including their ordering, are in excellent agreement with the available experimental results [3]. The enormous mixing among several fine-structure levels makes it very difficult to identify them correctly. Perhaps, that may be the reason for the lack of experimental results for these levels. We believe that our extensive calculated values can guide experimentalists identify the fine-structure levels [4]. From our radiative decay rates, we have also calculated radiative lifetimes of the fine-structure levels in Cu XVII. Our calculated lifetimes for the levels $3s 3p^2(^4P)$ are found to be in excellent agreement with the experimental results of Trabert et al. [5] compared to other available theoretical results. We predict new data for several levels where no other theoretical and/or experimental results are available.

References

- [1] A. Hibbert, *Comput. Phys. Commun.* **9**, 141 (1975)
- [2] R. Glass, A. Hibbert, *Comput. Phys. Commun.* **16**, 19 (1978)
- [3] T. Shirai et al., *J. Phys. Chem. Ref. Data* **20**, 12 (1991)
- [4] G. P. Gupta, K. M. Aggarwal, A. Z. Msezane, *Phys. Rev.* **A70**, 036501 (2004)
- [5] E. Trabert et al., *J. Opt. Soc. Am.* **B5**, 2173 (1988)

Levels energies, oscillator strengths, and lifetimes for transition in Pb III

C. Colón¹, A. Alonso-Medina¹, A. Zanón² and J. Albéniz³

¹*Dpto. de Física Aplicada, EUITI, Universidad Politécnica de Madrid (UPM), Spain*

²*Dpto. de Matemática Aplicada, EUITI, UPM Madrid, Spain*

³*Dpto. de Química Industrial y Polímeros, EUITI, UPM Madrid, Spain*

E-mail: cristobal.colon@upm.es

Information about the oscillator strengths and lifetimes has applications in many scientific fields. Data about atomic properties are relevant not only to spectroscopy, as these values are also of interest in a variety of other fields in physics and technology. In astrophysical applications this information can be used to determine elemental abundances from absorption spectra. These data are also essential to calculate the Stark width and shift parameters of spectral lines. In previous work [1-3] we have measured and calculated experimental and theoretical values for Pb III.

Transition Probabilities and oscillator strengths for several lines of astrophysical interest arising from $5d^96s^26p$, $5d^{10}6s1$, $5d^{10}6s^2$, $5d^{10}6p^2$, $5d^{10}6p7s$, and $5d^{10}6p6d$ configurations and some levels radiative lifetimes of Pb III has been calculated. These values were obtained in intermediate coupling (IC) and using ab initio relativistic Hartree-Fock calculations. We use for the IC calculations the standard method of least square fitting of experimental energy levels by means of computer codes from Cowan (1981). The inclusion in these calculations of the $5d^{10}6p7s$ and $5d^{10}6p6d$ configurations has facilitated us a complete assignment of the levels of energy of the Pb III. The system considered is complex, with high Z where both relativistic and correlation effects must be important. Least-square fitting of experimental energy levels partially account correlation effects not explicitly calculated in our work. Nevertheless and as we already waited, there are some noticeable discrepancies between our theoretical values and experimental data of oscillator strengths and lifetimes for the resonance lines 1048.9 and 1553.0 Å. These discrepancies have been studied with detail in the bibliography and we think that they can be corrected with the inclusion of core polarization effects. Oscillator strengths and radiative lifetimes obtained, although in general agreement with the rare experimental data [see e.g. 4-7], do present some noticeable discrepancies, that are studied in the text.

References

- [1] A. Alonso-Medina, C. Colón, A. Zanón, MNRAS **385**, 261 (2008).
- [2] C. Colón, A. Alonso-Medina, C. Herrán-Martínez, J. Phys. B: Atom. Mol. Opt. Phys. **32**, 3887 (1999).
- [3] C. Colón, A. Alonso-Medina, Physica Scripta **62**, 132 (2000).
- [4] T. Andersen, A. Kirkegaard Nielsen, G. Sorensen G., Physica Scripta **6**, 122 (1972).
- [5] W. Ansbacher, E. H. Pinnington, J. A. Kernahan, Can. J. Phys. **66**, 402 (1988).
- [6] H. -S. Chou, K. -N. Huang K, Chin. J. Phys **35**, 35 (1997).
- [7] L. J. Curtis et al., Physical Review A **63**, 042502 (2001).

This work has been supported by the project CCG07-UPM/ESP-1632 of the UPM. IV PRICIT of the CAM (Comunidad Autónoma de Madrid), SPAIN.

Hyperfine interaction induced decays in highly charged ions: Successful atomic lifetime measurements and puzzling problems

E. Träbert

*Astronomisches Institut, Ruhr-Universität Bochum, D-44780 Bochum, Germany, and
Lawrence Livermore National Laboratory, Livermore, CA 94550, USA
E-mail: traebert@astro.rub.de*

In Ni-like ions, the lowest excited configuration is $3d^9 4s$. The lowest excitation level, 3D_3 , can decay to the $3d^{10}$ ground state only by emission of M3 radiation. For the ion Xe^{26+} , the predicted level lifetime is about 15 ms. A measurement at an electron beam ion trap at Livermore has determined this value with an uncertainty of only about 1.5% [1]. In isotopes with a nonvanishing nuclear spin, hyperfine interaction mixes HFS sublevels of the 3D_3 level with those of 3D_2 ; the M3/E2 mixing reduces the lifetime of some sublevels. Again, the Livermore EBIT measurements have corroborated specific calculations [2].

An update of some older calculations of the hyperfine-induced decay rate of the nsnp $^3P_0^o$ [3, 4] levels in Be- and Mg-like ions has shifted the results by about 20%, close to those of recent other extensive calculations [5]. However, two experiments at the heavy-ion storage ring TSR (Heidelberg), one on Ti^{18+} ions [6], the other on $^{63,65}Cu^{17+}$ ions [7], find results that differ by much more than 20% from those vintage predictions. The reason for the discrepancy is not yet understood. The 3s3p $^3P_2^o$ level lifetimes in Mg-like ions of Ni (no HFS) and Cu (with HFS) [7] agree well with theory [7, 8].

ET acknowledges support from the German Research Association (DFG). Part of this work was performed under the auspices of the U.S. Department of Energy by Lawrence Livermore National Laboratory under Contract DE-AC52-07NA27344.

References

- [1] E. Träbert, P. Beiersdorfer, and G. V. Brown, *Phys. Rev. Lett.* **98** 263001 (2007).
- [2] K. Yao, M. Andersson, T. Brage, R. Hutton, P. Jönsson, and Y. Zou, *Phys. Rev. Lett.* **97**, 183001 (2006); Erratum: *Phys. Rev. Lett.* **98**, 269903 (2007).
- [3] J. P. Marques, F. Parente, and P. Indelicato, *Phys. Rev. A* **47** 929 (1993).
- [4] J. P. Marques, F. Parente, and P. Indelicato, *At. Data Nucl. Data Tab.* **55** 157 (1993).
- [5] M. H. Chen, K.-T. Cheng (private communication).
- [6] S. Schippers, E. W. Schmidt, D. Bernhardt, *et al.*, *Phys. Rev. Lett.* **98** 033001 (2007).
- [7] E. Träbert, J. Hoffmann, C. Krantz, S. Reinhardt, A. Wolf, and P. Indelicato (work in progress).
- [8] K. M. Aggarwal, V. Tayal, G. P. Gupta, F. P. Keenan, *At. Data Nucl. Data Tab.* **93** 615 (2007).

Einstein coefficients for activation barriers of equilibrium and non-equilibrium processes caused by Plank radiation

A. Stepanov

Byelorussian State University, National Ozone Monitoring Research and Educational Centre, 7-816 Kurchatov Street, 220064 Minsk, Republic of Belarus, E-mail: stepav@bsu.by

Analytical calculation of Einstein coefficients is made for activation barrier of the Boltzmann-Arrhenius model and an activation process model. For the activation process model an activation barrier is shown to have discrete energy structure due to its thermodynamic equilibrium with thermal radiation. This structure is determined by interaction of conformation substates of a molecule with thermal radiation. The Boltzmann-Arrhenius model represents an activation process as a result of the work of high-energy spectral components of thermal equilibrium radiation. The process is realized by overcoming a potential barrier with continuous energy structure. However, it is shown, that such process is essentially non-equilibrium and hard to achieve at thermal equilibrium radiation [1].

References

- [1] A. V. Stepanov, J. Mol. Struct.:THEOCHEM **805**, 87 (2007)

New transition probabilities of astrophysical interest in triply ionized lanthanum (La IV)

V. Fivet¹, É. Biémont^{1,2}, P. Palmeri¹ and P. Quinet^{1,2}

¹ *Astrophysique et Spectroscopie, Université de Mons-Hainaut, B-7000 Mons, Belgium*

² *IPNAS, Université de Liège, Sart Tilman, B-4000 Liège, Belgium*

E-mail: vanessa.fivet@umh.ac.be

Despite their low cosmic abundances, the lanthanides ($Z=57-71$) become increasingly important in astrophysics because they are strongly enhanced in some chemically peculiar (CP) stars. Up to now, triply ionized lanthanides have not been investigated in stellar spectra, the main reason being the lack of atomic data. According to Saha equation however, these ions are expected to be observed in hot-stars spectra. The main purpose of the present work is to fill in this gap and to provide the astrophysicists with the radiative data they need for a quantitative investigation of CP-stars high-resolution spectra.

During the meeting, we will present preliminary results obtained so far for triply ionized lanthanum (La IV). The accuracy of the new data will be assessed through comparison of the results obtained within the framework of two independent theoretical approaches, i.e. the partly relativistic Hartree-Fock method [1] and the fully relativistic multiconfigurational Dirac-Fock approach [2]. Homologous lighter ions will also be considered for testing the adopted model.

The present work on La IV is a continuation of a long-term effort carried out at Mons University in order to improve the radiative data of the rare-earth (RE) elements in their first ionization degrees. Results obtained previously for many RE atoms and ions are stored in the database DREAM on a web site of Mons University, Belgium (See [3] and the references therein).

References

- [1] R.D. Cowan, *The Theory of Atomic Structure and Spectra*, University of California Press, Berkeley (1981)
- [2] I.P. Grant, *Relativistic Quantum Theory of Atoms and molecules*, Springer-Verlag, New York (2007)
- [3] <http://www.umh.ac.be/~astro/dream.shtml>

A new method for determining minute long lifetimes of metastable levels

J. Gurell¹, P. Lundin¹, S. Mannervik¹, L.-O. Norlin² and P. Royen¹

¹*Department of Physics, Stockholm University, AlbaNova University Center, SE-10691 Stockholm, Sweden*

²*Department of Physics, Royal Institute of Technology, AlbaNova University Center, SE-10691 Stockholm, Sweden*

Radiative lifetime measurements of metastable states have been performed for many years utilizing stored ions. When measuring lifetimes of metastable states in a storage ring the signal may be greatly enhanced, compared to that from passive observation, by actively inducing transitions with one or more lasers. The basic principle of our laser probing technique has been to probe the population of the metastable state as a function of delay time after ion injection which gives us a population decay curve, see *e.g.* Ref. [1]. The introduction of lasers also increases the maximum possible measurable lifetime significantly. Currently the longest radiative lifetime measured at the storage ring CRYRING in Stockholm, Sweden, and to the best of our knowledge in storage rings in general, is 89 s in BaII, see Ref. [2]. For lifetimes longer than this collisional excitation of stored ground state ions becomes a problem since after a few seconds of storage the vast majority of the population of the metastable state under study will be originating from ions that were in the ground state when injected into the storage ring. During the analysis, this contribution is subtracted from the total fluorescence which gives a low S/N ratio, large uncertainties and eventually limits the maximum possible lifetime measurable.

A new method has therefore been proposed and its advantages concerning more accurate lifetime determinations of extremely long lived metastable states demonstrated, see Ref. [3]. Instead of monitoring the decay of the population of the metastable state relative to ion injection the contribution from collisional excitation is monitored directly. In contrast to the metastable state population itself, the collisional excitation grows stronger with increased storage time which results in a much higher S/N ratio at longer storage times and higher residual gas pressures and as a consequence the maximum possible radiative lifetime measurable increases. This technique has so far only been applied in two studies with lifetimes ranging from 16 to 32 s, the $5d\ ^2D_{5/2}$ state in BaII, see Ref. [3], and the $b\ ^4P_{5/2}$ state in TiII, submitted to J Phys B. This new technique has not yet been pushed to its limit but lifetimes of a few minutes will most probably be possible to measure.

References

- [1] P. Lundin, J. Gurell, L.-O. Norlin, P. Royen, S. Mannervik, P. Palmeri, P. Quinet, V. Fivet and É. Biéumont PRL **99** 213001 (2007)
- [2] J. Gurell, E. Biéumont, K. Blagoev, V. Fivet, P. Lundin, S. Mannervik, L.-O. Norlin, P. Quinet, D. Rostohar, P. Royen and P. Schef PRA **75** 052506 (2007)
- [3] P. Royen, J. Gurell, P. Lundin, L.-O. Norlin and S. Mannervik PRA **76** 030502(R) (2007)

Lifetime measurements of metastable states of astrophysical interest

J. Gurell¹, P. Lundin¹, S. Mannervik¹, L.-O. Norlin², P. Royen¹, P. Schef¹, H. Hartman³, A. Hibbert⁴, H. Lundberg⁵, K. Blagoev⁶, P. Palmeri⁷, P. Quinet^{7,8} and É. Biémont^{7,8}

¹*Department of Physics, Stockholm University, AlbaNova University Center, SE-10691 Stockholm, Sweden*

²*Department of Physics, Royal Institute of Technology, AlbaNova University Center, SE-10691 Stockholm, Sweden*

³*Lund Observatory, Lund University, Box 43, 22100 Lund, Sweden*

⁴*Department of Applied Mathematical and Theoretical Physics, Queen's University, Belfast BT7 1NN, Northern Ireland*

⁵*Department of Physics, Lund Institute of Technology, Box 118, 22100 Lund, Sweden*

⁶*Institute of Solid State Physics, Bulgarian Acad. of Sciences, 72 Tzarigradsko Chaussee, BG-1784 Sofia, Bulgaria*

⁷*Astrophysique et Spectroscopie, Université de Mons-Hainaut, B-7000 Mons, Belgium*

⁸*IPNAS, Université de Liège, Sart Tilman B15, B-4000 Liège, Belgium*

Under normal laboratory conditions metastable states are commonly depleted through collisions between particles. Under astrophysical conditions, however, low pressures and temperatures can make the mean free path of particles so long that ions in metastable states have time to decay spontaneously through forbidden transitions which are usually not observed in laboratory light sources. Since the intensity of these forbidden lines are strongly dependent on the frequency of particle collisions these transitions may be used as density probes of dilute astrophysical plasmas.

The super massive star η Carinae has attracted much attention recently. One of the surrounding regions referred to as the Strontium-filament contains ejecta from η Carinae and shows a number of forbidden lines from Sr II, Fe I, Ti II and Sc II. In order to use these lines as probes transition probabilities are needed which are either calculated or measured indirectly through lifetime measurements in combination with experimental branching fractions.

At the storage ring CRYRING in Stockholm, Sweden, lifetime measurements of metastable states have been performed for many years (see *e.g.* Ref. [1]) and recently lifetimes of metastable levels in Sc II and Ti II have been measured and submitted for publication together with new calculations. The experimental technique utilizes a laser probing technique and the resulting lifetimes are used in combination with astrophysical branching fractions deduced from spectra recorded with the STIS spectrograph on board the Hubble Space Telescope, see *e.g.* Ref. [2]. All measurements, which are ranging from 1-24 s, are complemented by theoretical calculations showing good agreement with the experimental values.

References

- [1] S. Mannervik, A. Ellmann, P. Lundin, L.-O. Norlin, D. Rostohar, P. Royen and P. Schef *Phys. Scr.* **T119** 49 (2005)
- [2] H. Hartman *et al.* *A&A* **397** 1143 (2003)

Spin-exchange effects in elastic electron scattering from linear triatomic radicals

M.-T. Lee¹, M. M. Fujimoto², S. E. Michelin³, and I. Iga¹

¹ *Departamento de Química, UFSCar, 13565-905, São Carlos, SP, Brazil*

² *Departamento de Física, UFPR, 81531-990 Curitiba, PR, Brazil*

³ *Departamento de Física, UFSC, 88040-900 Florianópolis, SC, Brazil*

E-mail: dlmt@ufscar.br

Low-energy electron collisions with atoms, molecules, radicals, and surfaces are, in general, strongly influenced by electron-exchange effects. Such effects can be easily characterized in the electron-impact spin-forbidden excitations (for instance, singlet-to-triplet transitions). Although exchange mechanism is also important in low-energy elastic electron-molecule collisions, its effects is usually masked since most experimental studies are performed using unpolarized electron sources and without spin analysis of the scattered beam. Limited experimental studies have been reported in the literature over the past years. For instance, spin-flip (SF) differential cross sections (DCSs) for elastic electron scattering by the Na and Hg atoms as well as by the open-shell O₂ and NO molecules were reported by Hegemann *et al.* [1]. Although significant spin-exchange effects were found for atomic targets, very small effects were observed for O₂ and NO. Lately, theoretical studies of da Paixão *et al.* [2] have shown that the almost isotropic polarization fractions (SPFs) of scattered electrons is mainly caused by the molecular orientation averaging, since gaseous targets are randomly oriented in space.

Recently, we reported a theoretical investigation on spin-exchange effects in elastic electron collisions with the open-shell C₂O radical [3] using the iterative Schwinger variational method (ISVM). In that study, we have shown that the exchange effects are strongly enhanced by the occurrence of resonances. In this sense, the calculated P'/P averaged over all orientations are no longer isotropic and deviate significantly from unity particularly at large scattering angles.

Here, we extend the spin-exchange study to two linear triatomic open-shell molecules, namely CNN and NCN. These two targets are isoelectronic of C₂O radical with the ground-state electronic configuration X³Σ⁻. As in C₂O, strong shape resonances are also present in the doublet- and quartet-coupling scattering channels for both targets in the low-incident energy range [3]. In this work, we report a calculation of spin-flip (SF) differential (DCSs) and integral cross sections (ICSs) as well as spin-polarization (SPFs) fractions for elastic electron scattering by CNN and NCN in the (1-10)-eV energy range. Our calculated SF DCSs and SPFs as well as the SF ICSs for these two targets will be presented during the EGAS.

This work is partially supported by the Brazilian agency CNPq.

[1] T. Hegemann, M. Oberste-Vorth, R. Vogts, and G. F. Hanne, *Phys. Rev. Lett.* **66** 2968 (1991).

[2] F. J. da Paixão, M. A. P. Lima, and V. McKoy, *Phys. Rev. A* **53** 1400 (1996).

[3] M. M. Fujimoto, S. E. Michelin, I. Iga, and M.-T. Lee, *Phys. Rev. A* **73** 012714 (2006).

Spectral properties of interactions in metallic endohedral fullerenes $Li_2@C_{60}$ and $Na_2@C_{60}$

Zapryagaev S.A., Butyrskaya E.V.

Voronezh State University. Russia

Endohedral fullerenes are of great interest due to their diversity applications as in technology so in fundamental research of interatomic interactions. Because of the robust carbon cage and its large hollow interior space fullerenes can be used as molecular containers and as building blocks of carbon-based nanotechnology. The program Gaussian 03 and HF method in basis 3-21G was used in calculation at present work to investigate a spectral properties of an interactions of Li_2 and Na_2 molecules encapsulated in C_{60} carbon cage that are produced endohedral metallic fullerenes $Li_2@C_{60}$ and $Na_2@C_{60}$. Encapsulating molecules inside fullerene C_{60} changes a structure and properties, both molecules as a carbon skeleton. According of Mulliken population data significant carry of electronic density from an encapsulated molecule on fullerene cage is observed. Except according of presented calculation a compression of encapsulated Na_2 molecule takes place. This compression is consequence of steric interaction of multielectronic Na_2 system from a carbon cage. This effect is not observed at encapsulate inside C_{60} Li_2 molecule having the smaller sizes then Na_2 molecule. On the contrary the internuclear $Li - Li$ distance increases, in comparison with free two-nuclear molecule Li_2 that shows an increase Mulliken charge atoms of lithium inside fullerene.

Redistribution of electronic density changes a picture of an oscillatory spectrum of the visitor's molecule and the fullerene too. The analysis of the form of oscillations for metallic fullerenes has shown, that all normal oscillations can be divided on two groups: - 6 oscillations in which atoms of metal take part and 174 oscillations of a carbon skeleton. Except of metallic atoms oscillation near balance position, oscillation of a metallic molecule as a whole inside fullerene and antiphase oscillations of atoms of an encapsulated molecule perpendicularly to nuclear line take place.

Frequencies of normal oscillations of encapsulated molecules Li_2 and Na_2 according to calculation are equal: 67, 93, 117, 145, 263*, 290 cm^{-1} for Li_2 and 9, 24, 63, 81, 209, 354* cm^{-1} for Na_2 . The symbol * notes the frequencies of nuclear oscillations near the balance position, equal for the main electronic term $X^1\Sigma_g^+$ of two-nuclear molecules Li_2 and Na_2 accordingly 352 cm^{-1} and 159 cm^{-1} . The fullerene spectrum according to downturn of system symmetry also changes: instead of 4 active in C_{60} IR modes the number of absorption bands in a fullerene spectrum increases. Optimization of metallic fullerenes structures and the calculation of IR spectra is executed for a case when metals are located on an C_2 axis of symmetry, and atoms of carbon in C_{60} are fixed and for a case of full optimization without the requirement of preservation of symmetry. For the case when atoms of metal are located on C_2 axis, reference of fullerene cage oscillation according to a new system symmetry is executed.

Simulation of fullerene formation

Zapryagaev S.A., Butyrskaya E.V.

Voronezh State University. Russia

The reason why C_{60} is by far the most abundant fullerene in carbon soot still remains unrevealed/ It is well known, that C_{60} fullerene is not energetically the most stable cluster among that clusters can be find in soot. For example C_{70} and C_{84} have larger binding energies per atom than C_{60} . Hence C_{60} should be less stable energetically than some other fullerenes. Nevertheless, C_{70} is the second most abundant and C_{84} the third. Besides, the production yields of them are much lower than of C_{60} . These facts imply the unimportance of binding energy for the production fullerenes. To elucidate a reason why C_{60} is the most abundant one need to unveil the process of fullerenes formation.

There are some formation models - "pentagon road", "fullerene road", "ring stacking model" and " C_{10} " reaction road. Pentagon road model bases on the curling of graphitic sheets through the incorporation of pentagons forms fullerenes. Fullerene road model assumes that the small fullerenes grow into lager ones through sequential C_2 additions. Ring stacking assumes that fullerenes are formed by sequential stacking of carbon rings. It is natural to expect that the C atoms react with each other to form small carbon clusters in the early stage of fullerene formation process. That is why the study of small carbon cluster is the important stage of fullerene formation.

At present work we optimize the ground -state geometries of small carbon clusters using the b3lyp method of Gaussian 03 program and simulate the fullerene formation according the " C_{10} " reaction road method proposed in [1]

References

- [1] Yusuke Ueno and Susumu Saito, Phys Rev. B77, 085403 (2008)

CROSS SECTIONS OF NEGATIVE ION PRODUCTION IN ELECTRON COLLISIONS WITH ADENINE MOLECULES

I.I.Shafranyosh, M.I.Sukhoviya, M.I.Shafranyosh, Fedorko R. O.

Department of Physics, Uzhgorod National University, Uzhgorod 88000, Ukraine

We report absolute cross sections for the formation negative ions resulting from electron interactions with adenine. Interest in experimental studies of the processes of electron-impact ion production in the molecules of biological relevance is related, first of all, to the significance of the problem of intracellular irradiation of biological structures by secondary electrons produced in the substance in quite considerable amounts under the influence of different-type radiation. It has been shown in our preliminary experiments carried out with the heterocyclic components of the above molecules [1–2] that under electron impact different physical processes occur: i.e. molecules excitation, ionization, dissociative excitation and dissociative ionization. Physical modeling of these processes and estimation of their radiobiological consequences require knowledge of their basic characteristics – absolute ionization cross sections. Reliable data on the ionization cross sections could be obtained only in the precise experiment, in which the role of environment is minimized. Such approach was applied in this work.

Production of negative ions of adenine molecules (nucleic acid base) has been studied using a crossed electron and molecular beam technique. The method developed by the authors enabled the molecular beam intensity to be measured and the electron dependences and the absolute values of the total cross sections of production of negative adenine ions to be determined. A five-electrode electron gun with a thoriated tungsten cathode was used as an electron beam source. Electron gun temperature was about 400K providing gun parameter stability during operation. Electrons having

passed the interaction region were trapped by a Faraday cup kept at the positive potential. Measurements were carried out at the 10^{-7} – 10^{-6} A electron beam current and the $\Delta E_{1/2} \sim 0.3$ eV (FWHM) energy spread. Electron gun was immersed into the longitudinal magnetic field (induction $B = 1.2 \cdot 10^2$ Tl). An electron energy scale was calibrated with respect to the resonance peak of the SF_6^- ion production, the position of which determined the zero point of the energy scale.

Using the technique developed by the authors, the absolute cross sections of the negative adenine ions formation have been determined for electron energy in the interval from 0.4 to 5.0 eV. It has been found that the maximal negative-ion formation cross section $\sigma = 6 \cdot 10^{-18}$ cm² was observed for an electron energy of 1.2 eV. Main contribution to the cross section was shown to result from the dissociative ionization cross section. It has been noted that due to the resonance mechanism of the negative adenine ions formation just at low incident electron energy considerable disorders in the nucleic acid macromolecules are probable.

References

- [1] Sukhoviya M.I., Slavik V.N., Shafranyosh I.I. *Biopolym. Cell.* **7**, 77 (1991) (in Russian).
- [2] Sukhoviya M.I., Shafranyosh M.I., Shafranyosh I.I. *Spectroscopy of Biological Molecules: New Directions* (Kluwer Acad. Publ.-Dordrecht /Boston /London) p.281 (1999).

Effect of divalent metal ions on the conformational transitions in poly(dA)+poly(dT) system

O. Ryazanova, O. Nesterov and V. Zozulya

Department of Molecular Biophysics, B. Verkin Institute for Low Temperature Physics and Engineering, NAS of Ukraine, 47, Lenin ave., 61103, Kharkov, Ukraine

Divalent metal ions strongly affect the polymeric molecules of nucleic acid. In particular, they can alter the stability of DNA double-helical structure and induce its aggregation in aqueous solutions. Synthetic homopolymer poly(dA)+poly(dT) system simulates properties of nucleic acids, which are independent on peculiarities of the primary structure.

The effect of Mg^{2+} , Ni^{2+} and Cd^{2+} ions on conformational transitions in duplex and triplex complexes formed by poly(dA) with poly(dT) is studied. Investigations were carried out in buffered solutions (pH6,9, 0,1 M NaCl), for polynucleotide concentrations of 0.1 — 0.3 mM (in nucleic bases) by the method of thermal denaturation with registration of melting profiles by absorbance change at 260 nm and 284 nm. The rate of heating was 1 °C/min. The concentration of metal ions in solutions were gradually elevated up to 50 mM in the case of Mg^{2+} , and 4 mM for Ni^{2+} and Cd^{2+} . Aggregation processes in the systems were detected by intensity of light scattering in the visible range at 540 nm. On the basis of data obtained, the diagrams of conformational transitions for poly(dA)+poly(dT)+ Me^{2+} system were plotted in the range of reversible transitions.

It is established that all studied divalent ions strongly increase the temperatures of triplex-to-duplex transition (3→2) for poly(dA)·2poly(dT). The Mg^{2+} and Ni^{2+} ions stabilize helix-to-coil (2→1) one for poly(dA)·poly(dT), and the midpoint temperatures of the transitions, T_m , are proportional to $\log[Me^{2+}]$. However, the Cd^{2+} ions destabilize 2→1 transition.

For Ni^{2+} and Cd^{2+} containing systems an aggregation of biopolymer was occurred under $[Me^{2+}] \geq 3$ mM, at the same time a reversibility of helix-to-coil transition was broken due to molecular condensation of poly(dA). Another picture has been observed for the poly(dA)+poly(dT)+ Mg^{2+} system. Under $[Mg^{2+}] \geq 15$ mM the thermodynamical stability of duplex and triplex structures becomes equal. Further increase of metal ions concentration results in the appearance of the disproportionality in the duplex polymer structure, which is revealed by the 2→3 transition for poly(dA)·poly(dT), as well as in occurring of only one 3→1 transition for poly(dA)·2poly(dT) system. Under $[Mg^{2+}] \geq 20$ mM the increased turbidity and an extremely high light scattering is revealed during melting transitions for the duplex and triplex polymers, which are disappeared after total separation of polynucleotide strands. This phenomenon is obviously conditioned by reversible fluctuating aggregation of polymer strands. Under $[Mg^{2+}] \geq 50$ mM the irreversible aggregation with polymer precipitation was observed even at room temperature.

It is necessary to note that effect of polymer aggregation is of biological significance since studied Na^+ and Mg^{2+} ion concentrations are close to physiological values.

Anomalous inhomogeneous broadening and kinetics properties of DMABN

K. Hubisz, T. Wróblewski, V.I. Tomin

*Institute of Physics, Pomeranian University,
76-200 Słupsk, Arciszewskiego 22B, Poland.
E-mail: tomin@apsl.edu.pl*

The anomalously large spectral inhomogeneity of the electronic bands ($\Delta\lambda \sim 145$ nm) of N, N-dimethylaminobenzonitrile (DMABN) in a polar solution of glycerol has been found and investigated [1,2]. In nonpolar solutions there is no substantial manifestation of inhomogeneous broadening.

In addition to the local excited (LE) band (~ 360 nm), the emission spectra distinctly display the band associated with internal charge transfer, the CT band having a maximum near 460 nm. The most interesting property of spontaneous emission by DMABN is an unusually strong dependence of emission bands on the exciting light wavelength in the range 290–430 nm. The character of the changes relates to both emission bands and looks as follows. First, the ratio of the intensity maxima of the components I_{LE}/I_{CT} decreases in favour of the charge transfer band. At $\lambda_{ex} = 350$ nm the entire spectrum is rather broad and blurred, and the band maximum is displaced to the red side by about 40 nm. A subsequent increase in λ_{ex} to 430 nm causes a further red shift of the entire emission spectrum to 495 nm. Thus, the resultant shift of the spectrum is anomalously great and attains 145 nm, with the dependence of the red shift on the excitation wavelength being almost linear.

The excitation spectra also depend substantially on the registration wavelength λ_{reg} . Characteristically, there is an additional structure in these spectra when recording is made in the range 390 – 420 nm.

Emission decay and anisotropy characteristics of these “red forms” excited at longwavelength edge of absorption were studied using methods of kinetic picosecond spectroscopy. The decay times and anisotropy of emission are close to the corresponding parameters of DMABN upon excitation at the absorption maximum near 300 nm. Results support the conclusion about luminescence nature of registered emission of DMABN at far antiStokes excitation.

The given data can be explained taking into account an existence of different conformers of the solute and dipole-dipole interactions between the solute and solvent molecules, with allowance for the statistics of the microenvironment, which leads to the appearance of a considerable inhomogeneous broadening of spectra when DMABN is placed into a polar solution. Hence, DMABN and some other charge transfer molecules in polar solution may exist as a set of various conformers differing by their solvate shells. Some of these conformers possesses absorption and emission spectra well shifted to the longwavelength and could be selectively excited on the red edge of absorption band.

References

- [1] V.I. Tomin, K. Hubisz, and Z. Mudryk, Z. Naturforsch., A: Phys.Sci. **58**, 529 (2003)
- [2] V.I. Tomin, Opt.Spectr. **101**, 2, 206 (2006)

Reexamination of the LeRoy-Bernstein formula for weakly bound molecules

Haikel Jelassi, Bruno Viaris de Lesegno and Laurence Pruvost

Laboratoire Aimé Cotton, CNRS II, bat 505, campus d'Orsay

91405 Orsay, France

E-mail: laurence.pruvost@lac.u-psud.fr

The energy law giving the eigen energies of a $-c_n/R^n - c_m/R^m$ potential (studied by LeRoy in 1980 [1]), is revisited. For $n = 3$, $m = 6$, an analytical law giving the density of states is deduced. In the context of weakly bound levels an energy law giving the vibrational number v versus the binding energy ϵ is given. We show that the well-known LeRoy-Bernstein formula [2] [3] has to be corrected by additional terms, with the first one varying as ϵ , the second one as ϵ^2 and the third as $\epsilon^{7/6}$ [4]. The use of such a law is discussed in the context of the photoassociation spectroscopy of long range molecular levels.

References

- [1] *Theory of deviations from the limiting near-dissociation behavior of diatomic molecules*, R. J. LeRoy, J. Chem. Phys. **73**, 6003 (1980).
- [2] *Dissociation energy and long-range potential of diatomic molecules from vibrational spacings of higher levels*, R. J. LeRoy and R. B. Bernstein, J. Chem. Phys. **52**, 3869 (1970).
- [3] *The Dissociation Energy of the Hydrogen Molecule Using Long-Range Forces*, W. C. Stwalley, Chem. Phys. Lett. **6**, 241 (1970).
- [4] *Reexamination of the LeRoy-Bernstein formula for weakly bound molecules*, H. Jelassi, B. Viaris de Lesegno, L. Pruvost, accepted to Phys. rev. A.

The singlet $X - A$ and $X - B$ absorption coefficient of the K_2 system

F. Talbi, M. Bouledroua, and K. Alioua

*Laboratoire de Physique des Rayonnements, Badji Mokhtar University,
B.P. 12, Annaba 23000, Algeria*

Transitions from the singlet $X^1\Sigma_g^+$ to the first excited $A^1\Sigma_u^+$ and $B^1\Pi_u$ states of the potassium dimer are studied quantum mechanically. Using the most recent data for the potential-energy curves for the $4s+4s$ and $4p+4s$ molecular systems and the corresponding dipole transition moments, the reduced absorption coefficients for temperatures ranging from 880 to 3000 K have been computed. The simulations of the absorption coefficient show that the bound-bound transitions are dominant in the red wing and reveal the occurrence of a satellite structure around the wavelength 1049 nm. The temperature effect on the satellite position and its amplitude has also been investigated and the results are compared with recent experimental data.

Atomic-like shell models for alkali trimers derived from *ab initio* calculations

Andreas W. Hauser¹, Carlo Callegari¹, Wolfgang E. Ernst¹ and Pavel Soldán²

¹*Institute of Experimental Physics, Graz University of Technology,
Petersgasse 16, A-8010 Graz, Austria*

²*Charles University in Prague, Faculty of Mathematics and Physics, Department of
Chemical Physics and Optics,
Ke Karlovu 3, CZ-12116 Prague 2, Czech Republic*

Alkali metal clusters have received great attention due to their role as bridge between atomic and solid state physics. Among the smallest clusters, the trimers are of special interest, since these systems provide complex spectra including Jahn-Teller distortions, yet the spectra are well defined and still accessible via *ab initio* calculations.

The experimental spectra, as well as *ab initio* calculations, show a regular pattern of electronic states. High level *ab initio* calculations [CCSD(T), CASPT2] provide detailed information about the participating electronic orbitals, and allow us to rationalize the observed patterns in terms of simplified shell models.

For the low-spin states of K_3 the standard electron-droplet model offers a qualitative explanation.¹ In this simplified picture the electronic states are interpreted as single-electron excitations into delocalized molecular orbitals with typical atomic-like shape. For the description of the quartet manifolds of K_3 , K_2Rb , KRb_2 and Rb_3 we utilize the eigenstates of a harmonic oscillator in a quantum-dot-like confining potential.²

References:

- 1) A. W. Hauser, C. Callegari, W. E. Ernst and Pavel Soldán, *J. Chem Phys.*, submitted
- 2) J. Nagl, G. Auböck, A. W. Hauser, O. Allard, C. Callegari, and W. E. Ernst, *Phys. Rev. Lett.* 100, 63001 (2008)

First observation and analysis of the $(1, 2)^1\Pi$ states of KCs

L. Busevica¹, R. Ferber¹, O. Nikolayeva¹, E. A. Pazyuk²,
A. V. Stolyarov², and M. Tamanis¹

¹*Laser Centre, University of Latvia, 19 Rainis Boulevard, LV-1586 Riga, Latvia*

²*Department of Chemistry, Moscow State University, Moscow, 119899, Russia*

E-mail: Laureta.Busevica@lu.lv

In spite of the fact that the KCs molecule is among prospective objects for production of ultracold polar molecules, empirical data on its ground state potential have been obtained only very recently [1]. There are still no experimental spectroscopic data on any of KCs excited state, and all existing information comes from ab initio calculations [2]. We present first observation of laser induced fluorescence (LIF) for the $(1, 2)^1\Pi$ states of KCs studied by Fourier transform spectroscopy using a Bruker IFS125HR, with 0.03 cm^{-1} resolution. KCs molecules were formed at 280°C in the sealed cylindrical glass cell containing K (natural isotope mixture) and Cs metals. The LIF $D(2)^1\Pi \rightarrow X^1\Sigma^+$ spectra have been excited by tuning within $15280 - 15140\text{ cm}^{-1}$ a diode laser with 130 mW Mitsubishi ML101J27 laser diode. The $B(1)^1\Pi \rightarrow X^1\Sigma^+$ LIF spectra have been obtained with excitation frequencies $14400 - 14500\text{ cm}^{-1}$ by a diode laser with 50 mW Hitachi HL6750 laser diode. Lasers were mounted in home made external cavity resonators (Littrow configuration), with a grating serving as a feedback source. Term values of the $(1, 2)^1\Pi$ states in KCs have been obtained by adding transition frequencies to the respective ground state $(v_X, J_X)X^1\Sigma^+$ term values using accurate $X^1\Sigma^+$ state energy level data from [1]. The dependencies of the $(1, 2)^1\Pi$ states term values on the factor $J(J + 1)$ have been plotted. In particular, for the $D(2)^1\Pi$ state the rotationless term values covered the energy range from ca. 15400 to 16400 cm^{-1} , spanning the J range from 16 to 205. Preliminary v_D identification was suggested. The dependencies have been compared with their theoretical counterparts based on calculations in [2]. The analysis has revealed a noticeable deviation from regular dependence caused, most probably, by spin-orbit interaction of the $D(2)^1\Pi$ state with the $(3)^3\Sigma^+$ state and, especially, with the very closely lying $(2)^3\Pi$ state, as predicted in [2]. The work on vibrational assignment and potential energy curves construction of the states under study is in progress.

Support by Latvian Science Council grant No. 04.1308 is gratefully acknowledged by Riga team. O.N. acknowledges support from European Social Fund. Moscow team acknowledges support by the Russian Foundation for Basic Researches grant No. 06-03-32330a.

References

- [1] R. Ferber, I. Klincare, O. Nikolayeva, M. Tamanis, A. Pashov, H. Knöckel and E. Tiemann, *J. Chem. Phys.*, to be published.
- [2] M. Korek et al., *Can. J. Phys.* 78, 977 (2000); M. Korek et al., *J. Chem. Phys.* 124, 094309 (2006); M. Aymar and O. Dulieu, private communications.

High resolution spectroscopy and IPA potential construction of $a^3\Sigma^+$ state in KCs

R. Ferber¹, O. Nikolayeva¹, M. Tamanis¹, K. Knöckel², E. Tiemann², and A. Pashov³

¹*Laser Centre, University of Latvia, 19 Rainis Boulevard, LV-1586 Riga, Latvia*

²*Institute of Quantum Optics, Leibniz University Hannover, Welfengarten 1, 30167 Hannover, Germany*

³*Department of Physics, Sofia University, 5 J. Bourchier blvd., 1164 Sofia, Bulgaria*

Study of $a^3\Sigma^+$ states of heteronuclear alkali dimers has a strong motivation in supplying necessary spectroscopic data for producing ultra-cold molecular species in their ground state. We present the analysis of high resolution laser induced fluorescence (LIF) spectra to the $a^3\Sigma^+$ state of KCs, see also [1]. The fluorescence has been studied using a Bruker IFS125HR Fourier transform spectrometer, with a typical resolution of 0.03 cm^{-1} . KCs molecules were produced at 280°C in a sealed cylindrical glass cell containing K and Cs metals. For excitation a single mode ring dye laser Coherent 699-21 with Rhodamine 6G dye was used as a light source. Excitation frequencies were selected between 16870 cm^{-1} and 17280 cm^{-1} and measured by a wavemeter (HighFinesse WS6) with about 0.015 cm^{-1} accuracy. The laser frequencies were tuned until the LIF signal to the $a^3\Sigma^+$ state of KCs, as monitored by the Fourier spectrometer in the preview mode, exhibited a maximal value. LIF observed between $13700\text{-}14200\text{ cm}^{-1}$ revealed clear hyperfine structure and therefore was attributed as fluorescence to the $a^3\Sigma^+$ state. In the same spectra LIF to the ground state was present as well. Only P and R transitions were observed in LIF to both the $a^3\Sigma^+$ and the $X^1\Sigma^+$ states. The upper state exited in our experiments is most likely $(4)^1\Sigma^+$ perturbed by $(3)^3\Sigma^+$ and $(2)^3\Pi$ states. Term values of the $a^3\Sigma^+$ state in KCs have been obtained by subtracting the transition frequencies from the respective excited state (v', J') term value. This term value was obtained by adding the energy of the corresponding level of the $X^1\Sigma^+$ state, calculated from the analysis in [1], to the respective (i.e. originating from the same upper state (v', J')) transition frequencies.

At current research stage we have assigned 681 LIF lines in 48 LIF progressions to the $a^3\Sigma^+$ state spanning v^* from 1 to 21 and J from 23 to 143. The symbol v^* means the preliminary current assignment of vibrational quantum numbers. A first empirical potential of the $a^3\Sigma^+$ state is presented, obtained by the Inverted Perturbation Approach (IPA) method [2]. The work on vibrational assignment and potential energy curve of the $a^3\Sigma^+$ state is still in progress.

Support by Latvian Science Council grant No. 04.1308 is gratefully acknowledged by the Riga team. O.N. acknowledges support from European Social Fund. The Hannover team acknowledges support through SFB407 by DFG. A. P. acknowledges partial support from the Bulgarian National Science Fund Grant No. VUF 202/06.

References

- [1] R. Ferber, I. Klincare, O. Nikolayeva, M. Tamanis, A. Pashov, H. Knöckel and E. Tiemann, J. Chem. Phys., to be published.
- [2] A. Pashov, W. Jastrzębski, and P. Kowalczyk, Comput. Phys. Commun. **128**, 622 (2000)

Determination of first-order molecular hyperpolarizability of ethyl 5-(4-aminophenyl)-3-amino-2,4-dicyanobenzoate using steady-state spectroscopic measurements and quantum-chemical calculations

Józef Heldt, Marek Józefowicz, Janina R. Heldt

*University of Gdansk, Institute of Experimental Physics,
ul. Wita Stwosza 57, 80-952 Gdansk, Poland*

In recent years, molecules with large optical non-linearities have been extensively studied due to their potential applications in various optical devices. Some organic molecules with donor and acceptor groups connected by a π -conjugated bridges show very large first-order hyperpolarizability (β). The existence of electronically excited states with strong intermolecular charge transfer (ICT) character is an essential prerequisite for large non-linear optical properties.

Ethyl 5-(4-aminophenyl)-3-amino-2,4-dicyanobenzoate (EAADCy) and its derivatives, organic molecules containing separate electron donor and electron acceptor groups, belong to biphenyl derivatives in which a large dipole moment change between ground (S_0) and the first excited (S_1) states as well as a large transition moment were measured. It is well known that first-order hyperpolarizability (β) depend on several spectroscopic parameters of the two-level model of organic molecule (J.L. Oudar, D.S. Chmla, *J. Chem. Phys.* **66** (1977) 2664):

$$\beta \propto \frac{\Delta\mu_{eg}M_{eg}^2}{E_{eg}^2} \quad (1)$$

where $\Delta\mu_{eg}$ – difference in dipole moment between ground and excited state, M_{eg} – transition dipole moment, E_{eg} – transition energy. Therefore, in this communication we present a scrupulous analysis of the first-order hyperpolarizabilities of molecules under study. The calculated (using semiempirical calculations, CAChe WS 5) β_{theo} values are discussed in relationship to the experimental data β_{exp} obtained from steady-state spectroscopic measurements.

Acknowledgements

This work was partially supported by the research grant of the University of Gdansk, BW-5200-5-0051-8.

Electronic structure of the $[\text{Au}_2(\text{dmpm})(\text{i} - \text{mnt})]$ complex

J. Muñiz, L.E. Sansores, A. Martínez, R. Salcedo

*Instituto de Investigaciones en Materiales, Universidad Nacional Autónoma de México.
Apartado Postal 70-360, México DF 04510, México*

Compound $[\text{Au}_2(\text{dmpm})(\text{i} - \text{mnt})]$ was synthesized by Tang et al [1] as part of a series of dinuclear gold compounds that have intra and inter molecular Au–Au interaction. In this work a theoretical study of this complex is presented. Full geometry optimization at MP2 level was performed on one and two molecules. The basis set used is LANL2DZ for Au and 6-31++G** for all other atoms. The structural parameters obtained for a single molecule show that the aurophilic interaction is present with a Au–Au distance of 3.0Å. A scanning of the potential energy surface at the MP2 level was done by changing the intermolecular gold–gold distance between two units of the compound and a minimum was found at 3.3Å with an interaction energy of 5 kcal/mol which is consistent with the binding energy found in the experiment on this type of complexes. Excited states calculations were also carried out to study the optical spectra observed. The results are in good agreement with those found in experiment, the emission and absorption bands are generated by Metal Ligand Charge Transfer (MLCT) and Metal Centered Charge Transfer (MCCT) interactions, respectively.

References

- [1] S.S Tang, C.-P. Chang, I.J.B. Lin, L.-S. Liou, J.-C. Wang, *Inorg. Chem.* **36**, 2294 (1997)

A lecture demonstration of quantum erasing on a photon-by-photon basis

Todorka L. Dimitrova¹ and Antoine Weis²

¹*Paisii Hilendarski University, Plovdiv, Bulgaria*

²*Physics Department, University of Fribourg, Switzerland*

The introduction of the wave-particle duality in quantum mechanics courses often starts by a discussion of the famous Gedankenexperiment in which a double slit is illuminated by single photons. The classical interference pattern on the screen can then be explained in terms of the superposition of a large number of single photon events, in which each of the photons has passed both slits simultaneously. In recent years we have developed two lecture demonstration experiments of this effect: a first version using a double slit with a single photon CCD camera [1,2], and a second version using two-path interference in a Mach-Zehnder interferometer (MZI) combined with photomultiplier detection [2]. In the latter apparatus we vary the path difference of the interfering beams periodically by modulating one of the MZI mirrors with a piezo-transducer, and displaying the outgoing light intensity on an oscilloscope. Using strong light and a photodiode one observes smooth fringes, while the use of strongly attenuated light, and a photomultiplier reveals the individual photon structure of the fringes. In that case photon clicks can also be rendered acoustically. This apparatus can be used to demonstrate many effects related to single photon interference in an undimmed large auditorium.

Recently we have extended the latter experiment for demonstrating the phenomenon of quantum erasing. Interference fringes are a consequence of the indistinguishability of the paths taken by the particle in the interferometer. Any attempt to put individual labels on the particles in each path leads to a disappearance of interference. This can be demonstrated in a simple way by inserting orthogonally oriented linear polarizers in the two paths of the MZI. When doing so the interference fringes on the screen are made to disappear. However, the which-way information imposed by the polarizers can be erased after the particles have left the interferometer. In practice this is realized by the insertion of a third polarizer, the eraser, oriented at $\pm 45^\circ$ before the screen. The erasing polarizer destroys the polarization labels and makes the interference reappear, a phenomenon called *quantum erasing*. In terms of classical wave superposition the phenomenon is readily understood, but its understanding at the single photon level presents some difficulties for students. From a didactical point of view it is a nice example for introducing the concept of entanglement: while being in the interferometer the external degree of freedom (path) of each photon is entangled with its internal state (polarization).

The versatile apparatus described above can be used to demonstrate quantum erasing on a photon-by-photon basis in an impressive manner.

References

- [1] A. Weis and R. Wynands, *Three demonstration experiments on the wave and particle nature of light*, PhyDid, 1/2 (2003) 67-73.
- [2] T. L. Dimitrova and A. Weis, *The wave-particle duality of light: a demonstration experiment*, Am. J. Phys. 76 (2008) 137-142.

Stark shift in the Cs clock transition frequency: A new experimental approach

J.-L. Robyr, P. Knowles, A. Weis

University of Fribourg, Department of Physics, Fribourg, Switzerland

The precision of microwave atomic clocks is approaching the 10^{-16} level, and at this precision, more refined accounting of the perturbations affecting the cesium hyperfine level splitting must be carefully considered. The AC Stark shift induced by blackbody radiation via the polarizability of the Cs atom is one such disturbance. The past few years have seen a renewed interest in the measurement and theoretical description of that effect. We report on progress towards the application of coherent population trapping (CPT) in a pump-probe experiment on a thermal atomic beam for a new measurement of the third order scalar and tensor polarizabilities that underlie the blackbody shift.

The polarizability, α , describes the energy shift of a level via $\Delta E(n, L_J, F, M_F) = -\frac{1}{2}\alpha\mathbb{E}^2$, and is traditionally expanded in a perturbation series whose first few terms are

$$\alpha = \alpha_0^{(2)}(n, L_J) + \alpha_0^{(3)}(n, L_J, F) + \alpha_2^{(3)}(n, L_J, F) \frac{3M_F^2 - F(F+1)}{I(2I+1)}.$$

Only the third-order perturbation terms $\alpha_0^{(3)}$ (scalar) and $\alpha_2^{(3)}$ (tensor) create a shift affecting the Cs hyperfine structure, and hence the clock transition frequency $\nu_{00}(3, 0 \rightarrow 4, 0)$. Recent examination of the theory underlying the polarizability[1] has corrected a long-hidden sign error, and several recent measurements of the AC and DC Stark shifts of ν_{00} are not consistent with each other. We wish to help clarify the situation by a new experiment.

The principle of the experimental method is to create a hyperfine coherence using CPT in an atomic beam, to allow the coherence to evolve for a certain time in controlled magnetic and electric fields, and finally to probe the phase accumulated in the field region. Part of the phase difference will be proportional to the differential level shifts produced by the applied electric field and thus give access to both the third-order scalar and tensor polarizabilities of the Cs ground state. We plan to measure the shifts in all accessible M_F levels, and not only in the $M_F=0$ clock transition states. A degenerate CPT version of the method was successfully used by us to measure[2] the tensor Stark shift $\alpha_2^{(3)}$, a value roughly two orders of magnitude smaller than the scalar $\alpha_0^{(3)}$ which dominates the contribution to the black body shift.

Details of the apparatus and the physics under study will be presented.

[1] S. Ulzega, A. Hofer, P. Moroshkin, and A. Weis, *Europhys. Lett.* **76**, 1074 (2006)

[2] C. Ospelkaus, U. Rasbach, and A. Weis, *Phys. Rev. A* **67**, 011402 (2003).

Magnetic Field Imaging With Arrays of Cs Magnetometers: Technology and Applications

P. Knowles^e, G. Bison^{e,h}, N. Castagna^e, A. Hofer^e,
 A. Mtchedlishvili^l, A. Pazgalev^{e,l,1}, A. Weis^e,
 and including the PSI nEDM collaboration^{a-l}

^a*Physikalisch Technische Bundesanstalt, Berlin, Germany*

^b*Laboratoire de Physique Corpusculaire, Caen, France*

^c*Jagellonian University, Cracow, Poland*

^d*Joint Institute for Nuclear Research, Dubna, Russia*

^e*University of Fribourg, Switzerland*

^f*Institut Laue Langevin, Grenoble, France*

^g*Laboratoire de Physique Subatomique et de Cosmologie, Grenoble, France*

^h*Biomagnetisches Zentrum Jena, Germany*

ⁱ*Katholieke Universiteit, Leuven, Belgium*

^j*Johannes-Gutenberg-Universität, Mainz, Germany*

^k*Technische Universität München, Germany*

^l*Paul Scherrer Institut, Villigen PSI, Switzerland*

¹*Ioffe Physical Technical Institute, St. Petersburg, 194021, Russia*

The precision measurement of magnetic fields is of interest for both applied and fundamental physics. In many of these cases, atomic cesium magnetometers pumped by a laser (LsOPM) or by a discharge lamp (LaOPM) and operating via simultaneous application of optical and magnetic resonance, have the necessary sensitivity[1]. The shift from using multiple lamps to using a single laser (with holographic beam splitting) as a light source for driving many sensors has improved the suitability of the LsOPM for use in multi-channel applications. A successful effort in the mass production of paraffin anti-relaxation coated Cs vacuum cells, along with a compact sensor design which maintains a high magnetic sensitivity (~ 20 fT/ $\sqrt{\text{Hz}}$), shows that the multi-sensor (~ 50) approach to field imaging is realistic with LsOPMs. The compact sensors ($30 \times 40 \times 40$ mm³) are vacuum compatible and, once assembled, relatively rugged and insensitive to vibration and shock. Successful all-digital control of the magnetometer, as performed by dedicated FPGA systems including real-time feedback between different sensors in the array, indicates that the initial hurdles slowing the creation of a fully operational compact multi-sensor optical magnetometry array have been overcome.

Developments related to the sensors and their in-array operation will be detailed. Future applications, such as the control of the magnetic field stability for the new neutron electron dipole moment experiment at PSI as well as in the domain of cardiomagnetic field imaging, will be explained.

[1] S. Groeger, A. S. Pazgalev, and A. Weis, Appl. Phys. B **80**, 645 (2005).

Performance of a compact dark state Magnetometer

R. Lammegger¹ and L. Windholz¹

¹*Institute of Experimental Physics TU-Graz, Petersgasse16, 8010 Graz*

Measuring magnetic fields by means of spectroscopic-optical methods has advantages in many respects. E.g. in best case the magnetic field sensor of an optical magnetometer can only be made of a (nonmagnetic) glass cell containing a tiny amount of an alkali metal non perturbing the external magnetic field. Moreover the optical sensor is working near room temperature. Thus unlike to the (in common more sensitive) superconducting quantum interference device (SQUID) magnetometer an extensive cooling down to cryogenic temperatures can be avoided.

We consider a compact vertical surface emitting laser (VCSEL) based dark state Magnetometer. In such kind of optical magnetometer the zeeman split (magnetic sensitive) components of the coherent population trapping (CPT) resonance spectrum are used to determine an external magnetic field. By applying the Breit-Rabi formula the value of the external magnetic field can be derived directly from the frequency of the magnetic sensitive CPT resonance components.

In our investigations the advantages and constraints of such a compact magnetometer type in terms of sensitivity, measurement bandwidth, noise and influence of magnetic field gradients are outlined. E.g. in our actual magnetometer setup a sensitivity down to $10\text{ pT}/\sqrt{\text{Hz}}$ is reached.

The work is founded by the Fonds zur Förderung der wissenschaftlichen Arbeit (FWF) (Project No.: L300-N02)

Laser-induced transport effect and laser induced-line narrowing mechanism for laser excitation in ^{87}Rb atomic vapors in a finite-size buffer-less cell.

A.Litvinov¹, G. Kazakov², B. Matisov²

¹*A.F. Ioffe Physico-Technical Institute RAS, St.Petersburg, Russia*

²*St. Petersburg State Polytechnic University, St.Petersburg, Russia*

Coherent population trapping (CPT) and double radio-optical resonance (DROR) are quantum nonlinear effects. Both these effects are the base for the creation of high precision magnetometers and atomic frequency standards.

We study the influence of the laser induced transport (LIT) [1] and the laser induced line narrowing (LILN) [2] effects on the DROR and CPT resonance line shape for excitation in ^{87}Rb atomic vapors in wall-coated and uncoated cell. We take into account both hyperfine and Zeeman structures of the ground and the excited states of ^{87}Rb atoms as well as the probabilities of spontaneous transitions. We investigate the dependence of the resonance shape on the length of the cell, on the type of boundary conditions, on the polarization and intensity of laser and microwave fields, and on the laser line width ("narrow-band" and "broad-band").

Laser induced transport in DROR: The first the LIT was predicted for three-level model in [1]. We show that the LIT takes place in buffer-less cell with real ^{87}Rb atoms. The physical essence of the LIT effect is the caused by the Doppler effect velocity-selectivity of the interaction of "narrow-band" laser field with atoms, resulting in Bennett dips and peaks in the velocity distribution of atoms in the ground state sublevels. Asymmetry of the two velocity distributions gives rise to the opposite-directed (along the laser propagation direction) fluxes of the atoms in the ground state sublevels. Therefore, a flux of the population inversion (or, equivalently, of the longitudinal magnetization) arises. This behavior one experimentally can observe as the transmission peak in the centre of the DROR signal [3]. LIT effect is most pronounced for "narrow-band" laser pumping.

Laser induced line narrowing in CPT resonance: The LILN of the CPT resonance realizes only in the case of excitation by "narrow-band" laser. We established that for the LILN mechanism the parameters (the amplitude and width) of the CPT resonance excited on hyperfine transition weakly depend on the cell size and the type of the coating [4]. When the components of the laser field are comparable the CPT resonance width depends linearly on the laser field intensity. This case was investigated in [5] where the formation of CPT resonance on Zeeman sublevels was studied. In contrast for the electromagnetically-induced transparency (EIT) effect (where one laser field is drive and the other - probe) the EIT width increases proportionally to the square root of the drive field intensity [6].

This work is supported by INTAS-CNES-NSAU grant, project 06-1000024-9321.

References

- [1] B. D. Agap'ev, M. B. Gornyi, and B. G. Matisov, *Sov.Phys. JETP* **65**, 1121 (1987).
- [2] M. S. Feld and A. Javan, *Phys.Rev.* **2**, 177 (1969).
- [3] A. S. Zibrov, A. A. Zhukov, V. P. Yakovlev et al., *JETP Letters* **83**, 168 (2006).
- [4] G. Kazakov, B. Matisov, A. Litvinov, and I. Mazets, *J. Phys. B* **40**, 3851 (2007).
- [5] A. Huss, R. Lammegger, and L. Windholz et al., *JOSA B* **23**, 1729 (2006).
- [6] A. Javan, O. Kocharovskaya, H. Lee et al., *Phys. Rev. A* **66**, 013805 (2002).

Population transfer, light storage, and superluminal propagation by bright-state adiabatic passage

G.G. Grigoryan¹, G. Nikoghosyan¹, A. Gogyan^{1,2}, Y.T. Pashayan-Leroy², C. Leroy², and S. Guérin²

¹*Institute for Physical Research, 0203, Ashtarak-2, Armenia*

²*Institut Carnot de Bourgogne, UMR 5209 CNRS - Université de Bourgogne, BP 47870, 21078 Dijon, France*

The practical implementation of quantum information requires to develop techniques of mapping of light pulses into the excitation of media in order to allow the subsequent retrieval of the stored information. Recently, broad attention has been focused on the possibility of "light-storage" under the conditions of electromagnetically induced transparency (EIT), as proposed by Fleischauer and Lukin [1]. The method is based on the existence of a dark state in Raman interaction of a Λ -type system. We present an alternative method for the storage and retrieval of optical information using adiabatic passage along a bright state (b-state). We present theoretical calculations demonstrating that a light storage can take place in media where EIT does not occur. This method is achieved for short pulses of interaction time shorter than the relaxation times. Such a bright state allows population transfer by a Stimulated Raman adiabatic passage using an intuitive pulse sequence (process named b-STIRAP), as demonstrated in $\text{Pr}^{+3}\text{Y}_2\text{SiO}_5$ [2].

In the present work we obtain an analytical solution of the set of Maxwell-Schrödinger equations describing the propagation of two laser pulses in a Λ -type medium for an intuitive pulse sequence. We show that it allows an effective storage and retrieval of an optical pulse. The probe pulse that is switched on later than the control pulse propagates in the medium with the velocity greater than the light velocity (superluminal propagation). When the control pulse is switched off, the shape of the probe pulse is mapped into the coherence of the lower states. After a subsequent switching on of the control pulse the probe pulse is shown to be completely restored.

We have analyzed population transfer process in a medium via b-state during the pulse propagation. We show that for specific interaction parameters one can achieve an efficient population transfer. We have estimated the maximal length up to which population transfer is still possible.

References

- [1] M. Fleischauer and M.D. Lukin, Phys. Rev. Lett. **84**, 5094 (2000)
- [2] J. Klein, F. Beil, and T. Halfmann, Phys. Rev. Lett. **99**, 113003 (2007)

Population switching of Na and Na_2 excited states by means of interference due to Autler-Townes effect

C. Andreeva^{1,2}, N. Bezuglov³, A. Ekers¹, K. Miculis¹, B. Mahrov¹, I. Ryabtsev⁴,
E. Saks¹, R. Garcia-Fernandez⁵, K. Bergmann⁵

¹*Laser Centre, University of Latvia, LV-1002 Riga, Latvia*

²*Institute of Electronics, Bulgarian Academy of Sciences, Sofia 1784, Bulgaria*

³*Faculty of Physics, St.Petersburg State University, 198904 St. Petersburg, Russia*

⁴*Institute of Semiconductor Physics, 630090 Novosibirsk, Russia*

⁵*University of Kaiserslautern, Dept. of Physics, D-67653 Kaiserslautern, Germany*

We present our results on the exploitation of interference effects for population switching of excited states. Our calculations show that spatial distribution of the atomic excitation can be controlled by employing the Autler-Townes effect [1] in a laser coupling scheme enabling Ramsey interference [2]. Interference fringes in the Autler-Townes spectra have been reported in [3] for the case of a closed three-level system coupled by a resonant pulsed pump laser in the first excitation step, creating time-varying dressed states, which were probed by a simultaneous probe pulse in the second excitation step. In our experiment, a supersonic sodium beam is crossed by two *cw* laser beams, which couple an open three-level ladder system. The lasers are focused in such a way that a strong and short (tightly focused) pump laser couples the two lower levels $|g\rangle$ and $|e\rangle$, and weak and long (less tightly focused) probe laser couples the intermediate $|e\rangle$ and the upper level $|f\rangle$. The pump laser thus creates two spatially varying dressed states, whose energy difference is determined by the pump field Rabi frequency and its detuning from resonance.

Our numerical calculations of density matrix equations of motion using the split propagation technique [4] show that with this arrangement the spatial distribution of populations of excited atomic or molecular states can be precisely controlled by varying the laser frequencies and intensities. When the frequencies of both laser are fixed, the excitation of the upper level can take place at two spatial locations. This leads to two alternative excitation pathways of the level $|f\rangle$, where the probability amplitude of this level after the second crossing point is determined by the constructive or destructive interference of both excitation pathways. Our simulations show [5] that interference fringes in the excitation spectrum of the upper level can be resolved when counter-propagating laser beams are used to avoid residual Doppler broadening. We show that moderate detunings of the strong dressing laser are favorable for the observation of interference effects. The experimental realization of the idea is in progress.

The work is supported by the EU TOK Project LAMOL, European Social Fund, Latvian Science Council, and RFBR Grant 05-02-16216.

References

- [1] S.H. Autler, C.H. Townes, *Phys.Rev.* **100**, 703 (1955).
- [2] N.F. Ramsey, *Molecular Beams* (Clarendon, Oxford, 1989).
- [3] S.R. Wilkinson, A.V. Smith, M.O. Scully, E. Fry, *Phys. Rev.* **A53** (1), 126 (1996).
- [4] M.D. Fiet, J.A. Fleck, A. Steiger, *J. Comput. Phys.* **47**, 412 (1982).
- [5] N.N. Bezuglov, R. Garcia-Fernandez, A. Ekers, K. Miculis, L.P. Yatsenko, K. Bergmann, "Consequences of optical pumping and interference for excitation and spectra in a coherently driven molecular ladder system" (in preparation).

High-rank polarization moments influence on the CPT resonance obtained on two-level degenerated system

E. Alipieva, E. Taskova, S. Gateva and G. Todorov

*Academician Emil Djakov Institute of Electronics, Bulg. Acad. Sc.,
72 Tzarigradsko Chaussee, 1784 Sofia, Bulgaria
E-mail: alipieva@ie.bas.bg*

In two-level degenerated system Coherent Population Trapping (CPT) resonance is due to the interference between the Zeeman sub-levels with $\Delta m=2$, created by interaction of resonance linear polarized laser beam with the atoms. The resonance is detected by sweeping magnetic field \mathbf{B}_0 around its zero value - Hanle configuration. The multiphoton processes and the low relaxation rate of the lower levels allow creation of coherences between sub-levels with $\Delta m>2$. The laser field transfers this coherence in the fluorescence from the upper level and thus changes the shape of CPT resonance.

The investigations were performed on the D_1 ^{87}Rb line ($F=2 \rightarrow F=1$ transition) in an uncoated cell. The comparative - theoretical and experimental investigation, performed of the shapes of the CPT resonances registered in fluorescence shows that the high-rank polarization moments (HRPMs, $\Delta m>2$) influence them at low excitation power and at high excitation powers as well. The HRPMs conversion is proved to cause the CPT resonance shape peculiarities at the center of the resonance: at low excitation power, a specific difference from the Lorentzian shape is observed, while at a high power of excitation, an inverted structure is registered [1].

All resonances in Hanle configuration are centered at zero magnetic field. The integration of the modulation and coherent spectroscopy allows resonances due to different polarization moments to be resolved and enlarge the application area of the investigations [2,3]. A.c. electromagnetic field (EMF) applied collinearly to the \mathbf{B}_0 modulates the frequency difference between the Zeeman sub-levels. The Larmor frequency becomes: $\omega = \omega_0 + \omega_1 \cos \Omega t$, where Ω is the EMF frequency. The intensity of the scattered from the atoms light is modulated and shows resonance increasing when EMF frequency is multiple to the Zeeman sub-levels difference. When EMF is applied the side-band resonance which corresponds to coherence created between $m=+2$ and $m=-2$ Zeeman sub-levels appears first. The parameters of this resonance in dependence of experimental conditions were investigated.

The results of this investigation are interesting for high-resolution spectroscopy, magnetometry, and metrology applications.

References

- [1] S. Gateva, L. Petrov, E. Alipieva, G. Todorov, V. Domelunksen, V. Polischuk, Phys. Rev. **A76**(2), 025401 (2007).
- [2] E. Alexandrov, O. Konstantinov, V. Perel, V. Khodovoy, JETP **45**, 503-510 (1963);
- [3] S. Pustelny, D.F. Jackson Kimball, S.M. Rochester, V.V. Yashchuk, W. Gawlik, D. Budker, Phys. Rev. **A73**, 023817 (2006).

Sub-Doppler fluorescence spectroscopy of Cs-vapour layers with nano-metric thickness

K. Vaseva¹, P. Todorov¹, S. Cartaleva¹, D. Slavov¹, S. Saltiel²

¹*Institute of Electronics, Bulgarian Academy of Sciences, 72 Tzarigradsko Shosse bld, 1784 Sofia, Bulgaria*

²*Sofia University, Faculty of Physics, 5 J. Bourchier boulevard, 1164 Sofia, Bulgaria
E-mail: petkoatodorov@yahoo.com*

The extensive study of alkali-vapor layers with nano-metric thickness L has been made possible through the development of cells of $L \leq 1 \mu\text{m}$, where the thickness of the vapor-layer can be varied in an interval around the wavelength λ of the irradiating light [1]. It was shown that the width of the fluorescence profiles increases with the cell thickness [2].

We present experimental and theoretical studies of the fluorescence spectra on the D_2 line of *Cs*-atomic-layers with $L = m\lambda$ ($m = 0.5, 0.75, 1, 1.25$), when irradiated by narrow-band laser light tuned around $\lambda = 852\text{nm}$. We use the theoretical model [3] based on the Optical Bloch Equations and obtain qualitative agreement between the theory and the experiment. The atomic systems are separated in two groups: closed and open. Well pronounced narrow dip in the fluorescence (superimposed on the top of the sub-Doppler-width fluorescence profile) is observed experimentally only for the open transitions suffering hyperfine/Zeeaman optical pumping, and for $L \geq \lambda$. In the case of closed transition, non-suffering population loss extremely small peculiarity in the fluorescence profile is observed for $L = 1.25\lambda$ [4]. Systematic comparison is made between the fluorescence profiles amplitude and width, estimated theoretically and experimentally. With laser power the amplitude and the width of the fluorescence profiles increase, for all cell thicknesses and all transitions. In agreement with the previous results [2], the width of the transition profiles is growing with L . However, we report here about the following new peculiarity: the enhancement rate of the transition width is not constant, namely it is larger for L varying in the interval $0.75\lambda \leq L \leq \lambda$ than that varying in the interval $\lambda \leq L \leq 1.25\lambda$.

We show that the width of the fluorescence profiles strongly depends on the layer thickness (with variations as small as 213nm). These results can be used for spectral investigations of atoms confined in nano volumes, as well as for spectroscopy of miniature gas discharges.

Authors are grateful to Prof. D. Sarkisyan for providing the nano-cell, as well as to INTAS (grant: 06-1000017-9001), Indo-Bulgarian program of cooperation in science and technology (grant No. BIn-2/07) and the French-Bulgarian Rila collaboration (French grant: 98013UK, Bulgarian grant: 3/10), for the partial support.

- [1] D. Sarkisyan, D. Bloch, A. Papoyan, M. Ducloy, *Opt. Commun.* **200**, 201 (2001).
- [2] D. Sarkisyan, T. Varzhapetyan, A. Sarkisyan, Yu. Malakyan, A. Papoyan, A. Lezama, D. Bloch, M. Ducloy, *Phys. Rev.* **A69**, 065802 (2004).
- [3] C. Andreeva, S. Cartaleva, L. Petrov, S. M. Saltiel, D. Sarkisyan, T. Varzhapetyan, D. Bloch, M. Ducloy, *Phys. Rev.* **A76**, 013837 (2007).
- [4] K. Vaseva, P. Todorov, D. Slavov, S. Cartaleva, K. Koynov, S. Saltiel, *ACTA PHYSICA POLONICA A*, Vol. **112**, No. 5, 865 (2007).

Absorption in the saturation regime of Cs-vapour layer with thickness close to the light wavelength

P. Todorov¹, S. Cartaleva¹, K. Vaseva¹, C. Andreeva¹, I. Maurin², D. Slavov¹,
S. Saltiel³

¹*Institute of Electronics, BAS, 72 Tzarigradsko Shosse boulevard, 1784 Sofia, Bulgaria*

²*Laboratoire de Physique des Lasers UMR 7538 du CNRS, Université Paris-13, France*

³*Sofia University, Faculty of Physics, 5 J. Bourchier boulevard, 1164 Sofia, Bulgaria*
E-mail: petkoatodorov@yahoo.com

Absorption spectrum of an atomic vapour layer, which thickness L is close to the wavelength of the irradiating light λ , shows a narrow structure on the Doppler broaden background. This is attributed to Dicke narrowing [1,2], which is due to the coherent contribution of all velocity group atoms into the narrow absorption signal at the position of the central frequency of the transition. This is possible because the Doppler shift is eliminated by the transient regime of atom-light interaction when the transient interaction time is shorter than the lifetime of the excited state. The maximum contribution of Dicke effect is achieved for $L = \lambda/2$, while the effect is cancelled at $L = \lambda[2]$. It has been shown that a revival (with an amplitude lower than that at $L = \lambda/2$) of the Dicke narrowing occurs for $L = (2n + 1)\lambda/2$. The maximum amplitude of the Dicke revival is for $L = (3/2)\lambda[2-5]$.

We present the absorption spectra in saturation regime on the D_2 line of Cs-vapour-layer with $L = (5/4)\lambda$, irradiated by tunable (around $\lambda = 852\text{nm}$ diode laser light[6]. The atomic gas is confined in a nano-cell [7]. Different saturation behavior for closed and open optical transitions reported before in [6,8,9] is studied for cell thickness $L = (5/4)\lambda$. For the closed transition, well pronounced Dicke narrowing is observed starting from low light intensity and it is preserved even on the saturation deep occurring at high intensity. On the contrary, the open transitions do not show Dicke resonance under the same conditions. The observations differ from those for $L = (3/2)\lambda$ [5], where the Dicke revival is observed for both closed and open transitions. The result is of basic importance for revealing of the influence of the optical pumping/saturation processes to the Dicke effect.

We thank D. Sarkisyan for nano-cell, D. Bloch and M. Ducloy for discussions, INTAS (gr. 06-1000017-9001) and Rila collaboration (French gr.: 98013UK, Bulgarian gr.: 3/10).

- [1] R. H. Romer, R. H. Dicke, Phys. Rev. **99**, 532(1955).
- [2] G. Dutier, A. Yarovitski, S. Saltiel, A. Papoyan, et. al., Europhys. Lett. **63**, 35 (2003).
- [3] D. Sarkisyan, T. Varzhapetyan, A. Sarkisyan, et. al., Phys. Rev. A **69**, 065802(2004).
- [4] I. Hamdi, P. Todorov, A. Yarovitski, G. Dutier, et. al., Laser Physics **15**, 987 (2005).
- [5] S. Cartaleva, K. Koynov, et. al., Proc. 34th EPS Conf., ECA vol.**31F**, P-4.008 (2007).
- [6] C. Andreeva, S. Cartaleva, L. Petrov, et. al., Phys. Rev. **A76**, 013837 (2007).
- [7] D. Sarkisyan, D. Bloch, A. Papoyan, M. Ducloy, Opt. Commun. **200**, 201 (2001).
- [8] S. Briaudeau, D. Bloch and M. Ducloy, Europhys. Lett. **35**, 337 (1996)
- [9] S. Briaudeau, S. Saltiel, D. Bloch, M. Ducloy, Phys. Rev. **A57**, R3169 (1998)

Dark and bright resonances in large J systems: example of K_2 molecule

M. Auzins, R. Ferber, I. Fescenko, L. Kalvans, and M. Tamanis

Laser Centre, University of Latvia, 19 Rainis Boulevard, LV-1586 Riga, Latvia

We report the results of an experimental as well as theoretical study of the dark and bright resonances in the ground state of systems with extremely large angular momentum. It is shown that, besides the well-known zero-magnetic field suppression of the absorption on $J_g = J \rightarrow J_e = J - 1$, J transitions caused by population trapping in the ground J_g state, optical pumping may induce enhanced absorption as well. This occurs if some conditions are met on $J_g = J \rightarrow J_e = J + 1$ transitions for small magnetic field B values. The latter effect becomes more pronounced if the J -value increases and disappears if a substantial fraction of the excited molecules can spontaneously decay to a level that is different from the one on which the absorption transition started. Bright resonance enhancement is substantially stronger for excitation with circularly polarized light than for excitation with linearly polarized light. The experiments were carried out with the K_2 molecule, and the results of our measurements agree reasonably well with numerical simulations that were based on the optical Bloch equations for the density matrix [1].

K_2 molecules were formed in a glass cell that contained K metal at a temperature of 170 °C, and which was placed between the poles of an electromagnet that produced a magnetic field B up to 10 kG. The Q-type $B(1)^1\Pi_u \leftarrow X^1\Sigma_g^+$ transition to the rovibronic level with $v_e = 0$ and $J_e = 104$ was excited by a diode laser with a Mitsubishi ML101J27 laser diode at the 15192.29 cm^{-1} transition frequency. The laser power in the cell was about 20 mW and the laser beam width about 2.5 mm. Dark resonances were observed in the intensities of linearly polarised laser induced fluorescence with polarization vectors \mathbf{E}_{obs} both parallel (I_{par}) and orthogonal (I_{ort}) to the exciting laser radiation polarization vector \mathbf{E}_{exc} , which was orthogonal to \mathbf{B} . We detected well pronounced dark resonance signals, with larger contrast in I_{par} by about 30% , and signal width about 6 kG, which agreed with theoretical predictions. Bright resonances had been neither detected nor predicted previously for such a system because of the presence of “leak” transitions to the J_i -levels other than the pumped J_g transition.

The authors are grateful for the support from the Latvian State Research programme in Material Science 1-23/50 and from the ERAF grant VPD1/ERAF/CFLA/05/APK/2.5.1/000035/018.

References

[1] K. Blush and M. Auzins, Phys. Rev. A **69**, 063806 (2004).

***F*-resolved bright and dark magneto-optical resonances at the cesium D1 line**

M. Auzinsh, R. Ferber, F. Gahbauer, A. Jarmola, and L. Kalvans

*The University of Latvia, Laser Centre, 19 Rainis Boulevard, LV-1586 Riga, Latvia
jarmola@latnet.lv*

We present detailed experimental and theoretical studies of *F*-resolved bright and dark magneto-optical resonances at D1 excitation of atomic cesium in a vapor cell [1]. Although these effects have been known for some time [2,3], experimental measurements [4,5] did not agree with theoretical predictions [6,7]. Previously studied systems have been difficult to model because several hyperfine levels contributed to the signal simultaneously. The advantage of the cesium D1 line system considered here is that the hyperfine splitting of the excited $6P_{1/2}$ state exceeds the Doppler width and therefore the hyperfine transitions from ground state levels $F_g = 3, 4$ to excited state levels $F_e = 3, 4$ can be studied individually despite Doppler broadening.

Cesium atoms in a vapor cell were excited by linearly polarized laser radiation from an external cavity diode laser and the laser induced fluorescence was detected with a photodiode in a direction perpendicular to the laser propagation and polarization. The magnetic field in the observation direction was scanned by means of a Helmholtz coil. The laboratory magnetic field in the other directions was compensated by two other Helmholtz coils. Experimentally obtained signals for various laser power densities and transit relaxation times were compared to the results of a theoretical calculation based on the optical Bloch equations, which averages over the Doppler contour of the absorption line and accounts for the contribution of all hyperfine levels, as well as mixing of magnetic sublevels in an external magnetic field.

In contrast to previous studies which could not resolve the hyperfine transitions, in this study there is excellent agreement between experiment and theory regarding the sign (bright or dark), contrast, and width of resonance. The results thus support the theoretical description of these resonances originally proposed in [6,7]. Renewed confidence in the theoretical underpinnings of these resonances and a detailed theoretical model could aid in the design of optical devices based on this effect.

We acknowledge support from the Latvian National Research Programme in Material Sciences Grant No. 1-23/50, the University of Latvia grant Y2-ZP04-100, the ERAF grant VPD1/ERAF/CFLA/05/APK/2.5.1./000035/018, and the INTAS projects 06-1000017-9001 and 06-1000024-9075. F. G., A. J., and L. K. acknowledge support from the ESF.

References

- [1] M. Auzinsh, R. Ferber, F. Gahbauer, A. Jarmola, and L. Kalvans, arXiv.org, arXiv:0803.0201.
- [2] R. W. Schmieder *et al.*, Phys. Rev. **A 2**, 1216 (1970).
- [3] G. Alzetta, A. Gozzini, L. Moi, and G. Orriols, Il Nuovo Cimento **B 36**, 5 (1976).
- [4] G. Alzetta *et al.*, Journal of Optics **B 3**, 181(2001).
- [5] A. V. Papoyan *et al.*, J. Phys. **B 36**, 1161 (2003).
- [6] F. Renzoni *et al.*, Phys. Rev. **A 63** 065401 (2001).
- [7] J. Alnis and M. Auzinsh, J. Phys. **B 34**, 3889 (2001).

Effects of hyperfine structure on the Autler-Townes splitting

T. Kirova¹, A. Ekers¹, N. N. Bezuglov^{1,2}, I. I. Ryabtsev³, K. Blushs¹, and M. Auzinsh¹

¹ *Laser Centre, University of Latvia, LV-1002 Riga, LATVIA*

² *Faculty of Physics, St.Petersburg State University, 198904 St. Petersburg, RUSSIA*

³ *Institute of Semiconductor Physics SB RAS, 630090, Novosibirsk, RUSSIA*

The Autler-Townes (AT) effect is associated with its typical doublet structure in the excitation spectrum [1], which is due to the dressing of two energy levels by strong coherent radiation field [2]; the dressed states can be observed by an auxiliary weak probe field coupled to some third level. It has been extensively studied in detail in atoms [3] and less extensively also in [4] molecules.

In our recent work [5] we have extended the studies of AT effect to atomic and molecular systems where hyperfine structure is present. In the case of a three-state ladder with hyperfine structure in Na coupled by two laser fields, simulations based on a theoretical model of solving the optical Bloch equations (OBE's)[6] show that application of a sufficiently strong coupling between the intermediate and the final states results in full resolution of the m_F Zeeman sublevels of the hyperfine levels F . This resolution, however, vanishes if the hyperfine levels can not be initially resolved spectroscopically, which is the case for most molecular systems.

Currently, work is in progress to understand the above effects in the case of both resolved and unresolved hyperfine structure and to predict possible experimental applications. Besides OBE's we employ an alternative method treating the laser-atom system by solving the Shrödinger's equation to obtain the time evolution of the probability amplitudes. Comparison with the simulations based on solving the OBE's shows the same energy positions of the m_F Zeeman sublevels under the action of a strong laser field but different widths and intensities of the AT peaks, since no cascading due to spontaneous emission is included. Simulations based on Shrödinger's equation show that the increase of the coupling field strength, compared to the separation between the hyperfine components, leads to rapid decrease (and eventually vanishing) of the intensity of all AT peaks besides the two side ones. The latter is explained in view of the creation of multiple dark states in a multilevel system coupled by a strong field.

Support by the EU FP6 TOK project LAMOL, ERDF project S35-ESS38-100, European Social Fund, Latvian Science Council, and RFBR grant No. 08-02-00220 is acknowledged.

References

- [1] S. H. Autler and C. H. Townes, *Phys. Rev.* **100**, 703 (1955)
- [2] C. Cohen-Tannoudji et al., *Atomo-Photon Interactions*, (Wiley, New York, 1992)
- [3] J. L. Picque and J. Pinard, *J. Physics B* **9**, L77 (1976); P. T. H. Fisk et al., *Phys. Rev. A* **33**, 2418 (1986); F. C. Spano, *J. Chem. Phys.* **114**, 276 (2001)
- [4] J. Qi et al., *Phys. Rev. Lett.* **83**, 288 (1999); R. Garcia-Fernandez et al., *Phys. Rev. A* **71**, 023401 (2005)
- [5] T. Kirova, et al., in: *Proceedings of the XIV National Conference "Laser Physics-2007"*, (Ashtarak, Armenia, 2008) in print
- [6] M. Auzinsh et al., *Opt. Commun.* **264**, 333 (2006)

Ladder and Lambda systems electromagnetically induced transparency in thin and extremely-thin cells

A. Sargsyan¹, M.G.Bason², D. Sarkisyan¹, Y. Pashayan-Leroy^{1,3}, A.K.Mohapatra²,
C. S. Adams²

¹*Institute for Physical Research, NAS of Armenia, Ashtarak-0203, Armenia*

²*Department of Physics, Durham University, Durham DH1 3LE, United Kingdom*

³*Laboratoire de Physique de l'Université de Bourgogne, Dijon, France*

The recent interest in the effect of electromagnetically induced transparency (EIT) phenomenon is caused by a number of important applications. We study the possibility for miniaturization of alkali cells for application in the EIT experiments without compromising the EIT resonance parameters [1].

We present results on an EIT ladder system of the ⁸⁵Rb, ⁸⁷Rb, 5S-5P-nD(mS) transitions with $n = 5$ as well as involving highly excited Rydberg states with $n = 26$ and $m = 48$. For this purpose a recently developed multi-region (MR) high temperature cell containing Rb vapor has been used. The construction of MR cell allows us to study EIT effect in atomic vapor of thickness $L = 4$ mm, 2 mm, and 0.5 - 6 μm . The design of MR cells with length L in the range of 30 nm - 10 mm will be presented. It is demonstrated that in 4 mm and 2 mm-long cells it is possible to realize a robust formation of EIT resonance in counter-propagating geometry [2] with a high contrast (50 - 60%) and with a sub-natural linewidth. The fine structure of 26 $D_{5/3, 3/2}$ has been measured. For 5S-5P-48S system a pronounced Stark broadening of the EIT resonance is observed. The short thickness of the cell allows one to provide a tight focusing to achieve high intensity. Under this condition efficient 2-photon absorption has been detected, even when the thickness L is reduced to 6 μm .

We present experimental and theoretical results on an EIT ladder system of the ⁸⁵Rb, ⁸⁷Rb, 5S-5P-5D for a pure Rb vapour column with L of the order of light wavelength ($\lambda = 780$ nm) and varying in the range of (0.75 to 6) λ . It is shown that in the case when coupling laser frequency is resonant with atomic transition the linewidth of the EIT resonance (6 to 8 MHz) is weakly dependent on the thickness as $\sim L^{-0.25}$. The explanation is that the contribution of atoms with small velocity projection in the laser radiation direction (i.e. atoms flying nearly parallel to the cell windows) is enhanced thanks to their longer interaction time with laser field [1]. Due to this atomic velocity-selectivity, the observed linewidth of the EIT resonance is more than by an order narrower than that expected from the inverse of the window-to-window flight time of the atoms. Meanwhile, direct influence of atom-wall collisions on the EIT resonance is well seen when there is a large detuning of the coupling laser with respect to resonance transition (EIT linewidth for this case achieves ~ 100 MHz). The slight dependence of the EIT linewidth for the case when coupling frequency is resonant with atomic transition allows us to detect EIT resonance (< 20 MHz) at the smallest thickness reported up to now $L = 0.75 \lambda = 585$ nm.

References

- [1] Y. Pashayan-Leroy, C. Leroy, A. Sargsyan, et. al., JOSA B, 24, 1829 (2007).
- [2] A. K. Mohapatra, T. R. Jackson, C. S. Adams, Phys. Rev. Lett. 98, 113003 (2007)

Saturation effects of Faraday rotation signals in Cs vapor nanocells: thickness-dependent effects

A. Sargsyan¹, D. Sarkisyan¹, A. Papoyan¹, Y. Pashayan-Leroy^{1,2}, C. Leroy²,
P. Moroshkin³ and A. Weis³

¹*Institute for Physical Research, NAS of Armenia, Ashtarak-2, 378410, Armenia*

²*Laboratoire de Physique de l'Université de Bourgogne, CNRS-UMR 5027, Dijon, France*

³*Département de Physique, Université de Fribourg, 1700 Fribourg, Switzerland*

Magneto-optical effects, in particular the nonlinear Faraday rotation (NFR), have proven to be powerful tools in the laser spectroscopy of atomic gases. Optical magnetometers based on ultra-narrow spectral features accompanied by a strong polarization rotation are under active development. Ordinary cm-sized alkali metal cells are basic elements of such types of optical magnetometers [1]. Recently, differences of the resonant absorption and fluorescence spectra on the D_2 line ($\lambda = 852$ nm) of Cs vapor were demonstrated [2] when exciting the transition either in a cell of $L = \lambda/2$ thicknesses and a $L = \lambda$ cell.

Here we present experimental and theoretical results of NFR signals for thicknesses $L = \lambda/2$ and $L = \lambda$ performed on the D_1 line $\lambda = 894$ nm of Cs vapor. The nanocell was placed inside Helmholtz coils and a crossed polarizer geometry was used. The beam of a frequency-tunable DFB diode laser ($\lambda = 894$ nm, spectral width $\gamma_L \sim 6$ MHz) irradiated the nanocell under an angle close to the normal in resonance with the D_1 line of Cs. Signals recorded with different laser intensities were compared. The magnetic field B was applied along the laser propagation direction and could be varied in the range of 1-20 G. Spectra of the NFR signal and absorption spectra for $L = \lambda/2$ and $L = \lambda$ were compared.

There are two main features: i) significant differences were observed between the NFR signal at $L = \lambda/2$ (~ 450 nm) and at $L = \lambda$. In the $L = \lambda/2$ cell, the Dicke-narrowed absorption profile causes a stronger nonlinear Faraday rotation than in the $L = \lambda$ (while in an ordinary cm-sized cell a length increase leads to increase of the NFR signal), accompanied by a significant spectral narrowing down to 20 MHz. ii) at relatively high intensities (> 10 mW/cm²) the spectrum of the NFR signal for $L = \lambda/2$ simply broadens, while for $L = \lambda$, the NFR signal vanishes completely due to strong optical-pumping. The different behaviors for $L = \lambda/2$ and $L = \lambda$ is more pronounced in the NFR signals than in the absorption spectra. A theoretical model taking optical pumping effects into account gives a good agreement with the experiment.

A simple magnetometer based on the NFR signal in a nanocell with $L = \lambda/2$ could be developed. A sensitivity of several tens of mG is expected together with a spatial resolution in the nanometer range was achieved. This may prove useful for measurements of strongly inhomogeneous magnetic fields.

References

- [1] D. Budker, W. Gawlik, D. Kimball, S. Rochester, V. Yaschuk, A. Wies, Rev. Mod. Phys. **74**, 1153 (2002) and reference therein.
- [2] C. Andreeva, S. Cartaleva, L. Petrov, S. M. Saltiel, D. Sarkisyan, T. Varzhapetyan, D. Bloch, M. Ducloy, Phys. Rev. A **76**, 013837 (2007) and reference therein.

Magneto-optical resonances in atomic rubidium at D1 excitation in ordinary and extremely thin cells

L. Kalvans¹, M. Auzinsh¹, R. Ferber¹, F. Gahbauer¹,
A. Jarmola¹, A. Papoyan², D. Sarkisyan²

¹*Laser Centre of the University of Latvia, 19 Rainis Boulevard, LV-1586, Riga, Latvia*

²*Institute for Physical Research, NAS of Armenia, Astarak-0203, Armenia*

We present the results of a detailed experimental and theoretical investigation of nonlinear magneto-optical resonances at D1 excitation of atomic rubidium in both ordinary and extremely thin vapor cells. These sub-natural linewidth resonances have been known for some time [1,2] and continue to be the subject of intriguing investigations and a valuable tool for fine-tuning theoretical models [3]. In this work, magneto-optical resonances are observed in both cells and can be bright or dark, depending on which hyperfine transition is excited. However, in a normal cell individual hyperfine transitions cannot be resolved because of Doppler broadening. The use of extremely thin cells (ETCs) represents a rather new experimental technique and allows the experimenter to realize direct sub-Doppler spectroscopy [4]. The thickness of the cell L used in this study varies in the range from 150 nm to 1600 nm. By comparing results obtained from both cells, one obtains useful information about how Doppler broadening influences the shape and contrast of the resonances.

In this study experimental results from an ordinary Rb vapor cell and an ETC filled with Rb are compared to theoretical calculations based on the optical Bloch equations, which have proven to be well suited to describe the signals obtained in ordinary vapor cells [3]. The vapor cells were placed inside a three-axis Helmholtz coil system and excited with a diode laser manufactured by Toptica, GmbH. The polarization of the exciting laser radiation was perpendicular to the magnetic field, which was scanned, and the fluorescence was observed in the direction along the magnetic field. In order to test how well our model can describe ETC behavior, we study resonances at different laser powers, beam cross-sections, and wall separations L , and compare the experimental measurements with the results of calculations based on the model. By requiring the model to take into account so many different parameters, it will be possible to either validate the model as is for the case of the ETC or to identify new effects that should be taken into account when modelling the signals obtained with ETCs.

We acknowledge support from the Latvian National Research Programme in Material Sciences Grant No. 1-23/50, the University of Latvia grant Y2-ZP04-100, the ERAF grant VPD1/ERAF/CFLA/05/APK/2.5.1./000035/018, and the INTAS projects 06-1000017-9001 and 06-1000024-9075. A. J., F. G., and L. K. acknowledge support from the ESF project.

References

- [1] R. W. Schmieder *et al.*, Phys. Rev. A **2**, 1216 (1970)
- [2] G. Alzetta, A. Gozzini, L. Moi, and G. Orriols, Il Nuovo Cimento B **36**, 5 (1976)
- [3] M. Auzinsh *et al.*, arXiv:0803.0201v1 [physics.atom-ph]
- [4] D. Sarkisyan, D. Bloch, A. Papoyan, and M. Ducloy, Opt. commun. **200**, 201 (2001)

Frequency-modulation spectroscopy of coherent population trapping resonances

A.Yu. Samokotin¹, A.V. Akimov¹, N.N. Kolachevsky¹, Yu.V. Vladimirova²,
V.N. Zadkov², A.V. Sokolov¹, V.N. Sorokin¹

¹*P. N. Lebedev Physical Institute,*

Leninsky pr., 53, 119991 Moscow, Russia

²*International Laser Center and Faculty of Physics,*

M. V. Lomonosov Moscow State University,

199899 Moscow, Russia

E-mail: samokotin@gmail.com

Resonance of coherent population trapping (CPT) is one of nonlinear effects in three-level atomic systems in so-called Λ -configuration. The resonance appears when a bichromatic optical field with certain frequency and phase correlations between its components is applied to the system. The ultimate spectral width of the CPT resonance is determined by the coherency time between the lower levels of the Λ -system and can amount to several tens of hertzs. A high Q-factor of CPT resonances enables to use them as frequency references and in magnetometry.

One of the simplest experimental methods to create two phase-correlated light fields is a frequency modulation (FM) of a monochromatic light field. In the case of diode laser, the FM of light is achieved via modulation of the injection current.

In this work we experimentally investigated CPT resonances on Zeeman sublevels of ⁸⁷Rb D₁-line excited by FM-modulated laser field and considered possible applications to magnetometry. The laser was tuned to $F = 2 \rightarrow F = 1$ transition, such that a chain of three Λ -systems can be excited by the sidebands of the field. The FM field contains a number of harmonics which relative amplitudes depend on modulation parameters, and thus a number of CPT resonances of different amplitudes are excited at corresponding frequencies. The experimental results are confirmed by the recent theoretical consideration of FM spectroscopy of CPT resonances [1,2].

Since the frequency of the CPT resonance depends on magnetic field, the FM spectroscopy allows to measure magnetic field applied to the Rb vapors. We recorded a number of CPT resonances in two Rb cells (with and without buffer gas) at different values of an external magnetic field. Our experimental setup allows to measure magnetic fields in the range 10-100 G with 0.05% accuracy. Non-linear Zeeman effect, playing a significant role in such fields, is studied in details.

References

- [1] J. Vladimirova et al., Laser Physics Lett., 3(9), 427-436 (2006).
- [2] Yu.V. Vladimirova et al., J. of Theor. and Exp. Phys., **96**, 629 (2003).

Pump-probe spectroscopy: a survey of the spectra for four polarization combinations in degenerate two-level atoms

K. Dahl, L. Spani Molella, R.-H. Rinkleff, and K. Danzmann

*Albert-Einstein-Institut, Max-Planck-Institut für Gravitationsphysik and
Institut für Gravitationsphysik, Leibniz Universität Hannover
Callinstrasse 38, D-30167 Hannover, Germany
E-mail: rolf-hermann.rinkleff@aei.mpg.de*

The optical properties of a cesium atomic beam driven on a resonant hyperfine transition in the D₂ line were experimentally investigated as a function of the probe-laser frequency. In the present experiment the coupling laser drove the hyperfine transition $6s\ ^2S_{1/2}, F=4$ — $6p\ ^2P_{3/2}, F=5$ and was actively locked to it by means of frequency modulation spectroscopy. The probe-laser frequency was scanned around the same transition [1]. The coupling and probe absorption spectra were measured also in a range of probe-laser intensities large enough to affect the pump-laser absorption. We present an experimental survey of the coupling and probe absorption spectra for four polarization combinations ($\pi\sigma^+, \pi\sigma, \sigma^-\pi, \sigma^-\sigma^+$).

For all polarization combinations the probe-laser absorption profiles showed electromagnetically induced absorption (EIA), a spectrum characterized by a peak on the ordinary absorption profile. The observed coupling-laser absorption profiles could be described by “absorption within transparency”, i.e. the absorption in the region around the two-photon resonance was smaller than the absorption corresponding to the one-photon transition induced by the coupling laser, and at the two-photon resonance an extra absorption peak on this curve was measured.

For investigations with laser beams of counterrotating circular polarizations ($\sigma^-\sigma^+$) the coupling-laser absorption profiles showed at various laser powers a surprising behavior as function of the laser powers. We detected a transition of the two-photon resonance peak from absorption to more transparency when the probe-laser exceeded the constantly held coupling-laser power [2]. Furthermore, a switch was observed for a constant probe-laser power when varying the coupling-laser power. In all these cases the probe-laser absorption profiles showed EIA signals. These findings are the experimental confirmation of published theoretical predictions [3]. However, for phase measurements, no corresponding switch from positive to negative parametric dispersion or from negative to positive dispersion was observed.

The work was supported by the grant SFB407 of the Deutsche Forschungsgemeinschaft.

References

- [1] L. Spani Molella, R.-H. Rinkleff, K. Danzmann, *Appl. Phys. B* **90**, 273 (2008)
- [2] K. Dahl, L. Spani Molella, R.-H. Rinkleff, K. Danzmann, *Optics Letters* (in press)(2008)
- [3] C. Goren, A. D. Wilson-Gordon, M. Rosenbluh, H. Friedman, *Phys. Rev. A* **69**, 053818 (2004)

Dark resonance narrowing in uncoated rubidium vacuum vapor cell

Z. Grujić, M. Mijailović, D. Arsenović, M. Radonjić and B. M. Jelenković

*Institute of Physics
Pregrevica 118, Belgrade-Zemun, Serbia
E-mail: zoran.grujic@phy.bg.ac.yu*

The CPT (Coherent Population Trapping) phenomena has been intensely investigated due to its narrow resonance suitable for precision measurements, magnetometry and atomic clocks etc. Different approaches were applied in order to make these resonances narrower in alkali vapor cells: coated cells in order to preserve atomic coherence after collision with the cell wall, use of buffer gas cells to increase atom time of flight through laser beam, and nanocells.

In our experiment we use spatially separated pump and probe laser beams in order to induce Ramsey type CPT narrowing [1]. The probe laser beam (diameter of 1.5 mm) is placed in the center of pump beam which has a ring like profile. Outside diameter of the pump laser beam is very close to the Rb cell diameter of 25 mm, while its inner is larger than the probe laser diameter. Both pump and probe laser beams are obtained from a single ECDL (External Cavity Diode Laser), locked to the $F_g = 2 \rightarrow F_e = 1$ transition at D1 line of ^{87}Rb . Thus, some Rb atoms are first pumped into the dark state by the pump laser beam, then travel through the "dark region" between the pump and the probe beam before they reach the pump laser beam. The dark state and induced Zeeman coherences created by pump are experimentally detected in the probe beam absorption. Related work has been published by A. S. Zibrov and A. B. Matsko [2]. Obtained narrow resonances widths, shapes depend of "dark region" length and pump and the probe laser intensities.

Our theoretical model relies on solving time-dependent optical Bloch equations and takes into account different atomic velocities and angles of atom propagation in respect to the laser beams. It is shown that experiment and theory are in a good agreement for different probe and pump beam polarizations and intensities.

References

- [1] Z.D. Grujić, M.M. Mijailović, B.M. Panić, M. Minić, A.G. Kovačević, M. Obradović, B.M. Jelenković and S. Cartaleva, Acta Physica Polonica A, No 5, **112**, 799 (2007).
- [2] A. S. Zibrov and A. B. Matsko, Physical Review A, **112**, 013814

Quantum search with trapped ions

S. Ivanov, P. Ivanov and N. Vitanov

Department of Physics, Sofia University, James Bourchier 5 blvd, 1164 Sofia, Bulgaria

We propose an ion trap implementation of Grover's quantum search algorithm for an unstructured database of arbitrary length N . The experimental implementation is appealingly simple because the linear ion trap allows for a straightforward construction, in a single interaction step and without a multitude of Hadamard transforms, of the reflection operator, which is the engine of the Grover algorithm. Consequently, a dramatic reduction in the number of the required *physical* steps takes place, to just $\mathcal{O}(\sqrt{N})$, the same as the number of the *mathematical* steps. The proposed setup allows for demonstration of both the original (probabilistic) Grover search and its deterministic variation, and is remarkably robust to imperfections in the register initialization.

The observability of atoms

Gebhard von Oppen

Institut für Optik und Atomare Physik, Technische Universität Berlin

Atomic particles differ fundamentally from macroscopic objects. In every measurement with moderate spatial resolution, macroscopic objects can be observed continuously. Free atoms, however, are observed discontinuously. Their observation is based on discrete, spontaneously occurring elementary events, which can be counted. During free flight, atoms are principally unobservable. As a consequence, identical atomic particles are indistinguishable, whereas macroscopic twin-bodies can be distinguished [1, 2].

In this contribution I'll show you that the difference in observability provides the key for an experimentally oriented understanding of the "spooky" phenomena of quantum dynamics and of the appearance of chance in physics. In particular, I'll consider:

1. The presence of statistical and thermal noise in all measurements: Noise is neglected in classical dynamics (mechanics and electrodynamics), but justifies the concept of chance in statistical thermodynamics. Accordingly, classical dynamics describes only reversible processes, whereas statistical thermodynamics also applies to irreversible processes.
2. The transition from quantum to classical physics: Quantum dynamics is not a generalization of classical dynamics, but describes an idealization of nature opposite to the ideal of classical dynamics. The two theories apply to opposite extremes on a scale of observability [2].
3. Space-time reality: "...we have to abandon the description of atomic events as happenings in space and time" (Einstein, Infeld: The evolution of physics). A description in space and time is only justified for objects, which can be observed continuously, but not for atomic particles. Therefore, atoms must not be idealized as mass-points, and a thermodynamic ensemble of free atoms is fundamentally different from the mechanical model of the ideal gas [3].
4. The approaches of physics to nature: The objects of physics must be observable. Otherwise they cannot be investigated experimentally. For being observable, the objects must be coupled spontaneously to the environment. This spontaneous coupling prohibits an exact reproducibility of experiments. As a consequence of this insufficiency on the experimental side, theory cannot image nature exactly, but describes idealizations of nature. Presently, physics is based on three idealizations: Classical dynamics, statistical physics and quantum dynamics.
5. From decomposition to isolation: The objects of classical dynamics can be decomposed. But by decomposing, one produces components, which are not any more observable continuously. One ultimately obtains the isolated objects of quantum dynamics[1].

References:

- [1] G. v. Oppen, Physics Uspekhi **39**, 617 (1996)
- [2] G. von Oppen, Eur. Phys. J. Special Topics **144**, 3 (2007)
- [3] Bergmann, Schaefer, Lehrbuch der Experimentalphysik, Band 1 (12. Auflage, 2009), in print

Characterization of a High Precision Cold Atom Gyroscope

T. Leveque, A. Gauguet, W. Chaibi and A. Landragin

LNE-SYRTE, CNRS UMR 3630, Observatoire de Paris

61 avenue de l'Observatoire, 75014 Paris, France

E-mail : thomas.leveque@obspm.fr

We investigate the limits of our inertial sensor using a cold atom interferometer. In contrast with previous atomic setups, emphasis was placed on the long term stability and compactness of the device thanks to the use of laser cooled atoms. Moreover it has been designed to give access to all six axes of inertia (three accelerations and three rotations) [1]. The expected improvement in stability will enable to consider applications in inertial navigation, geophysics and tests of general relativity.

Caesium atoms are loaded from a vapour into two independent magneto-optical traps for 140 ms. Two caesium clouds are then launched into two opposite parabolic trajectories using moving molasses at 2.4 m.s^{-1} , with an angle of 8° with respect to the vertical direction. At the apex of their trajectory, the atoms interact successively with three Raman laser pulses, which act on the matter-wave as beam splitters or mirrors, and generate an interferometer of 80 ms total interaction time. The use of two atomic sources allows discrimination between the acceleration and rotation.

The sensitivity to acceleration is $5,5 \times 10^{-7} \text{ m.s}^{-2}$ at one second, limited by residual vibration on our isolation platform. Concerning the rotation, the sensitivity is $2,3 \times 10^{-7} \text{ rad.s}^{-1}$ at one second, limited by the quantum projection noise in the detection. After 1000 seconds of integration time, we achieve a sensitivity of $1 \times 10^{-8} \text{ rad.s}^{-1}$. Moreover, we have performed studies of all possible sources of drift on the rotation signal. Among others, we measured the effect of the two photon light shift during the Raman laser pulses. We also identified the main limit of the stability, which is linked to fluctuations of the atomic trajectories inducing Raman laser wave-front changes.

We characterize the accuracy of our gyroscope in term of bias and scaling factor. In this purpose, we record rotation phase shift as a function of the interrogation time and rotation rate. The rotation shift behaves as the square of the interrogation time and linearly with the projection of the Earth's rotation rate, which is modulated by turning the interferometer in the horizontal plane. The linearity of our sensor was demonstrated with an agreement better than 0.01% and the bias was determined with an accuracy of $5 \times 10^{-8} \text{ rad.s}^{-1}$. Currently, we are developing a new method to enable measurements in noisy environments which will be crucial for applications in the field of inertial navigation.

References

- [1] B. Canuel, F. Leduc, D. Holleville, A. Gauguet, J. Fils, A. Viridis, A. Clairon, N. Dimarcq, Ch.J. Bordé, and A. Landragin, "Six-Axis Inertial Sensor Using Cold-Atom Interferometry", Phys. Rev. Lett. 97 010402 , 2006.

Electron capture of methane molecule by proton impact

F. Shojaei Baghini, M.A. Bolorizadeh, R. Fathi, and E. Ghanbari Adivi¹

Physics Department, Shahid Bahonar University of Kerman, Kerman, Iran and

¹*Physics Department, Isfahan University, Isfahan, Iran*

mabolori@mail.uk.ac.ir

Potential scattering is implemented to the electron capture of fast projectiles colliding with molecular targets. The electron capture channel is a two step reaction especially at higher projectile energies. The two step reactions are described quantum mechanically by second Born term in the Born series. This has been shown in a series of articles for the ion-atom collisions in the literature [1,2]. We have adopted an active electron model to study the electron capture by protons colliding with a molecule. A central potential composed of a long range potential (Coulomb) and two short range (Yukawa) ones were deduced to simulate methane.

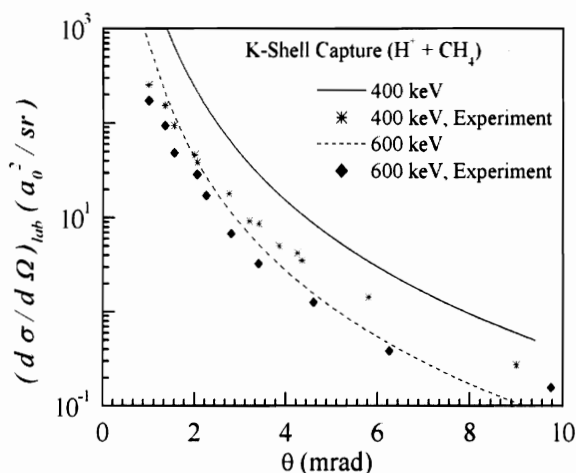


Figure 1. Differential cross sections for the electron capture from K-shell of carbon in methane by proton impact. The results are compared with the experimental data of [4] at 400 and 600 keV impact energy.

Applying this model, the first and the second order terms for the amplitudes of the electron capture reaction under the three body FWL formalism was calculated. This method was applied to electron capture from atomic target where successful results were obtained [3]. The results of the current work are plotted in Figure 1 and compared with the available experimental data in the literature [4]. The method is applicable in the high energy region. At 600 and 400 keV, the calculated results are overestimated at small angle as compared with the experimental results. Nonetheless, the errors of the experiment are high as reported.

References

- [1] P. S. Vinitisky, Yu. V. Popov, and O. Chuluunbaatar, *Phys. Rev. A* **71**, (2005) 012706
- [2] J.H. McGuire, P.R. Simony, O.L. Weaver, and J. Macek, *Phys. Rev. A* **26** (1982) 1106
- [3] E. Ghanbari Adivi, et al, *Phys. Rev. A* **75** (2007) 022704.
- [4] B G Lindsay, W S Yu and R F Stebbings *J. Phys. B: At. Mol. Opt. Phys.* **38** (2005) 1977

Excitation of the Xe I $6s$ metastables to the $6p$ and $7p$ configurations

Ch. Berenguer¹, K. Katsonis¹, R. Srivastava², L. Sharma², R.E.H. Clark³, A.D. Stauffer⁴

¹ *GAPHYOR, Lab. de Physique des Gaz et des Plasmas, UMR 8578, Univ. Paris-sud
91405 Orsay, FRANCE*

² *Dept. of Physics, Indian Institute of Technology, Roorkee 247667 INDIA*

³ *Nuclear Data Section, IAEA, Vienna, AUSTRIA*

⁴ *Dept. of Physics and Astronomy, York University, Toronto, ON, M3J1P3 CANADA
E-mail: chloe.berenguer@u-psud.fr, GAPHYOR.lpgp@u-psud.fr*

Because of the importance of Xe plasmas in contemporary industrial applications, especially for ionic propulsion and Tokamak plasmas in the divertor region, we have carried out Collisional-Radiative (C-R) modeling of Xe. Most of the experimental energy levels needed for the C-R model are available in an extended review by NIST [1]. Coulomb approximation calculations [2] based on the experimental energy levels lead to a basic set of transition probabilities in LS/jK coupling. *Ab initio* quantum methods (mainly CATS [3] and GRASP92) complete the data sets needed in the C-R model.

We address here one specific case of electron impact cross section evaluation. This process, together with spontaneous emission, plays an important role in the spectral emission mechanism, defining the bulk of the line intensities and of the energy transfer. For low temperature plasma regions the Xe I metastable levels $1s^3/1s^5$ are significantly populated and, notably, are more easily excited than the ground level, while excitation of the latter is hindered by the considerable energetic gap separating the Xe I ground level from the excited ones. Therefore, evaluation of the excitation rates of the metastables is very important.

Measurement and calculation of the Xe I $6s - 6/7p$ electron impact excitation cross sections have many gaps, hindering the evaluation of the corresponding rate coefficients and hence the development of satisfactory C-R models which are needed for diagnostics and modeling of low temperature plasmas. Recent theoretical work on $6s - 6/7p$ electron collision excitation has been carried out using relativistic quantum theory [4]. Cross sections obtained by these calculations are compared here to DW calculation results obtained with ACE [5], CTMC and empirical formulas and two experiments [6,7]. From these data an evaluation of the electron impact excitation cross sections from the Xe I $6s$ metastable levels to the levels of the $6p$ and $7p$ configurations has been recently completed [8].

References

- [1] E.B. Saloman, *J. Phys. Chem. Ref. Data* **33** 765 (2004).
- [2] K. Katsonis, Jun Yan, R.E.H. Clark, Bin Duan, Hong Zhang, Ch. Berenguer, XXV ICPEAC Conference, 25-31 July 2007, Freiburg (Germany).
- [3] <http://aphysics2.lanl.gov/tempweb/>
- [4] R. Srivastava, A.D. Stauffer, L. Sharma, *Phys. Rev. A* **74** 012715 (2006).
- [5] R.E.H. Clark, J. Abdallah Jr., G. Czanak, J.B. Mann, R.D. Cowan, Report LA-11436-M, Vol. II (1988).
- [6] A.A. Mityureva, V.V. Smirnov, *Opt. Spektrosk.* **74** 6 (1993).
- [7] R.O. Jung, J.B. Boffard, L.W. Anderson, C.C. Lin, *Phys. Rev. A* **72** 022723 (2005).
- [8] K. Katsonis, Ch. Berenguer, Report LPGP-GA-21 (2008).

Parametrization of NeI spectrum for $2p^5 5g$, $6g$, $7g$ configurations using semiempirical method

Anisimova G.P.¹, Efremova E.A.¹, Tsygankova G.A.¹

¹*St.-Petersburg State University*

Petergof, Uljanovskaja st., 1, NIIF-SPbSU, St.-Petersburg, 198504, Russia.

E-mail: efremovakat@inbox.ru

The paper presents results of numerical study of the fine structure parameters (the radial integrals in the energy operator matrix) for $2p^5 5g$, $2p^5 6g$ and $2p^5 7g$ configurations of a neutral Neon atom. The angle coefficients for the radial integrals were obtained taking into account the following interactions in the Breit's Hamiltonian: electrostatic, spin-orbit (own and foreign), spin-spin and orbit-orbit [1].

The energy operator matrix for "hole" configurations can be calculated either using fractional parentage coefficients or via free momentums representation. In the latter case it is assumed that the atom's state is described exclusively by the individual quantum numbers of particular electrons. The energy operator matrix obtained via free momentum representation was transformed to $LSJM$ - and j_1KJM -representations. For vector types of coupling the energy operator matrix has 24 matrix elements each of which is a linear combination of 18 fine structure parameters.

The calculations are based on the empirical data namely the energies of the fine structure experimentally obtained with the high precision [2, 3].

The classification of the fine structure levels for $2p^5 5g$, $2p^5 6g$ and $2p^5 7g$ of NeI was given in jK -coupling representation. The calculation of the parameters is also accomplished using the energy operator matrix given in jK -coupling representation. The numerical calculation is based on the Newton's method applied to the set of non-linear equations. The unknowns for the equations were the parameters of the fine structure as well as the expansion coefficients of wave functions in jK -coupling basis. The initial approximation for Newton's method was derived using least-squares method.

As a result of numerical study a set of the fine structure parameters was obtained. Substitution of these parameters into the energy operator matrix and follow-up diagonalization for all the coupling types yields the energies, which fully agree with the energies obtained experimentally. Expansion coefficients for LS - and JK -bases, gyromagnetic ratio and level compositions in LS -basis were also obtained. It can be concluded that the highly-excited $2p^5 5g$, $2p^5 6g$ and $2p^5 7g$ configurations of NeI are close to jK -coupling model.

References

- [1] Anisimova G.P., Efremova E.A., Tsygankova G.A., Vestnik of St.-Petersburg State University. **Series 4. Part 3.**, 49 (2007)
- [2] Chang E.S., Schoenfeed W.G., Biemont E., Quinet P., Palmeri P., Phys. Scr. **V. 49.**, 26 (1994)
- [3] Saloman E.B., Sansonetti C.J. Wavelengths, J. Phys. Chem. Ref. data. **V. 33. N 4**, 1113 (2004).

Ab initio calculations of aluminium-like calcium

R. Karpuškienė, P. Bogdanovich and O. Rancova

Institute of Theoretical Physics and Astronomy of Vilnius University

A. Goštauto st. 12, 01108 Vilnius, Lithuania

E-mail: olga@itpa.lt

This work presents theoretical investigation of Ca VIII ion of aluminium isoelectronic sequence. The *ab initio* study of Ca VIII was performed within the configuration interaction approximation in the basis of transformed radial orbitals with a variable parameter [1]. Relativistic effects were accounted for within the Breit-Pauli approximation.

The ground configuration $3s^23p$ and excited configurations $3s3p^2$, $3s^23d$, $3p^3$, $3s3p3d$, $3s^24s$, $3s^24p$, $3s^24d$, $3s^24f$, $3s3p4s$ and $3s3p4p$ are studied. The first calculation of energy spectra was performed in the basis of admixed configurations made by virtual excitations from 3l- and 4l-shells. The second calculation was performed in the extended basis of admixed configurations made by the virtual excitations not only from 3l- and 4l- shells, but also from the closed shells 2s- and 2p-. This way enables us to take into account core polarization effects.

The obtained energy spectra of ground configuration $3s^23p$ and excited configurations $3s3p^2$, $3s^23d$, $3p^3$ and $3s3p3d$ were compared with available data [2-3]. We supplement our results with the energy spectra of highly excited configurations $3s^24s$, $3s^24p$, $3s^24d$, $3s^24f$, $3s3p4s$ and $3s3p4p$ as well. The obtained energy levels of these configurations (except $3s^24p$ and $3s3p4p$) are compared with data from [4].

The comparison of the obtained results and the data presented by other authors show that the core polarization is important and has a considerable influence on the accuracy of theoretical energy spectra.

The multiconfiguration wave functions determined as a result of the energy matrix diagonalization were used to calculate the wavelengths and the characteristics for the electric dipole transitions from the excited configurations. The radiative lifetimes of the excited levels were also calculated and compared with the available data.

These calculations have been performed using the resources of the European Commission project RI026715 BalticGrid and LitGrid project.

References

- [1] P. Bogdanovich, R. Karpuškienė, Lith. J. Phys. **39**, 193 (1999)
- [2] E. Landi, P.J. Storey, C.J. Zeippen, Astrophys. J. **607**, 640 (2004)
- [3] U.I. Safronova et al, Atomic Data and Nuclear Data Tables **84**, 1 (2003)
- [4] J. Sugar, C. Corliss, J. Phys. Chem. Ref. Data **14**, Suppl. 2, 1 (1985)

Isotope shifts of forbidden lines of Lead

T.J. Wąsowicz, S. Werbowy, R. Drozdowski, J. Kwela

*Institute of Experimental Physics, University of Gdansk, ul. Wita Stwosza 57,
80-952 Gdansk, Poland*

The $6s^26p^2$ ground configuration of Pb I gives rise to five levels 1S_0 , $^3P_{2,1,0}$ and 1D_2 . In the $6s^26p$ ground configuration of Pb II only two levels $^2P_{1/2}$ and $^2P_{3/2}$ appear. Since electric-dipole (E1) transitions between the states of the same parity are forbidden, all the levels of these configurations are metastable. In the second-order radiation theory weak magnetic-dipole (M1), electric-quadrupole (E2) or mixed type (M1+E2) transitions between these levels are permitted.

In the experiment the isotope shifts (IS) of forbidden lines 461.9 nm ($6p^2\ ^1S_0 \rightarrow 6p^2\ ^3P_1$; M1), 531.5 nm ($6p^2\ ^1S_0 \rightarrow 6p^2\ ^3P_2$; E2), 733.2 nm ($6p^2\ ^1D_2 \rightarrow 6p^2\ ^3P_1$; M1+E2) of Pb I and 710.2 nm ($6p\ ^2P_{3/2} \rightarrow 6p\ ^2P_{1/2}$; M1+E2) of Pb II between four stable isotopes (204, 206, 207, 208) were measured. The observation of isotopic structure of multipole lines is very difficult because of relatively small shifts (see Table 1) and the components of the isotope structure are partly or completely unresolved. For such a case the computer simulation technique becomes very useful. Such a computer technique has been recently used by us in the analysis of the IS spectra of electric-dipole (E1) lines of Pb I [1] and Pb II [2]. By variation of free parameters describing the line shape and positions of individual components the calculated profiles were fitted into the recorded spectra. In the case of the M1+E2 transitions the E2 admixtures (see e.g. [3]) were also taken into account as a fixed parameter. Moreover, using the King plots we were able to separate the two contributions to the total isotope shift, namely the mass and the field shifts. These results may prove to be useful for future studies of PNC in Pb.

Table 1: Measured isotope shifts relative to the 208 isotope of lead (in mK).

Line (nm)	Transition	$\delta\nu_i^{207CG,A}$	$\delta\nu_i^{206,A}$	$\delta\nu_i^{204,A}$
461.9	$6p^2\ ^1S_0 \rightarrow 6p^2\ ^3P_1$	4.9 (1.1)	7.8 (1.3)	14.6 (3.4)
531.5	$6p^2\ ^1S_0 \rightarrow 6p^2\ ^3P_2$	8.1 (1.5)	13.0 (1.2)	24.2 (5.4)
733.2	$6p^2\ ^1D_2 \rightarrow 6p^2\ ^3P_1$	5.6 (0.6)	8.8 (1.0)	16.3 (2.4)
710.2	$6p\ ^2P_{3/2} \rightarrow 6p\ ^2P_{1/2}$	10.8 (1.9)	17.3 (2.3)	32.7 (5.6)

Acknowledgment

This work was supported by the University of Gdansk, grant BW 5200-5-0053-8.

References

- [1] T.J. Wąsowicz, J. Kwela, Phys. Scr. **77**, 025301 (2008)
- [2] T.J. Wąsowicz, R. Drozdowski, J. Kwela, Eur. Phys. J. D **36**, 249 (2005)
- [3] T.J. Wąsowicz, Phys. Scr. **76**, 294 (2007)

Solid ^4He stabilized by charged impurities below the solidification pressure of pure helium

P. Moroshkin, V. Lebedev, A. Weis

University of Fribourg, Department of Physics, Fribourg, Switzerland

The coexistence of a ^4He crystal with superfluid ^4He is a model system for investigating fundamental aspects of the growth and melting of crystals. Here we present a study of a dramatic effect [1] that occurs during the melting of solid ^4He doped with nanoscopic impurities — alkali atoms, clusters, ions, and electrons: the doped part of the crystal remains solid under conditions at which pure helium is liquid. We refer to this structure as an iceberg. If the structure disintegrates in a static electric field of several kV/cm fragments of the iceberg containing unequal amounts of electrons and positive ions move towards either the positive or the negative electrode. These events are accompanied by electric current pulses that have allowed us to determine the number density of charged particles in the sample to be of order of $10^{14} - 10^{15} \text{ cm}^{-3}$. We consider the iceberg as being an aggregation of positively charged particles (snowballs) and electron bubbles.

Using interferometry we have found [1] that the density of the solid structure (iceberg) lies between the densities of pure liquid and pure solid helium. On the other hand, a comparison of laser-induced fluorescence spectra of neutral Cs atoms trapped in the iceberg with those in bulk solid ^4He indicates that the iceberg has the same density and crystalline structure (bcc, hcp) as the bulk solid ^4He . We therefore suggest that the iceberg is in fact a porous structure filled with liquid helium.

- [1] P. Moroshkin, A. Hofer, S. Ulzega, A. Weis, *Nature Physics* **3**, 786 (2007).

Spectroscopy of Ba atoms isolated in solid He matrix

P. Moroshkin, V. Lebedev, A. Weis

University of Fribourg, Department of Physics, Fribourg, Switzerland

We present the results of a new spectroscopic study of Ba-doped solid ^4He . Ba atoms are introduced into the solid He matrix by means of laser ablation from a metallic target surrounded by solid He. This allows us to produce a sample with up to 10^{15} Ba atoms per cm^3 . By exciting the sample with a pulsed-laser tuned over 440 – 690 nm we have found a number of fluorescence lines, some of which were not detected in earlier studies [1,2]. Our analysis shows that the Ba atoms are excited at the single-photon $6s^2\ ^1S_0 - 6s6p^1P_1$ transition at 540 nm and at least at 6 different two-photon transitions at 530, 568, 618, 632, 650, and 675 nm. The decay of highly excited states populated by the two-photon transitions proceeds via a cascade of fluorescence transitions including triplet-triplet and intercombination lines, as well as other so far unidentified lines.

We have also performed a systematic study of the absorption and fluorescence spectra of the single-photon $6s^2\ ^1S_0 - 6s6p^1P_1$ transition and their dependence on helium pressure. The spectral line is blueshifted and broadened by the interaction with the matrix. The shift and the broadening increase with the He pressure following the trend already observed in pressurized liquid helium.

- [1] H. Bauer, M. Beau, D. Friedl, C. Marshand, K. Miltner, H. J. Reyher, *Phys. Lett. A* **146**, 134 (1990).
- [2] S. I. Kanorsky, M. Arndt, R. Dziewior, A. Weis, T. W. Hänsch, *Phys. Rev. B* **49**, 3645 (1994).

New Measurement of the $2S$ Hyperfine Splitting in Atomic Hydrogen

A. Matveev^{1,2}, J. Alnis¹, C. Parthey¹, N. Kolachevsky^{1,2}, T.W. Hänsch^{1,3}

¹ *MPI für Quantenoptik, Hans-Kopfermann Str. 1, 85748 Garching, Germany*

² *P.N. Lebedev Physics Institute, Leninsky prosp. 53, 119991 Moscow, Russia*

³ *Ludwig-Maximilians University, Geschwister-Scholl-Platz 1, 80539 Munich, Germany*

Recent advances in laser stabilization, optical frequency measurements and preparation of cold atomic samples open possibility to compare optical frequencies to the 17th decimal place [1] which significantly overcomes the accuracy of the best Cs fountain clocks defining the SI second [2]. Besides this impressive result there exist many other examples when spectroscopy in the optical domain allows for more accurate measurements than classical radio-frequency techniques.

In 2003 we have developed a new optical method for measuring the $2S$ hyperfine splitting in atomic hydrogen by help of two-photon spectroscopy of the $1S-2S$ transition [3]. By measuring the frequency difference between two optical fields at 243 nm driving $1S(F=0) \rightarrow 2S(F=0)$ and $1S(F=1) \rightarrow 2S(F=1)$ two-photon transitions in a nearly-zero magnetic field one can derive the frequency of the $2S$ hyperfine splitting $f_{\text{hfs}}(2S)$. Accurate experimental value $f_{\text{hfs}}(2S)$ allows for accurate tests of quantum electrodynamics theory since the specific difference $D_{21} = 8f_{\text{hfs}}(2S) - f_{\text{hfs}}(1S)$ can be calculated with a high accuracy [4].

In 2008 we have remeasured the $f_{\text{hfs}}(2S)$ frequency using an ultra-stable vibrationally- and temperature-compensated optical cavity as an optical frequency reference [5]. The diode laser at 972 nm locked to this cavity has a spectral line width of less than 0.5 Hz while its frequency drift is on the level of 50 mHz/s. The excellent stability of this new laser oscillator (the Allan deviation reaches 2×10^{-15} in less than 1 s) allows for accurate measurement of the $2S$ hyperfine splitting.

The two photon transitions between different hyperfine sublevels are excited by the second harmonic of a dye laser [3], while its frequency is continuously compared to the frequency of the second harmonic of the stabilized diode laser at 972 nm. The new measurement possesses a significantly improved statistics which, in turn, allows for more detailed study of systematic effects. The preliminary analysis of experimental data gives us a value of $f_{\text{hfs}}(2S) = 177\,556\,840(5)$ Hz which uncertainty is about 5 times less than the most accurate direct radio frequency measurement performed up to date [6].

[1] T. Rosenband *et al.*, *Science* **319**, 1808 (2008).

[2] S. Bize *et al.* *J. Phys. B: At. Mol. Opt. Phys.* **38** S44968, (2005).

[3] N. Kolachevsky, M. Fischer, S.G. Karshenboim, T.W. Hänsch, *Phys. Rev. Lett.* **92**, 033003 (2004).

[4] S.G. Karshenboim and V.G. Ivanov, *Phys. Lett. B* **524**, 259 (2002).

[5] J. Alnis, A. Matveev, N. Kolachevsky, Th. Udem, and T.W. Hänsch, arxiv:0801.4199.

[6] N.E. Rothery and E.A. Hessels, *Phys. Rev. A* **61**, 044501 (2000).

High Resolution Laser Spectroscopy of Scandium

Yu.P. Gangrsky¹, K.P. Marinova¹, S.G. Zemlyanoi¹, M. Avgoulea², J.Billowes²,
P.Campbell², B. Cheal², B. Tordoff², M. Bissel³, D.H. Forest³, M. Gardner³, G.
Tungate³, J. Huikari⁴, H. Penttila⁴ and J. Aysto⁴

¹*FLNR Joint Institute for Nuclear Research, 141980 Dubna, Moscow Region, Russia*

²*Shuster Building, University of Manchester, Manchester M13 9PL, UK*

³*School of Physics and Astronomy, University of Birmingham, B15 2TT, UK*

⁴*Accelerator Laboratory, University of Jyvaskyla SF-405 51, Finland*

Collinear laser spectroscopy experiments on the ScII transition $3d4s^3D_2 \rightarrow 3d4p^3F_3$ at $\lambda \approx 363.1$ nm were performed on the $^{42-46}\text{Sc}$ isotopic chain using an ion guide isotope separator with a cooler-buncher [1]. Hyperfine structure constants, nuclear moments, isotope and isomer shifts of five ground states and two isomers, $^{44,45}\text{Sc}$, were measured.

Among the investigated nuclei the ^{45}Sc isotope deserves closer attention because along with several other odd-A nuclei in the lower $1f_{7/2}$ shell it has a positive parity isomeric state with $I^\pi = 3/2^+$. Such excited states have been explained [2] in the framework of the Nilsson model: the Nilsson $3/2^+$ orbital of the sd shell and the lowest orbital of the $1f_{7/2}$ shell approach each other for increasing deformation, thereby producing a low-lying well deformed core excited state. The value of Q_0 obtained from the laser spectroscopic data in this work is nearly two times larger, than the one of [2]. The unusually large quadrupole moment of the isomeric state of ^{45}Sc is the most striking feature of the present data. This surprising fact remains so far unexplained.

The preliminary analysis performed to date can only provide estimates of the expected upper and lower limits of the radii changes. No drastic contradiction with the overall radii trend in the $f_{7/2}$ shell is found. While the odd-even staggering is reduced compared with Ca and Ti, it is consistent with that observed in K, the only other odd-Z element studied in this region. Although qualitative, the new information on Sc charge radii changes constitutes a valuable contribution to the systematic of nuclear charge radii in the Ca region.

1. Billowes J., *Hyp. Int.* **162** (2005) 63.
2. Styszen J. *et al.*, *Nucl. Phys. A* **262** (1976) 317.

$L\alpha_1$, $L\alpha_2$, $L\beta_1$, $L\beta_2$ and $L\gamma$ satellites in the X-ray emission spectra

S. Poonia

*Division of Natural Resources and Environment,
Central Arid Zone Research Institute, Jodhpur - 342 003, Rajasthan, India*

The X-ray satellites $L\alpha'$, $L\alpha''$, $L\alpha'''$, $L\alpha''''$, $L\alpha_3$, $L\alpha_4$, $L\alpha_5$, $L\alpha^{ix}$, $L\alpha^x$, $L\alpha_s$, $L\beta_1^I$, $L\beta_1^{II}$, $L\beta_1^{III}$, $L\beta_1^{IV}$, $L\beta_2^I$, $L\beta_2^{(b)}$, $L\beta_2^{II}$, $L\beta_2^{(c)}$, $L\gamma_1'$, $L\gamma_2'$, $L\gamma_2''$ and $L\gamma'_{2,3}$ observed in the L-emission spectra in elements with $Z = 26$ to 92 , have been calculated. The energies of various transitions have been calculated by available Hartree-Fock-Slater using the semi-empirical Auger transition energies in the doubly ionized atoms and their relative intensities have been estimated by considering cross-sections of singly ionized $2x^{-1}$ ($x \equiv s, p$) states and then of subsequent Coster-Kronig (CK) and shake off processes. In both these processes initial single hole creation is the prime phenomenon and electron bombardment has been the primary source of energy. The calculated spectra have been compared with the measured satellite energies in L emission spectra. Their intense peaks have been identified as the observed satellite lines. The one to one correspondence between the peaks in calculated spectra and the satellites in measured spectra has been established on the basis of the agreement between the separations in the peak energies and those in the measured satellite energies. Group of transitions under the transition schemes $L_3M_x-M_xM_{4,5}$, $L_2M_x-M_xM_{4,5}$, $L_3M_x-M_xN_{4,5}$ and $L_2M_x-M_xN_{4,5}$ ($x \equiv 1-5$), which give rise to these satellites have been identified. It is observed that the satellite $L\beta_2^{(b)}$ in all these spectra can be assigned to superposition of ${}^3F_4-{}^3G_5$ and ${}^3F_4-{}^3D_3$ transitions and that this must be the most intense of all these satellites, contributing in order of decreasing intensity. Each of the remaining satellites is found to have different origin in different elements. The possible contributions of suitable transitions to all these lines have also been discussed.

References:

1. Y. Cauchois and C. Sénémaud, *X-ray Wavelength Tables*, 2nd ed., Pergamon Press, Oxford, pp. 217-314, (1978).
2. S. Poonia and S. N. Soni, *Indian J. Pure and Appl. Phys.* **38** (2000) 133-138.
3. S. N. Soni and S. Poonia, *J. Phys. Chem. Solids* **61** (2000) 1509-1518.
4. S. Poonia and S. N. Soni, *J. Phys. Chem. Solids* **62** (2001) 503-511.
5. S. Poonia and S. N. Soni, *J. Electron. Spectrosc. Relat. Phenom.* **122** (2002) 27-36.
6. S. N. Soni and S. Poonia, *Indian J. Phys.* **76B** (2002) 11-16.
7. S. Poonia and S. N. Soni, *Indian J. Pure and Appl. Phys.* **40** (2002) 786-794.
8. Surendra Poonia and S. N. Soni, *Indian J. Pure and Appl. Phys.* **45** (2007) 119-126.

Origin of X-ray satellites spectra in the $L\alpha_1$, $L\alpha_2$, region

S. Poonia

*Division of Natural Resources and Environment,
Central Arid Zone Research Institute, Jodhpur - 342 003, Rajasthan, India*

The X-ray satellites $L\alpha_3$, $L\alpha_4$, $L\alpha_5$, $L\alpha'$, $L\alpha^{ix}$, $L\alpha^x$ and $L\alpha_s$ observed in the L-emission spectra in elements with $Z = 40$ to 92 , have been calculated. The energies of various transitions have been calculated by available Hartree-Fock-Slater using the semi-empirical Auger transition energies in the doubly ionized atoms and their relative intensities have been estimated by considering cross - sections of singly ionized $2x^{-1}$ ($x \equiv s, p$) states and then of subsequent Coster-Kronig (CK) and shake off processes. In both these processes initial single hole creation is the prime phenomenon and electron bombardment has been the primary source of energy. The calculated spectra have been compared with the measured satellite energies in L-emission spectra. Their intense peaks have been identified as the observed satellite lines. The one to one correspondence between the peaks in calculated spectra and the satellites in measured spectra has been established on the basis of the agreement between the separations in the peak energies and those in the measured satellite energies. Group of transitions under the transition schemes $2p_{3/2}^{-1}3x^{-1}3d_{5/2}^{-1}$ and $2p_{3/2}^{-1}3x^{-1}3d_{3/2}^{-1}$ ($x \equiv s, p, d$) which give rise to these satellites have been identified. It has been established that six satellites in the $L\alpha_1$ and remaining one satellite observed in $L\alpha_2$ region of the X-ray spectra of various elements and named α_3 , α_4 , α_5 , α' , α^{ix} , α^x and α_s in order of increasing energy are mainly emitted by $2p_{3/2}^{-1}3d^{-1}3d^{-2}$ transitions. On the basis of agreement between computed spectra and measured satellites, It is observed that the satellite α_3 in ${}_{40}\text{Zr}$ to ${}_{48}\text{Cd}$ and α' in ${}_{74}\text{W}$ to ${}_{92}\text{U}$ is emitted by the superposition of the most intense transition ${}^3F_4\text{-}{}^3F_4$, contributing in order of decreasing intensity. It has been well established that the transition ${}^1F_3\text{-}{}^1G_4$ is the main source of the emission of the satellite α_4 in the spectra of elements with $Z = 40\text{-}48$. The same transition ${}^1F_3\text{-}{}^1G_4$ and other two transitions namely ${}^1P_1\text{-}{}^1D_2$ and ${}^1F_3\text{-}{}^1D_2$ have been proved to be the main origin of the satellite, α^{ix} , reported in the range $Z = 74\text{-}92$. Further, the line α_5 in the spectra of elements with $Z = 40 - 48$ has been assigned to mainly the ${}^3D_3\text{-}{}^3F_4$, ${}^3D_2\text{-}{}^3F_3$, ${}^1P_1\text{-}{}^1D_2$ and ${}^1F_3\text{-}{}^1D_2$ transitions. Finally, the satellite α^x , reported in the spectra of elements with $Z = 74\text{-}92$, has been associated with the transition ${}^3D_3\text{-}{}^3F_4$. The satellite $L\alpha_s$ of the $L\alpha_2$ region, observed in the spectra of elements ${}_{73}\text{Ta}$ to ${}_{90}\text{Th}$ is assigned to the superposition of three transitions ${}^3P_1\text{-}{}^3D_1$, ${}^3D_2\text{-}{}^3D_3$ and ${}^3D_2\text{-}{}^3D_1$. The possible contributions of other transitions of the $2p_{3/2}^{-1}3x^{-1}3d_{5/2}^{-1}$ and $2p_{3/2}^{-1}3x^{-1}3d_{3/2}^{-1}$ ($x \equiv s, p, d$) array having appreciable intensities, have also been discussed.

VUV Spectroscopy of Xe IX

H.P. Garnir, É. Biémont, S. Enzonga Yoca and P. Quinet

Institut de Physique Nucléaire, Atomique et Spectroscopie
Université de Liège
Sart Tilman B15, B4000 LIEGE BELGIUM
hpgarnir@ulg.ac.be

The spectrum of xenon ions has been recorded by the beam-foil method in the 10-110 nm wavelength range and many lines of Xe VII-VIII have been analysed [1]. In our spectra, we have looked for lines belonging to 8 times ionized Xe. Some of the lines attributed to Xe IX have been pinpointed by a careful analysis of the line intensity variation with the beam energy [2]. For those lines, the lifetimes of the upper level have been measured by analyzing beam-foil decay curves (one of the rare methods able to provide experimental data in these multicharged ions).

Our measurements will be compared with theoretical values calculated by a relativistic Hartree-Fock approach including core-polarization effects and by a purely relativistic multiconfiguration Dirac-Fock method.

During the meeting, we will describe our experiment and present our new results.

References

- [1] É. Biémont, M. Clar, V. Fivet, H.-P. Garnir, P. Palmeri, P. Quinet, and D. Rostohar, *Eur. Phys. J. D* **44**, 23 (2007)
- [2] H.P. Garnir, *Journal of Physics: Conference Series*, *accepted for publication*

Improved atomic data for platinum group elements

V. Fivet¹, É. Biémont^{1,2}, P. Palmeri¹, P. Quinet^{1,2}, L. Engström³, H. Lundberg³
and H. Nilsson⁴

¹ *Astrophysique et Spectroscopie, Université de Mons-Hainaut, B-7000 Mons, Belgium*

² *IPNAS, Université de Liège, Sart Tilman, B-4000 Liège, Belgium*

³ *Department of Physics, Lund Institute of Technology, PO Box 118,
SE-22100 Lund, Sweden*

⁴ *Lund Observatory, Lund University, PO Box 43, SE-22100 Lund, Sweden
E-mail: vanessa.fivet@umh.ac.be*

The spectra of the elements situated in the sixth row of the periodic table ($72 < Z < 86$) are still poorly known due to the lack of laboratory analysis and to the complexity of their electronic configurations of the type $4f^{14}5d^N nl$ and $4f^{14}5d^{N-1}nl n'l'$ ($N=3-10$, $nl, n'l'=6s, 6p, 6d, \dots$).

The aim of the present work is to provide a large amount of new atomic data for neutral and lowly ionized sixth row elements. The astrophysicists need these accurate data for refining their models in nucleosynthesis, for determining the chemical composition of CP stars, for the diagnostic of plasmas and for cosmochronology. Radiative parameters for some of these elements are also strongly needed for research oriented toward controlled thermonuclear fusion.

In the present work, radiative lifetimes of selected sixth row ions have been measured using TR-LIF spectroscopy[1] developed at the Lund Laser Centre by Prof. Svanberg and his group. The new results have been used to assess the accuracy of calculations performed with a Hartree-Fock-plus-Relativistic-corrections model that takes configuration interaction and core-polarization effects into account[2,3].

By combining experimental lifetimes and theoretical branching fractions, we have determined new oscillator strengths and transition probabilities. We will discuss the results obtained for the following ions: Ta III ($Z=73$), W II, W III ($Z=74$) et Pt II ($Z=78$). These results will be stored in the database DESIRE (**D**atabas**E** on **S**ixth **R**ow **E**lements) [4,5] on a website of the University of Mons-Hainaut.

References

- [1] H.L. Xu , A. Persson, S. Svanberg, K.B. Blagoev, G. Malcheva, V. Penchev and É. Biémont, *Phys. Rev. A* **70**, 0425058 (2004)
- [2] R.D. Cowan, *The Theory of Atomic Structure and Spectra*, University of California Press, Berkeley (1981)
- [3] P. Quinet, P. Palmeri, É. Biémont, M.M. McCurdy, G. Rieger, E.H. Pinnington, M.E. Wickliffe and J.E. Lawler, *Mon. Not. R. Astron. Soc.* **307**, 934 (1999)
- [4] V. Fivet, P. Quinet, P. Palmeri, É. Biémont and H.L. Xu, *J. Electron. Spectrosc. Relat. Phenom.* **156-158**, 250 (2007)
- [5] <http://www.umh.ac.be/~astro/desire.shtml>

Impact of high-order moments on the statistical modeling of transition arrays

F. Gilleron¹, J.C. Pain¹, J. Bauche² and C. Bauche-Arnoult²

¹*Commissariat à l'Energie Atomique, Centre DAM Île-de-France, Bruyères-le-Châtel, 91297 ArpaJon Cedex, France*

²*Laboratoire Aimé Cotton, CNRS II, Bâtiment 505, 91405 Orsay, France*

The impact of high-order moments on the statistical modeling of transition arrays in complex spectra is studied [1]. It is shown that a departure from the Gaussian, which is usually employed in such approach, may be observed even in the shape of unresolved spectra due to the large value of the kurtosis coefficient. The use of a Gaussian shape may also overestimate the width of the spectra in some cases. Therefore, it is proposed to simulate the statistical shape of the transition arrays by the more flexible generalized Gaussian distribution which introduces an additional parameter - the power of the argument in the exponential - that can be constrained by the kurtosis value. The relevance of the new statistical line distribution is checked by comparisons with smoothed spectra obtained from detailed line-by-line calculations. The departure from the Gaussian is also confirmed through the analysis of $2p \rightarrow 3d$ transitions of recent absorption measurements [2-4]. A numerical fit is proposed for an easy implementation of the new statistical profile in atomic-structure codes.

[1] F. Gilleron, J. C. Pain, J. Bauche and C. Bauche-Arnoult, *Phys. Rev. E* **77**, 026708 (2008)

[2] C. Chenais-Popovics *et al.*, *Astrophys. J. Suppl. Ser.* **127**, 275 (2000).

[3] J. Bruneau *et al.*, *Spectral Opacity experiments*, (Symposium Science on large lasers, Saclay, 1997).

[4] J. E. Bailey *et al.*, *J. Quant. Spectrosc. Radiat. Transfer* **81**, 31 (2003).

Exact and statistical methods for computing the distribution of states, levels and E1 lines in atomic spectra

J.C. Pain and F. Gilleron

*Commissariat à l'Energie Atomique,
Centre DAM Île-de-France, Bruyères-le-Châtel, 91297 Arpajon Cedex, France*

We propose different methods in order to determine the distribution $P(M)$ of quantum states M (projection of total angular momentum J) inside a relativistic or non-relativistic configuration. This distribution is used to calculate: (i) the distribution of levels [1] of a configuration and (ii) the number of electric-dipolar (E1) lines between two configurations.

First, an efficient recursive approach is presented for an exact calculation of $P(M)$ [2]. Second, the statistical approach of Bauche *et al.* [3] is improved to account for high- l spectators (e.g. i^1p^N) which occur for instance in electron capture into high-lying Rydberg states in collisions between multiply charged ions and light target gases [4]. In that case, $P(M)$ may exhibit a plateau, which can neither be modeled by a Gaussian nor by a Gram-Charlier expansion series. We show that the Generalized Gaussian, whose exponent is completely determined by the kurtosis (reduced fourth-order centered moment) α_4 of $P(M)$, is more suited for such cases. We propose an analytical formula for the evaluation of the number of E1 lines with a larger range of applicability.

[1] E. U. Condon and G. H. Shortley, *The Theory of Atomic Spectra* (Cambridge: Cambridge University, 1935).

[2] F. Gilleron and J. C. Pain, to be published.

[3] J. Bauche and C. Bauche-Arnoult, *J. Phys. B: At. Mol. Phys.* **20**, 1659 (1987).

[4] P. Hvelplund, H. K. Haugen, H. Knudsen, L. Andersen, H. Damsgaard and F. Fukusawa, *Phys. Scr.* **24**, 40 (1981).

Laser optogalvanic spectroscopy of Lanthanum in Spectral range of Rhodamine 6G.

Nighat Yasmin, R Islam

*Laser Development Division, National Institute of Lasers and Optronics Nilore
Islamabad*

Hyperfine structure studies of some of the allowed transitions of La I has been carried out by high resolution Doppler limited laser optogalvanic spectroscopy. A narrow bandwidth (500 KHz) Autoscan ring dye laser (899-29) pumped by argon ion laser model Innova series 200 (coherent Corp) has been employed to investigate the hyperfine structure in the wavelength range 5600-6200 Å of Rhodamine 6G in connection with a commercially available hollow cathode. Sixteen transitions of La I have been observed involving twenty five levels, twelve with odd and thirteen with even parity. A comparison with the previous data available in the literature has also been made.

The recorded spectra were analyzed using Casimir's formula which yields the expression for the shift of a hyperfine component from the center of the gravity. Then we formulate four simultaneous equations for the four unknown quantities A , B , A' and B' according to the expression. i.e;

$$\Delta\nu_{12} = A\frac{K_1-K_2}{2} + \frac{3B}{8} \frac{[K_1(K_1+1)-K_2(K_2+1)]}{IJ(2I-1)(2J-1)} + A'\frac{K'_1-K'_2}{2} + \frac{3B'}{8} \frac{[K'_1(K'_1+1)-K'_2(K'_2+1)]}{I'J'(2I'-1)(2J'-1)}$$

A computer program based on Gauss elimination technique is then employed to determine the hyperfine structure constants i.e. A , B , A' and B' for lower and upper energy levels. The curve obtained through the utilization of these empirically evaluated hyperfine structure constants is then matched with the experimental data through another computer program for the best-fit values.

Here we present the analyzed data of only few transitions. Experimentally obtained hyperfine structure constants (in MHz) of these transitions along with the transition wavelengths are shown below.

Lower level						Upper level							
Å	E(cm ⁻¹)	Config.	Term	J		A	B	E (cm ⁻¹)	Config.	Term	J	A	B
5677.707	2668.2	5d ² (³ F)6s	⁴ F	3/2	-487.3	62.88	20338.3	5d ² (³ F)6p	⁴ F ^o	3/2	254.8	97.63	
5690.6	0.00	5d6s ²	² D	3/2	141.2	44.78	17567.49	5d6s(³ D)6p	⁴ P ^o	1/2	2892.1	0.00	
5699.241	13747.28	3d ³	⁴ F	9/2	-63.8	-26.2	31287.646	5d6s(³ D)7s	⁴ D	7/2	-565.5	800	
5699.348	4121.572	5d ² (³ F)6s	⁴ F	9/2	489.5	32.18	21662.51	5d ² (³ F)6p	² G ^o	7/2	283.5	55	
5720.009	3494.58	5d ² (³ F)6s	⁴ F	7/2	461.3	21.6	20972.22	5d ² (³ F)6p	-	5/2	-65.74	37.42	
5742.922	7231.36	5d ² (³ P)6s	⁴ P	1/2	2460.0	0.00	24639.27	5d ² (³ P)6p	⁴ S ^o	3/2	-197.3	26.0	
5744.384	7679.94	5d ² (³ P)6s	⁴ P	5/2	798.5	826.6	25083.42	5d ² (³ P)6p	⁴ D ^o	7/2	67.5	820.2	
5821.975	9960.96	5d ² (¹ G)6s	² G	7/2	-289.2	72.40	27132.5	5d ² (¹ G)6p	² G ^o	7/2	69.1	42.6	
5829.692	7490.46	5d ² (³ P)6s	⁴ P	3/2	936	37.6	24639.27	5d ² (³ P)6p	⁴ S ^o	3/2	-221	-140	
5845.034	1053.2	5d6s ²	² D	5/2	182.1706	54.213	18157.0	5d6s(³ D)6p	⁴ P ^o	5/2	651.5	115	

Investigation of the even parity states of group II-B elements (Zn, Cd and Hg)

Ali Nadeem

Photonics Division, National Institute of Lasers and Optronics (NILOP), Islamabad, Pakistan

Systematic studies of the group-IIIB (Zn, Cd, Hg) elements have been carried out to investigate highly excited even-parity triplet states. The inter-combination msn p 3P_1 levels of these atoms can be populated relatively easily using ultra violet laser light and can serve as intermediate levels. The lack of spectroscopic studies on the bound states of these atoms is primarily due to the fact that their ionization potentials lies in the VUV region. As already said, their resonance transitions lie in the UV region (Cd, Zn) and in the VUV region (Hg). Consequently, multi-photon and multi-step ionization techniques have not been employed so far to probe the highly excited states of these atoms. The experimental set-up comprised of two frequency doubled dye lasers simultaneously pumped by a common Q-switched Nd:YAG (532nm; 355nm) laser operating at 10Hz repetition rate and 7ns pulse duration. To record the spectra, a thermionic diode ion detector working in the space charge limited mode was used. The change in the diode current due to the photo-ion production was measured as a voltage drop across a 100 k Ω load resistor.

The new observations for cadmium include the term energies and quantum defects of 5snd 3D_2 ($11 < n < 52$) and 5sns 3S_1 ($12 < n < 38$) Rydberg series whereas the 5snd 1D_2 series have been detected from $n = 11$ to 26. The appearance of 5snd 1D_2 is because the $\Delta S = 0$ selection rule is relaxed, then triplet to singlet transitions are observable. The ratio of the transition probabilities in cadmium indicates that the 1P_1 contribution to the 3P_1 wave function is 0.2%, whereas in zinc it is 0.02% and in mercury it is 3.2%. The singlet-triplet mixing determines the intensities of the excited triplet states. The relative intensities of the excited states have been described according to electric dipole selection rules. The first ionization potential of cadmium has been determined from the unperturbed 5snd 3D_2 series. From the termination of the Rydberg series we have estimated the net electric field present in the interaction region using the $E(\text{V/cm}) = 1.23 \times 10^9 n_m^5$ relation. During experiments on zinc the two metastable levels 4s4p 3P_0 and 4s4p 3P_2 also get populated through collisions. The average thermal energy of atoms corresponding to 823K is 572cm^{-1} which is sufficient to populate these fine structure components in zinc. New observations include 4snd 3D_2 ($14 < n < 55$) and 4sns 3S_1 ($15 < n < 35$) Rydberg series excited from the 4s4p 3P_1 level. In addition, 4snd 3D_3 ($13 < n < 49$) and 4snd 3D_1 ($10 < n < 20$) series including few members of the 4sns 3S_1 series were also observed exciting the 4s4p 3P_0 and 4s4p 3P_2 states, respectively. The wave function mixing in zinc is very small therefore no singlet transitions are detected. In mercury we have observed the even-parity 6snd 3D_2 ($25 < n < 52$) series and few levels of the 6sns 3S_1 series. Although the wave function mixing of the 1P_1 and 3P_1 is much higher than for Cd and Zn and thus the 6snd 1D_2 series should be present with high intensity compared to that in zinc and cadmium, these series is completely absent in the spectra of mercury.

New levels of Pr I discovered via infrared spectral lines

Z. Uddin¹, L. Windholz¹, F. Akber², M. Jahangir², I. Siddiqu¹

¹*Institute of Experimental Physics, Technical University of Graz, Austria*

²*Department of Physics, University of Karachi, Pakistan*

The Fourier transform (FT) spectrum of Praseodymium [1] shows hundreds of spectral lines in the infrared and far infrared region, many of them are unclassified. We have classified lot of them by their hyperfine (hf) structures and level energy differences. Still we found a number of lines, which could not be explained as transitions between known levels; this indicated that up to now unknown energy levels of Pr are involved. Some of the hyperfine structures in the FT spectrum have a very good signal to noise ratio, thus a fit of these structure was possible. In this way we found 15 new levels of Pr I. For one of them we give the following details:

The line 8954.659 Å is a line already classified [2] as a transition between the upper level 31787 cm⁻¹ (J = 5.5, odd parity) and the lower level 20622.7 cm⁻¹ (J = 6.5, even parity). However, the hf structure in the FT spectrum does not match with the hf structure corresponding to this transition. A fit of the hf structure suggested a transition 4.5 - 4.5 with hyperfine constant A of the lower level close to 810 MHz. With help of this value we identified the lower level to be 11713 cm⁻¹, J = 4.5, even parity. Adding the wave number of the line (center of gravity wavelength corrected to 8954.681 Å), we introduced a new upper level 22877 cm⁻¹, J = 4.5, odd parity. This new level of Pr I explains 10 lines shining up in the FT spectra. Six of them were already known but unclassified lines, three of them are new lines, one classification was wrong (see table). From the line 5419.935 Å we determined the final value of the level energy, 22877.524 cm⁻¹, assuming that the energy 4432.24 cm⁻¹ of the lower level is correct.

Lines classified by new level 22877.524 cm⁻¹, J = 4.5, A = 932 MHz, odd parity:

Wavelength (Å)	Lower level with even parity			Remarks
	J	Energy (cm ⁻¹)	A (MHz)	
5419.935	4.5	4432.24	929	unclassified line
6035.419	5.5	6313.25	756.3	unclassified line
6117.513	3.5	6535.52	979	unclassified line
7346.179	5.5	9268.75	976	new line
7714.313	3.5	9918.17	1057	unclassified line
8349.517	5.5	10904.07	301	new line
8825.330	4.5	11549.61	1064	unclassified line
8954.681	4.5	11713.22	818.5	wrong classified line
9471.136	3.5	12321.92	870.5	new line
9671.920	4.5	12519.72	693	unclassified line

[1] B. Gamper, Diploma thesis, Graz 2007, unpublished

[2] A. Ginibre-Emery, PhD thesis, Paris 1988

New lines of atomic niobium in Fourier transform spectra with enhanced sensitivity

Alev Er¹, Ipek K. Öztürk¹, Gönül Başar¹, Sophie Kröger², Günay Başar³,
Andrey Jarmola⁴, Maris Tamanis⁴, and Ruvin Ferber⁴

Istanbul University, Faculty of Science, Physics Department, 34134 Vezneciler, Istanbul, Turkey

Technische Universität Berlin, Institut für Optik und Atomare Physik, Hardenbergstr.36, 10623 Berlin, Germany

Technical University of Istanbul, Faculty of Science and Letters, Physics Engineering Department, 34469 Maslak, Istanbul, Turkey

University of Latvia, Faculty of Physics and Mathematics, Laser Centre, 19 Rainis Blvd., Riga LV-1586, Latvia

This work is a continuation of our hyperfine structure studies of the atomic niobium. Recently, the spectrum of Nb from a hollow cathode discharge was recorded in the wavelength region from 330 nm to 800 nm with a high-resolution Bruker IFS 125HR Fourier transform spectrometer in Riga with resolution of 0.02 cm^{-1} [1]. To increase the sensitivity of the Fourier transform measurements, an interference filter was introduced in the beam pass to limit the spectral range of the light that came from the hollow cathode discharge and entered to the Fourier transform spectrometer. We used different interference filters in the range of 410 nm to 670 nm, each with spectral bandwidth of about 10 nm. By this method a strong increase of the signal-to-noise ratio has been obtained. Even lines that had not been seen at all in the previous measurements by Fourier transform spectroscopy (without filter), now become clearly visible. The measured spectra include some previously unknown Nb spectral lines not listed in the wavelength tables [2,3] as well as lines without classification [2]. The hyperfine structure profiles of the spectral lines have been analyzed with a least-squares-fit procedure assuming a Doppler profile. Experimental hyperfine structure constants A of atomic niobium were determined. For unclassified lines, several fits were performed assuming different values of angular momentum J for the fine structure levels involved. The J values of the best fit together with the resulting hyperfine structure constants A , provide relevant information for the classification of the transitions.

Riga team acknowledges support from LZP grant No. 04.1308. A.J. is grateful for support from ESF grant.

- [1.] A. Er et al., paper in preparation
- [2.] C. J. Humphreys and W.F. Meggers, National Bureau of Standards, Vol. 34, (1945)
- [3.] Frederick, M. Phelps III, M.I.T. Wave-Length Table, Volume 2: Wavelength by element, The MIT Press, Cambridge, Massachusetts, London, England (1991).

Configuration interaction effects in the fine- and hyperfine structure of the even configuration system of tantalum atom

J. Dembczyński, M. Elantkowska, J. Ruczkowski

*Chair of Quantum Engineering and Metrology, Faculty of Technical Physics, Poznan
University of Technology, Nieszawska 13B, 60-965 Poznan, Poland
E-mail: jerzy.dembczynski@put.poznan.pl*

The experimental work of L. Windholz and co-workers, concerning observation of the tantalum spectrum, yield many informations about new energy levels and hyperfine structure splittings.

We contribute the results of the complex parametric studies of the fine- and hyperfine structure of the mentioned element up to second-order of perturbation theory. The work has been performed for the systems including 36 even configurations. The values of the radial parameters describing the one- and many-body interactions effects on atomic structure are given. We predicted values of energy levels and their A- and B- hyperfine structure constants, also for experimentally levels not observed up to now.

This work was supported by Polish Ministry of Science and Higher Education under the project N519 033 32/4065

Extended analysis of the even configurations of Ta II

Ewa Stachowska¹, Jerzy Dembczyński¹ and Laurentius Windholz²

¹*Chair of Quantum Engineering and Metrology, Poznań University of Technology,
Poznań, Poland*

²*Institute of Experimental Physics, Graz University of Technology, Graz, Austria*

The structure of Ta II is of particular interest in astrophysical studies, especially of chemically peculiar stars, such as χ Lupi.

This work extends the analysis of the complex atomic structure of the tantalum ion, using extensive fine and hyperfine structure calculations of the system of the following 25 even configurations :

$5d^4 + 5d^3n'g$ ($n'=5-6$) + $5d^36s + 5d^36d + 5d^26s^2 + 5d^26sn'g$ ($n'=5-6$) + $5d^26sn''d$ ($n''=6-10$)
+ $5d^26sn'''s$ ($n'''=7-10$) + $5d^25f6p + 5d^26p^2 + 5d6s^2n''d$ ($n''=6-7$) + $5d6s6p^2 + 5d5f6s6p$
+ $5d5f6s7p + 5d6s6d7s$.

Previously only low lying levels of the $(5d + 6s)^4$ configuration system up to 40000 cm^{-1} were well known, identification supported by their hyperfine structure. Levels of higher configurations, from 70000 cm^{-1} upwards are found, but their identification is still lacking and further study is needed. Results will be presented at the conference.

This work was partially supported by PUT (project DS 63-029/08).

Search for new electronic levels in singly ionized europium Eu II

B. Furmann

*Chair of Quantum Engineering and Metrology
Faculty of Technical Physics, Poznan University of Technology
boguslaw.furmann@put.poznan.pl*

Experimental search for new electronic levels in rare earths, combined with determination of the parameters, which allow a correct classification of those levels, such as J quantum number, g_J factor or hyperfine structure constants A and B, has an significant influence on both the improvement of precision of the theoretical description of interactions in particular atoms (particularly in a semi-empirical method) and some applications in other branches of physics, e.g. investigations of abundance of particular atoms or ions in stellar atmospheres [1].

In the case of europium ion Eu II the electronic levels system is slightly different from the typical pattern of other lanthanides. The known electronic levels of the odd configurations $4f^76s$ and $4f^75d$ have energies in the range $0-17500\text{ cm}^{-1}$. Above this value a large gap is present and the next levels can be found at the energies above 50000 cm^{-1} . On the other side, theoretical predictions [2] yield an energy gap in the system of electronic levels, but only covering the range $17500-26000\text{ cm}^{-1}$; at energy values between 26000 cm^{-1} and 50000 cm^{-1} several tens of electronic levels should occur. The tables of spectral lines of Eu II [3] contain several tens of unclassified spectral lines.

In the present contribution results of search of new electronic levels, based on investigations of the hyperfine structure of unclassified spectral lines with the method of laser induced fluorescence in a hollow cathode discharge, are presented. The method of investigation has been similar to the one applied earlier for praseodymium ion [4]. On the basis of the measured hyperfine A constants and determined fluorescence channels wavelengths, combined with g_J values presented in [3], it has been possible to assign the levels investigated to the theoretically predicted ones, however, their energies have not been determined so far. A plan of continuations of the investigations is presented.

The work has been supported by Poznan University of Technology under project No 63-029/2008

References

- [1] C. Travaglio, D. Galli, R. Gallino, M. Busso, *The Astrophys. Journal* **521**, 691-702, (1999)
- [2] J. Dembczynski, M. Elantkowska, J. Ruczkowski "Private communication"
- [3] H. N. Russel, W. Albertson, and D. N. Davis, *Phys. Rev* **60** , 641-656, (1941)
- [4] B. Furmann, D. Stefanska, J. Dembczynski, E. Stachowska, *Physica Scripta* **72**, 300-308, (2005)

Analysis of the odd configurations of tantalum atom search for configurations containing f electrons

B. Arcimowicz, J. Dembczyński

*Chair of Quantum Engineering and Metrology, Faculty of Technical Physics, Poznan
University of Technology, Nieszawska 13B, 60-965 Poznan, Poland
E-mail: bronislaw.arcimowicz@put.poznan.pl*

Recently the structure of tantalum atom has been extensively investigated, in particular by three groups: from Graz, Hamburg and Poznań. So far the energies of more than 260 electronic levels, belonging to odd configurations of tantalum atom, have been established and their hyperfine structures have been determined. Attempts at classification of those levels, based on the semi-empirical calculations, have been made. The wavefunctions obtained in this procedure have further been used to calculate the A and B hyperfine structure constants. However, only for less than twenty lowest-lying levels a satisfactory agreement has been obtained. Results of the analysis indicated a strong configurations interaction. Semi-empirical calculations performed in the multiconfiguration approximation $5d^4n'p + 5d^36sn'p + 5d^26s^2n'p$ (where $n'=6-10$) with conservation of the values of effective quantum numbers n_{eff} have still omitted several levels with energies in the range $40000-50000 \text{ cm}^{-1}$. It suggested the existence of other configurations, which positions were, however, inconsistent with predictions based on multiconfiguration Hartree-Fock calculations. Taking into account 27 or 28 configurations, including additional configurations of the type $5d36sn''f + 5d26s2n''f + 5d4n''f$ (where $n''=5-7$), although it has improved the consistency of the fitted parameters g_J and the levels energies with the respective experimental values, it nevertheless has not solved some differences. In the subsequent stage of calculations an attempt of reduction of the configuration basis to merely 9 configurations has been made, but simultaneously some hitherto not considered interactions in the second order perturbation theory have been included. A better precision of these calculations allowed to determine the positions of configurations $5d^35f6s$ and $5d^25f6s^2$. The lowest-lying level of the former configuration containing the f electron is the recently found level of the energy $E = 47740.71 \text{ cm}^{-1}$ with the value of hyperfine structure constant $A = -2500 \text{ MHz}$. For many levels the deciding test of classification have been the hyperfine structure constants B, which varied strongly, since the values of the constants A have been very close to each other. The results obtained are discussed in detail within this work

References

- [1] N. Jaritz, L. Windholz, U. Zaheer, M. Farooq, B. Arcimowicz, R. Engleman Jr, J. C. Pickering, H. Jäger and G. H. Guthöhrlein, Phys. Scr **74**, 211-217 (2006)

Program package for semi-empirical analysis of the fine- and hyperfine structure of complex atoms

J. Ruczkowski, J. Dembczyński, M. Elantkowska

*Chair of Quantum Engineering and Metrology, Faculty of Technical Physics, Poznan
University of Technology, Nieszawska 13B, 60-965 Poznan, Poland
E-mail: jerzy.dembczynski@put.poznan.pl*

The experimental work combined with semi-empirical calculations is a very efficient tool for the investigations of the fine- and hyperfine structure of the complex atoms.

We present a set of programs for the analysis of the fine- and hyperfine structure. The input data for the calculations are : the fine structure energy levels, the g_J -factors and the hyperfine structure (hfs) A and B constants of experimentally observed levels. In order to avoid mistakes, all input data are set once in the initial input file and are transferred between the programs automatically.

The programs are used for the analysis of electron systems containing any number of configurations up to four open shells. In the energy matrix generated, all kinds of electrostatic, magnetic and correlated electrostatic and magnetic interaction, up to second order perturbation theory, were included.

As a result, we obtain predicted energy values for all the levels of the system considered, their exact spectroscopic description, eigenvector amplitudes and also g_J -factors and hfs A and B constants.

The program package contains supplementary programs useful for clear presentation of results of calculations and their analysis.

This work was supported by Polish Ministry of Science and Higher Education under the project N519 033 32/4065

Procedure for precise determination of the hyperfine structure constants A, B, C and D. Example of lanthanum atom

M. Elantkowska, J. Ruczkowski, J. Dembczyński

Chair of Quantum Engineering and Metrology, Faculty of Technical Physics, Poznan University of Technology, Nieszawska 13B, 60-965 Poznan, Poland
E-mail: jerzy.dembczynski@put.poznan.pl

High precision measurements of the hyperfine structure (hfs) splittings of electronic levels, especially by rf-spectroscopic methods [1, 2, 3] make it possible to study even fairly complicated aspects of the interaction between electron shells and the nucleus, which can result in determination of the nuclear moments with high accuracy. We report the parametrization method of the hyperfine structure which takes into account simultaneously one and two-body effects appearing in the second order perturbation theory.

The analysis of the hfs of the even configurations of La atom was performed in the basis of 3 configurations taking into account all possible interactions predicted by many-body fine structure theory. In order to include the J-off-diagonal effects in the hyperfine structure, direct diagonalization of the matrix containing J-diagonal as well as J-off-diagonal elements has to be performed (in the basis of $\Psi(\textit{configuration}, vSLJF)$ states). Usually, the "repulsion" effects of the neighbouring levels with the same quantum number F are considered. It requires the precision up to 16 significant digits. The diagonal part of this matrix consists of coefficients corresponding to particular components of the energy of a hyperfine structure sublevel E_F : center of gravity of *hfs* energy W_J and the experimental *hfs* constants A, B, C and D. These parameters are treated as free in the fitting procedure of the experimental and the calculated *hfs* energies (E_F). The differences between E_F and $E_{F\pm 1}$ values are equal to experimentally determined hyperfine structure intervals. Values of J-off-diagonal matrix elements are fixed.

As a result, we obtain final values of the hyperfine structure constants, which can be used again to determine the radial *hfs* parameters.

This work was supported by Polish Ministry of Science and Higher Education under the project N519 033 32/4065

References

- [1] Y. Ting, Phys.Rev. **108**, 295, (1957)
- [2] W.J. Childs, L.S. Goodman, Phys.Rev. **A3**, 25, (1971)
- [3] W.J. Childs, U. Nielsen, Phys.Rev. **A37**, 6, (1988)

Investigations of the Hyperfinestructure of Praseodymium in the IR-Region with the help of FTS

Bettina Gamper¹ and Laurentius Windholz¹

¹ *Institute of Experimental Physics, Graz University of Technology,
Petersgasse 16, 8010 Graz, Austria*

The density of the spectral lines of praseodymium is very high. Therefore there are a lot of unknown and not classified lines and levels. One kind of investigation one can do is to analyze the fourier-transform-spectra (FTS). That is exactly what we did in the IR-region of praseodymium. In this region there are a lot of lines which are not classified and therefore not related to a spectral transition between two energetic levels. If you look through the FTS you can immediately see and then also analyze the characteristic hyperfinestructure of several transitions.

With the help of FTS we could classify about 200 new spectral lines. That does not mean that they are all already related to a spectral transition, some of them are just marked as here is a line. The reason why we could not assigne each line to a transition is that either the intensity of a line was to weak to see all of their components or that there was a blend-situation between several ennergetic transitions. One very successful way to solve such a problem is to make some investigations via laserinduced fluorescencespectroscopy. That would be the next step in our work.

Another thing which we did was that we could correct some energies or hyperfineconstants of already known levels or also give a more precise center of gravity of some lines. As well we could relate a lot of already classified lines to a spectral transition between two previously known energetic levels.

Of course it also was possible to find some new energylevels. That can be done via fitting some very intens lines. For example we calculated the following two new levels:

level energy/ cm^{-1}	J value	A value/ MHz	parity	investigated line/ \AA
20467.49	2.5	800	o	9293.848
22442.19	7.5	961	o	9319.011

A clear indication that those new energetic levels are correct is that they also explain other lines in the spectra.

Investigation of the hyperfine structure of Ta I-lines

P. Głowacki¹, L. Windholz² and J. Dembczyński¹

¹*Chair of Quantum Engineering and Metrology, Poznań University of Technology
Nieszawska 13B, 60-965 Poznań, Poland*

²*Institute of Experimental Physics, Graz University of Technology Petersgasse 16,
A-8010 Graz, Austria*

E-mail: przemyslaw.glowacki@doctorate.put.poznan.pl

Investigations of the hyperfine structure in tantalum began in the thirties of 20th century [1,2]. Numerous research groups all over the world obtained many experimental results concerning the tantalum spectrum [3,4,5]. The theoretical group under supervision of Prof. Dembczyński included all known experimental results in a semi-empirical analysis of the electronic structure of tantalum atom. This calculations show that there are still plenty of predicted energy levels that require experimental confirmation or discovery.

In our experimental investigations we used a hollow cathode lamp producing free Ta atoms by sputtering, which were excited by a tunable dye laser operating with coumarine 102 (480-510nm). The laser-induced fluorescence was detected. Several spectral lines, which appear in a Fourier transform spectra (FTS) and were unclassified, were excited. The energy of some electronic levels and the values of their hyperfine constants A and B were obtained.

Table I. Ta I lines investigated and classified by laser excitation.

Excitation wavelength [Å, air]	Even level		Odd level	
	Energy [cm ⁻¹]	J	Energy [cm ⁻¹]	J
4870.082	new 54024.941	3.5	33497.154	4.5
4900.354	53598.985	3.5	33197.724	3.5
4909.322*	55080.053	4.5	34716.237	5.5
4909.395*	20646.702	3.5	41010.121	2.5
4934.261	23912.929	4.5	44173.713	4.5
4939.771*	27412.440	1.5	a 47650.666	1.5
5000.391	25655.493	2.5	45648.307	3.5
5000.981	22761.279	3.5	42751.800	3.5

* - new center of gravity, a - level predicted by calculation from FTS, confirmed by LIF methods

This work was performed within the project of WTZ PL07/2007.

References

- [1] E. McMillan, N.S. Grace, Phys. Rev. **44**, 949-950 (1933)
- [2] Gisolf and Zeeman, Nature **132**, 566 (1933)
- [3] G.H. Guthöhrlein, L. Windholz, Z.Phys D **27**, 343-347 (1993)
- [4] B.Arcimowicz, A. Huss, S. Roth, N. Jaritz, D. Messnarz, G.H. Guthöhrlein, H. Jäger, L. Windholz, Eur. Phys J. D **13**, 187-194 (2001)
- [5] N. Jaritz, L. Windholz, U. Zaheer, M. Farooq, B. Arcimowicz, R. Engleman Jr, J.C. Pickering, H. Jäger, G.H. Guthöhrlein, Phys. Scr. **74**, 211-217 (2006)

Perturbed intensity distribution of hyperfine components of Praseodymium-I lines

I. Siddiqui, B. Gamper, G.H. Guthöhrlein and L. Windholz

*Institut für Experimentalphysik, Techn. Univ. Graz, A-8010 Graz, Petersgasse 16,
windholz@tugraz.at*

Excitation of Praseodymium-I atoms with wavelength 578.051 nm led to observation of laser-induced fluorescence signal at 618.3 nm with anomalous intensity distribution of the hyperfine components. The recorded structure appeared to be a convolution of more than one structures apparently depicting an excitation and fluorescence blend situation, which may be observed when investigating Praseodymium atoms, due to the high level density. But the same structure appeared also on all other fluorescence channels, thus we had to conclude that more than one transition is always excited, and that either two lower or two upper levels form a narrow spaced pair. These levels could disturb each other, explaining also the quite unusual intensity distribution of the hyperfine patterns. The first part of the structure showed small components on both sides of the huge diagonal components, indicating $\Delta J = 0$. From the spacing of the components, a transition between levels with high angular momentum, $15/2 - 15/2$, was suggested, while the strong decrease of the intensity of the diagonal components indicated small J-values. A fit of the structure with $15/2 - 15/2$ gave A-factors which did not coincide with A-factors of already known levels, thus we had to conclude that we have excited a transition where lower and upper level were up to now unknown. Nevertheless, by an analysis of the wave numbers of the observed fluorescence lines we were able to locate the upper level of the excited transition at a wave number of 32486.80 cm^{-1} , with $J = 15/2$ and even parity. Excitation with wavelength 618.3 nm confirmed our assumptions concerning energy and J of this upper level without doubt; its A-factor was 552.5 MHz . Thus we were able to find also the wave numbers of the pair of lower levels excited with 578.051 nm. In further investigation we found that another third level is located very close to this pair.

These levels are

$15192.090 \text{ cm}^{-1}$, $J = 15/2$, $A = 730 \text{ MHz}$, odd parity

$15191.906 \text{ cm}^{-1}$, $J = 13/2$, $A = 730 \text{ MHz}$, odd parity

$15191.233 \text{ cm}^{-1}$, $J = 13/2$, $A = 666 \text{ MHz}$, odd parity

During our systematic investigations we found three other new upper levels, which could be excited from this level triplet, all showing disturbed intensities of the hyperfine components.

Investigation of the hyperfine structure of Pr I lines in the region 5630 Å to 5830 Å

Shamim Khan, Syed Tanweer Iqbal, Imran Siddiqui and Laurentius Windholz

*Institut für Experimentalphysik, Techn. Univ. Graz, A-8010 Graz, Petersgasse 16,
windholz@tugraz.at*

We investigated the hyperfine structures of several spectral lines of Praseodymium by using laser excitation in a hollow cathode discharge. Up to now seventeen unknown energy levels with odd parity, nine levels with even parity and one ionic odd level were found. The region investigated is in between 5630 Å and 5830 Å. The excitation source is a R-6G ring-dye laser pumped by a solid state diode-pumped, frequency doubled Nd:Vanadate (Nd:YVO₄) Verdi V-18 laser system. The dye was pumped at 7.5 W power of pumping source. We recorded characteristic hyperfine patterns, from which we determined both J-values and magnetic dipole interaction constants A of the combining levels. Using these constants and excitation and fluorescence wavelengths, we were able to find the energies of the new levels. The excitation wavelengths were taken from FT Spectra [1].

Levels confirmed by a second laser excitation are given in the following table.

	Excitation Wavelength	Signal/Noise in FT Spectra	Discovered Odd Levels	
	Å		J	Energy/ cm ⁻¹
1	5739.179	6	7.5	25370.613
2	5656.938	7	6.5	26036.412
3	5634.304	22	5.5	26848.512
4	5828.609	4	2.5	28513.813
5	5808.605	17	8.5	28694.509
6	5720.270	4	6.5	30135.271
7	5721.189	4	6.5	30509.771
8	5647.923	2	3.5	30828.498
9	5635.388	3	5.5	31562.583
			Discovered Even Levels	
	Å		J	Energy/cm ⁻¹
10	5630.85	20	7.5	28474.777
11	5669.693	3	5.5	29363.344
12	5659.606	1	4.5	30485.255
13	5636.680	4	4.5	31962.250

Reference:

1. B.Gamper, Diploma Thesis, Technical University of Graz, 2007 (Unpublished)

Correction of Pr I energy levels values due to Fourier transform spectra and laser excitation

G. Krois, G.H. Guthöhrlein and L. Windholz

*Institut für Experimentalphysik, Techn. Univ. Graz, A-8010 Graz, Petersgasse 16,
windholz@tugraz.at*

The electronic ground state configuration of ${}_{59}\text{Pr}^{141}$ is $[\text{Xe}]4f^36s^2$, with ground state level ${}^4I_{9/2}$. Excitation of one or more electrons of the open f-shell or one of the s-electrons forms a huge number of metastable and excited state levels. In our level data base on Pr we use in moment approximately 1100 levels of odd and 750 levels of even parity, but this list of levels is quite far from being complete.

Due to the high number of levels, the line density is also very high, in average 5 to 10 lines per Å. In our line list (based on ref.[1]) we have now 20000 spectral lines. Thus, only with the help of their hyperfine structure the transitions, explaining the lines, can be selected. This classification is supported by a specially developed computer program (ref.[2]), which is now extended to show immediately a part of a Fourier transform spectrum (FTS) [3], and allows to compare easily calculated hyperfine patterns with structures appearing in the FTS (of course for this the hyperfine constants of the combining levels must be known).

Accurate center of gravity (cog.) wavelengths, obtained from our calibrated FTS, allows to determine more accurate level energies (usually we use for this the vacuum wave number in cm^{-1}). Starting from the ground level (which has odd parity), a huge number of energies of even upper levels could be corrected. The same is true for upper odd levels, taking the lowest even level, 4432.24 cm^{-1} , as basis.

Without accurate level energy and without correct excitation and emission wavelength a certain transition can not be identified in the FTS and can not be excited in laser spectroscopic studies. This information is given quite often insufficient, as we have recently seen for example in ref. [4]. We repeat here the data for one level, published as new in [4]: Excitation wavelengths 5885.76; 5829.5; 5800.19; 5707.90 Å, energy 28698.51 cm^{-1} , odd parity, fluorescence wavelengths 4465.23; 5101.76; 5144.97 Å, $A = 767.4(3.3) \text{ MHz}$.

Identifying with the help of the given A-factor hyperfine structures which may be decays of this level, we determined a level energy between $28698.073 \text{ cm}^{-1}$ and $28698.103 \text{ cm}^{-1}$, depending on the treated line. Moreover, we performed laser excitation with cog. wavelength 5800.48 Å, and came to 28698.03 cm^{-1} . These different results for the level wave number show, that the energy differences between the even lower levels are not completely correct. Assuming $28698.103 \text{ cm}^{-1}$ as most reliable, we re-calculate the excitation wavelengths given in [4] to be 5885.957, 5829.801, 5800.456, 5708.234 Å and the fluorescence wavelengths to be 4466.053, 5102.419, 5145.418 Å in full agreement with position and pattern of lines appearing in the FTS. Taking into account the wavelength differences up to 0.5 Å and the high line density, it is nearly impossible to identify the lines mentioned in [4]. In general, the energies in [4] are more reliable than the wavelengths, since the conversion from vacuum wave number to air wavelength was done quite insufficient.

[1] A.Ginibre, Thesis, (Paris 1988); [2] L.Windholz, G.Guthöhrlein, Phys. Scr. T105, 55-60 (2003); [3] B.Gamper, diploma thesis (T.U. Graz, 2007); [4] B.Furmann, A.Krzykowski, D.Stefanska, J.Dembczynski, Phys. Scr. 74, 658 (2006)

Normal spectral emissivity depending on atomic composition for two nickel-based and two ferrous-based alloys at 684.5 nm

C. Cagran¹, H. Reschab¹, R. Tanzer², W. Schützenhöfer², A. Graf², G. Pottlacher¹

¹*Institut für Experimentalphysik, TU Graz, Petersgasse 16, 8010 Graz, Austria*

²*Böhler Edelstahl GmbH & Co KG, Mariazellerstrasse 25, 8605 Kapfenberg, Austria*

The Subsecond Thermophysics Workgroup at TU Graz mainly investigates thermophysical properties, such as electrical resistivity, specific heat capacity and density of solid and liquid metals and alloys as a function of temperature. A fast pulse-heating system is used, which also allows the determination of normal spectral emissivity under pulse heating conditions. For this purpose, a laser polarimeter, proposed in the 1980's and later developed by R. M. A. Azzam for the determination of optical constants without any moving parts, was adapted for this μ s-pulse heating experiment.

The change in polarization of a laser beam reflected off the surface of the wire-shaped sample material during a pulse heating experiment enables the measurement of temperature-dependent normal spectral emissivity at melting and in the liquid state at the used laser wavelength. Knowledge of emissivity and its behaviour throughout the liquid phase can improve the understanding of interacting effects between light and the molten alloy. The industrial cooperation partner Böhler Edelstahl GmbH & Co KG is interested in emissivity data for numerical simulations of plastic deformation and remelting processes as well as for process optimisation.

As observed from numerous experiments with various sample materials the liquid state behaviour of normal spectral emissivity at 684.5 nm can be classified into three groups, namely increasing, decreasing and constant emissivity with increasing temperature. Based on this finding, it can be shown that the behaviour of normal spectral emissivity in conjunction with the radiometric temperature measurement is needed to achieve reliable thermophysical properties of liquid metals.

Within this presentation normal spectral emissivity data at 684.5 nm for two nickel-based alloys (Nimonic 80A and Inconel 718), as well as the austenitic steel X2CrNiMo18-14-3 and another ferrous-based alloy at melting and in the liquid state are presented.

Research supported by Böhler Edelstahl GmbH & Co KG and the „Forschungsförderungsgesellschaft mbH, Sensengasse 1, 1090 Wien, Austria“, project 812972.

Identification of atomic structure in measurement data, depending on the used set of units

T. Hüpf¹, C. Cagran¹, G. Pottlacher¹, G. Lohöfer²

¹*Institut für Experimentalphysik, Technische Universität Graz, Austria*

²*Institut für Materialphysik im Weltraum, DLR Köln, Germany*

Hardly any scientific topic can be treated without a closer specification of quantities. In natural sciences this is commonly done by choosing an appropriate, standardized system of units, generally the SI, or sometimes a ratio of selected quantities. With such an approach numerical data are compared to a well-defined unit and reported as a fraction or multiple thereof.

The presented work wants to demonstrate how the choice of different units can lead to a totally different presentation of results, which might help to reveal yet unseen coherences. This idea is reviewed on the example of measurements performed with a fast pulse heating method.

Using this pulse heating technique wire shaped samples are resistively volume heated as part of a fast capacitor discharge circuit. Time resolved electrical measurements with sub- μ s resolution include the current through and the voltage drop across the specimen. Surface radiance from the samples is detected by pyrometers and the thermal expansion of the sample can be monitored by means of a custom-made fast CCD-camera. Based on these measured quantities, temperature-dependent thermophysical properties such as enthalpy, isobaric heat capacity, electrical resistivity and thermal expansion can be deduced.

During the compilation of specific enthalpy results for numerous pure elements we observed an organisation according to the periodic system of the elements. By using *molar* instead of *specific* units the same results become rearranged and show the established law of Dulong-Petit.

The project: *Electrical Resistivity Measurement of High Temperature Metallic Melts* is sponsored by the FFG-ASAP programme.

Electronic Wavefunction Microscopy using slow-photoelectron Imaging

M. M. Harb[1], A. Ollagnier[1], S. Cohen[2], F. Lépine[1], F. Robicheaux[3], M. Vrakking[4] and C. Bordas[1]

[1]Université Lyon 1; CNRS; LASIM, UMR 5579, 43 bd. du 11 novembre 1918, F-69622 Villeurbanne, France.

[2]Atomic and Molecular Physics Laboratory, Physics Department, University of Ioannina, 45110 Ioannina, Greece.

[3]Department of Physics, 206 Allison Lab, Auburn University, AL 36849-5311, USA.

[4]FOM-Institute AMOLF, Kruislaan 407, 1098 SJ Amsterdam, The Netherlands.

Photoelectron imaging spectroscopy has recently emerged as a powerful tool capable of providing detailed information on the microscopic properties of matter. In a standard velocity map imaging (VMI) experiment eV kinetic energy electrons or ions are projected towards a 2D position sensitive detector. Therefore the obtained image corresponds to the classical projection of a Newton sphere that, in principle, allows a direct reconstruction of the initial 3D velocity distribution of the particles. Improvements on the standard VMI set-up, allowing the study of meV electrons, led to the recording of 2D patterns which are drastically modified with respect to those obtained with high kinetic energy electrons. The most striking effect is the observation of radial signal modulations due to quantum interferences [1]. Moreover, ionic core gives rise to a re-scattering ionization channel [2]. Simulations based on wavepacket propagation have been performed and we have shown that when ionization of Hydrogenic atoms occurs via a Stark resonance above the saddle point energy, the measured image represents a direct projection of the bound component of the electronic wavefunction magnified to macroscopic dimensions by a factor 106. Hence it is fully justified to consider the meV-VMI apparatus as a photoionization microscope, corresponding to the smallest Youngs slit experimental set-up ever implemented [3, 4]. For a non-hydrogenic atom, on the other hand, the presence of the electronic core leads to mixing of the parabolic electronic states which modifies the wavefunction. As a consequence, a smooth evolution of the interferogram patterns with energy is expected. Experimental results on Xe and Li will be presented and discussed.

[1] C. Nicole, H.L. Offerhaus, F. Lépine, C. Bordas, and M. Vrakking, Phys. Rev. Letters 88 (2002) 133001. [2] C. Nicole, I. Sluimer, F. Rosca-Pruna, M. Warntjes, M.J.J. Vrakking, C. Bordas, F. Texier and F. Robicheaux, Phys. Rev. Lett. 85 (2000) 4024. [3] C. Bordas, F. Lépine, C. Nicole and M. Vrakking, Phys. Rev. A68 (2003) 012709. [4] F. Lépine, S. Zamith, A. de Snaijer, Ch. Bordas and M.J.J. Vrakking, Phys. Rev. Lett. 93 (2004) 233003.

On a self-sustained oscillating mode for operation of a glow discharge

E. Dimova, D. Zhechev and V. Steffekova

*Institute of Solid State Physics, Bulgarian Academy of Sciences
72 Tzarigradsko Chaussee Blvd., BG-1784 SOFIA, BULGARIA
e-mail: spectron@issp.bas.bg*

Numerous glow discharge (GD) applications are based on its stable mode for operation. From another point of view, the gaseous plasma in a GD is known as a typical nonlinear dynamical "open system" with a large number of degrees of freedom. Within these frames a GD modification, i.e. hollow cathode discharge (HCD) should possess one more additional degree of freedom due to the specific Penning ionization of sputtered atoms. A self-sustained oscillating mode for operation of a hollow cathode discharge (HCD) is analyzed based on an equivalent glow discharge RCL scheme. The oscillation takes place under i - V operating point of positive differential resistance and its frequency (\approx kHz) depends on the discharge current value. The self-sustained instabilities correlate with the plasma space structure in the cathode cavity.

If the value η is a small deviation of the continuous discharge current i_0 , i.e. $i = i_0 + \eta$, the equation

$$a \left(\frac{\partial \eta}{\partial t} \right)^2 + b \left(\frac{\partial \eta}{\partial t} \right) + d = 0$$

is found to describe a non damping oscillating function $\eta(t)$ under some combinations (a, b, d) of reasonable data values characterizing glow discharge plasma in general.

Atomic beam measurements of the Cs $7d^2D_{3/2}$ hyperfine parameters with two-photon fluorescence spectroscopy

A. Kortyna and V. Fiore

*Department of Physics, Lafayette College
Easton, PA 18042, U.S.A.*

The hyperfine intervals of the $7d^2D_{3/2}$ manifold are measured by interrogating an effusive beam of atomic cesium with resonant two-photon laser-induced-fluorescence spectroscopy. This work adapts the laser system previously used to measure hyperfine splittings in a vapor cell [1]. Two external-cavity diode lasers drive the two-step excitation of the $7d^2D_{3/2}$ state. One laser is center locked to a $6s^2S_{1/2}(F'') \rightarrow 6p^2P_{3/2}(F')$ transition using magnetic dithering and a servo-feedback circuit. The second laser is scanned over the $6p^2P_{3/2}(F') \rightarrow 7d^2D_{3/2}(F)$ transitions.

The scanned laser's frequency scale is calibrated with an electro-optic modulator. Phase modulation introduces sidebands to the laser frequency at precise intervals. As the laser frequency is scanned across an atomic feature, the sidebands cause the feature to be repeated at intervals equal to the modulation frequency, providing calibration frequency markers. High accuracy is achieved by directly referencing the modulation frequency to the $^{87}\text{Rb } 5s^2S_{1/2}(F=1) \leftrightarrow 5s^2S_{1/2}(F=2)$ ground-state hyperfine transition using an atomic frequency standard. To enhance resolution, nonlinear fitting of Voigt profiles is used to locate the centroid of each fluorescence peak. The observed linewidths are 8.2 ± 0.1 MHz, and the hyperfine intervals are determined with overall uncertainties of 200 kHz. The uncertainty includes contributions from the fitting procedure, jitter in the frequency scale calibration, and statistical uncertainty.

The hyperfine intervals are used to generate the magnetic dipole coupling constant $A = 7.36 \pm 0.03$ MHz and the electric quadrupole coupling constant, $B = -0.1 \pm 0.2$ MHz. This result is the first time a constraint has been placed on the B coupling constant. The A coupling constant is in good agreement with a previous measurement [2] but with an order of magnitude improvement in resolution. This result does not agree with a relativistic-all-order calculation [3], but this disagreement is anticipated because of the difficulty of modeling electron correlation effects. Our resolution is sufficient to provide a benchmark value for testing future improvements in high-precision theory. This work is generously supported by Lafayette College and by the U.S. National Science Foundation through Grant Numbers PHY-0244684, PHY-0653107, and ECCS-0722610.

References

- [1] A. Kortyna, N. A. Masluk, and T. Bragdon, *Phys. Rev. A*, **74**, 022503 (2006).
- [2] G. Belin, L. Homgren, and S. Svanberg, *Physica Scripta* **14**, 39 (1976).
- [3] M. Auzinsh, K. Bluss, R. Ferber, F. Gahbauer, A. Jarmola, M. S. Safronova, U. I. Safronova, and M. Tamanis, *Phys. Rev. A* **75**, 022502 (2007).

ELECTRON SCATTERING BY CADMIUM ATOMS

O.B.Shpenik, E.E.Kontros, I.V.Chernyshova

Institute of Electron Physics, National Academy of Sciences of Ukraine

21 Universitetska str., Uzhgorod 88017, Ukraine

E-mail: an@zvl.iep.uzhgorod

We have performed an investigation of elastic and inelastic scattering of monoenergetic electrons by cadmium atoms. The specific feature of the experiment is that, using a hypocycloidal electron spectrometer, the total electron scattering cross-section, electron energy loss spectra as well as constant residual energy spectra (threshold excitation spectra) were measured at the same experimental conditions as well as the ionization cross-section and excitation function for the lower atomic levels near the threshold.

The experiments were performed using a vapour-filled cell: an electron beam was formed by a hypocycloidal electron monochromator [1], passed through the vapour-filled cell, then through a hypocycloidal electron analyser and was detected by a deep Faraday cup. Inelastically scattered electrons were registered by a separate detector and measured by a digital picoammeter. Cadmium vapour was supplied to the cell from a separate reservoir, its temperature being kept by 20 – 30 °C below the cell temperature. To provide spectrometer operation, the axial magnetic field of ~ 150 Oe strength was used produced by Helmholtz rings. The detector of positive ions was located directly in the cell, performed in a shape of a flat electrode, protected by a metallic grid and positioned at a distance of 5 mm from the electron beam.

The threshold excitation spectra of Cd atom, measured at different values of the residual electron energy from 0 to 1 eV, have shown a metastable 5^3P - level, then a resonance 5^1P_1 - level and the $6^{3,1}S$ - level to be the most effectively excited by electrons.

Taking into account the fact that the hypocycloidal analyzer enables all the inelastically scattered electrons to be detected within 0.5 – 1.5 eV near the level excitation threshold, we have measured the excitation functions for the lower $5^3P_{0,1,2}$ -, 5^1P_1 -, as well as 6^3S_1 - and 6^1S_1 - levels. The form of the excitation function of the $5^3P_{0,1,2}$ - and 5^1P_1 - levels is very close to the optical excitation functions of ($5^1S_0 - 5^3P_1$) and ($5^1S_0 - 5^1P_1$) spectral lines, measured earlier [2].

The work was carried out in part in the framework of the agreement No. F014/309 – 2007 of DFFD of the Ministry of Education and Science of Ukraine.

References

- [1] N.I.Romanyuk, O.B.Shpenik, I.A.Mandy, F.F.Papp, I.V.Chernyshova, Tech. Phys. 63, 138-147 (1993).
- [2] N.M.Erdevdy, O.B.Shpenik, V.S.Vukstich, Opt.Spectr. 97, 559-565 (2004).

Probing surface vibrations of amorphous solids by helium atom scattering

W. Steurer¹, B. Holst^{1,*}, J. R. Manson², and W. E. Ernst¹

¹ Institute of Experimental Physics, Graz University of Technology, Austria

² Department of Physics, Clemson University, South Carolina, USA

contact: wolfram.steurer@tugraz.at

While helium atom scattering has been a well established method for the investigation of ordered surface structures, the technique has only recently shown its great potential for the non destructive probing of the vibrational state density at amorphous interfaces [1,2]. No diffraction can be observed from such interfaces but the energy transfer from the beam to the surface and vice versa reveals valuable information about vibrational frequencies in a way that is purely surface sensitive with no penetration into the bulk. In the experiment, a nearly monochromatic beam of neutral He atoms of about 20 meV kinetic energy impinges on the sample surface. Some helium atoms will exchange kinetic energy and momentum with the surface via creation or annihilation of surface phonons while others scatter elastically and do not change their kinetic energy. Upon arriving at the detector the kinetic energy of the atoms is obtained by measuring their time-of-flight. The observed spectrum of energies is related to the differential reflection coefficient and, as shown in our recent publication [1], a surface phonon spectral density can be obtained. Procedures to determine the vibrational state density at an amorphous silica surface and compare it with theoretical models, will be described in this contribution.

[1] W. Steurer et al., Phys. Rev. Lett. 99, 035503 (2007).

[2] W. Steurer et a., Phys. Rev. Lett. 100, 135504 (2008)

* present address: Department of Physics and Technology, University of Bergen, Norway

Towards Direct Frequency Comb Spectroscopy using Quantum Logic

Birgit Brandstätter, Borge Hemmerling, Lukas An der Lan, Piet O. Schmidt

Institut für Experimentalphysik, Universität Innsbruck, Technikerstrasse 25, A-6020 Innsbruck, Austria

A possible change of the fine-structure constant over cosmological time scales derived from quasar absorption lines is currently strongly debated. One of the difficulties turns out to be the lack of precise laboratory data on transition lines of elements with a complex level structure such as Ti^+ and Fe^+ [1].

We challenge this problem by developing a versatile experimental setup in which spectroscopy ions are sympathetically cooled by magnesium ions in a linear Paul trap. Using quantum logic techniques, initial state preparation and state detection of the spectroscopy ion can be very efficient. Owing to the complex level structure of these spectroscopy ions, repumping from unwanted states is required. We plan to implement this by applying an appropriately tailored optical frequency comb.

We will present the latest status of our experimental setup and simulation results on the expected fluorescence signal from a Ca^+ test candidate. We furthermore present schemes based on quantum logic techniques to interrogate single ions in order to further improve the accuracy of the spectroscopic data.

[1] J. C. Berengut, V. A. Dzuba, V. V. Flambaum, M. V. Marchenko and J. K. Webb, arXiv:physics/0408017 (2006)

Towards Cryogenic Surface Ion Traps

Michael Niedermayr¹, Muir Kumph¹, Piet Schmidt¹, Rainer Blatt^{1,2}

¹*Institut für Experimentalphysik, Universität Innsbruck, Technikerstrasse 25, 6020 Innsbruck, Austria*

²*Institut für Quantenoptik und Quanteninformation, Österreichische Akademie der Wissenschaften, Otto- Hittmair-Platz 1, 6020 Innsbruck*

One promising approach for scalable quantum information processing (QIP) architectures is based on miniaturized surface ion traps [1]. These traps with dimensions in the sub- $100\mu\text{m}$ range can be fabricated by photolithography techniques [2]. Generally, experimental results indicate that the heating rate of the ions increases with decreasing trap dimensions. The mechanism of this heating is not yet fully understood. However, the heating rate can be reduced by several orders of magnitude when the trap electrodes are cooled from room temperature to 4K [3, 4]. Within a new experiment which is presently set up we intend to investigate surface traps at low temperatures in a cryogenic system. These traps will be applied for quantum simulations, for fundamental investigations of large-scale entanglement and for precision measurements enhanced by quantum metrology techniques employing entangled particles.

[1]D. Kielpinski et al., Nature 417, 709 (2002)

[2]J. Chiaverini et al., Quantum Inf. Comput. 5, 419 (2005)

[3]J. Labaziewicz et al., Phys. Rev. Lett. 100, 013001 (2008)

[4]L. Deslauriers et al., Phys. Rev. Lett. 97, 103007 (2006)

CROSS SECTIONS FOR ELASTIC ELECTRON COLLISIONS WITH SMALL ALCOHOLS

I. Iga^{*}, I. P. Sanches^{*}, R. T. Sugohara[†], M. G. P. Homem^{*} and M. T. Lee^{*}

^{}Departamento de Química, UFSCar, 13565-905 São Carlos, SP, Brazil*

[†]Departamento de Física, UFSCar, 13565-905 São Carlos, SP, Brazil

E-mail: diig@ufscar.br

Recently, there is a clear interest on studies of electron scattering by molecules due to their key role to physical and chemical transformations in fields of diverse nature, such as industrial plasmas, radiation damage in biomaterials, etc. Despite these facts, for most targets of interest, cross sections values are often not easily available. For instance, electron collisions cross sections with oxygen containing-organic molecules are very scarce. Therefore, in this contribution we will present electron scattering cross sections for methanol and ethanol.

Concerning these simple alcohols, their discovery in interstellar space and in the atmospheres of planets in the solar system has motivated recent studies of electron interaction with such species. Also the amount of ethanol vapors in our atmosphere is certainly expected to increase in the near future since it is a renewable energy source that is being increasingly used as an important bio-fuel to replace at least partially the usages of fossil fuels. Nevertheless, information available on the interaction of intermediate energy electrons and alcohols is still quite limited and mainly directed to the ionization processes [1].

In this work we have carried out studies of elastic scattering of electrons in the intermediate energy range, from ionization threshold to 1 keV. In our experiments [2], an electron beam interacts with a gaseous beam formed by alcohol vapors and the intensities of elastically scattered electrons are measured as a function of scattering angle in the (6° - 130°) angular range. The relative flow technique [3] is used to convert the experimental electron intensities to absolute differential cross sections. Results of measured cross sections and their comparison with the calculated data using the independent atom model at the static-exchange-polarization level of approximation will be presented during the Conference.

We acknowledge support by the Brazilian agencies: CNPq and FAPESP.

References

- [1] R. Rejoub, C. D. Morton, B. G. Lindsay, and R. F. Stebbings, *J. Chem. Phys.* **118**, 1756-1760 (2003) **38** 3477 (2005) and references therein..
- [2] I. Iga, I. P. Sanches, E. de Almeida, R. T. Sugohara, L. Rosani, and M. T. Lee, *J. Electron Spectr. Relat. Phenom* **155** 7 (2007).
- [3] S. K. Srivastava, A. Chutjian, and S. Trajmar, *J. Chem. Phys.* **63** 2659 (1975).

Contents

Evening Lecture

- EL 1** **R.F. Curl jr.** (Nobel Price in chemistry 1996)
A brief History of Elemental Carbon

Plenary Lectures

- PL 1** **S. Haroche**
Non-demolition photon counting and field quantum state reconstruction in a cavity: a new way to look at light
- PL 2** **M. Quack**
Theory and Spectroscopy of Parity Violation in Chiral Molecules
- PL 3** **J. Kluge**
Precision Experiments with Heavy Ions
- PL 4** **J. Schmiedmayer**
Atom Chips: Integrated circuits for matter waves
- PL 5** **F. Riehle**
Optical Atomic clocks at the Frontiers of metrology
- PL 6** **A. Weis, P. Moroshkin, V. Lebedev, A. Hofer**
Alkali Atoms, Dimers, Exciplexes and Clusters in 4He Crystals
- PL 7** **M. Scully**
Generation of short wavelength radiation via Coherent hyper Raman Superradiance
- PL 8** **G.M. Tino**
Cold Atom Interferometry for Gravitational Experiments
- PL 9** **Ch. Blondel**
Photodetachment microscopy in a magnetic field
- PL 10** **P. Corkum**
Laser induced-Tunneling, Electron Diffraction and Molecular Orbital Imaging
- PL 11** **A. Scrinzi**
Few-electron dynamics in the interaction with strong fields

Invited Progress Reports

- PR 1** **R. Wester**
Molecular Reaction Dynamics at Low Energies
- PR 2** C. Champenois, G. Hagel, M. Houssin, C. Zumsteg, F. Vedel, **M. Knoop**
1, 2, 3 Photons for Trapped Ion Spectroscopy
- PR 3** **M. Richter**, A.A. Sorokin
Non-linear Photoionization in the Soft X-ray Regime
- PR 4** **U. Becker**
Multi-photon ionization and excitation of the rare gases by Free Electron Laser radiation
- PR 5** F. Lang, K. Winkler, C. Strauss, R. Grimm, **J. Hecker-Denschlag**
Ultracold deeply-bound Rb₂ molecules
- PR 6** **P. Barker**
Manipulating cold molecular gases with intense optical fields

- PR 7** **J.R. Crespo Lopez-Urrutia, S. W. Epp, and J. Ullrich**
Resonant laser spectroscopy in the soft x-ray region
- PR 8** **V.L. Sukhorukov**
Resonances in Rare Gas Atoms: Many-Electron Theory and Experiment
- PR 9** **R. Kienberger**
Attosecond spectroscopy in atoms and solids
- PR 10** **J. Mauritsson**
Above, Around, and Below Threshold Ionization using Attosecond Pulses

Contributed Papers

- CP 1 F. Ferlaino, S. Knoop, M. Mark, M. Berninger, H. Schöbel, H.C. Nägerl, R. Grimm
Few-body physics with ultracold Cs atoms and molecules
- CP 2 L. Pruvost, H. Jelassi, B. Viaris de Lesegno
Weakly bound molecules: Analysis by the Lu-Fano method coupled to the LeRoy-Bernstein model.
- CP 3 M. Aymar, J. Deiglmayr, O. Dulieu
Calculations of static polarizabilities of alkali dimers and alkali hydrides. Prospects for alignment of ultracold molecules
- CP 4 L. van Buuren, C. Sommer, M. Motsch, M. Schenk, W.H. Pinkse, G. Rempe
Electrostatically extracted cold molecules from a cryogenic buffer gas
- CP 5 H.-D. Kronfeldt, H. Schmidt, B. Sumpf, M. Maiwald, G. Erbert, G. Tränkle
In-situ non-invasive quality control of packaged meat using a micro-system external cavity diode laser at 671 nm for Raman spectroscopy
- CP 6 D. Pinegar, C. Diehl, R. van Dyck, K. Blaum
 $^3\text{H}/^3\text{He}$ mass ratio experiment MPIK/UW-PTMS in the context of ν -mass measurements
- CP 7 S. Nic Chormaic, D. Gleeson, V. Minogin
Optical microtraps for cold atoms based on near-field diffraction
- CP 8 Th. Becker, Th. Germann, P. Thoumany, G. Stania, L. Urbonas, T. Hänsch
Optical Spectroscopy of Rubidium Rydberg Atoms with a 297nm Frequency Doubled Dye Laser
- CP 9 K. V. Rodriguez, V. Y. Gonzalez, L. U. Ancarani, D. M. Mtnik, G. Gasaneo
Helium $^{1,3}\text{S}$ excited states obtained with an angular correlated configuration interaction method
- CP 10 G. Gaigalas, E. Gaidamauskas, Z. Rudzikas
Atomic structure calculations of Cm^{+4} and Am^{+3} ions
- CP 11 G. Gaigalas, E. Gaidamauskas, J. Bieron, S. Frizsche, P. Jönsson
MCHF calculations of the electric dipole moment of radium induced by the nuclear Schiff moment
- CP 12 Sølve Selstø, J. Bengtsson, E. Lindroth
On the solution of the time dependent Dirac equation for hydrogen-like system
- CP 13 M. Safronova, R. Pal, D. Jiang, U. Safronova
Calculation of parity-nonconserving amplitude in Ra^+
- CP 14 M. Safronova, M.G. Kozlov, W.R. Johnson
Development of the CI + all-order method for atomic calculations
- CP 15 K. V. Rodriguez, V. Y. Gonzalez, L. U. Ancarani, D. M. Mtnik, G. Gasaneo
Ground state wavefunctions for two-electron systems with finite nuclear mass
- CP 16 O.Y. Khetselius
Laser separation and detecting the isotopes and nuclear reaction products and relativistic calculating the hyperfine structure parameters in the heavy-elements
- CP 17 A.V. Glushkov, O.Y. Khetselius, A.A. Svinarenko
QED approach to the photon-plasmon transitions and diagnostics of the space plasma turbulence

- CP 18 A.V. Glushkov
QED theory of laser-atom and laser-nucleus interaction
- CP 19 Kh. Yu. Rakhimov
Quantum dynamics of planar hydrogen atom in a billiard with moving boundaries
- CP 20 V.L. Sukhorukov, B.M. Lagutin, I.D. Petrov, A. Ehresmann, L. Werner, s. Klumpp, K.H. Schartner, H. Schmoranzer
Interchannel interaction in orientation and alignment of Kr $4p^4mp$ states in the excitation region of $3d^9np$ resonances
- CP 21 O. Rancova, P. Bogdanovich, R. Karpuskiene
Application of new quasirelativistic approach for treatment of oxygen-like Iron and Nickel
- CP 22 Y.S. Kozhedub, D.A. Glazov, I.I. Tupitsyn, V.M. Shabaev, G. Plunien
Relativistic recoil and higher-order electron correlation corrections to the transition energies in Li-like ions
- CP 23 R. Jursenas
Coupled tensorial forms of atomic two particle operator
- CP 24 V.K. Gudym, E.V. Andreeva
The binominal potential of electron-proton interaction alternative to the Coulomb law
- CP 25 J. Bengtsson, E. Lindroth, S. Selstø
The dynamics of meta-stable states described with a complex scaled Hamiltonian
- CP 26 L.U. Ancarani, G. Gasaneo
A simple parameter-free wavefunction for the ground state of three-body systems
- CP 27 L.U. Ancarani, G. Gasaneo, F.D. Colavecchia, C. Dal Capello
($e, 3e$) and ($\gamma, 2e$) processes on helium: interplay of initial and final states
- CP 28 M.A. Bolorizadeh, R. Fathi, E. Gahnbari-Adivi, F. Shojaei
A three body approach to calculate the differential cross sections for the excitation of H and He atoms by proton impact
- CP 29 F. Umarov, A. Dzhurakhalov
The peculiarities of elastic and inelastic energy losses at low-energy ion-surface interactions
- CP 30 R. Lomsadze, M. Gochitashvili, B. Lomsadze, N. Tsiskarishvili, D. Kugarashvili
Study of Mechanism in Alkali Metal Ion Inert Gas Atom Interaction
- CP 31 I.I. Shafranyosh, R.O. Fedorko, V.I. Marushka, T.A. Snegurskaya, V.V. Perehanets, V.V. Stetsovych
Studies of superelastic electron scattering by the metastable Thallium atoms
- CP 32 O.B. Shpenik, A.N. Zaviopulo
Ionization and Dissociative Ionization of Adenine Molecules by Electron Impact near Threshold
- CP 33 L. E. Machado, I. Iga, L. M. Brescansin, M.-T. Lee
Absorption effects in intermediate-energy electron scattering by difluoroethylene
- CP 34 S. Houamer, Y. Popov, C. Champion, C. Dal Capello
Charge transfer in collision of protons with water molecule and atomic helium at high energy
- CP 35 S.Y. Kurskov, A.S. Kashuba
 $Ar(3p^5 4p)$ states excitation in low-energy Ar-Ar collisions
- CP 36 S. Gedeon, V. Lazur
Low-energy electron scattering from calcium
- CP 37 J. Loreau, M. Desouter-Lecomte, F. Rosmej, N. Vaeck
Ab initio calculation of $H + He^+$ electron transfer cross sections
- CP 38 G. Purohit, U. Hitawala, K.K. Sud
TDCS for inner-shell ($e, 2e$) processes on alkali and alkali earth atoms Na, K, Be, Mg and Ca
- CP 39 P. Syty
The relativistic J-matrix method in scattering of electrons from model potentials and small atoms
- CP 40 V.S. Melezhik, P. Saeidian, P. Schmelcher
Multichannel atomic scattering and confinement-induced resonances in waveguides

- CP 41 E. Ovcharenko, A. Gomonai, Yu. Hutykh
Excitation of forbidden $4d^9 5s^2 \ ^2D_{5/2} - 4d^{10} 5s \ ^2P_{3/2}$ transition in In^{2+} ion at electron- In^+ ion collisions
- CP 42 A.O. Lindahl, P. Andersson, C. Diehl, O. Forstner, K. Wendt, D.J. Pegg, D. Harnstorp
The electron affinity of Tungsten
- CP 43 M. Czarnota, D. Banás M. Berset, D. Chmielewska, J-Cl. Dousse, J. Hoszowska, Y-P Maillard, O. Mauron, M. Pajek, M. Polasik, P.A. Raboud, J. Rzakiewicz, K. Stabkowska, Z. Sujkowski
High resolution measurements of molybdenum L-shell satellites and hypersatellites excited by oxygen and neon ions
- CP 44 L. Bandurina, V. Gedeon
Electron-impact scattering on boron
- CP 45 E. Baszanowska, R. Drozdowski, P.Kaminski, G. von Oppen
Observation of He-He collisions using the anticrossing method
- CP 46 V. A. Kartoshkin, S.P. Dmitriev, N.A. Dovator
Spin-exchange cross sections at the interaction between ground state rubidium and metastable helium atoms
- CP 47 V. A. Kartoshkin
Spin exchange and redistribution of the spin-polarization at the interaction between ground state alkali atoms and nitrogen atoms in gas discharge
- CP 48 L. Klosowski, M Piwinski, D. Dziczek, K. Pleskacz, S. Chwirot
Large angle e-He scattering - coincidence experiment with magnetic angle changer
- CP 49 M.T. Bouazza, C. Benseddik, M. Bouledroua
Diffusion coefficient and viriel coefficient of Krypton Atoms in a Argon Gas at Low and Moderate Temperature
- CP 50 M.T. Bouazza, M. Bouledroua
A theoretical report on ultracold collisions of two monatomic Cesium
- CP 51 V.M.Entin, I.I.Beterov, I.I. Ryabtsev, D.B. Tretyakov
Tomography of laser cooled atoms in MOT using Rydberg state excitation
- CP 52 M. Mestre, F. Diry, B. Viaris de Lesegno, L. Pruvost
Spatial light modulators for cold atom manipulation
- CP 53 O. Gorceix, Q. Beaufils, R. Chicireanu, T. Zanon, A. Crubellier, B. Laburthe-Tolra, E. Maréchal, L. Vernac, J-C. Keller
All-optical Bose-Einstein condensation of Chromium atoms and rf spectroscopy of cold Cr_2 molecules
- CP 54 M. Seliger, U. Hohenester, G. Pfanner
Entangled photons from excitonic decay in artificial atoms
- CP 55 J. Grond, U. Hohenester, J. Schmiedmayer
Optimizing number squeezing when splitting a mesoscopic condensate
- CP 56 I.E. Mazets, T. Schumm, J. Schmiedmayr
Breakdown of integrability in a quasi-one-dimensional ultracold bosonic gas
- CP 57 J-F. Clément, J-P. Brantut, M. Robert de St. Vincent, G. Varoquaux, R.A. Nyman, A. Aspect, T. Bourdel, P. Bouyer
Light-shift tomography in an optical-dipole trap
- CP 58 H. Knöckel, S. Liu, I. Sherstov, C. Lisdat, E. Tiemann
Matter wave interferometry with K_2 molecules
- CP 59 E. Maréchal, B. Laburthe-Tolra, L.Vernac, J.-C. Keller, O. Gorceix
A magnetic lens for cold atoms tuned by a rf field
- CP 60 T. Pfau, Th. Lahaye, J. Metz, B. Fröhlich, T. Koch, A. Greismaier
Stability and d-wave collapse of a dipolar BEC
- CP 61 K. Chebakov, N. Kolachevsky, A. Akimov, I. Tolstikhina, P. Rodionov, S. Kanorsky, V. Sorokin
Blue cooling transitions of thulium atom

- CP 62 J.Szczepkowski, R. Abdoul, R. Gartman, W. Gawlik, M. Witkowski, J. Zachorowski, M. Zawada
Free-fall expansion of finite-temperature Bose-Einstein condensed gas in the non Thomas-Fermi regime
- CP 63 N. Kolachevsky, E. Tereschenko, M. Egorov, A. Sokolov, A. Akimov, V. Sorokin
Resonance Interaction between Cold Rb Atoms and a Frequency Comb
- CP 64 M. Witkowski, R. Gartman, W. Gawlik, J. Szczepkowski, M. Zawada
Optical tailoring of spatial distribution of the BEC and non-degenerate cold atoms. Non-periodic optical lattice
- CP 65 F. Tantussi, N. Porfido, F. Prescimone, V. Mangasuli, M. Allegrini, E. Arimondo, F. Fuso
Laser techniques for atom-scale technologies
- CP 66 F. Fuso, M. Bassu, F. Tantussi, L. Strambini, G. Barillaro, M. Allegrini
Emission from Silicon/Gold nanoparticle systems
- CP 67 I. Ulfat, J. Adell, J. Sadowski, L. Ilver, J. Kanski
As_{3d} Core Level Photoemission Studies of (GaMn)As annealed under As capping
- CP 68 N. Alinejad, M. Jahangir, F. Izadi
Pulsed laser Deposition Simulation for Graphite Target using Monte-Carlo Method
- CP 69 C. Diehl, D. Pinegar, R. S. Van Dyck Jr, K. Blaum
Precision Measurement of the ³He-³H mass ratio with the MPIK/UW-PTMS
- CP 70 A. Alonso-Medina, C. Colón, C. Herrán-Martínez
Measured of different atomic parameters of some elements (Ca, Sn, Pb) in a plasma generated by Laser-Induced Breakdown Spectroscopy (LIBS)
- CP 71 T. Carette, C. Drag, C. Blondel, C. Delsart, C. Froese Fischer, M. Godefroid, O. Scharf
Isotope shift in the electron affinity of sulfur
- CP 72 A.K. Kazansky, N.M. Kabachnik
Theoretical study of attosecond chronoscopy of strong-field atomic photoionization
- CP 73 A.V. Glushkov, O.Y. Khetselius, A.V. Loboda
Generation of ultra-short X-ray pulses in cluster system during ionization by femto-second optical pulse
- CP 74 J. Alnis, A. Matveev, T. W. Hänsch, C. Parthey, N. Kolachevsky
Long-term stability of high-finesse Fabry-Perot resonators made from Ultra-Low-Expansion glass
- CP 75 H.-D. Kronfeldt, H. Schmidt
Application of Surface-Enhanced-Raman-Scattering (SERS) for In-Situ Detection of PAHs in Sea-Water
- CP 76 S. Qamar Hussain, M. Saleem, A. Baig
Laser Based Isotopic Separation of Atoms
- CP 77 D. Gleeson, V. Minogin, S. Nic Chormaic
Atomic fluorescence coupled into a thin optical fibre
- CP 78 D.U. Matrasulov, T.A. Ruzmetov, D.M. Otajanov, P.K. Khabibullaev, A.A. Saidov, F.C. Khanna
Nonlinear dynamics of atoms in a cavity
- CP 79 G.G. Grigoryan, Y. Pashayan-Leroy, C. Leroy, S. Guèrin
Storage of optical pulses in solids despite fast relaxation
- CP 80 M. Motsch, M. Zeppenfeld, G. Rempe, W. Pinkse
Purcell-enhanced Rayleigh scattering into a Fabry-Perot cavity
- CP 81 M. Agre
Circular and elliptical dichroism effects in two-photon disintegration of atoms and molecules
- CP 82 I. L. Glukhov, V. D. Ovsyannikov
Thermal ionization of alkali Rydberg atoms
- CP 83 V.D. Ovsyannikov, E. Yu. Ilinova
Hyperpolarizabilities of multiplet Rydberg states in alkali and alkaline-earth atoms
- CP 84 N. N. Bezuglov, K. Miculis, A. Ekers, J. Denskat, C. Giese, T. Amthor, M. Weidemüller
Penning ionization of cold Rb Rydberg atoms due to long-range dipole-dipole interaction

- CP 85 I.I.Beterov, I.I. Ryabtsev, D.B. Tretyakov, N.N Bezuglov, A. Ekers, V.M. Entin
Ionization of alkali-metal Rydberg atoms by blackbody radiation
- CP 86 B. T. Torosov, N.V. Vitanov
Level-crossing transition between mixed states
- CP 87 S.Werbowy, J. Kwela
M1-E2 interference in the Zeeman spectra of Bi I
- CP 88 E. Efremova, G. Anisimova, R. Semenov, G. Tsygankova
Numerical investigation of Ne I for 2p55g configuration and Ar I for 3p55g configuration Zeeman structure
- CP 89 A. Papoyan, G. Hakhumyan, A. Atvars, M. Auzinsh, D. Sarkisyan
Method for quantitative study of atomic transitions in magnetic field based on vapor nanocell with $L = \lambda$
- CP 90 D. Glazov, A. Volotka, V. Shabaev, I. Tupitsyn, G. Plunien
g factor of boronlike ions
- CP 91 V. Chernushkin, V. Ovsianikov
Magnetolectric Jones spectroscopy of Li and Na atoms
- CP 92 A. Kamenski, V. Ovsianikov
Radiative transition probabilities from D Stark states in orthohelium
- CP 93 M. Ryabinina, L. Melnikov
Light-induced quasi-static polarization in hydrogen-like atom under the action of strong electromagnetic laser field
- CP 94 G.Skolnik, N. Vujicic, T. Ban, S. Vdovic, G. Pichler
Doppler-free spectroscopy of rubidium atoms placed in a magnetic field
- CP 95 M. Pawlak, M. Bylicki
Electric field influence on the hydrogen atom embedded in a plasma
- CP 96 B. Schnizer, Th. Heubrandtner, E. Rössl, M. Musso
Dynamic and geometric phases in the Stark Zeeman effect of the hyperfine structure of one-electron atoms
- CP 97 A. Costescu, C. Stoica, S. Spanulescu
New analytical relativistic formulae for the total photoeffect cross section for the K-shell electrons
- CP 98 N.L. Manakov, S.I. Marmo, S.Sviridov
Two-photon above-threshold ionization by a VUV-light
- CP 99 N.L. Manakov, S.I. Marmo, S.Sviridov
Above-threshold polarizability of alkali-metal and noble gas atoms
- CP 100 V. Richardson, J. Dardis, P. Hayden, P. Hough, E.T. Kennedy, J.T. Costello, S. Dsterer, W. Li, A. Azima, H. Redlin, J. Feldhaus, D. Cubaynes, D. Glijer, M. Meyer
Ionisation in Intense Superposed XUV + NIR Laser Fields
- CP 101 V.L.Sukhorukov, I.D. Petrov, H. Hotop
Photoionization of excited rare gas atoms $Rg(mp5(m+1)p J=0-3)$ in the autoionization region
- CP 102 S.Y. Yousif Al-Mulla
Spin dependent exchange scattering from ferromagnetic materials
- CP 103 K. Alioua, M. Bouledroua, A. Allouche, and M. Aubert-Frécon
Far-wing collisional broadening of the Na(3s-3p) line by helium
- CP 104 S. Chelli, M. Bouledroua
Excited and ground potassium monatoms perturbed by helium
- CP 105 L. Reggami, M. Bouledroua
Pressure broadening of calcium resonance line perturbed by helium
- CP 106 E. Saks, I. Sydoryk, N. N. Bezuglov, I. I. Beterov, K. Miculis, A. Ekers
Broadening and intensity redistribution in the atomic hyperfine excitation spectra due to optical pumping in the weak excitation limit

- CP 107 B. Mahrov, C. Andreeva, N. Bezuglov, K. Miculis, E. Saks, M. Bruvelis, A. Ekers
Reconsideration of spectral line profiles affected by transit time broadening
- CP 108 G. Auböck, J. Nagl, C. Callegari, W.E. Ernst
Alkali doped Helium Droplets in a Magnetic Field
- CP 109 J. Nagl, G. Auböck, A.W. Hauser, O. Allard, C. Callegari, W.E. Ernst
Quartet alkali trimers on He nanodroplets: Laser spectroscopy and ab initio calculations
- CP 110 R. Hefferlin
Group Dynamics of 2-Atom Even-Electron Molecules and Ions
- CP 111 A. Dantan, P. Herskind, J. Marler, M. Albert, M.B. Langkilde-Lauesen, M. Drewsen
11:30 Cavity-QED with ion Coulomb crystals
- CP 112 U. Hohenester, A. Eiguren, S. Scheel, E.A. Hinds
11:45 Spin flip lifetimes in superconducting atom chips
- CP 113 A. Cerè, V. Parigi, M. Abad, F. Wolfgramm, A. Predojevic, M. Mitchell
12:00 Interaction-Free Measurement of the Degree of Polarization of an Atomic Ensemble
- CP 114 J. Koperski, M. Krosnicki, M. Strojecki
12:15 Entangled atom-pairs from dissociated dimers: an experimental test of Bell inequality for atoms
- CP 115 G. Casa, A. Castrillo, G. Galzerano, R. Wehr, A. Merlone, D. Di Serafino, P. Laporta, L. Gianfrani
11:00 Primary gas thermometry by means of near-infrared laser absorption spectroscopy and determination of the Boltzmann constant
- CP 116 V. Batteiger, M. Herrmann, S. Knünz, A. Ozawa, A. Vernaleken, G. Saathoff, M. Semczuk, F. Zhu, H. Schuessler, Th. Hänsch, T. Udem
11:15 Towards precision spectroscopy in the XUV
- CP 117 P.F. Staunum, K. Hojbjerg, R. Wester, M. Drewsen
11:30 Probing isotope effects in chemical reactions using single ions
- CP 118 N.A. Matveeva, A.V. Taichenachev, A.M. Tumaikin, V.I. Yudin
11:45 Laser cooling of unbound atoms in nondissipative optical lattice
- CP 119 R. Lammegger, E. Breschi, G. Kazakov, G. Mileti, B. Matisov, L. Windholz
11:30 Investigations on the lin||lin CPT and its application in quantum sensors
- CP 120 J. Klein, F. Beil, T. Halfmann
11:45 Optically Driven Atomic Coherences: from the gas phase to the solid state
- CP 121 F. A. Hashmi, M. A. Bouchene
12:00 Slowing light and coherent control of susceptibility in a duplicated two-level system
- CP 122 T. Pfau, R. Heidemann, U. Raitzsch, V. Bendkowsky, B. Butscher, R. Löw
12:15 Rydberg excitation of a Bose-Einstein Condensate
- CP 123 S. Kreim, K. Blaum, H. Kracke, A. Mooser, W. Quint, C. Rodegheri, S. Ulmer, J. Walz
11:30 Progress towards a high-precision measurement of the g-factor of a single, isolated (anti)proton in a double Penning trap
- CP 124 R. E. Zillich, M. Leino, A. Viel
11:15 Helium-4 Clusters Doped with Excited Rubidium Atoms
- CP 125 M. Koch, J. Lanzersdorfer, G. Auböck, J. Nagl, C. Callegari, and W. E. Ernst
11:30 Progress in optically-detected spin-resonance on helium droplets
- CP 126 I.I. Ryabtsev, D.B. Tretyakov, I.I. Beterov, V.M. Entin
11:45 Effect of finite detection efficiency on the observation of the dipole-dipole interaction of a few Rydberg atoms
- CP 127 A.V. Glushkov, O.Yu. Khetselius, S.V. Malinovskaya, Yu. V. Dubrovskaya
Energy approach to discharge of metastable nuclei during negative muon capture
- CP 128 A.V. Glushkov
Resonance phenomena in heavy ions collisions and structurization of positron spectrum
- CP 129 O.Y. Khehtselius
Dynamics of the resonant levels for atomic and nuclear ensembles in a laser pulse: optical bi-stability effect and nuclear quantum optics

- CP 130 A.V. Glushkov, O.Y.Khetselius, E.P. Gurnitskaya, Yu. V. Dubrovskaya, D.E. Sukharev
Spectroscopy of the hadronic atoms and superheavy ions: Spectra, energy shifts and widths, hyperfine structure
- CP 131 K. Katsonis, Ch. Berenguer, R. Srivastava, L. Sharma, R. Clark, M. Cornille, A.D. Stauffer
Ar I transition probabilities and excitation cross sections involving the 4s metastable levels and the 4/5p configurations
- CP 132 G. Malcheva, K. Blageov, R. Mayo, M. Ortiz, J. Ruiz, L. Engström, H. Lundberg, S.Svanberg, H. Nilsson, P. Quinet, E. Biémont
Radiative data in the Zr I spectrum
- CP 133 G.P. Gupta
Energy levels, oscillator strengths and lifetimes in C1 IV
- CP 134 G.P. Gupta
Large scale CIV 3 calculations of fine-structure energy levels and lifetimes in Al-like copper
- CP 135 C. Colon, A. Alonso-Medina, A. Zanon, J. Albeniz
Levels energies, oscillator strengths, and lifetimes for transition in Pb III
- CP 136 E. Träbert
Hyperfine interaction induced decays in highly charged ions
- CP 137 A. Stepanov
Einstein coefficients for activation barriers of equilibrium and non-equilibrium processes caused by Plank radiation
- CP 138 V. Fivet, E. Biemont, P. Palmeri, P. Quinet
New transition probabilities of astrophysical interest in triply ionized lanthanum (La IV)
- CP 139 J. Gurell, P. Lundin, S. Mannervik. L.O.Norlin, P. Royen
A new method for determining minute long lifetimes of metastable levels
- CP 140 J. Gurell, P. Lundin, S. Mannervik. L.O.Norlin, P. Royen, P. Schef, H. Hartman, A. Hibbert, H. Lundberg, K. Blageov, P. Palmeri, P. Quinet, E. Biémont
Lifetime measurements of metastable states of astrophysical interest
- CP 141 M.-T. Lee, M. Fujimoto, S. Michelin, I. Iga
Spin-exchange effects in elastic electron scattering from linear triatomic radicals
- CP 142 S. Zapryagaev, E.Butyrskaya
Spectral properties of interactions in endohedral fullerenes Li₂@c₆₀ and Na₂@C₆₀
- CP 143 S. Zapryagaev, E.Butyrskaya
Simulation of fullerene formation
- CP 144 I.I.Shafranyosh, M.I.Sukhoviya, M.I.Shafranyosh, R.O. Fedorko
Cross sections of negative ion production in electron collisions with Adenine molecules
- CP 145 O. Ryazanova, O. Nesterov, V. Zozulya
Effect of divalent metal ions on the conformational transitions in poly(dA)+poly(dT) system
- CP 146 K. Hubisz, T. Wroblewski, V.I. Tomin
Anomalous inhomogeneous broadening and kinetics properties of DMABN
- CP 147 L. Pruvost, H. Jelassi, B. Viaris de Lesegno
Reexamination of the LeRoy-Bernstein formula for weakly bound molecules
- CP 148 F. Talbi, M. Bouledroua, K. Alioua
The singlet X -A and X -B absorption coefficient of the K₂ system
- CP 149 A. W. Hauser, C. Callegari, W.E. Ernst, P. Soldán
Atomic-like shell models for alkali trimers derived from ab initio calculations
- CP 150 L. Busevica, R. Ferber, O. Nikolayeva, E. Pazyuk, A. Stolyarov, M. Tamanis
First observation and analysis of the (1; 2)¹Π states of KCs
- CP 151 O. Nikolayeva, R. Ferber, M. Tamanis, K. Knöckel, E. Tiemann, A. Pashov
High resolution spectroscopy and IPA potential construction of a³Σ⁺ state in KCs

- CP 152 J. Heldt, M. Józefowicz, J. R. Heldt
Determination of first-order molecular hyperpolarizability of ethyl 5-(4-aminophenyl)-3-amino-2,4-dicyanobenzoate using steady-state spectroscopic measurements and quantum-chemical calculations
- CP 153 L.E. Sansores, J. Muniz, A. Martinez, R. Salcedo
Electronic structure of the $[\text{Au}_2(\text{dmpm})(i - \text{mnt})]$ complex
- CP 154 T. L. Dimitrova, A. Weis
A lecture demonstration of quantum erasing on a photon by photon basis
- CP 155 J.L. Robyr, P. Knowles, A. Weis
Stark shift in the Cs clock transition frequency
- CP 156 P. Knowles, G. Bison, N. Castagna, A. Hofer, A. Mtehdlishvili, A. Pazgalev, A. Weis
Magnetic Field Imaging With Arrays of Cs Magnetometers: Technology and Applications
- CP 157 R. Lammegger, L. Windholz
Performance of a compact dark state Magnetometer
- CP 158 A. Litvinov, G. Kazakov, B. Matisov
Laser-induced transport effect and laser induced-line narrowing mechanism for laser excitation in ^{87}Rb atomic vapors in a finite-size buffer-less cell
- CP 159 G.G. Grigoryan, G. Nikoghosyan, A. Gogyan, Y.T. Pashayan-Leroy, C. Leroy, S. Guerin
Population transfer, light storage, and superluminal propagation by bright-state adiabatic passage
- CP 160 C. Andreeva, N. Bezuglov, A. Ekers, K. Miculis, B. Mahrov, I. Ryabtsev, E. Saks, R. Garcia-Fernandez, K. Bergmann
Population switching of Na and Na₂ excited states by means of interference due to Autler-Townes effect
- CP 161 E. Alipieva, E. Taskova, S. Gateva, G. Todorv
High-rank polarization moments influence on the CPT resonance obtained on two-level degenerated system
- CP 162 K. Vaseva, P. Todorov, S. Caraleva, D. Slavov, S. Saltiel
Sub-Doppler fluorescence spectroscopy of Cs-vapour layers with nano-metric thickness
- CP 163 P. Todorov, S. Cartaleva, K. Vaseva, C. Andreeva, I. Maurin, D. Slavov, S. Saltiel
Absorption in the saturation regime of Cs-vapour layer with thickness close to the light wavelength
- CP 164 M. Auzins, R. Ferber, I. Fescenko, L. Kalvans, M. Tamanis
Dark and bright resonances in large J systems
- CP 165 M. Auzinsh, R. Ferber, F. Gahbauer, A. Jarmola, L. Kalvans
F-resolved bright and dark magneto-optical resonances at the cesium D_1 line
- CP 166 T. Kirova, A. Ekers, N. N. Bezuglov, I. I. Ryabtsev, K. Blushs, M. Auzinsh
Effects of hyperfine structure on the Autler-Townes splitting
- CP 167 A.Sargsyan, M.G. Bason, D. Sarkisyan, Y. Pashayan-Leroy, A.K. Mohapatra, C.S. Adams
Ladder and lambda systems electromagnetically induced transparency in thin and extremely-thin cells
- CP 168 A. Sargsyan, D. Sarkisyan, A. Papoyan, Y. Pashayan-Leroy, C. Leroy, P. Moroshkin, A. Weis
Saturation effects of Faraday rotation signals in Cs vapor nanocells: thickness-dependent effects
- CP 169 L. Kalvans, M. Auzinsh, R. Ferber, F. Gahbauer, A. Jarmola, A. Papoyan, D. Sarkisyan
Magneto-optical resonances in atomic rubidium at D_1 excitation in ordinary and extremely thin cells
- CP 170 A.Y. Samokotin, A.V. Akimov, N.N. Kolachevsky, Y. V. Vladimirova, V.N. Zadkov, A.V. Sokolov, V. N. Sorokin
Frequency-modulation spectroscopy of coherent population trapping resonances
- CP 171 K. Dahl, L. Spani, R.H. Rinkleff, K. Danzmann
Pump-probe spectroscopy: a survey of the spectra for four polarization combinations in degenerate two-level atoms
- CP 172 Z. Grujic, M. Mijailovic, D. Arsenovic, M. Radonjic, B. M. Jelenkovic
Dark resonance narrowing in uncoated rubidium vacuum vapor cell

- CP 173 S. S. Ivanov, P. Ivanov, N. Vitanov
Quantum search with trapped ions
- CP 174 G. von Oppen
The observability of atoms
- CP 175 T. Leveque, A. Gauguet, W. Chaibi, A. Landragin
Characterization of a high precision cold atom gyroscope
- CP 176 F. Shojaei Baghini, M. A. Bolorizadeh, R. Fathi, E. Ganhbari Adivi
Electron capture of methane molecule by proton impact
- CP 177 Ch.Berenguer, K. Katsonis, R. Srivastava, L. Sharma, R. Clarks, A.D. Stauffer
Excitation of the Xe I 6s metastables to the 6p and 7p configurations
- CP 178 G. P. Anisimova, E. Efremova, G. A. Tsygankova
Parametrization of Ne I spectrum for 2p55g, 6g, 7g configurations using semiempirical method
- CP 179 R. Karpuskiene, P. Bogdanovich, O. Rancova
Ab initio calculations of aluminium-like calcium
- CP 180 T.J. Wasowicz, S. Werbowy, R. Drozdowski, J. Kwela
Isotope shifts of forbidden lines of Lead
- CP 181 P. Moroshkin, V. Lebedev, A. Weis
Solid ^4He stabilized by charged impurities below the solidification pressure of pure helium
- CP 182 P. Moroshkin, V. Lebedev, A. Weis
Spectroscopy of Ba atoms isolated in solid He matrix
- CP 183 A. Matveev, J. Alnis, C. Parthey, N. Kolachevsky, T. W. Hänsch
New Measurement of the 2S Hyperfine Splitting in Atomic Hydrogen
- CP 184 Yu.P. Gangrsky, K.P. Marinova, S.G. Zemlyanoi, M. Avogoulea, J. Billowes, P. Campbell, B. Cheal, B. Tordoff, M. Bissel, D.H. Forest, M. Gardner, G. Tungate, J. Huikari, H. Penttila, J. Aysto
High Resolution Laser Spectroscopy of Scandium
- CP 185 S. Poonia
 $L_{\alpha 1}$, $L_{\alpha 2}$, $L_{\beta 1}$, $L_{\beta 2}$ and L_{γ} satellites in the X-Ray emission spectra
- CP 186 S. Poonia
Origin of X-Ray satellites spectra in the $L_{\alpha 1}$ and $L_{\alpha 2}$ region
- CP 187 H.P. Garnir, E. Biemont, S. Enzonga Yoca, P. Quinet
VUV Spectroscopy of Xe IX
- CP 188 V. Fivet, E. Biémont, P. Palmeri, P. Quinet, L. Engström, H. Lundberg, H. Nilsson
Improved atomic data for platinum group elements
- CP 189 F. Gilleron, J. c. Pain, J. Bauche, C. Bauche-Arnoult
Impact of high-order moments on the statistical modeling of transition arrays
- CP 190 J. C. Pain, F. Gilleron
Exact and statistical methods for computing the distribution of states, levels and E1 lines in atomic spectra
- CP 191 Y.Nighat, R. Islam
Laser optogalvanic spectroscopy of Lanthanum in Spectral range of Rhodamine 6 G
- CP 192 A. Nadeem
Investigation of the even parity states of group II-B elements (Zn, Cd and Hg)
- CP 193 Z. Uddin, L. Windholz, F. Akber, M. Jahangir, I. Siddiqui
New levels of Pr I discovered via infrared spectral lines
- CP 194 A. Er, I.K. Öztürk, Gö. Basar, S. Kroeger, Gü. Basar, A. Jarmola, M. Tamanis, R. Ferber
New lines of atomic niobium in Fourier transform spectra
- CP 195 J. Dembczynski, M. Elantkowska, J. Ruczkowski
Configuration interaction effects in the fine- and hyperfine structure of the even configuration system of tantalum atom

- CP 196 E. Stachowska, J. Dembczynski, L. Windholz
Extended analysis of the even configurations of Ta II
- CP 197 B. Furmann
Search for new electronic levels in singly ionized europium Eu II
- CP 198 B. Acrimowicz, J. Dembczynski
Analysis of the odd configurations of tantalum atom – search for configurations containing f electrons
- CP 199 J. Dembczynski, M. Elantkowska, J. Ruczkowski
Program package for semi-empirical analysis of the fine- and hyperfine structure of complex atoms
- CP 200 M. Elantkowska, J. Ruczkowski, J. Dembczynski
Procedure for precise determination of the hyperfine structure constants A, B, C and D. Example of lanthanum atom
- CP 201 B. Gamper, L. Windholz
Investigations of the Hyperfinestructure of Praseodymium in the IR-Region with the help of FTS
- CP 202 P. Glowacki, L. Windholz, J. Dembczynski
Investigation of the hyperfine structure of Ta I - - lines
- CP 203 I. Siddiqui, B. Gamper, G.H. Guthöhrlein, L. Windholz
Perturbed intensity distribution of hyperfine components of Praseodymium-I lines
- CP 204 S. Khan, S.T. Iqbal, I. Siddiqui, L. Windholz
Investigation of the hyperfine structure of Pr I - lines in the region 5630 Å to 5772 Å
- CP 205 G. Krois, G.H. Guthöhrlein, L. Windholz
Correction of Pr I energy level values due to Fourier transform spectra and laser excitation
- CP 206 H. Reschab, C. Cagran, R. Tanzer, W. Schützenhöfer, A. Graf, G. Pottlacher
Normal spectral emissivity depending on atomic composition for two nickel-based and two ferrous-based alloys at 684.5 nm
- CP 207 T. Hüpf, C. Cagran, G. Pottlacher, G. Lohöfer
Identification of atomic structure in measurement data, depending on the used set of units
- CP 208 S. Cohen, M. M. Harb, A. Ollagnier, S. Cohen, F. Lepine, F. Robicheaux, M. Vrakking, C. Bordas
Electronic Wavefunction Microscopy using slow-photoelectron Imaging
- CP 209 E. Dimova, D. Zhechev, V. Steflekova
On a self-sustained oscillating mode for operation of a glow discharge
- CP 210 A. Kortyna and V. Fiore
Atomic beam measurements of the Cs $7d\ ^2D_{3/2}$ hyperfine parameters with two-photon fluorescence spectroscopy
- CP 211 O.B. Shpenik, E.E. Kontros, I.V. Chernyshova
Electron scattering by Cadmium atoms
- CP 212 W. Steurer, B. Holst, J.R. Manson, W.E. Ernst
Probing surface vibrations of amorphous solids by helium atom scattering
- CP 213 B. Brandstätter, B. Hemmerling, L. An der Lan, P.O. Schmidt
Towards Direct Frequency Comb Spectroscopy using Quantum Logic
- CP 214 M. Niedermayr, M. Kumph, Piet Schmidt, Rainer Blatt
Towards Cryogenic Surface Ion Traps
- CP 215 I. Iga, I. P. Sanches, R. T. Sugohara, M. G. P. Homem and M. T. Lee
Cross sections for elastic electron collisions with small alcohols

Author Index

Abad	M	CP 113
Abdoul	R.	CP 62
Acrimowicz	B.	CP 198
Adams	C.s.	CP 167
Adell	J.	CP 67
Agre	M.Ya.	CP 81
Akber	F.	CP 193
Akimov	A.	CP 61
Akimov	A.	CP 63
Akinov	A.V.	CP 170
Albéniz	J.	CP 135
Albert	M	CP 111
Alinejad	N.	CP 68
Alioua	K.	CP 103
Alioua	K.	CP 148
Alipieva	E.	CP 161
Allard	O.	CP 109
Allegrini	M.	CP 65
Allegrini	M	CP 66
Allouche	A.	CP 103
Alnis	J.	CP 183
Alnis	J.	CP 74
Alonso-Medina	A.	CP 70
Alonso-Medina	A.	CP 135
Amthor	T.	CP 84
Ancarani	L.U.	CP 9
Ancarani	L.U.	CP 15
Ancarani	L.U.	CP 26
Ancarani	L.U.	CP 27
An der Lahn	L.	CP 213
Andersson	P.	CP 42
Andreeva	C.	CP 107
Andreeva	C.	CP 160
Andreeva	C.	CP 163
Andreeva	E.V.	CP 24
Anisimova	G.P.	CP 88
Anismova	G.P.	CP 178
Arimondo	E.	CP 65
Arsenovic	D.	CP 172
Aspect	A.	CP 57
Atvars	A.	CP 89
Aubert-Frécon	M.	CP 103
Auböck	G-	CP 108
Auböck	G.	CP 109
Auböck	G.	CP 125
Auzinsh	M.	CP 89
Auzinsh	M.	CP 164
Auzinsh	M.	CP 165
Auzinsh	M.	CP 166
Auzinsh	M	CP 169
Avgoulea	M.	CP 184
Aymar	M.	CP 3
Aysto	J.	CP 184
Azima	A.	CP 100
Baig	M.A.	CP 76
Ban	T.	CP 94
Banás	D.	CP 43

Bandi	T.N.	CP 7
Bandurina	L.	CP 44
Barillaro	G.	CP 66
Barker	P.F.	PR 6
Basar	Gü.	CP 194
Basar	Gö.	CP 194
Bason	M.G.	CP 167
Bassu	M.	CP 66
Baszanowska	E.	CP 45
Batteiger	V.	CP 116
Bauche	J.	CP 189
Bauche-Arnoult	C.	CP 189
Beaufils	Q.	CP 53
Becker	Th.	CP 8
Becker	U.	PR 4
Beil	F.	CP 120
Bendkowsky	V.	CP 122
Bengtsson	J.	CP 12
Bengtsson	J.	CP 25
Beninger	M.	CP 1
Benseddik	C.	CP 49
Berenguer	Ch.	CP 131
Berenguer	Ch.	CP 177
Bergmann	K.	CP 160
Berset	M	CP 43
Beterov	I.I.	CP 51
Beterov	I.I.	CP 85
Beterov	I.I.	CP 106
Beterov	I.I.	CP 126
Bezuglov	N.N.	CP 84
Bezuglov	N.N.	CP 85
Bezuglov	N.N.	CP 106
Bezuglov	N.N.	CP 107
Bezuglov	N.	CP 160
Bezuglov	N.N.	CP 166
Biémont	E.	CP 132
Biémont	E.	CP 138
Biémont	E.	CP 140
Biémont	E.	CP 187
Biémont	E.	CP 188
Bieron	J.	CP 11
Billowes	J.	CP 184
Bison	G.	CP 156
Bissel	M.	CP 184
Blagoev	K.	CP 132
Blagoev	K.	CP 140
Blatt	R.	CP 214
Blaum	K.	CP 6
Blaum	K.	CP 69
Blaum	K.	CP 123
Blondel	C.	PL 9
Blondel	C.	CP 71
Blushs	K.	CP 166
Bogdanovic	P.	CP 21
Bogdanovic	P.	CP 179
Bolorizadeh	M.A.	CP 28
Bolorizadeh	M.A.	CP 176
Bordas	C.	CP 208
Bouazza	M.T.	CP 49
Bouazza	M.T.	CP 50

Bouchene	M.A.	CP 121	Czarnota	M.	CP 43
Bouledroua	M.	CP 49	Dahl	K.	CP 171
Bouledroua	M.	CP 50	Dal Cappello	C.	CP 27
Bouledroua	M.	CP 103	Dal Cappello	C.	CP 34
Bouledroua	M.	CP 104	Dantan	A.	CP 111
Bouledroua	M.	CP 105	Danzmann	K.	CP 171
Bouledroua	M.	CP 148	Dardis	J.	CP 100
Bourdel	T.	CP 57	de St. Vincent	M.R.	CP 57
Bouyer	P.	CP 57	Deiglmayr	J.	CP 3
Brandstätter	B.	CP 213	Delsart	C.	CP 71
Brantut	J.P.	CP 57	Delsart	C.	PL 9
Brescansin	L.M.	CP 33	Dembczynski	J.	CP 195
Breschi	E.	CP 119	Dembczynski	J.	CP 196
Bruvelis	M.	CP 107	Dembczynski	J.	CP 198
Busevica	L.	CP 150	Dembczynski	J.	CP 199
Butscher	B.	CP 122	Dembczynski	J.	CP 200
Butyrskaya	E.V.	CP 142	Dembczynski	J.	CP 202
Butyrskaya	E.V.	CP 143	Denskat	J.	CP 84
Bylicki	M.	CP 95	Desouter-Lecomte	M.	CP 37
Cagran	C.	CP 206	di Serafino	D.	CP 115
Cagran	C.	CP 207	Diehl	Ch.	CP 6
Callegari	C.	CP 108	Diehl	C.	CP 42
Callegari	C.	CP 109	Diehl	Ch.	CP 69
Callegari	C.	CP 125	Dimitrova	T.L.	CP 154
Callegari	C.	CP 149	Dimova	E.	CP 209
Campbell	P.	CP 184	Diry	F.	CP 52
Carette	T.	CP 71	Dmitriev	S.P.	CP 46
Cartaleva	S.	CP 162	Dousse	J.Cl.	CP 43
Cartaleva	S.	CP 163	Dovator	N.A.	CP 46
Casa	G.	CP 115	Drag	C.	CP 71
Castagna	N.	CP 156	Drag	C.	PL 9
Castrillo	A.	CP 115	Drewsen	M.	CP 111
Cerè	A.	CP 113	Drewsen	M.	CP 117
Chaeal	B.	CP 184	Drozdowski	R.	CP 45
Chaibi	W.E.	CP 175	Drozdowski	R.	CP 180
Chaibi	W.	PL 9	Dsterer	S.	CP 100
Champenois	C.	PR 2	Dubrovskaya	Yu.V.	CP 127
Champion	C.	CP 34	Dubrovskaya	Yu.V.	CP 130
Chebakov	K.	CP 61	Dulieu	O.	CP 3
Chelli	S.	CP 104	Dzhurakhalov	A.A.	CP29
Chernushkin	V.V.	CP 91	Dziczek	D.	CP 48
Chernyshova	I.V.	CP 211	Efremova	E.A.	CP 88
Chicireanu	R.	CP 53	Efremova	E.A.	CP 178
Chmielewska	D.	CP 43	Egorov	M.	CP 63
Chwirot	S.	CP 48	Ehresmann	A.	CP 20
Clark	R.E.H.	CP 131	Eiguren	A.	CP 112
Clark	R.E.H.	CP 177	Ekers	A.	CP 84
Clément	J.F.	CP 57	Ekers	A.	CP 85
Cohen	S.	CP 208	Ekers	A.	CP 106
Colavecchia	F.D.	CP 27	Ekers	A.	CP 107
Colón	C.	CP 135	Ekers	A.	CP 160
Colón	C.	CP 70	Ekers	A.	CP 166
Corkum	P.	PL 10	Elantowska	M.	CP 195
Cornille	M.	CP 131	Elantowska	M.	CP 199
Costello	J.T.	CP 100	Elantowska	M.	CP 200
Costescu	A.	CP 97	Engström	L.	CP 132
Crespo Lopez-U.	J.R.	PR 7	Engström	L.	CP 188
Crubellier	A.	CP 53	Entin	V.M.	CP 51
Cubaynes	D.	CP 100	Entin	V.M.	CP 85
Curl	R.F., jr.	EL 1	Entin	V.M.	CP 126

Enzonga Yoca	S.	CP 187	Ghanbari Adivi	E.	CP 28
Epp	S.W.	PR 7	Ghanbari Adivi	E.	CP 176
Er	A.	CP 194	Giafrani	L.	CP 115
Erbert	G.	CP 5	Giese	C.	CP 84
Ernst	W.E.	CP 108	Gilleron	F.	CP 189
Ernst	W.E.	CP 109	Gilleron	F.	CP 190
Ernst	W.E.	CP 125	Glazov	D.A.	CP 22
Ernst	W.E.	CP 149	Glazov	D.A.	CP 90
Ernst	W.E.	CP 212	Gleeson	D.	CP 77
Fathi	R.	CP 28	Glijer	D.	CP 100
Fathi	R.	CP 176	Glowacki	P.	CP 202
Fedorko	R.O.	CP 144	Glukhov	I.L.	CP 82
Fedorko	R.O.	CP 31	Glushkov	A.V.	CP 17
Feldhaus	J.	CP 100	Glushkov	A.V.	CP 18
Ferber	R.	CP 150	Glushkov	A.V.	CP 73
Ferber	R.	CP 151	Glushkov	A.V.	CP 127
Ferber	R.	CP 164	Glushkov	A.V.	CP 128
Ferber	R.	CP 165	Glushkov	A.V.	CP 130
Ferber	R.	CP 169	Gochitashvili	M.	CP 30
Ferber	R.	CP 194	Godefroid	M.	CP 71
Ferlaino	F.	CP 1	Gogyan	A.	CP 159
Fescenko	I.	CP 164	Gomonai	A.	CP 41
Fiore	V.	CP 210	Gonzalez	V.Y.	CP 15
Fivet	V.	CP 138	Gonzalez	V.Y.	CP 9
Fivet	V.	CP 188	Gorceix	O.	CP 53
Forest	D.H.	CP 184	Gorceix	O.	CP 59
Forstner	O.	CP 42	Graf	A.	CP 206
Fritzsche	S.	CP 11	Griesmaier	A.	CP 60
Froese Fischer	C.	CP 71	Grigoryan	G.G.	CP 79
Fröhlich	B.	CP 60	Grigoryan	G.G.	CP 159
Fujimoto	M.M	CP 141	Grimm	R.	CP 1
Furmann	B.	CP 197	Grimm	R.	PR 5
Fuso	F.	CP 65	Grond	J.	CP 55
Fuso	F.	CP 66	Grujic	Z.	CP 172
Gahbauer	F.	CP 165	Gudym	V.K.	CP 24
Gahbauer	f.	CP 169	Guérin	S.	CP 159
Gaidamauskas	E.	CP 10	Guérin	S.	CP 79
Gaidamauskas	E.	CP 11	Gupta	G.P.	CP 133
Gaigalas	G.	CP 10	Gupta	G.P.	CP 134
Gaigalas	G.	CP 11	Gurell	J.	CP 139
Galzerano	G.	CP 115	Gurell	J.	CP 140
Gamper	B.	CP 201	Gurnitskaya	E.P.	CP 130
Gamper	B.	CP 203	Guthöhrlein	G.H.	CP 203
Gangersky	Yu.P.	CP 184	Guthöhrlein	G.H.	CP 205
Garcia-Fernandez	R.	CP 160	Hagel	G.	PR 2
Gardner	M.	CP 184	Hakhumyan	G.	CP 89
Garnir	H.P.	CP 187	Halfmann	T.	CP 120
Gartman	R.	CP 62	Hänsch	T.W.	CP 8
Gartman	R.	CP 64	Hänsch	T.W.	CP 74
Gasaneo	G.	CP 9	Hänsch	T.W.	CP 116
Gasaneo	G.	CP 15	Hänsch	T.W.	CP 183
Gasaneo	G.	CP 26	Hanstorp	D.	CP 42
Gasaneo	G.	CP 27	Harb	M.M.	CP 208
Gateva	S.	CP 161	Haroche	S.	PL 1
Gauguet	A.	CP 175	Hartman	H.	CP 140
Gawlik	W.	CP 62	Hashmi	F.A.	CP 121
Gawlik	W.	CP 64	Hauser	A.W.	CP 109
Gedeon	S.	CP 36	Hauser	A.W.	CP 149
Gedeon	V.	CP 44	Hayden	P.	CP 100
Germann	Th.	CP 8	Hecker-Denschlag	J.	PR 5

Hefferlin	R.	CP 110	Kanski	J.	CP 67
Heidemann	R.	CP 122	Karpuskiene	R.	CP 21
Heldt	J.	CP 152	Karpuskiene	R.	CP 179
Heldt	J.R.	CP 152	Kartoshkin	V.A.	CP 46
Hemmerling	B.	CP 213	Kartoshkin	V.A.	CP 47
Herrán-Martínez	C.	CP 70	Kashuba	A.S.	CP 35
Herrmann	M.	CP 116	Katsonis	K.	CP 131
Herskind	P.	CP 111	Katsonis	K.	CP 177
Heubrandtner	Th.	CP 96	Kazakov	G.	CP 119
Hibbert	A.	CP 140	Kazakov	G.	CP 158
Hinds	E.A.	CP 112	Kazansky	A.K.	CP 72
Hitawala	U.	CP 38	Keller	J.C.	CP 53
Hofer	A.	PL 6	Keller	J.C.	CP 59
Hofer	A.	PL 6	Kennedy	E.T.	CP 100
Hohenester	U.	CP 54	Khabibullaev	P.K.	CP 78
Hohenester	U.	CP 55	Khan	Sh.	CP 204
Hohenester	U.	CP 112	Khanna	F.C.	CP 78
Hojbjerre	K.	CP 117	Khetselius	O.Yu.	CP 16
Holst	B.	CP 212	Khetselius	O.Yu.	CP 17
Homem	M.G.P.	CP 215	Khetselius	O.Yu.	CP 73
Hoszowska	J.	CP 43	Khetselius	O.Yu.	CP 127
Hotop	H.	CP 101	Khetselius	O.Yu.	CP 129
Houamer	S.	CP 34	Khetselius	O.Yu.	CP 130
Hough	P.	CP 100	Kienberger	R.	PR 9
Houssin	M.	PR 2	Kirova	T.	CP 166
Hubisz	K.	CP 146	Klein	J.	CP 120
Huikari	J.	CP 184	Klosowski	L.	CP 48
Hüpf	Th.	CP 207	Kluge	H.-J.	PL 3
Hussain	S.Q.	CP 76	Klumpp	S.	CP 20
Hutyach	Yu.	CP 41	Knöckel	K.	CP 151
Iga	I.	CP 33	Knöckl	H.	CP 58
Iga	I.	CP 141	Knoop	S.	CP 1
Iga	I.	CP 215	Knoop	M.	PR 2
Ilinova	E.Yu.	CP 83	Knowles	P.	CP 155
Ilver	L.	CP 67	Knowles	P.	CP 156
Imre	A.	CP 41	Knünz	S.	CP 116
Islam	R.	CP 191	Koch	M.	CP 125
Ivanov	S.	CP 173	Koch	T.	CP 60
Ivanov	P.	CP 173	Kolachevsky	N.	CP 61
Izadi	F.	CP 68	Kolachevsky	N.	CP 63
Jahangiri	M.	CP 68	Kolachevsky	N.	CP 74
Jahangir	M.	CP 193	Kolachevsky	N.	CP 170
Jarmola	A.	CP 165	Kolachevsky	N.	CP 183
Jarmola	A.	CP 169	Kontros	E.E.	CP 211
Jarmola	A.	CP 194	Koperski	J.	CP 114
Jelassi	H.	CP 2	Kortyna	A.	CP 210
Jelassi	H.	CP 147	Kozhedub	Y.S.	CP 22
Jelenkovic	B.M.	CP 172	Kozlov	M.G.	CP 14
Jiang	D.	CP 13	Kracke	H.	CP 123
Johnson	W.R.	CP 14	Kreim	S.	CP 123
Jönsson	P.	CP 11	Kröger	S.	CP 194
Józefowicz	M.	CP 152	Krois	G.	CP 205
Jursenas	R.	CP 23	Kronfeldt	H.D.	CP 5
Kabachnik	N.M.	CP 72	Kronfeldt	H.D.	CP 75
Kalvans	L.	CP 164	Krosnicki	M.	CP 114
Kalvans	L.	CP 165	Kumph	M.	CP 214
Kalvans	L.	CP 169	Kuparashvili	D.	CP 30
Kamenski	A.A.	CP 92	Kurskov	S.Yu.	CP 35
Kaminski	P.	CP 45	Kwela	J.	CP 180
Kanorsky	S.	CP 61	Kwela	J.	CP 87

Laburthe-Tolra	B.	CP 53	Marmo	S.I.	CP 98
Laburthe-Tolra	B.	CP 59	Marmo	S.I.	CP 99
Lagutin	B.M.	CP 20	Martinez	A.	CP 153
Lahaye	Th.	CP 60	Marushka	V.I.	CP 31
Lammegger	R.	CP 119	Matisov	B.	CP 119
Lammegger	R.	CP 157	Matisov	B.	CP 158
Landragin	A.	CP 175	Matrasulov	D.U.	CP 78
Lang	F.	PR 5	Matveev	A.	CP 74
Langkilde-Lauesen	M.B.	CP 111	Matveev	A.	CP 183
Lanzersdorfer	J.	CP 125	Matveeva	N.A.	CP 118
Laporta	P.	CP 115	Maurin	I.	CP 163
Lazur	V.	CP 36	Mauritsson	J.	PR 10
Lebedev	V.	PL 6	Mauron	O.	CP 43
Lebedev	V.	CP 181	Mayo	R.	CP 132
Lebedev	V.	CP 182	Mazets	I.E.	CP 56
Lee	M.T.	CP 33	Melezhik	V.S.	CP 40
Lee	M.T.	CP 141	Melnikov	L.A.	CP 93
Lee	M.T.	CP 215	Merlone	A.	CP 115
Leino	M.	CP 124	Mestre	M.	CP 52
Lépine	F.	CP 208	Metz	J.	CP 60
Leroy	C.	CP 159	Meyer	M.	CP 100
Leroy	C.	CP 168	Michelin	S.E.	CP 141
Leroy	C.	CP 79	Miculis	K.	CP 84
Leveque	T.	CP 175	Miculis	K.	CP 106
Li	W.	CP 100	Miculis	K.	CP 107
Lindahl	A.O.	CP 42	Miculis	K.	CP 160
Lindroth	E.	CP 12	Mijailovic	M	CP 172
Lindroth	E.	CP 25	Mileti	G.	CP 119
Lisdat	Chr.	CP 58	Minogin	V.	CP 7
Litvinov	A.	CP 158	Minogin	V.	CP 77
Liu	S.	CP 58	Mitchell	M.W.	CP 113
Loboda	A.V.	CP 73	Mitnik	D.M.	CP 15
Lohöfer	G.	CP 207	Mitnik	D.M	CP 9
Lomsadze	R.	CP 30	Mohapatra	A.K.	CP 167
Lomsadze	B.	CP 30	Mooser	A.	CP 123
Loreau	J.	CP 37	Moroshkin	P.	PL 6
Löw	R.	CP 122	Moroshkin	P.	CP 168
Lundberg	H.	CP 132	Moroshkin	P.	CP 181
Lundberg	H.	CP 140	Moroshkin	P.	CP 182
Lundberg	H.	CP 188	Motsch	M.	CP 4
Lundin	P.	CP 139	Motsch	M.	CP 80
Lundin	P.	CP 140	Msezane	A.Z.	CP 134
Machado	L.E.	CP 33	Mtchedlishvili	A.	CP 156
Mahrov	B.	CP 107	Muniz	J.	CP 153
Mahrov	B.	CP 160	Musso	M.	CP 96
Maillard	Y.P.	CP 43	Nadeem	A.	CP 192
Maiwald	M.	CP 5	Nägerl	H.C.	CP 1
Malcheva	G.	CP 132	Nagl	J.	CP 108
Malinovskaya	S.V.	CP 127	Nagl	J.	CP 109
Manakov	N.L.	CP 98	Nagl	J.	CP 125
Manakov	N.L.	CP 99	Nesterov	O.	CP 145
Mangasuli	V.	CP 65	Nic Chormaic	S.	CP 7
Mannervik	S.	CP 139	Nic Chormaic	S.	CP 77
Manson	J.R.	CP 212	Niedermayr	M.	CP 214
Mannervik	S.	CP 140	Nighat	Y.	CP 191
Maréchal	E.	CP 53	Nikoghosyan	G.	CP 159
Maréchal	E.	CP 59	Nikolayeva	O.	CP 150
Marinova	K.P.	CP 184	Nikolayeva	O.	CP 151
Mark	M.	CP 1	Nilsson	H.	CP 132
Marler	J.	CP 111	Nilsson	H.	CP 188

Norlin	L.O.	CP 139	Pruvost	L.	CP 2
Norlin	L.O.	CP 140	Pruvost	L.	CP 52
Nyman	R.A.	CP 57	Pruvost	P.	CP 147
Ollagnier	A.	CP 208	Purohit	G.	CP 38
Ortiz	M.	CP 132	Quack	M.	PL 2
Otajanov	D.M.	CP 78	Quinet	P.	CP 132
Ovcharenko	E.	CP 41	Quinet	P.	CP 138
Ovsiannikov	V.D.	CP 82	Quinet	P.	CP 140
Ovsiannikov	V.D.	CP 83	Quinet	P.	CP 187
Ovsiannikov	V.D.	CP 91	Quinet	P.	CP 188
Ovsiannikov	V.D.	CP 92	Quint	W.H.	CP 123
Ozawa	A.	CP 116	Raboud	P.A.	CP 43
Öztürk	I.K.	CP 194	Radonjic	M.	CP 172
Pain	J.C.	CP 189	Raitzsch	U.	CP 122
Pain	J.c.	CP 190	Rakhimov	Kh.Yu	CP 19
Pajek	M.	CP 43	Rancova	O.	CP 21
Pal	R.	CP 13	Rancova	O.	CP 179
Palmeri	P.	CP 138	Redlin	H.	CP 100
Palmeri	P.	CP 140	Reggami	L.	CP 105
Palmeri	P.	CP 188	Rempe	G.	CP 4
Papoyan	A.	CP 168	Rempe	G.	CP 80
Papoyan	A.	CP 89	Reschab	H.	CP 206
Papoyan	A.	CP 169	Resmej	F.	CP 37
Parigi	V.	CP 113	Richardson	V.	CP 100
Parthey	C.	CP 74	Richter	M.	PR 3
Parthey	C.	CP 183	Riehle	F.	PL 5
Pashayan-Leroy	Y.T.	CP 79	Rinkleff	R.H.	CP 171
Pashayan-Leroy	Y.T.	CP 159	Robicheaux	F.	CP 208
Pashayan-Leroy	Y.T.	CP 167	Robyr	J.L.	CP 155
Pashayan-Leroy	Y.T.	CP 168	Rodegheri	C.	CP 123
Pashov	A.	CP 151	Rodionov	P.	CP 61
Pawlak	M.	CP 95	Rodriguez	K.V.	CP 9
Pazgalev	A.	CP 156	Rodriguez	K.V.	CP 15
Pazyuk	E.A.	CP 150	Rössl	E.	CP 96
Pegg	D.J.	CP 42	Royen	P.	CP 139
Penttila	H.	CP 184	Royen	P.	CP 140
Perehanets	V.V.	CP 31	Ruczkowski	J.	CP 195
Petrov	I.D.	CP 20	Ruczkowski	J.	CP 199
Petrov	I.D.	CP 101	Ruczkowski	J.	CP 200
Pfanner	G.	CP 54	Rudzikas	Z.	CP 10
Pfau	T.	CP 60	Ruiz	J.	CP 132
Pfau	T.	CP 122	Ruzmetov	T.A.	CP 78
Pichler	G.	CP 94	Ryabinina	M.V.	CP 93
Pinegar	D.	CP 6	Ryabtsev	I.I.	CP 51
Pinegar	D.	CP 69	Ryabtsev	I.I.	CP 85
Pinkse	P.W.H.	CP 4	Ryabtsev	I.I.	CP 126
Pinkse	P.W.H.	CP 80	Ryabtsev	I.I.	CP 160
Piwinski	M.	CP 48	Ryabtsev	I.I.	CP 166
Pleskacz	K.	CP 48	Ryazanova	O.	CP 145
Plunien	G.	CP 22	Rzadkiewicz	J.	CP 43
Plunien	G.	CP 90	Saathoff	G.	CP 116
Polasik	M.	CP 43	Sadowski	J.	CP 67
Poonia	S.	CP 185	Saeidian	S.	CP 40
Poonia	S.	CP 186	Safronova	M.	CP 13
Popov	Y.	CP 34	Safronova	M.	CP 14
Porfido	N.	CP 65	Safronova	Ul.	CP 13
Pottlacher	G.	CP 206	Saidov	A.A.	CP 78
Pottlacher	G.	CP 207	Saks	E.	CP 106
Predojevic	A.	CP 113	Saks	E.	CP 107
Prescimone	F.	CP 65	Saks	E.	CP 160

Salcedo	R.	CP 153	Soldán	P.	CP 149
Saleem	M.	CP 76	Sommer	Ch.	CP 4
Saltiel	s.	CP 162	Sorokin	A.A.	PR 3
Saltiel	S.	CP 163	Sorokin	V.	CP 61
Samokotin	A.Yu.	CP 170	Sorokin	V.	CP 63
Sanches	I.P.	CP 215	Sorokin	V.N	CP 170
Sansores	L.E.	CP 153	Spani Molella	L.	CP 171
Sargsyan	A.	CP 167	Spanulescu	S.	CP 97
Sargsyan	A.	CP 168	Srivastava	R.	CP 131
Sarkisyan	D.	CP 89	Srivastava	R.	CP 177
Sarkisyan	D.	CP 167	Staanum	P.F.	CP 117
Sarkisyan	D.	CP 168	Stabkowska	K.	CP 43
Sarkisyan	D.	CP 169	Stachowska	E.	CP 196
Scharf	O.	CP 71	Stania	G.	CP 8
Schartner	K.H.	CP 20	Stauffer	A.D.	CP 131
Scheel	S.	CP 112	Stauffer	A.D.	CP 177
Schef	P.	CP 140	Steflekova	V.	CP 209
Schenk	M.	CP 4	Stepanov	A.	CP 137
Schmelcher	P.	CP 40	Stetsovykh	V.V.	CP 31
Schmidt	H.	CP 5	Steurer	W.	CP 212
Schmidt	H.	CP 75	Stoica	C.	CP 97
Schmidt	P.O.	CP 213	Stolyarov	A.V.	CP 150
Schmidt	P.O.	CP 214	Strambini	L.	CP 66
Schmiedmayr	J.	PL 4	Strauss	c.	PR 5
Schmiedmayer	J.	CP 55	Strojecki	M.	CP 114
Schmiedmayer	J.	CP 56	Sud	K.K.	CP 38
Schmoranzer	H.	CP 20	Sugohara	R.T.	CP 215
Schnizer	B.	CP 96	Sujkowski	Z.	CP 43
Schöbel	H.	CP 1	Sukharev	D.E.	CP 130
Schuessler	H.	CP 116	Sukhorukov	V.L.	PR 8
Schumm	T.	CP 56	Sukhorukov	V.L.	CP 20
Schützenhöfer	W	CP 206	Sukhorukov	V.L.	CP 101
Scrinzi	A.	PL 11	Sukhoviya	M.I	CP 144
Scully	M.O.	PL 7	Sumpf	B.	CP 5
Seliger	M.	CP 54	Svanberg	S.	CP 132
Selsto	S.	CP 12	Svinarenko	A.A.	CP 17
Selsto	S.	CP 25	Sviridov	S.A.	CP 98
Semczuk	M.	CP 116	Sviridov	S.A.	CP 99
Semenov	R.I.	CP 88	Sydoryk	I.	CP 106
Shabaev	V.M.	CP 22	Syty	P.	CP 39
Shabaev	V.M.	CP 90	Szczepkowski	J.	CP 62
Shafranyosh	I.I.	CP 31	Szczepkowski	J.	CP 64
Shafranyosh	I.I.	CP 144	Taichenachev	A.V.	CP 118
Shafranyosh	M.I.	CP 144	Talbi	F.	CP 148
Sharma	L.	CP 131	Tamanis	M.	CP 150
Sharma	L.	CP 177	Tamanis	M.	CP 151
Sherstov	I.	CP 58	Tamanis	M.	CP 164
Shojaei Baghini	F.	CP 28	Tamanis	M.	CP 194
Shojaei Baghini	F.	CP 176	Tantussi	F.	CP 65
Shpenik	O.B.	CP 32	Tantussi	F.	CP 66
Shpenik	O.B.	CP 211	Tanweer Iqbal	S.	CP 204
Siddiqui	I.	CP 193	Tanzer	R.	CP 206
Siddiqui	I.	CP 203	Taskova	E.	CP 161
Siddiqui	I.	CP 204	Tereschenko	E.	CP 63
Skolnik	G.	CP 94	Thoumany	P.	CP 8
Slavov	D:	CP 162	Tiemann	E.	CP 58
Slavov	D.	CP 163	Tiemann	E.	CP 151
Snegurskaya	T.A.	CP 31	Tino	G.M.	PL 8
Sokolov	A.	CP 63	Todorov	G.	CP 161
Sokolov	A.V.	CP 170	Todorov	P.	CP 162

Todorov	P.	CP 163	Werbowy	S.	CP 87
Tolstikhina	I.	CP 61	Werbowy	S.	CP 180
Tomin	V.I.	CP 146	Werner	L.	CP 20
Tordoff	B.	CP 184	Wester	R.	PR 1
Torosov	B.T.	CP 86	Wester	R.	CP 117
Träbert	E.	CP 136	Windholz	L.	CP 119
Tränkle	G.	CP 5	Windholz	L.	CP 157
Tretyakov	D.B.	CP 51	Windholz	L.	CP 193
Tretyakov	D.B.	CP 85	Windholz	L.	CP 196
Tretyakov	D.B.	CP 126	Windholz	L.	CP 201
Tsiskarishvili	N.A.	CP 30	Windholz	L.	CP 202
Tsygankova	G.A.	CP 88	Windholz	L.	CP 203
Tsygankova	G.A.	CP 178	Windholz	L.	CP 204
Tumaikin	A.M.	CP 118	Windholz	L.	CP 205
Tungate	G.	CP 184	Winkler	K.	PR 5
Tupitsyn	I.I.	CP 22	Witkowski	M.	CP 62
Tupitsyn	I.I.	CP 90	Witkowski	M.	CP 64
Uddin	Z.	CP 193	Wolframm	F.	CP 113
Udem	Th.	CP 116	Wróblewski	T.	CP 146
Ulfat	I.	CP 67	Yousif Al-Mula	S.Y.	CP 102
Ullrich	J.	PR 7	Yudin	V.I.	CP 118
Ulmer	S.	CP 123	Zachorowski	J.	CP 62
Umarov	F.F.	CP 29	Zadkov	V.N	CP 170
Urbonas	L.	CP 8	Zanon	T.	CP 53
Vaeck	N.	CP 37	Zanón	A.	CP 135
van Buuren	L.	CP 4	Zapryagaev	S.A.	CP 142
van Dyck	R.	CP 6	Zapryagaev	S.A.	CP 143
van Dyck	R.S.	CP 69	Zavilopulo	A.N.	CP 32
Varoquaux	G.	CP 57	Zawada	M.	CP 62
Vaseva	K.	CP 162	Zawada	M.	CP 64
Vaseva	K.	CP 163	Zemlyanoi	S.G.	CP 184
Vdovic	S.	CP 94	Zeppenfeld	M.	CP 80
Vedel	F.	PR 2	Zhechev	D.	CP 209
Vernac	L.	CP 53	Zhu	F.	CP 116
Vernac	L.	CP 59	Zillich	R.E.	CP 124
Vernakelen	A.	CP 116	Zozulya	V.	CP 145
Viaris de Leseugno	B.	CP 2	Zumsteg	C.	PR 2
Viaris de Leseugno	B.	CP 52			
Viaris de Leseugno	B.	CP 147			
Viel	A.	CP 124			
Vitanov	N.	CP 173			
Vitanov	N.V.	CP 86			
Vladimirova	Yu.V.	CP 170			
Volotka	A.V.	CP 90			
von Oppen	G.	CP 45			
von Oppen	G.	CP 174			
Vrakking	M	CP 208			
Vujicic	N.	CP 94			
Walz	J.	CP 123			
Wasowicz	T.J.	CP 180			
Wehr	R.	CP 115			
Weidemüller	M.	CP 84			
Weis	A.	PL 6			
Weis	A.	CP 154			
Weis	A.	CP 155			
Weis	A.	CP 156			
Weis	A.	CP 168			
Weis	A.	CP 181			
Weis	A.	CP 182			
Wendt	K.	CP 42			